



1 **Desorption Lifetimes and Activation Energies Influencing Gas-Surface Interactions and**
2 **Multiphase Chemical Kinetics**

3

4 *Daniel A. Knopf^{1,2,*}, Markus Ammann³, Thomas Berkemeier⁴, Ulrich Pöschl⁴, Manabu Shiraiwa^{5,*}*

5 1. School of Marine and Atmospheric Sciences, Stony Brook University, Stony Brook, New York,
6 USA.

7 2. Department of Chemistry, Stony Brook University, Stony Brook, New York, USA.

8 3. Laboratory of Environmental Chemistry, Paul Scherrer Institute, Villigen, Switzerland

9 4. Multiphase Chemistry Department, Max Planck Institute for Chemistry, Mainz, Germany

10 5. Department of Chemistry, University of California Irvine, California, USA

11 *Correspondence to:* *daniel.knopf@stonybrook.edu; m.shiraiwa@uci.edu



12 **Abstract**

13 Interfacial and multiphase chemical processes involving gases typically involve adsorption and
14 desorption onto liquid or solid substrates. The desorption energy, which depends on the
15 intermolecular forces between adsorbate and substrate, determines the residence time of chemical
16 species at the interface. In this study, we demonstrate how variations in desorption energy and
17 temperature influence the net uptake or release of gas species, which in turn affects the rates of
18 surface and bulk reactions, surface-bulk exchange, and the equilibration time scales of gas-particle
19 partitioning. We survey experimentally and theoretically derived desorption energies to develop a
20 parameterization that enables the prediction of desorption energies based on the molecular weight,
21 polarizability, and oxygen to carbon ratio of the desorbing chemical species independent of
22 substrate-specific properties, which is possible because of the dominating role of the desorbing
23 species' polarizability. The data and analyses compiled in this study provide new insights into the
24 relationship between desorption energy and enthalpies of vaporization and solvation, reflecting the
25 central role of desorption in the multiple steps of interfacial exchange and multiphase processes,
26 including mass accommodation and heterogeneous chemical reactions. Practical implications are
27 discussed for gas-particle partitioning, organic phase changes, secondary organic aerosol
28 formation, and indoor surface chemistry. We conclude that future research in aerosol, atmospheric,
29 and environmental physical chemistry, air quality, climate, and Earth system science as well as
30 chemical engineering and materials science may benefit from further insight and constraints on the
31 influence of desorption lifetimes and energies on multiphase processes and their temperature
32 dependence.

33



34 **1. Introduction**

35 The interaction of gases with condensed phase matter via heterogeneous or multiphase reactions
36 is of importance for a variety of disciplines such as chemical engineering, catalysis, materials
37 science, and environmental and atmospheric chemistry (Cussler, 2009; Chorkendorff and
38 Niemantsverdriet, 2007; Finlayson-Pitts and Pitts, 2000; Ravishankara, 1997; Solomon, 1999;
39 Hoffmann et al., 1995; Beller et al., 2012; Hanefeld and Lefferts, 2018). In the atmosphere, gas-
40 particle interactions and multiphase chemical processes involve gaseous and condensed-phase
41 species manifesting in condensation, gas-particle partitioning, and alteration in the
42 physicochemical properties of aerosol particles and cloud droplets (Pöschl et al., 2007; Kolb et al.,
43 2010; Rudich et al., 2007; George and Abbatt, 2010; Pöschl and Shiraiwa, 2015; Moise et al.,
44 2015; Ammann et al., 2013; Crowley et al., 2013; Kroll et al., 2011; Donahue et al., 2011; Jimenez
45 et al., 2009; Abbatt and Ravishankara, 2023; Ravishankara, 1997; Penkett et al., 1979; Hoffmann
46 and Edwards, 1975; Davidovits et al., 2006). The dramatic effects of multiphase reactions in the
47 atmosphere are most impressively demonstrated by the large-scale stratospheric ozone depletion
48 (ozone hole) over the south pole during Antarctic winter and spring, where inactive gaseous
49 chlorine species are converted to active gas species on cloud particles (Solomon, 1999; Rowland,
50 1991).

51 Atmospheric aerosol particles and environmental interfaces are often chemically complex
52 systems comprising multiple components in multiple phases. The large compositional variety of
53 airborne particulate matter and gas species including reactive radicals, oxidants, and volatile
54 inorganic and volatile organic compounds (VOCs), in addition to the wide temperature and
55 humidity range present in the atmosphere, poses challenges to resolve multiphase chemical
56 kinetics on a molecular level. The underlying molecular processes are important for the scientific



57 understanding and reliable description of gas uptake and chemical transformation of aerosols
58 (Shiraiwa et al., 2011a; Berkemeier et al., 2013; Zhou et al., 2013; Abbatt et al., 2012; Kolb et al.,
59 2010; Schwartz, 1986; Hanson and Lovejoy, 1995; Hanson et al., 1996; Shen et al., 2022; Willis
60 and Wilson, 2022), the chemical evolution of secondary organic aerosol (SOA) including the
61 partitioning of semivolatile species (Shiraiwa and Seinfeld, 2012; Shiraiwa et al., 2013b; Perraud
62 et al., 2012; Donahue et al., 2011; Ingram et al., 2021), and the impact of multiphase reactions on
63 the particles' activation as cloud condensation nuclei (CCN) or ice-nucleating particles (INPs)
64 (Slade et al., 2015; Slade et al., 2017; Petters et al., 2006; Wang et al., 2012; Wang and Knopf,
65 2011; Knopf et al., 2018; Knopf and Alpert, 2023).

66 Atmospheric multiphase reactions usually involve the adsorption of gas species at the surface of
67 a liquid or solid material (Langmuir, 1918, 1916, 1915; IUPAC, 1997), which can be regarded as
68 physisorption or chemisorption depending on the nature and intensity of the surface interaction.
69 Physisorption is caused by weak intermolecular interactions (van der Waals, hydrogen bond, ionic
70 and hydrophobic interactions, Table 1) with energies up to $\sim 50 \text{ kJ mol}^{-1}$, whereas chemisorption
71 involves changes of chemical bonds with higher interaction energies (Desjonqueres and Spanjaard,
72 1996; Masel, 1996; Pöschl et al., 2007). The process of reversible adsorption is easiest to depict
73 on solid surfaces but applies also to liquid surfaces, where it is coupled to the exchange with the
74 bulk liquid (Langmuir, 1918, 1916, 1915; Nathanson, 2004; Ringeisen et al., 2002a, b; Behr et al.,
75 2001; Morris et al., 2000; Masel, 1996; Nathanson et al., 1996; Rettner et al., 1996; Donaldson
76 and Anderson, 1999; Donaldson et al., 1995; Donaldson, 1999; Pöschl et al., 2007).

77 According to the Frenkel equation, the desorption lifetime (τ_{des}) of a surface-adsorbed chemical
78 species (adsorbate) follows an Arrhenius-type behavior (Arrhenius, 1889b; Arrhenius, 1889a;
79 Laidler, 1949; Frenkel, 1924; Laidler et al., 1940):



$$\tau_{\text{des}} = \frac{1}{k_{\text{des}}} = \frac{1}{A_{\text{des}}} e^{\left(\frac{E_{\text{des}}^0}{RT}\right)}, \quad (1)$$

81 where k_{des} is a first-order desorption rate coefficient, A_{des} is a pre-exponential factor, in more
82 detail discussed below, R is the gas constant, and T is temperature. E_{des}^0 is the desorption energy
83 with the energy reference of the gas molecule at rest at $T = 0$ K. E_{des}^0 is referred to as the activation
84 energy of desorption. In terms of the theory of the kinetics of desorption, desorption is always
85 considered an activated process, independent of whether E_{des}^0 corresponds to just the energy
86 difference between gas and adsorbed state or also include an energy barrier on top of that (Knopf
87 and Ammann, 2021). In case of physisorption, E_{des}^0 is equal to the negative value of the enthalpy
88 of adsorption with a correction for the change in degree of freedom between gas and adsorbed
89 phase (see below and Knopf and Ammann, 2021; Kolasinski, 2012).

90 Atmospheric trace gases and water vapor undergo reversible adsorption on aerosol, cloud, and
91 ground surfaces over a wide range of temperatures from below 200 to above 300 K. The rate of
92 interfacial processes, which may involve reversible, reactive and catalytic steps, generally depends
93 on the concentration of surface-adsorbed reactants and hence on τ_{des} . Especially at low
94 temperatures, high values of τ_{des} can (over)compensate for the low rates of thermally activated
95 chemical reactions and diffusion and thereby enhance the overall gas uptake (Ammann et al., 2013;
96 Crowley et al., 2013; Kolb et al., 2010; Pöschl et al., 2007).

97 Further factors influencing gas uptake are competitive co-adsorption of other species (Pöschl et
98 al., 2001; Pöschl et al., 2007; Slade and Knopf, 2014; Kaiser et al., 2011; Springmann et al., 2009;
99 Shiraiwa et al., 2009), solvent dynamics and polarization effects (Ringeisen et al., 2002b; Morris
100 et al., 2000; Klassen et al., 1997; Nathanson et al., 1996; Jungwirth et al., 2006), thermodynamics
101 and kinetics of surface – bulk exchange and bulk diffusivity in viscous liquids (Lakey et al., 2016;



102 Berkemeier et al., 2016; Steimer et al., 2015; Shiraiwa et al., 2014; Shiraiwa et al., 2013a; Houle
103 et al., 2018; Wiegel et al., 2017; Davies and Wilson, 2015; Marshall et al., 2016; Marshall et al.,
104 2018), and phase separations or heterogeneous structures in the condensed phase (You and
105 Bertram, 2015; You et al., 2014; You et al., 2012; Bertram et al., 2011; Huang et al., 2021).

106 The further processes influencing gas-particle interactions and multiphase chemical kinetics
107 include mass transport to the condensed phase by gas-phase diffusion and accommodation at the
108 interface; chemical reactions at the surface following Langmuir-Hinshelwood or Eley-Rideal type
109 mechanisms; dissolution, diffusion, and chemical reactions in the bulk. Together with desorption,
110 these processes may proceed sequentially or in parallel for multiple chemical species, which can
111 be described by appropriate differential equations and numerical models (Shiraiwa et al., 2010;
112 Shiraiwa et al., 2009; Ammann and Pöschl, 2007; Pöschl et al., 2007; Shiraiwa et al., 2012; Wilson
113 et al., 2022).

114 Traditionally, the uptake of trace gases by solid and liquid particles or substrates has often been
115 analyzed by the so-called resistor model, treating each of the above processes in analogy to parallel
116 or serial resistors in an electrical circuit (Schwartz, 1986; Worsnop et al., 2002; Hanson and
117 Lovejoy, 1995; Hanson et al., 1994; Ammann et al., 2013; Crowley et al., 2010). Despite
118 constraints and limitations such as the required approximations regarding steady state and mixing,
119 and a limited capability to describe multicomponent systems, the resistor model has proven to be
120 useful for the investigation and characterization of various processes and substrates, including
121 mineral dust, ice, sulfuric acid, and organic and inorganic particles (Pöschl et al., 2007; Hanson,
122 1997; Davidovits et al., 2006; Crowley et al., 2010; Kolb et al., 2010; Hanson et al., 1994; Ammann
123 et al., 2013; Ammann et al., 2003; Knopf et al., 2005; Li and Knopf, 2021). In the resistor model



124 approach, the uptake of a gas species with reaction at the surface and in the bulk is described by
125 the following or equivalent equations (Pöschl et al., 2007):

$$126 \quad \frac{1}{\gamma} = \frac{1}{\alpha_s} + \frac{1}{\frac{1}{\Gamma_b + \Gamma_{sb}} + \Gamma_s}. \quad (2)$$

127 Here, γ is the uptake coefficient, defined as the overall loss rate from the gas phase normalized to
128 the gas kinetic collision rate, and α_s is the surface accommodation coefficient, which represents
129 the probability for a gas molecule colliding with the surface to be accommodated at the surface for
130 period longer than the duration of an elastic scattering process (Pöschl et al., 2007). The term Γ_s
131 represents the normalized loss rate due to surface reaction, Γ_{sb} is the normalized rate of surface to
132 bulk transfer, and Γ_b is the normalized loss rate in the bulk-phase induced by solubility, diffusion
133 and reaction (Hanson et al., 1994; Ammann et al., 2013; Crowley et al., 2013; Kolb et al., 2010;
134 Ammann and Pöschl, 2007; Pöschl et al., 2007; Wilson et al., 2022; Shiraiwa and Pöschl, 2021).
135 By virtue of the coupled nature of the involved elementary processes, the desorption rate can
136 influence the rates of all other surface and bulk processes involving this species, i.e., k_{des} can
137 influence Γ_s , Γ_{sb} , and Γ_b (Pöschl et al., 2007). For example, the terms Γ_s and Γ_{sb} , governed by the
138 competition between desorption and surface reaction or between desorption and surface to bulk
139 transfer, respectively, are inversely proportional to k_{des} and can be expressed as follows:

$$140 \quad \Gamma_s = \alpha_s \frac{k_s}{k_{des}}, \quad (3)$$

$$141 \quad \Gamma_{sb} = \alpha_s \frac{k_{sb}}{k_{des}}. \quad (4)$$

142 Here, k_s is a first-order rate coefficient of chemical reaction at the surface; k_{sb} is a first-order rate
143 coefficient for the transfer of molecules from the surface into the bulk (solvation); k_{bs} is a first-
144 order rate coefficient for the transfer of molecules from the bulk to the surface. The overall rate of
145 transfer of a gas molecule into the bulk of a liquid or (semi)solid particle also depends on k_{des} and



146 can be expressed by the bulk accommodation coefficient, α_b (Pöschl et al., 2007; Edwards et al.,
147 2022):

$$148 \quad \alpha_b = \alpha_s \frac{k_{sb}}{k_{sb} + k_s + k_{des}} . \quad (5)$$

149 Hence, the desorption rate coefficient is a critical parameter influencing all processes involved
150 in the uptake of a gas species by condensed matter (Li and Knopf, 2021).

151 The role of reversible adsorption and desorption has been addressed in many studies of gas
152 uptake and heterogeneous chemistry in particular for the decoupling of mass transport and
153 chemical reaction (Kolb et al., 1995; Hanson and Ravishankara, 1991; Kolb et al., 2010; Ammann
154 et al., 2013; Crowley et al., 2013; Pöschl and Shiraiwa, 2015). For example, kinetic multilayer
155 model analyses of measured uptake coefficients for OH radicals on levoglucosan substrates
156 (Arangio et al., 2015) and the heterogeneous reaction of ozone with oleic acid aerosol (Berkemeier
157 et al., 2021) demonstrated the intertwined nature of surface accommodation, desorption, and
158 surface reaction. To determine a best estimate for the surface reaction rate coefficient, it was thus
159 necessary to assume a realistic value for α_s and τ_{des} derived from molecular dynamics simulations
160 (Vieceli et al., 2005; von Domaros et al., 2020). *Li and Knopf* (2021) made use of the temperature-
161 dependent measurement of OH uptake to decouple τ_{des} from surface reactivity. The intimate
162 coupling of adsorption and desorption with other multiphase processes has also been discussed in
163 the context of many other reaction systems. These include the uptake of SO₂ into sulfuric acid
164 (Jayne et al., 1990; Ammann and Pöschl, 2007), adsorption of acetone on ice and HNO₃ on mineral
165 dust (Bartels-Rausch et al., 2005; Vlasenko et al., 2009; Cwiertny et al., 2008; Usher et al., 2003),
166 ozonolysis in liquid, viscous, and solid particles (Knopf et al., 2005; Berkemeier et al., 2016;
167 Steimer et al., 2015; Shiraiwa et al., 2011a; Hearn and Smith, 2007; Pöschl et al., 2001; Shiraiwa
168 et al., 2009; Zhou et al., 2013; Kahan et al., 2006; Kwamena et al., 2004; Mu et al., 2018; Knopf



169 et al., 2011; Willis and Wilson, 2022), and gas-particle partitioning of SOA (Shiraiwa et al., 2013a;
170 Ingram et al., 2021; Schervish and Shiraiwa, 2023). Accordingly, the design and interpretation of
171 heterogeneous and multiphase reaction rate measurements should include a careful assessment
172 whether reversible adsorption is an important or even rate-limiting step, whereby the applicable
173 kinetic regime, may vary with reaction time and conditions (Berkemeier et al., 2013; Berkemeier
174 et al., 2016; Shiraiwa et al., 2014; Ingram et al., 2021; Willis and Wilson, 2022). Hence, desorption
175 lifetimes and related activation energies are important for describing the interaction of gas phase
176 and condensed phase species.

177 To address and elucidate these issues, the remainder of this article is structured as follows: In
178 Section 2, we discuss the molecular interactions underlying adsorption and desorption, and we
179 outline the relevant thermodynamic equations and parameters. In Section 3, we compile and
180 present a comprehensive set of desorption energies and thermodynamic parameters for
181 environmentally and atmospherically relevant gas species and substrates. In Section 4, we evaluate
182 the role of the desorption energy in reactive and non-reactive gas uptake by solid and liquid
183 substrates considering characteristic tropospheric temperatures by exploratory kinetic flux model
184 simulations. In Section 5, we develop and present a simplified parameterization for estimating E_{des}^0
185 based on the gas species' polarizability and oxygen to carbon (*O:C*) ratio. Section 6 outlines the
186 role of E_{des}^0 in selected atmospheric implications including the formation and properties of viscous
187 secondary organic aerosol (SOA). We conclude the document with a summary and open questions.

188

189 **2. Thermodynamic Relations**

190 A detailed discussion of the microscopic and thermodynamic treatments of adsorption and
191 desorption and implications for uncertainties in E_{des}^0 is given in *Knopf and Ammann (2021)*. Here



192 we provide the key relationships and concepts needed to follow our assumptions when applying
193 literature obtained E_{des}^0 values for derivation of a parameterization.

194 Typically, the adsorption rate is a measure of the amount of gas molecules that adsorb on the
195 surface as a consequence of gas kinetic collisions. In the atmospheric sciences this is often
196 expressed with α_s (Kolb et al., 2010), defined as the probability that a gas kinetic collision leads
197 to adsorption. Adsorption can be considered a non-activated process, though in presence of an
198 energy barrier, adsorption has to be treated as an activated process (Knopf and Ammann, 2021).
199 The corresponding energy barrier directly impacts α_s (Knopf and Ammann, 2021). In contrast,
200 desorption is always treated as an activated process, even in the absence of an energy barrier. The
201 explicit treatment of an additional energy barrier when deriving adsorption and desorption rates is
202 given in *Knopf and Ammann (2021)*. Here we solely consider E_{des}^0 as reported in the literature,
203 independent of whether an additional activation barrier was included in the analysis. As discussed
204 below, the choice of adsorbate model and standard state will impact the value and uncertainties in
205 E_{des}^0 (Knopf and Ammann, 2021; Savara, 2013; Campbell et al., 2016).

206 Adsorption proceeds spontaneously and this implies an exergonic process with the
207 thermodynamic condition (Bolis, 2013):

$$208 \quad \Delta G_{\text{ads}}^0 = \Delta H_{\text{ads}}^0 - T\Delta S_{\text{ads}}^0 < 0, \quad (6)$$

209 where ΔG_{ads}^0 represents the standard Gibbs free energy change of adsorption, ΔH_{ads}^0 is the
210 standard enthalpy change of adsorption (in this case negatively defined), ΔS_{ads}^0 is the standard
211 entropy change of adsorption, and T is temperature. Adsorption of a gas on a substrate results in
212 an increase of order, thus, $\Delta S_{\text{ads}}^0 < 0$. This is because the degrees of freedom of the adsorbed
213 molecules are more constrained than in the gas phase. Often, the adsorbed molecule may be
214 considered a 2D ideal gas, a 2D ideal lattice gas, or an ideal hindered translator on the surface,



215 with the motion perpendicular to the surface strongly constrained but with varying freedom parallel
216 to the surface (Hill, 1986; Campbell et al., 2016; Savara et al., 2009; Sprowl et al., 2016). Since
217 $\Delta S_{\text{ads}}^0 < 0$, the change in enthalpy ΔH_{ads}^0 has to be negative. The adsorption enthalpy is determined
218 by the binding energy of a gas on the surface, thus on the molecular interactions between gas
219 species and substrates, including hydrogen bonds and van der Waals forces (Poe et al., 1988;
220 Valsaraj and Thibodeaux, 1988; Valsaraj, 1988b, a; Goss and Eisenreich, 1995a; Goss, 1993,
221 1994a; Valsaraj, 1994; Valsaraj et al., 1993). The van der Waals forces comprise London
222 dispersion forces between instantaneously induced dipoles, Debye forces between permanent and
223 induced dipoles, and Keesom forces between permanent dipoles (IUPAC, 1997). For organic
224 molecules, the strength of both van der Waals and hydrogen bonds depends on the polarity of
225 functional groups and commonly follows the order (Jeffrey, 1997; Jeffrey and Saenger, 1991;
226 Vinogradov and Linnell, 1971):

227 Amide > Acid > Alcohol > Ketone \approx Aldehyde > Amine > Ester > Ether > Alkane .

228 Table 1 gives an overview of intermolecular forces active among functional groups present in
229 typical gas- and condensed-phase atmospheric species. While all molecules exhibit van der Waals
230 forces, their thermodynamic properties are largely determined by the number and type of hydrogen
231 bonds they can form. The presence of charged groups, e.g., due to a dipole moment, can
232 significantly increase binding energy. The hydrogen bond strength in liquid water is around 10-19
233 kJ mol^{-1} (Hakem et al., 2007), and with a few exceptions, usually involving fluorine, the energies
234 associated with hydrogen bonding are typically less than 20-25 kJ mol^{-1} per hydrogen bond
235 (Steiner, 2002; Jeffrey, 1997; Jeffrey and Saenger, 1991; Brini et al., 2017; IUPAC, 1997).

236 The complexity of the adsorption processes can go beyond the 2D ideal gas, 2D ideal lattice gas,
237 and hindered translator model depending on how physisorption and chemisorption are considered.



238 For example, the Kisliuk precursor mechanism allows for more complex configurations of the
239 adsorbate that could include adsorbate-adsorbate interactions (Kisliuk, 1957; Tully, 1994;
240 Campbell et al., 2016; Kisliuk, 1958). Hence, the overall adsorbate-substrate binding energy may
241 involve contributions from adsorbate-surface as well as adsorbate-adsorbate interactions (see e.g.
242 Meyer et al., 2001). Moreover, the binding energy may vary between different types of adsorption
243 sites co-existing on real surfaces, depending on the morphology and chemical heterogeneities of
244 the substrate (Kolasinski, 2012). In view of the complex mixture of substances present in the
245 atmosphere, such effects and variations are not explicitly resolved in this study. Instead, we assume
246 that the energetics of reversible adsorption on atmospheric surfaces can be approximated by
247 effective average values characterizing the binding energy to the substrate. The assumption of
248 reversible adsorption and desorption has been crucial in studies of gas uptake and heterogeneous
249 or multiphase chemical reactions when decoupling mass transport and chemical reaction (Kolb et
250 al., 2010; Hanson and Ravishankara, 1991; Ammann et al., 2013; Crowley et al., 2013; Pöschl and
251 Shiraiwa, 2015; Li and Knopf, 2021). The assumption of reversible adsorption directly leads to
252 $\Delta H_{\text{ads}}^0 = -\Delta H_{\text{des}}^0$ and $\Delta S_{\text{ads}}^0 = -\Delta S_{\text{des}}^0$, where ΔH_{des}^0 and ΔS_{des}^0 represent the changes in the
253 desorption enthalpy and entropy, respectively.

254 The free energy change is the driving force for desorption from the thermodynamic point of
255 view. The Frenkel equation, given by Eq. (1), is usually applied to describe the kinetics of
256 desorption. By itself it does not differentiate between physisorption and chemisorption. For the
257 description and understanding of atmospheric heterogeneous and multiphase kinetics, it is useful
258 to treat chemisorption as a chemical reaction following physisorption (Pöschl et al., 2007; Hanson
259 et al., 1994; George and Abbatt, 2010), as expressed in Eqs. (2) to (5). We note that the energy
260 range of 50 kJ mol^{-1} mentioned above to distinguish between physisorption and chemisorption is



261 not necessarily appropriate, if chemisorption is reflecting the fact that chemical bonds are formed
 262 or disrupted. Large molecules may undergo a multitude of van der Waals and hydrogen bonds
 263 adding up to large interaction energies, which would still be considered physisorption. As outlined
 264 above, for these cases we regard the adsorption process to be reversible.

265 *Knopf and Ammann* (2021) have provided the thermodynamic and microscopic equations, the
 266 latter based on conventional transition state (TS) theory, that are implicitly included in the Frenkel
 267 equation, while accounting for the choice of standard states. For example, for the case of a 2D
 268 ideal gas as adsorbate model, the desorption rate expressed in thermodynamic quantities is

$$269 \quad k_{\text{des}} = \kappa \left(\frac{k_{\text{B}}T}{h} \right) \frac{(N_{\text{TS}}/\mathcal{A})^0}{(N_{\text{ads}}/\mathcal{A})^0} e^{-\Delta G_{\text{des}}^0/RT} = \kappa \left(\frac{k_{\text{B}}T}{h} \right) e^{-\Delta G_{\text{des}}^0/RT}, \quad (7)$$

270 where κ is a transmission coefficient giving the probability with which an activated complex
 271 proceeds to desorption (Kolasinski, 2012), k_{B} is the Boltzmann constant, and h is the Planck
 272 constant. Furthermore, we assume the standard concentration of molecules in the TS, $(N_{\text{TS}}/\mathcal{A})^0$,
 273 is equal to the standard concentration of adsorbed molecules, $(N_{\text{ads}}/\mathcal{A})^0$, i.e., $\frac{(N_{\text{TS}}/\mathcal{A})^0}{(N_{\text{ads}}/\mathcal{A})^0} = 1$.

274 In microscopic quantities, k_{des} is derived as

$$275 \quad k_{\text{des}} = \kappa \left(\frac{k_{\text{B}}T}{h} \right) \left(\frac{q_{\text{TS}}^0}{q_{\text{ads}}^0} \right) \frac{(N_{\text{TS}}/\mathcal{A})^0}{(N_{\text{ads}}/\mathcal{A})^0} e^{-\frac{E_{\text{des}}^0}{RT}}, \quad (8)$$

276 where q_{TS}^0 and q_{ads}^0 are the standard partition functions for the TS and adsorbate, respectively,
 277 evaluated using standard molar volume and area. Equations (7) and (8) clearly demonstrate the
 278 importance of the choice of standard state when comparing measured k_{des} and evaluated E_{des}^0 .

279 Looking at the equations for k_{des} allows to derive the pre-exponential factor of the Frenkel
 280 equation as (Knopf and Ammann, 2021)

$$281 \quad A_{\text{des}} = \kappa \left(\frac{k_{\text{B}}T}{h} \right) \left(\frac{q_{\text{TS}}^0}{q_{\text{ads}}^0} \right) = \kappa \left(\frac{k_{\text{B}}T}{h} \right) \frac{(N_{\text{TS}}/\mathcal{A})^0}{(N_{\text{ads}}/\mathcal{A})^0} e^{\Delta S_{\text{des}}^0/R}, \quad (9)$$



282 where q'_{TS} and $q_{\text{ads},2\text{D}}$ are the partition functions for the TS and adsorbate, respectively. The
283 microscopic interpretation of A_{des} shows that A_{des} depends on temperature and the choice of
284 adsorbate model, expressed as partition functions. The thermodynamic interpretation of A_{des}
285 demonstrates its dependency on standard concentrations and the change in entropy when desorbing
286 from the substrate surface into the activated TS.

287 We can now interpret A_{des} for the case of a 2D ideal gas adsorbate model. If we assume $\kappa \approx 1$,
288 and adsorbate and TS are 2D ideal gases with similar numbers of possibilities (neglecting
289 vibrations), i.e., $\frac{q'_{\text{TS}}}{q_{\text{ads}}} = 1$, then we obtain $A_{\text{des}} \approx \frac{k_{\text{B}}T}{h} = 6 \times 10^{12} \approx 10^{13} \text{ s}^{-1}$ at room temperature
290 (298 K). This is the commonly applied value for the pre-exponential factor. In this case, Eq. (9)
291 demonstrates that the change in ΔS_{des}^0 must be negligible. However, significant deviations from
292 this benchmark factor can occur. For example, if going from the adsorbate state to the activated
293 TS coincides with $\Delta S_{\text{des}}^0 > 0$, and thus $\frac{q'_{\text{TS}}}{q_{\text{ads}}} > 1$, implying more degrees of freedom in the TS, then
294 $A_{\text{des}} > 10^{13} \text{ s}^{-1}$. In contrast, if the TS is more constrained, e.g., only a limited number of molecular
295 orientations are allowed, then $\Delta S_{\text{des}}^0 < 0$, and thus $\frac{q'_{\text{TS}}}{q_{\text{ads}}} < 1$, then $A_{\text{des}} < 10^{13} \text{ s}^{-1}$. A similar analysis
296 has been provided for the 2D ideal lattice gas adsorbate model (Knopf and Ammann, 2021). A_{des}
297 varies between 180 and 300 K for a 2D ideal gas and 2D ideal lattice gas adsorbate model by about
298 a factor of 2 and 3, respectively, indicating minor temperature effects (Knopf and Ammann, 2021).
299 However, A_{des} can differ by about 3 orders of magnitude between the 2D ideal gas and 2D ideal
300 lattice gas adsorbate models.

301 Experimental studies usually yield pre-exponential factors in the range between 1×10^{11} to
302 $1 \times 10^{12} \text{ s}^{-1}$ for smaller molecules such as methane and $1 \times 10^{13} \text{ s}^{-1}$ for larger alkanes (Fichthorn and
303 Miron, 2002). For large adsorbates, A_{des} can be several orders of magnitude larger (Fichthorn and



304 Miron, 2002). For example, adsorption of benzene and toluene by graphite surfaces exhibit A_{des}
305 of about 10^{15} and 10^{19} s^{-1} , respectively (Ulbricht et al., 2006). In general, the larger the adsorbate
306 molecule, the larger A_{des} (Ulbricht et al., 2006).

307 Nevertheless, for this study and the compilation of literature data of E_{des}^0 , we have assumed a
308 constant pre-exponential factor $A_{\text{des}} = 1 \times 10^{13} \text{ s}^{-1}$, being aware of the underlying assumptions
309 discussed above. We justify this approach by noting that our aim is to derive E_{des}^0 estimates for
310 complex substrate systems, including multicomponent and multiphase aerosol particles, which will
311 impose additional uncertainties in E_{des}^0 . Due to the involvement of entropic contributions to the
312 pre-exponential factor, experimentally derived A_{des} values often contain not well-documented
313 implicit standard state assumptions (related to experimental surface to volume ratios) (Donaldson
314 et al., 2012b; Campbell et al., 2016; Savara, 2013) and thus carry more uncertainty than the E_{des}^0
315 obtained from the slope of temperature dependent data.

316 Figure 1 displays the dependency of τ_{des} on E_{des}^0 and temperature using the Eq. (1). As
317 illustrated in Fig. 1a, the temperature dependency of τ_{des} increases with increasing E_{des}^0 .
318 Calculations have been performed with $A_{\text{des}} = 10^{13} \text{ s}^{-1}$, while the shading represents the
319 application of A_{des} being one order of magnitude greater or smaller, thereby covering the typical
320 temperature dependency of A_{des} . Clearly, temperature can significantly increase the residence time
321 of a molecule on the substrate surface, by several orders of magnitude, thereby, potentially,
322 allowing different reaction pathways. It is also evident that uncertainties in A_{des} directly translate
323 into corresponding uncertainties in τ_{des} . Hence, assuming $A_{\text{des}} = 10^{13} \text{ s}^{-1}$ in the analysis of
324 literature data will yield uncertainties in E_{des}^0 values. For example, one order of magnitude
325 uncertainty in A_{des} , changes E_{des}^0 by $\sim 4\text{-}6 \text{ kJ mol}^{-1}$ over a temperature range of 210 to 300 K.
326 Conversely, an uncertainty of E_{des}^0 by 5 kJ mol^{-1} imposes an uncertainty in τ_{des} of about a factor



327 of ~ 7 - 17 for a similar temperature range. These interdependencies are further outlined in Fig. 1b
328 showing typical τ_{des} for given temperatures and E_{des}^0 , again derived assuming $A_{\text{des}} = 10^{13} \text{ s}^{-1}$.
329 This discussion implies an uncertainty in our E_{des}^0 values of about $\pm 5 \text{ kJ mol}^{-1}$. However, as
330 outlined in detail in *Knopf and Ammann (2021)*, additional uncertainties in E_{des}^0 can arise when
331 the appropriate adsorbate model is not known and if the surface coverage of the adsorbate is
332 uncertain. For example, for a given τ_{des} , E_{des}^0 can differ by 10 - 15 kJ mol^{-1} when assuming either
333 a 2D ideal gas or 2D ideal lattice gas adsorbate model. If a surface is assumed to be pristine but
334 actual coverage is about 20% , E_{des}^0 may be uncertain by 10 - 20 kJ mol^{-1} . In summary, literature
335 E_{des}^0 values applied in this analysis, assuming a conservative estimate, may be uncertain by up to
336 $\sim \pm 15 \text{ kJ mol}^{-1}$.

337 The approach adopted here also applies to liquid substrates. This is straightforward for poorly
338 soluble gases. For soluble gases, however, the full thermochemical cycle also involves the
339 dissolved state (Donaldson, 1999). Despite this additional complication, the formulations shown
340 above, linking the adsorbed state with the gas phase state, remain useful. We also note that the
341 system free energy change upon adsorption of a gas on a liquid manifests in a surface tension
342 change, with the Gibbs adsorption isotherm relating the surface tension change to surface excess
343 (Kolasinski, 2012; Donaldson, 1999).

344

345 **3. Compilation of Desorption Energies for Solid and Liquid Substrates**

346 To derive a parameterization of E_{des}^0 applicable to typical gas-aerosol particle systems,
347 literature values of E_{des}^0 reflecting typical atmospheric constituents or serving as aerosol surrogates
348 have been compiled. If available, E_{des}^0 reflects values derived from lowest surface coverage,
349 preferentially below one monolayer. Tables A1-A7, A8, and A9-A15 provide thermodynamic and



350 physicochemical literature values for gas-to-solid, gas-to-ice, and gas-to-liquid substrate
351 interactions, respectively. For derivation of E_{des}^0 and τ_{des} values, we use Eq. (1) and assume
352 $A_{\text{des}} = 10^{13} \text{ s}^{-1}$, if not otherwise noted. We assume the temperature effect on A_{des} (proportional
353 to T , see Eq. (9)) and changes in the desorption entropy to be negligible compared to the Arrhenius
354 factor (Eq. (8)). The tables include the parameters E_{des}^0 , τ_{des} , and for the gas species the molar
355 mass (M), enthalpy of vaporization (ΔH_{vap}), polarizability (α), dipole moment (μ), $O:C$, and
356 enthalpy of solvation (ΔH_{sol}). Lastly, the dielectric constant or relative permittivity of the substrate
357 (ϵ_r) is given. E_{des}^0 values are obtained from different experimental techniques and theoretical
358 studies described briefly below.

359

360 **3.1 Experimental and theoretical techniques yielding desorption energies**

361 Temperature programmed desorption (TPD), sometimes also termed thermal desorption
362 spectroscopy (TDS), is an experimental technique where the flux of desorbing molecules is
363 observed as the surface temperature is increased. TDS can yield coverages, activation energies,
364 and pre-exponential factors for desorption (Ulbricht et al., 2006). Thermal gravimetry with
365 differential scanning calorimetry (TG-DSC) determines the amount and rate (velocity) of change
366 in the mass of a sample as a function of temperature or time in a controlled atmosphere in addition
367 to thermophysical and thermoplastic properties derived by DSC (Giraudet et al., 2006). In general,
368 if heats of adsorption are measured experimentally by, e.g., calorimetric methods, the accurate
369 thermodynamic definitions have to be applied since heat is not a state function (Bolis, 2013). In
370 Knudsen cells and diffusion tubes coupled to mass spectrometric detection (KN) the rate of
371 molecules desorbing from a substrate can be selectively measured (Caloz et al., 1997; Koch and
372 Rossi, 1998a; Tolbert et al., 1987; Alcalá-Jornod et al., 2000). Scattering experiments of molecular



373 beams (MB) are applied to directly measure desorption from and adsorption of gas species to solid
374 or liquid substrates (Thomson et al., 2011; Morris et al., 2000; Nathanson et al., 1996). While
375 straightforward in use and interpretation for solid surfaces in high vacuum, the developments
376 around using MB techniques for atmospherically relevant volatile liquids is experimentally
377 challenging and also data interpretation with respect to desorption is less straightforward
378 (Nathanson, 2004; Ringeisen et al., 2002b; Morris et al., 2000; Klassen et al., 1997; Nathanson et
379 al., 1996; Gao and Nathanson, 2022), as discussed below. Inverse gas chromatography (IGC)
380 applies the solid of interest as the chromatographic sorbent (stationary phase) and yields sorption
381 coefficients of gas species (Mader et al., 1997). Vacuum microbalance (VM) determines the
382 change in weight due to adsorbed gases (Rouquerol and Davy, 1978; Thomas and Williams, 1965).
383 The desorption rate can be determined by measuring the time evolution of the adsorbed phase by
384 using diffuse reflectance infrared Fourier transform spectroscopy (DRIFT), while the gas phase is
385 monitored by selected-ion flow-tube mass spectrometry (SIFT-MS) and long path transmission
386 Fourier transform infrared spectroscopy (FTIR) (Romanias et al., 2016). Since measurement of the
387 desorption rate requires pressures in the molecular flow regime, this is only straightforward for
388 low vapor pressure materials, such as mineral dust or dry salts. For high vapor pressure materials
389 (aqueous or organic liquids and ice) or materials featuring complex microstructure (mineral dust,
390 soot), complications arise from the convolutions of pore space (Woodill et al., 2013; Keyser et al.,
391 1991), bulk liquid diffusion (Koop et al., 2011; Pöschl et al., 2007), gas phase diffusion (Knopf et
392 al., 2015; Fuchs and Sutugin, 1971; Fuchs, 1964; Seinfeld and Pandis, 1998; Pöschl et al., 2007)
393 and other coupled processes, making the determination of desorption life time an indirect and often
394 difficult task. Kinetic uptake (KU) experiments operated in the molecular flow regime can yield
395 estimates of species' surface residence times (Alcala-Jornod et al., 2000; Koch and Rossi, 1998b;



396 Koch et al., 1997). KU experiments using laminar flow tube reactors can also yield estimates of
397 the residence time of adsorbed species via determination of the Langmuir equilibrium constant
398 (Pöschl et al., 2001; von Hessberg et al., 2008; Slade and Knopf, 2013). Vibrational spectroscopy
399 (VS) is used to study the interaction of molecules with, e.g., ice surfaces, by examining the shifted
400 dangling hydrogen bond of ice in presence of an adsorbed molecule (Silva and Devlin, 1994).
401 Surface tension (ST) measurements of adsorbing gases on liquid substrates can yield directly the
402 thermodynamic parameters describing adsorption (Hauxwell and Ottewill, 1968; Donaldson,
403 1999), and the molecular level relationship between surface excess and surface coverage can be
404 assessed by direct spectroscopy (Lee et al., 2016).

405 IGC derives sorption coefficients which can yield estimates of E_{des}^0 via the van't Hoff equation
406 (Goss and Eisenreich, 1996). For experimental TPD and TDS desorption data analysis usually the
407 Redhead equation (Redhead, 1962) is applied that considers the heating rate and gas species
408 surface coverage. k_{des} derived from DRIFT studies yields τ_{des} which allows derivation of E_{des}^0
409 according to Eq. (1), with similar constraints with respect to effusion times from packed powder
410 samples (Woodill et al., 2013; Keyser et al., 1991). MB methods allow to uniquely differentiate
411 thermal desorption of molecules from those undergoing elastic or inelastic scattering, or from those
412 undergoing exchange with the bulk and/or reaction. For solid surfaces the interpretation is
413 straightforward, and corresponding desorption lifetimes can directly be observed. For liquid
414 surfaces, this is less straightforward, since the trajectory of a desorbing molecule may involve
415 diffusion into and out of the near-surface bulk layers (Faust et al., 2013), so that the 'surface
416 residence time' is not strictly a true desorption lifetime. Equilibrium measurements of surface
417 tension as a function of partial pressure of the trace gas allows to determine ΔG_{ads}^0 and ΔH_{ads}^0 , if
418 the latter is assumed to be independent of temperature (Donaldson, 1999).



419 The choice of standard states can impact data interpretation. Standard free energies of formation
420 are typically referenced to 1 bar or 1 mol L⁻¹ (at 298 K) (Donaldson et al., 2012b). Commonly it
421 can be assumed that standard enthalpy values are not strongly dependent on the choice of standard
422 state, because the dependence of enthalpy on pressure is weak (Donaldson et al., 2012b). However,
423 the standard entropies of phase transfer will depend on the choice of the standard-state (Donaldson
424 et al., 2012b; Knopf and Ammann, 2021; Campbell et al., 2016; Savara, 2013). Further
425 complications arise when choosing standard states for different adsorbate-surface interactions
426 (Campbell et al., 2016). This can impact standard state surface concentrations, equilibrium
427 constants and rate constants, and renders the adsorbate chemical potential dependent on surface
428 coverage (Campbell et al., 2016; Savara, 2013).

429 Molecular dynamics (MD) simulations can provide estimates of the residence time of gas
430 species at a surface or interface (Vieceli et al., 2005). MD simulations can yield residence times at
431 the interface or substrate surface and as such an estimate of τ_{des} . Then, for given A_{des} and
432 temperature, E_{des}^0 can be estimated using Eq. (1). Density functional theory (DFT) represents a
433 computational quantum mechanical modelling method to compute the electronic structure of
434 matter (Meng et al., 2004). Monte Carlo (MC) methods based on computational algorithms rely
435 on repeated random sampling to obtain numerical results (Remorov and Bardwell, 2005). Grand
436 canonical Monte Carlo (GCMC) simulations account for density fluctuations at fixed volume and
437 temperature and represents the preferred choice for the investigation of interfacial phenomena
438 (Croteau et al., 2009). (Collignon et al., 2005) A theoretical approach to the description of the
439 electronic structure of molecules adsorbed on solid surfaces and surface reactions is the embedded
440 cluster theory (ECT) (Whitten, 1993). This allows ab initio calculations of molecular properties of
441 the lattice-adsorbate system. The dipped adcluster model (DAM) is applied to study chemisorption



442 and surface reactions in which an adcluster (admolecule + cluster) is dipped onto the electron bath
443 of a solid metal (Nakatsuji, 1987). This treatment allows to derive adsorption energies (Hu and
444 Nakatsuji, 1999).

445

446 **3.2 Atmospherically Relevant Gas-Substrate Systems**

447 **Gas Adsorption by Solid Substrates.** Gas adsorption is the first step when describing the
448 reactivity between trace gases and solid interfaces (Kolb et al., 2010; Pöschl et al., 2007). It also
449 constitutes a significant removal process of gaseous organic compounds by partitioning between
450 gas and solid phases (Goss and Eisenreich, 1996, 1995b; Goss, 1993). Mineral dust particles are
451 the most abundant aerosol particles globally by mass, providing ample solid surface area for
452 adsorption of gaseous species (Usher et al., 2003; Tang et al., 2016). Atmospheric soot particles
453 also represent a solid surface which allows for multiphase chemistry involving adsorption and
454 reaction of atmospheric oxidants (Pöschl et al., 2001; Shiraiwa et al., 2009; Kaiser et al., 2011;
455 Springmann et al., 2009), though soot can be complex consisting of solid graphite structures coated
456 by organic carbon, the latter being amorphous or soft in nature (Bond et al., 2013; China et al.,
457 2013; Cappa et al., 2012). Also, amorphous solid organic particles (Virtanen et al., 2010; Koop et
458 al., 2011; Shiraiwa et al., 2017b) provide solid substrates that serve as adsorption and reactive sites
459 for trace gas species (Knopf et al., 2018; Slade et al., 2017; Slade and Knopf, 2014, 2013; Houle
460 et al., 2018; Hearn and Smith, 2007; Lakey et al., 2016; Berkemeier et al., 2016; Steimer et al.,
461 2015; Shiraiwa et al., 2011a; Li and Knopf, 2021; Li et al., 2020).

462 In the atmosphere, adsorbing trace gases including oxidants, radicals, and VOCs compete with
463 adsorbing water for substrate surface sites. A mineral dust surface is usually hydroxylated and
464 covered by a monolayer of water at about 20-30% relative humidity (Usher et al., 2003; Tang et



465 al., 2016; Goss, 1994b). Adsorption of water by mineral dust is also crucial for our understanding
466 of the ability of dust particles to serve as CCN (Tang et al., 2016) and INPs (Kanji et al., 2017;
467 Knopf et al., 2018; Knopf and Koop, 2006; Hoose and Möhler, 2012; Knopf and Alpert, 2023).
468 Since water vapor is abundant in our environment, adsorption of a reactive or non-reactive gas
469 species will likely always proceed in competition with co-adsorbing water molecules (Kaiser et
470 al., 2011; Springmann et al., 2009). Reactive uptake of O₃ and OH radicals by insoluble organic
471 aerosol surfaces has been shown to decrease as humidity increases, following a Langmuir-
472 Hinshelwood mechanism, where water vapor co-adsorbs and competes for surface sites (Pöschl et
473 al., 2001; Slade and Knopf, 2014). Condensation of water may lead to dissolution of soluble gas
474 species and coating material on top of solid substrates, e.g., present as an aqueous organic coating
475 on soot (Charnawskas et al., 2017). Those cases should then be considered as a solid substrate
476 covered by a liquid layer and adsorption or uptake processes should be treated as proceeding on a
477 liquid substrate. Tables A1-A7 present a compilation of E_{des}^0 and other molecular parameters for
478 a selection of atmospherically relevant reactive and non-reactive trace gases interacting with
479 various solid substrates serving as surrogates of aerosol particles.

480

481 **Gas Adsorption by Ice.** Ice is among the most abundant solid materials on the Earth's surface.
482 Roughly 50% of the northern hemisphere landmass is covered by ice and snow in winter (Bartels-
483 Rausch, 2013). Adsorption of trace gases on ice impact gas-phase chemistry in the stratosphere
484 and upper troposphere (Solomon, 1999; Borrmann et al., 1996; Voigt et al., 2006), snow chemistry
485 and boundary layer gas-phase chemistry over perennial and permanent snowpacks and gas-phase
486 chemistry above sea-ice (Bartels-Rausch et al., 2014; Artiglia et al., 2017; Raso et al., 2017;
487 George et al., 2015; McNeill et al., 2012; Abbatt et al., 2012; Jeong et al., 2022; McNamara et al.,



488 2021). Partitioning of gases to ice in polar and high-alpine snow also result in signals in ice cores
489 used to reconstruct past climates and environmental conditions (Vega et al., 2015). In comparison
490 to other solid materials, ice is a high-temperature material existing in the environment at
491 temperatures relatively close to its melting point. As in other molecular solids this leads to surface
492 premelting and thus a disordered interface, also referred to as quasi-liquid layer, the properties of
493 which are a matter of ongoing debate (Bartels-Rausch et al., 2014; Asakawa et al., 2016; Cho et
494 al., 2002; Slater and Michaelides, 2019). Since this layer is the interface with which adsorbing
495 gases interact, the mutual interplay between the properties of the disordered interface and the
496 nature of the interaction of gases have spurred speculations about whether it should be treated as
497 a thin aqueous solution layer or a purely solid surface. Recent spectroscopic evidence indicates
498 that soluble gases form solvation shells similar as in liquid water without, however, modifying the
499 remaining ice structure significantly (Bartels-Rausch et al., 2017). Thus under typical
500 atmospherically relevant conditions with low coverages of volatile gases, the surface remains
501 dominated by the properties of ice. A template for this may be the case of HCl adsorption on ice,
502 for which singly hydrogen bonded HCl is adsorbed at the outermost surface (Kong et al., 2017),
503 while upon hydration and dissociation, chloride enters deeper into the interface (Zimmermann et
504 al., 2016; McNeill et al., 2007; McNeill et al., 2006). This is in accord with a low desorption energy
505 and thus low coverage with molecular HCl (Table A8). This behavior can mask the weak
506 temperature dependence of the total coverage by HCl (molecular and dissociated). Similar
507 conclusions come from MB experiments, e.g., with NO_y compounds, where the desorption kinetics
508 are characterized directly (Lejonhuthun et al., 2014). An exception may be the case of H₂O itself,
509 where the MB experiments may not have been able to resolve singly hydrogen bonded H₂O
510 desorbing, but only completely hydrated ones desorbing more slowly (Kong et al., 2014b; Kong



511 et al., 2014a). Therefore, adsorption on ice may well be considered as adsorption within the
512 simplified scheme adopted in this work even for very soluble and more straightforwardly for less
513 soluble molecules. Table A8 summarizes the thermodynamic literature data on gas species
514 adsorption by ice substrates applied in this study.

515

516 **Gas Adsorption by Water and Aqueous Solutions.** Liquid water and aqueous solutions are a
517 dominant form of condensed matter in the environment including aerosol particles, clouds, or
518 ocean surfaces. In aerosol particles, aqueous solutions may range from dilute solutions at very high
519 humidity and at or close to the point of activation into a cloud droplet to very concentrated
520 supersaturated solutions at low relative humidity. High solute strength solutions may yield highly
521 viscous, semi-solid and glassy particle phase states occurring throughout the atmosphere (Shiraiwa
522 et al., 2017b; Koop et al., 2011; Mikhailov et al., 2009; Zobrist et al., 2008; Klassen et al., 1998).
523 Decreasing bulk diffusivity in these viscous phases increases the relative importance of the
524 desorption lifetime as exchange with the bulk is retarded (Behr et al., 2009; Knox and Phillips,
525 1998; Li and Knopf, 2021) (see Eq. (4)).

526 The notion that adsorbed molecules on liquid surfaces represent a distinct feature comes from
527 both spectroscopic and kinetic evidence. MB experiments of HCl on deuterated sulfuric acid
528 clearly identified collision-, adsorption-, and desorption trajectories (Behr et al., 2001; Morris et
529 al., 2000; Gao and Nathanson, 2022), as a direct and unique manifestation of Langmuir's view of
530 adsorption (Langmuir, 1918). The time the HCl molecule spends on the surface is directly related
531 to E_{des}^0 and A_{des} . In other cases studied by the MB technique, the picosecond scale hydrogen bond
532 exchange dynamics and fast diffusion (nanoseconds – microseconds for diffusion into and out of
533 depths of several nanometers) prevented unambiguous separation of pure desorption from



534 trajectories including entry into the liquid (Ringeisen et al., 2002a, b; Brastad et al., 2009; Faust
535 and Nathanson, 2016; Faust et al., 2016; Faust et al., 2013). Similar conclusions about adsorption
536 – desorption trajectories in the case of H₂O(g) on liquid water may be drawn from different isotope
537 exchange kinetics for HDO with H₂O and H₂¹⁸O with H₂O that require different degrees of
538 hydration on the water surface (Davidovits et al., 2011, 2006). The suggestion that a distinct
539 population of H₂O molecules exists that is singly hydrogen bonded at the liquid water surface
540 comes from detailed interpretation of IR spectra in line with theory (Devlin et al., 2000). The high
541 vapor pressure of environmentally relevant liquids and other difficulties (including those related
542 to fast exchange with the bulk liquid) prevent direct determination of desorption kinetics for many
543 relevant trace gas – substrate pairs. In spite of this situation, we suggest to apply the same concept
544 of converting desorption energies (derived from partitioning or chromatographic methods) into
545 desorption lifetimes as for solid surfaces, from which the concepts described in the introduction
546 section have been developed.

547 The fact that molecules at the aqueous solution or liquid water – air interface experience a
548 different environment than in the bulk liquid is straightforward. The density drops over molecular
549 length scales and the hydrogen bond dynamics and orientation in water and aqueous solutions on
550 average lead to a strongly asymmetric environment at the interface (Brini et al., 2017; Ahmed et
551 al., 2021; Hao et al., 2022). This leads to specific molecular interaction options (as described
552 above) and in turn to specific binding energies as result of these. Changes to the equilibrium
553 surface tension of aqueous solutions in response to adsorption of gases is the consequence of the
554 changes in the surface free energy. Its temperature dependence is reflecting the energy gain as a
555 result of the sum of these interactions. Tables A9 to A15 are a compilation of E_{des}^0 for a range of
556 inorganic and organic trace gases on pure water or on aqueous solutions. The simplest case H₂O(g)



557 on H₂O(l), exhibits a single hydrogen bond and a corresponding low E_{des}^0 value. Among the given
558 families of species, interaction energies scale with molar mass or the degree of substitution with
559 functional groups that alter the amount of weak or strong molecular interactions. The degree of
560 substitution may be represented by the dipole moment (μ) and $O:C$ for organic molecules as
561 outlined in the discussion of parameterized E_{des}^0 . The presence of hydrophilic functional groups
562 with strong hydrogen bonding interaction options leads to correspondingly larger E_{des}^0 . Since these
563 groups also interact with the hydrogen bonding network of water, these interactions are sensitive
564 to the presence of other solutes or, especially, ions (Demou and Donaldson, 2002; Lee et al., 2019;
565 Ohrwall et al., 2015; Ekholm et al., 2018).

566

567 **4. Impact of Desorption Lifetime on Gas Uptake**

568 To assess the impact of τ_{des} on multiphase chemical kinetics, the kinetic multi-layer models of
569 aerosol surface and bulk chemistry (K2-SURF, KM-SUB) are applied (Shiraiwa et al., 2010;
570 Shiraiwa et al., 2009). These models are based on the PRA framework (Ammann and Pöschl, 2007;
571 Pöschl et al., 2007) and describe the gas-particle interface by implementation of several model
572 compartments and molecular layers in which species can undergo mass transport and chemical
573 reactions. Here, the compartments included are: gas phase, near-surface gas phase, sorption layer,
574 quasi-static surface layer, and a number of bulk layers.

575 Gas-phase diffusion of a species X from the gas phase to the near-surface gas-phase surrounding
576 the particle is treated by the net flux of gas-phase diffusion:

$$577 \quad J_{g,X} = 2\pi(d_p + 2\lambda D_g)([X]_g - [X]_{gs}), \quad (10)$$

578 where d_p is the particle diameter, λ is the mean free path, D_g is the gas diffusivity and $[X]_g$ and
579 $[X]_{gs}$ are concentrations of X in the gas and near-surface gas phases, respectively (Pöschl et al.,



580 2007; Knopf et al., 2015; Li et al., 2018). The mass balance and rate equation for X in the near-
 581 surface gas phase can be described as:

$$582 \quad \frac{d[X]_{gs}}{dt} = \frac{J_{g,X} - (J_{ads,X} - J_{des,X})A_s}{V_{gs}}, \quad (11)$$

583 where A_s is the particle surface area and V_{gs} is the volume of the near-surface gas phase. $J_{des,X}$ is
 584 the desorption flux defined as $J_{des,X} = k_{des,X}[X]_s = \tau_{des,X}^{-1}[X]_s$. $J_{ads,X}$ is the adsorption flux defined
 585 as $J_{ads,X} = \alpha_{s,X}J_{coll,X}$, where $\alpha_{s,X}$ represents the surface accommodation coefficient, and the
 586 collision flux is defined as $J_{coll,X} = \frac{1}{4}\omega_X[X]_{gs}$ with ω_X being the mean thermal velocity of X.

587 The surface-layer reaction (SLR), involving only the adsorbed species, X(s), or components of
 588 the quasi-static layer, Y(ss), such as $X(s) + Y(ss) \rightarrow$ products, is described by the second-order
 589 rate coefficient k_{SLR} . The surface reaction rate is described as $L_s = k_{SLR}[X]_s[Y]_{ss}$. The mass
 590 balance and rate equations for X in the near-surface gas phase and at the surface can be described
 591 as below:

$$592 \quad \frac{d[X]_s}{dt} = J_{ads,X} - J_{des,X} - L_s - J_{s,b,X} + J_{b,s,X}, \quad (12)$$

593 where $J_{s,b,X}$ and $J_{b,s,X}$ are the fluxes from the surface to the near-surface bulk and from the near-
 594 surface bulk to the surface of X, respectively ($J_{s,b,X} = J_{bsb,X} = 0$ in the absence of bulk diffusion),
 595 and treated as a function of the bulk diffusion coefficient. The reactive uptake coefficient, γ , is
 596 usually the experimentally accessible parameter and the one used in atmospheric modeling studies.
 597 γ of a gas species X is defined as

$$598 \quad \gamma_X = \frac{J_{ads,X} - J_{des,X}}{J_{coll,X}}. \quad (13)$$

599

600 **Simulation of reactive gas uptake by solid substrates.** We apply the kinetic double-layer model
 601 of aerosol surface chemistry (K2-SURF; (Shiraiwa et al., 2009)) to investigate the sensitivity of γ



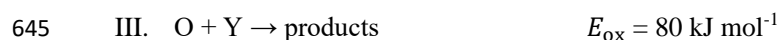
602 to the desorption lifetime for a solid substrate. The surface reaction of an adsorbed species X with
603 condensed species Y is considered, while surface-bulk exchange and bulk diffusion and reaction
604 are not considered for simplicity. The α_s on an adsorbate-free substrate is assumed to be one for
605 all simulations. Figure 2 shows the dependence of γ on τ_{des} and k_{SLR} at constant temperature. γ
606 values represent steady-state values. Higher k_{SLR} leads to higher γ at fixed τ_{des} due to faster
607 surface reaction rates. At fixed k_{SLR} , longer τ_{des} leads to higher surface concentrations of X, and
608 consequently to higher surface reaction rates and γ . In turn, with sufficiently long residence times
609 of the adsorbed gas species, low k_{SLR} can still lead to high values of γ . It is evident that different
610 pairs of τ_{des} and k_{SLR} can yield the same γ value. Furthermore, when k_{SLR} is known, uncertainties
611 in τ_{des} can result in large differences in γ . This exercise demonstrates that experimentally derived
612 γ values do not sufficiently constrain the heterogeneous reaction process to yield unambiguous
613 τ_{des} and k_{SLR} values, unless a significant parameter space is covered by the experiment to constrain
614 them individually. For instance, at large enough gas phase partial pressure the surface gets
615 saturated (fully covered by the adsorbate), which leads to decoupling of τ_{des} and k_{SLR} (Knopf et
616 al., 2011; Artiglia et al., 2017; Berkemeier et al., 2016; Steimer et al., 2015). However, this is often
617 not possible due to technical constraints. Therefore, constraining τ_{des} by application of E_{des}^0 , or
618 best estimates of E_{des}^0 , can significantly improve our molecular understanding of the underlying
619 processes in multiphase chemical kinetics and support the development of parameterizations for
620 modelling purposes.

621 Figure 3 displays the temperature dependence of γ with E_{des}^0 of 30 – 50 kJ mol⁻¹. The pre-
622 exponential frequency factor A_{des} was set to 10¹³ s⁻¹ and k_{SLR} was set to (a) 10⁻¹² and (b) 10⁻⁹ cm²
623 s⁻¹. Temperature dependence of k_{SLR} was not considered in these simulations to evaluate only the
624 effects of temperature-dependent τ_{des} on γ . The modeling results suggest that γ depends strongly



625 on temperature, where lower temperatures yield higher γ values. This is because lower
626 temperatures lead to longer τ_{des} and hence higher surface concentrations of X and reaction rates.
627 Generally, γ is more temperature-dependent at higher values of E_{des}^0 . However, if E_{des}^0 is close to
628 values typical for chemisorption ($\sim 50 \text{ kJ mol}^{-1}$), γ is close to 1 in this calculation. Further away
629 from this special case and natural cap of $\gamma = 1$, γ increases by about two orders of magnitude over
630 a temperature range of 80 K. These modeling results indicate that extrapolating multiphase
631 chemical kinetics acquired at room temperature to lower temperatures, can result in significantly
632 different reactive uptake coefficients. Clearly, a detailed understanding of the molecular processes
633 is necessary when applying multiphase reaction kinetics to environmental and atmospheric
634 conditions.

635 Even though the above simulations clearly suggest potentially large effects of the temperature
636 dependence of τ_{des} on γ , surface reaction rate coefficients are also temperature dependent which
637 in turn affect γ as well (Li and Knopf, 2021; Li et al., 2020). To further investigate the role of
638 temperature on heterogeneous reaction kinetics, we apply the K2-SURF model to heterogeneous
639 reactions between O_3 and polycyclic aromatic hydrocarbons (PAHs) adsorbed on soot. This
640 reaction proceeds with a multi-step Langmuir-Hinshelwood mechanism that includes I) O_3
641 physisorption, II) decomposition of O_3 into long-lived reactive oxygen intermediates (ROIs, O
642 atoms), and III) reactions of O atoms with PAHs (Shiraiwa et al., 2011b):



646 The activation energy for physisorbed O_3 to dissociated into chemisorbed O ($E_{\text{a,pc}}$) is $\sim 40 \text{ kJ mol}^{-1}$
647 and the activation energy for O reacting to oxidation products (E_{ox}) is $\sim 80 \text{ kJ mol}^{-1}$ (Berkemeier



648 et al., 2016; Shiraiwa et al., 2011b). Temperature dependence of the reaction rate coefficients of
649 reactions II and III are considered using an Arrhenius equation. We examine the response of this
650 reaction system to changes in initial E_{des}^0 of O_3 (reaction I) and temperature.

651 Figure 4 shows the results of such simulations. Higher E_{des}^0 yields higher surface concentrations
652 of physisorbed O_3 , and hence higher concentrations of O and reaction rates, yielding higher γ
653 values. γ decreases as temperature decreases, which is in contrast to above sensitivity studies
654 shown in Fig. 3. This is because the overall temperature dependency of the gas uptake is mostly
655 determined by the temperature dependency of the rate-limiting reaction III and also influenced by
656 thermally-activated chemical reaction II. Although physisorbed O_3 molecules can reside
657 significantly longer on the PAH surface at lower temperatures, the decrease in the formation rate
658 of ROIs and subsequent oxidation reaction rate govern γ , suggesting lower γ values at lower
659 temperatures.

660 Clearly, E_{des}^0 and activation energies for chemical reactions are crucial parameters to predict
661 multiphase chemical kinetic processes under tropospheric conditions. Conducting temperature-
662 dependent reactive uptake experiments of known reaction systems can be used to determine
663 coupled desorption lifetimes and reaction rates (e.g., Kerbrat et al., 2010; Li and Knopf, 2021).
664 For example, *Li and Knopf (2021)* measured the reactive uptake of OH radicals by triacontane for
665 temperatures between 213 and 293 K. By having a temperature-dependent multiphase kinetics data
666 set, E_{des}^0 and k_{SLR} could be decoupled and individually assessed.

667

668 **Non-reactive gas uptake into liquids simulation studies.** To demonstrate the effect of τ_{des} on
669 equilibration timescale of non-reactive gas uptake by a liquid substrate, the kinetic multi-layer
670 model for aerosol surface and bulk chemistry (KM-SUB) (Shiraiwa et al., 2010) was applied (Fig.



671 5). We simulate non-reactive uptake of species X with initial gas-phase and particle-phase
672 concentrations of 1 ppb and zero, respectively. The Henry's law constant of X was set to be 1×10^{-5}
673 $\text{mol cm}^{-3} \text{atm}^{-1}$ at 298 K and its temperature dependence was considered using the van't Hoff
674 equation with solvation enthalpy of 20 kJ mol^{-1} ; these values are consistent with ozone solvation
675 into water (Sander, 2015). The temperature dependence of the Henry's law constant is shown in
676 Fig. S1. The particle phase is assumed to be liquid with a bulk diffusion coefficient of $10^{-5} \text{ cm}^2 \text{ s}^{-1}$
677 and the temperature dependence of bulk diffusivity is not considered in this simulation for
678 simplicity. Different E_{des}^0 values of $10 - 80 \text{ kJ mol}^{-1}$ were used and the temperature dependence of
679 τ_{des} was considered using the Frenkel equation (see Eq. (1) and Fig. 1). Equilibration timescale is
680 defined as the time after which the particle-phase concentration deviates by less than a factor of
681 $1/e$ from the equilibrium or steady-state value.

682 The results of such simulations are shown in Fig. 5. The simulation demonstrates that for E_{des}^0
683 $\leq 30 \text{ kJ mol}^{-1}$, the timescales of desorption are much shorter than the timescale of diffusion and
684 the equilibration timescales are insensitive to E_{des}^0 . At higher E_{des}^0 , the increase of desorption
685 lifetime leads to the increase of the equilibration timescale, as molecules reside longer time in the
686 sorption layer; in fact, the majority of molecules reside on the surface and the partitioning is
687 governed by the surface process. At $E_{\text{des}}^0 \geq 80 \text{ kJ mol}^{-1}$, longer desorption lifetime leads to
688 saturation of the sorption layer, and hence also saturation of the equilibration timescale.

689 The calculations for Fig. 5 represent an open system in which the gas-phase concentration of X
690 is held constant. *Wilson et al.* (2021) investigated equilibration timescales for gas uptake of PAHs
691 on soot surfaces in the closed system, i.e., where a fixed amount of X is distributed between the
692 gas and particulate phases. In that study, equilibration timescales were either controlled by the
693 adsorption or by the desorption process, depending on whether the particle surface was under- or



694 oversaturated with X at the start of the model simulations, respectively. Temperature strongly
695 influenced equilibration timescales in the desorption-controlled regime, whereas particle number
696 concentrations influenced adsorption-controlled systems. Note that in the presence of chemical
697 reactions in the gas phase or on the surface, the partitioning equilibrium can be perturbed and adopt
698 a quasi-stationary state that differs from thermodynamic equilibrium.

699 For reactions occurring in liquids, the same features apply as for the case of surface reactions on
700 solids, i.e., the temperature dependence of an activated reaction may counteract the temperature
701 dependencies of desorption and solubility, e.g., for the reactions on sulfuric acid aerosol of HCl
702 with HONO (Longfellow et al., 1998; Ammann et al., 2013) or with ClONO₂ (Shi et al., 2001).
703 These cold sulfuric acid aerosols, but also viscous aqueous organic aerosols are also at the same
704 time high solute strength systems. The situation then is very complex since viscosity is modulated
705 by temperature and humidity, thereby impacting diffusion and salting out effects, and thus,
706 ultimately, solubility and kinetics (Edebeli et al., 2019; Li and Knopf, 2021; Li and Shiraiwa,
707 2019).

708

709 **5. Derivation of a Parameterization of the Desorption Energy**

710 Thermodynamic and chemical parameters given in Tables A1-A15 provide the basis to derive
711 E_{des}^0 estimates for application in multiphase chemical kinetics involving atmospheric gas species
712 and aerosol particles. This analysis includes over 500 gas species-substrate systems. As discussed
713 above, we note the underlying caveats in this analysis. The pre-exponential factor is set to 10^{13} s^{-1} .
714 ¹. The dependence of E_{des}^0 on adsorbate model and surface coverage is neglected. Thus, a highly
715 accurate prediction of E_{des}^0 is not possible. However, the goal here is to provide a best estimate of
716 E_{des}^0 in agreement with this training data set (Tables A1-A15) to enable improved analyses of



717 environmental multiphase chemical kinetics under the wide range of thermodynamic conditions
718 encountered in the Earth's environment. Furthermore, it would be desirable to predict E_{des}^0 from
719 commonly measured and accessible parameters, e.g., derived by mass spectroscopy, such as molar
720 mass, molecular structure, and oxidation state.

721 Following our previous discussion on the intermolecular bonding between adsorbate and
722 substrate, gas species polarizability, α , should serve as predictor of E_{des}^0 . Larger α should, in
723 general, coincide with an increase in E_{des}^0 . The oxidation state of an organic gas species,
724 represented in a simplified way by the ratio $O:C$, reflects the number of oxygenated functional
725 groups, typically monitored by mass spectrometry (Isaacman-VanWertz et al., 2018). An increase
726 in the gas species' oxidation state should also yield an increase in E_{des}^0 . Figure 6 displays a
727 multilinear regression analysis using all available data including solid, ice, and liquid substrates
728 (Tables A1-A15) to derive a relationship between E_{des}^0 , α , and $O:C$. Figure S3 depicts the same
729 data in more detail as two separate plots. Figure 6 indicates that E_{des}^0 increases with increasing α
730 and $O:C$, as one would expect from considerations of intermolecular bonding discussed above.
731 This is also corroborated by a principal component analysis given in Fig. S2, showing significant
732 correlation between E_{des}^0 and α . The regression analysis yields the following model (with an $R^2 =$
733 0.559 and a root mean squared error (RMSE) = 25.4):

$$734 \quad E_{\text{des}}^0(\alpha, O:C) = 25.895 + 2.330\alpha + 12.367(O:C) . \quad (14)$$

735 Figure 7 shows α as a function of molar mass and $O:C \leq 1$. Note that the few data for the three
736 gas species with $O:C \geq 1$, namely CO_2 (Table A3), formic acid (Table A7), and, peroxyacetyl
737 nitrate, PAN (Table A8) are colored as $O:C = 1$ for better visibility of the overall training set.
738 Figure 6 shows the few data points for $O:C > 1$. The data show a strong linear correlation between
739 α and M , where $O:C$ appears to play a less significant role. This can be understood by realizing



740 that a carbon atom in a molecule contributes three times more to α than an oxygen atom (Bosque
741 and Sales, 2002), discussed in more detail below. Hence, the number of methylene groups can
742 dominate α for larger molecules. Thus, the polarizability can be described, applying regression
743 analysis, as a linear function of molar mass ($R^2 = 0.952$ and $RMSE = 2.765$):

$$744 \quad \alpha(M) = -0.837 + 0.128M, \quad (15)$$

745 shown as a red line in Fig. 7.

746 We can now combine Eqs. (14) and (15) to obtain a parameterization to calculate E_{des}^0 from
747 knowledge of the gas species' molar mass and $O:C$:

$$748 \quad E_{\text{des}}^0(M, O:C) = 25.895 + 2.330(-0.837 + 0.128M) + 12.367(O:C). \quad (16)$$

749 Figure 8 shows E_{des}^0 values derived from Eq. (16) using M and $O:C$ values given by the training
750 datasets as input. Similarly to Fig. 7, we have color-coded $O:C$ for values up to one for better data
751 visibility. Figure S4 shows E_{des}^0 values derived from Eq. (16) using arbitrary M and $O:C$ values.
752 E_{des}^0 shows a linear relationship with M where deviation from linearity is only found at $M < 250$
753 g mol^{-1} . Figure 8B demonstrates that gas species with larger $O:C$ show larger E_{des}^0 . To understand
754 this trend in the data, we have to address the role of the gas species' dipole moment and substrate
755 in the derivation of the E_{des}^0 values. Equation (16) provides estimates of E_{des}^0 without specifically
756 addressing substrate properties. As discussed, its dependency solely on M and $O:C$ is
757 advantageous for application to complex gas species-particle composition data. Considering the
758 underlying uncertainties due to unknown applied standard states, adsorbate model, and assumed
759 prefactor, this parameterization is accurate within those limits. However, one would expect that
760 gas species' μ and the substrate's ϵ_r impact E_{des}^0 .

761 We recommend application of this parameterization (Eq. (16)) for gas species with $O:C \lesssim 1$.

762 Due to the few data points at $O:C \gtrsim 1$, E_{des}^0 could be significantly under- or overestimated in this



763 range. For example, for CO₂ (Table A3), tabulated $E_{\text{des}}^0 = 16.4 \text{ kJ mol}^{-1}$, while the parameterization
764 yields 61.8 kJ mol^{-1} . In the case of formic acid (Table A7), the tabulated $E_{\text{des}}^0 = 94.6 \text{ kJ mol}^{-1}$,
765 while the parameterization yields 62.4 kJ mol^{-1} . Hence, when applying Eq. (16) to gas species with
766 $O:C \gtrsim 1$, considering additional information or constraints is recommended.

767 For our data set, the principal component analysis in Fig. S2 indicates no strong correlation
768 between ϵ_r and E_{des}^0 . Fig. 9 corroborates the negligible dependence of E_{des}^0 on ϵ_r . However, one
769 would expect that greater μ , α , and ϵ_r result in larger E_{des}^0 due to enhanced molecular interactions.
770 The derivation of our parameterization exploited the strong dependency of E_{des}^0 on α . We suggest
771 that the underlying reason for this dependency is the competing effects of μ and α on E_{des}^0 as
772 outlined below.

773 Small molecules with polar groups can exert significant dipole moments while the polarizability
774 is still small. As depicted in Fig. S5, smaller molecules exert greater μ while $O:C$ values are high
775 and α is low (see also Fig. 7). Note that alkanes and PAHs in the data set, following common
776 convention, have zero dipole moments. Gas species with greater μ may interact more strongly with
777 polarizable substrates expressed by ϵ_r , yielding larger E_{des}^0 . However, as the gas molecules become
778 larger, their α increases, e.g., by the addition of methylene groups (Bosque and Sales, 2002),
779 thereby dominating over the impact of μ on E_{des}^0 . Figure S3 supports this trend where molecules
780 with largest α have low $O:C$ and small μ . Hence, this data set yields a negative correlation between
781 μ and α . As a consequence, for larger molecules the role of the molecule's μ interacting with the
782 substrate becomes less important. Thus, in a way, the range of available desorption data could be
783 responsible for the negligible correlation between E_{des}^0 and substrate ϵ_r (Fig. 9). In other words,
784 polarizability α , which is strongest for molecules with small μ and low $O:C$, compensates and
785 dominates the impact of the dipole moment on E_{des}^0 and, in turn, renders the substrate of less



786 importance for parameterizing E_{des}^0 . This is also evident in Fig. 10, where the scatter of
787 parameterization-derived E_{des}^0 values is largest for molecules with lower M and lower α . We can
788 attribute the scatter in E_{des}^0 at lower M to the competing contributions of the gas species' μ , here
789 accounted by $O:C$ and α . These may be the reasons why E_{des}^0 can be reasonably parameterized
790 from our data set without accounting for the substrate's ϵ_r and gas species' μ . Though, we would
791 expect with more available data, the role of gas species' μ and substrate's ϵ_r to likely be resolved
792 in a parameterization.

793 Considering the significant number of data and omission of substrate specific properties in the
794 parameterization, the scatter in E_{des}^0 is not very large. This suggests that this parameterization can
795 serve as a reasonable first estimate of E_{des}^0 for a complex environmental substrate such as an
796 aerosol particle. We would expect that with increasing number of desorption data that include
797 larger molecules with larger $O:C$ or μ and applied known standard states and adsorbate models,
798 the scatter in E_{des}^0 at lower molar masses can be resolved.

799

800 **Relationship Between Desorption Energy and Enthalpy of Vaporization.** To examine the
801 relationship between E_{des}^0 and ΔH_{vap} , we have plotted the data given in supplemental tables (not
802 the parameterized values) separated for the different substrate types in Fig. 11. Our data supports
803 a positive correlation between E_{des}^0 and ΔH_{vap} , where E_{des}^0 for most instances is larger than ΔH_{vap} .
804 The role of $O:C$ in the relationship between E_{des}^0 and ΔH_{vap} is not clearly identifiable for the cases
805 that include all, solid, and ice substrates data. However, for liquid substrates, the data suggest that
806 for given ΔH_{vap} , larger $O:C$ yields larger E_{des}^0 . As shown above, larger $O:C$ correlates with a
807 larger μ , which may exert a greater impact on E_{des}^0 in the case of a liquid substrate. In fact, the
808 interaction strength at the surface often exceeds the enthalpy of condensation between gas and its



809 condensed liquid for the same species family, e.g., in the case of methyl-substituted benzenes (Raja
810 et al., 2002; Bruant and Conklin, 2002), but also for other species like alcohols, acids, amines and
811 ketones (Mmereki et al., 2000) and alkanes (Goss, 2009) and halogenated alkanes (Bruant and
812 Conklin, 2001). This indicates that the aqueous solution – air interface allows for a two-
813 dimensional environment in which the intermolecular interactions are as important as in the
814 condensed phase of the adsorbate alone (Valsaraj, 1988b, 2009).

815

816 **Relationship Between Desorption Energy and Enthalpy of Solvation for Aqueous**

817 **Substrates.** To examine the relationship between E_{des}^0 and ΔH_{solv} , we have plotted the data for
818 liquid substrates, consisting mostly of water and few aqueous solutions (Tables A9 to A15) in Fig.
819 12. Despite the scatter in the data, a positive correlation between E_{des}^0 and ΔH_{solv} can be identified.
820 The data falls symmetrically around the 1:1 line, indicating no strong bias. Thus, E_{des}^0 and ΔH_{solv}
821 values are much closer correlated than E_{des}^0 and ΔH_{vap} (Fig. 11).

822 The relationship between E_{des}^0 and ΔH_{solv} shown in Fig. 12 can be understood in the following
823 way. For large non-polar molecules, the free energy cost of entering the aqueous solution is mostly
824 driven by enthalpic changes, because hydrogen bonds need to be disrupted to form a cavity around
825 the molecule (Kronberg, 2016; Valsaraj, 1988b; Brini et al., 2017). The surface energy in that
826 cavity is then driven by the surface energy of pure water and the hydrophobic interactions with the
827 solute (Chandler, 2005). This is then somewhat similar to the situation when the same molecule is
828 adsorbed at the aqueous solution – air interface. Thus, for the larger non-polar molecules, the
829 contribution of the enthalpy of cavity formation can be identified as a dominating factor of the
830 solvation process, which in turn depends on the intermolecular strength between adsorbing



831 molecule and liquid. This, hence, can explain the correlation between E_{des}^0 and ΔH_{solv} for the case
832 of the non-polar molecules.

833 For small non-polar molecules, the transfer to the aqueous phase is mostly entropy-driven,
834 because the hydrogen bonds do not need to be disrupted but need to reorganize around the solute
835 (Kronberg, 2016; Shinoda, 1992, 1977; Hvidt, 1983; Brini et al., 2017). Polar molecules would be
836 comparable to ions, but also in this case, the size and charge distribution determine the cost of
837 solvation through the number and strength of hydrogen bonds to water, which lead to a correlation
838 of and ΔH_{solv} with the number of hydrophilic groups. The latter also determine E_{des}^0 (i.e., $O:C$
839 correlates with μ). Among the small organic molecules contained in Fig. 12, with the increasing
840 presence of hydrophilic functional groups, the larger $O:C$ ratios lead to larger E_{des}^0 . For these
841 reasons, the relationship between E_{des}^0 and ΔH_{solv} shown in Fig. 12 supports the specific and
842 physical interaction model at the aqueous solution – air interface mentioned above: E_{des}^0 scales
843 with the magnitude of hydrophobic interactions for non-polar molecules and with the presence of
844 hydrophilic functional groups (i.e., $O:C$ correlates with μ) for polar molecules, and thus the
845 correlation with ΔH_{solv} is a logical consequence.

846 Note that since both E_{des}^0 and ΔH_{solv} are correlated, and are mostly independent of temperature
847 (Hildebrand and Scott, 1964) within the idealized concept presented here, the temperature
848 dependence of τ_{des} may apparently dominate the temperature dependence of solvation when
849 $E_{\text{des}}^0 > \Delta H_{\text{solv}}$. This idea of parallel behavior of desorption and solvation is also supported by a
850 very recent experimental study that provides in situ measurements of the uptake of gas-phase water
851 into ionic liquids at the gas-liquid interface using ambient pressure X-ray photoelectron
852 spectroscopy (Broderick et al., 2019). These measurements indicate that, dependent on water mole
853 fraction and temperature, solvation is governed by similar thermodynamics as relevant for crossing



854 the gas-liquid interface during the mass-transfer process (Broderick et al., 2019). The positive
855 correlation between the E_{des}^0 and ΔH_{solv} values displayed in Fig. 12 supports this notion, ascribing
856 the molecular interactions controlling τ_{des} and solvation an important role in the molecular
857 understanding of gas-substrate interactions.

858

859 **6. Atmospheric Implications**

860 The discussion in the above sections demonstrated the importance of accurate knowledge of E_{des}^0
861 for the representation of multiphase chemical reactions across various environmental interfaces
862 and phase states including aerosol particles. Analyses of experimentally conducted multiphase
863 chemical kinetics studies as well modeling the detailed processes that lead to the physicochemical
864 transformation of particles and define their atmospheric fate will greatly benefit from improved
865 estimates of E_{des}^0 (Su et al., 2020; Zheng et al., 2020; Shiraiwa et al., 2017b; Shiraiwa et al., 2017c;
866 Shrivastava et al., 2017b; Shrivastava et al., 2017a; Li and Knopf, 2021; Kaiser et al., 2011;
867 Springmann et al., 2009; Mu et al., 2018; Hems et al., 2021; Laskin et al., 2015). Below we discuss
868 further relevant atmospheric chemistry processes that connect to and/or make use of E_{des}^0 including
869 gas-particle partitioning, secondary organic aerosol (SOA) formation, indoor air chemistry, and
870 glass transition of OA particles.

871 **Gas-Particle Partitioning.** Organic aerosol is ubiquitous, consists of numerous chemical
872 species, and represents a large mass fraction (20–90%) of the total submicron particles in the
873 troposphere (Nizkorodov et al., 2011; Jimenez et al., 2009; Hallquist et al., 2009; Kanakidou et
874 al., 2005). The formation of SOA proceeds by complex pathways including reaction and mass
875 transport in the gas and condensed phases. The equilibration timescale for gas-particle partitioning
876 for SOA particles of varying viscosity has been evaluated (Shiraiwa and Seinfeld, 2012;



877 Berkemeier et al., 2020; Schervish and Shiraiwa, 2023; Li and Shiraiwa, 2019). In some of those
878 modeling studies a fixed $\tau_{\text{des}} = 10^{-9}$ s, which corresponds to about $E_{\text{des}}^0 = 22$ kJ mol⁻¹ at 293 K,
879 was applied. The simulation results shown in Fig. 5, however, demonstrated that we can expect
880 significant changes in condensed phase equilibration times for gas-particle partitioning when E_{des}^0
881 and temperature change. Our tabulated data suggests that oxygenated VOCs will exert larger E_{des}^0
882 and, as such, longer τ_{des} .

883 It has been shown that SOA oxidation products with a variety of functional groups fall into
884 molecular corridors characterized by a tight inverse correlation between volatility (or saturation
885 mass concentration, C_0) and molar mass as depicted in Fig. 13 (Li et al., 2016; Shiraiwa et al.,
886 2014). They are constrained by two boundary lines corresponding to the volatility of n-alkanes
887 C_nH_{2n+2} and sugar alcohols $C_nH_{2n+2}O_n$, which we now identify as “van der Waals” and “hydrogen-
888 bonding” dominated boundaries. This interpretation can be understood by the governing
889 intermolecular forces. For example, using the EVAPORATION model (Compernelle et al., 2011),
890 the vapor pressures for alkane, ketone, alcohol, and acid with a molecular weight of about 142 g
891 mol⁻¹ at 298 K yield: $p^0(C_{10}H_{22}) = 1.73$ hPa, $p^0(H_7C_3C(O)C_5H_{11}) = 0.084$ hPa, $p^0(C_9H_{19}OH) =$
892 0.023 hPa, and $p^0(C_7H_{15}COOH) = 1.62 \times 10^{-3}$ hPa, respectively. The decrease of about three orders
893 of magnitude in the vapor pressure between the alkane and the carboxylic acid is mainly due to
894 two carboxylic acid molecules forming hydrogen bonds, resulting in a dimer. A highly-oxidized
895 amide having ketone and alcohol groups such as $N=CC(O)C(O)C(O)CO$ and $M = 149.146$ g mol⁻¹
896 has $p^0 = 8.93 \times 10^{-7}$ hPa. This is due to the fact that this molecule not only establishes the van der
897 Waals forces such as London dispersion and Keesom forces but also hydrogen bonding with three
898 hydrogen bond donors and multiple hydrogen bond acceptors. As can be seen in Fig. 13, the change
899 in C_0 derived from decane to C_0 of the highly-oxidized amide spans the identified molecular



900 corridor around $M = 145 \text{ g mol}^{-1}$, indicating that the van der Waals forces and the number of
901 hydrogen bonds that can be established by a particular molecule may fundamentally describe the
902 volatility range of the organic species.

903 Keeping this approach in mind, we can ask: what are the extreme limits of the saturation mass
904 concentration? The smallest organic molecule is methane, only prone to London dispersion forces.
905 $p^0(\text{CH}_4) = 46000 \text{ hPa}$ with $\log_{10}(C_0) = 10.5$, which corresponds to the upper bound of the
906 molecular corridor. Ammonia (NH_3) has a similar molar mass as CH_4 but has lower vapor pressure,
907 because NH_3 can establish two hydrogen bonds. N_2O_5 does not form hydrogen bonds and locates
908 above the alkane line. The lower bound of the molecular corridor is mainly defined by the
909 molecule's permanent dipole moments and number of hydrogen bonds it can entertain. Clearly,
910 these attributes are likely to be found in larger and highly-oxidized compounds. Water constitutes
911 a peculiarity when looking at its position in the $C_0 - M$ framework depicted in Fig. 13. There is no
912 other molecule with this small size that can form four hydrogen bonds. Sulfuric acid (H_2SO_4) can
913 also form four hydrogen bonds and locates close to the lower bound of the molecular corridor. As
914 molecules become larger, there are steric hindrances that likely inhibit stronger intermolecular
915 bonding, whereas water with its small size is ideal. This reason may ultimately limit the lower
916 bound of the molecular corridor and thus the lowest volatilities experienced by OA species.

917 As we have discussed above, E_{des}^0 and ΔH_{vap} are positively correlated and E_{des}^0 in most cases
918 is larger than ΔH_{vap} (Fig. 11). Also, we found that gas species with higher $O:C$, and thus larger μ ,
919 exhibit larger E_{des}^0 values. This indicates that intermolecular interactions at the interface are as
920 important as in the condensed phase of the adsorbate alone (Valsaraj, 2009, 1988b). We expect
921 this also to hold for the case of SOA formation. It is generally observed that the composition of
922 the organic matrix, barring any mass-transport limitations, has little influence on the gas-particle



923 partitioning equilibrium (Donahue et al., 2012; Donahue et al., 2011). Oxygenated VOCs have
924 higher $O:C$ and larger μ . Saturation vapor pressure or volatility provides guidance in this regard
925 (Epstein et al., 2010), however, our study suggests that considering desorption, i.e., E_{des}^0 values,
926 can impact equilibrium times of gas-particle partitioning as outlined in the gas uptake multilayer
927 model simulations discussed in section 4.

928 Figure 13A shows that the compiled data sets fall within the $C_0 - M$ framework. In comparison,
929 Fig. 13B shows the distribution of SOA oxidation products (916 different species) in the $C_0 - M$
930 space evaluated previously by Shiraiwa et al. (2014). Since the gas species discussed in this work
931 cover a similar C_0 and M range as the SOA oxidation products, we can apply the parameterization
932 of E_{des}^0 to provide estimates of E_{des}^0 for gas species typically involved in SOA gas-particle
933 partitioning. This will allow a more detailed understanding and prediction of SOA formation, in
934 particular for temperatures typically encountered in the troposphere during transport.

935 We derive E_{des}^0 of SOA oxidation products by application of Eq. (14). Since we know the
936 molecular structure of the SOA oxidation products, we can calculate polarizability using the
937 equation provided by Bosque and Sales (2002), instead of using Eq. (15):

$$938 \quad \alpha = 1.51\#C + 0.17\#H + 0.57\#O + 1.05\#N + 2.99\#S + 2.48\#P + 0.22\#F + \\ 939 \quad 2.16\#Cl + 3.29\#Br + 5.45\#I + 0.32, \quad (20)$$

940 where $\#C$, $\#H$, $\#O$, $\#N$, $\#S$, $\#P$, $\#F$, $\#Cl$, $\#Br$, and $\#I$ represent the respective numbers of atoms in
941 the molecule.

942 Figure 14 displays E_{des}^0 values for the data set of SOA oxidation products as a function of
943 molar mass and its dependence on $O:C$ and polarizability. Figures S6 provides the same analysis
944 using parameterization Eq. (16). For the majority of data points the predicted E_{des}^0 values are within
945 $\pm 10\%$ of the values shown in Fig. 14 and within the expected general uncertainty of E_{des}^0 as



946 discussed above. Figure 14A demonstrates the impact of $O:C$ on E_{des}^0 , where alkanes, constituting
947 the upper bound in the molecular corridor, have the lowest E_{des}^0 for a given molar mass. With
948 increasing molecule $O:C$, E_{des}^0 increases as expected from our previous analyses and discussions.
949 The largest impact of molecule $O:C$ is at smallest molar masses. Figure 14B corroborates the
950 strong correlation between molar mass and polarizability. Figure S6 depicts a tighter correlation
951 of E_{des}^0 with molar mass and polarizability due to the linear representation of polarizability (Eq.
952 (15)). Estimates of E_{des}^0 for these SOA oxidation products will allow refinement of gas-particle
953 partitioning time scales, specifically when temperature changes are considered as outlined in our
954 example shown in Fig. 5.

955 Gas-particle partitioning plays an important role in chemical transport models, which describe
956 the long-distance transport and chemical degradation of atmospheric constituents. In these models,
957 gas-particle partitioning is often treated with instantaneous-equilibration approaches. Desorption
958 lifetimes crucially determine the position of partitioning steady states and thus affect chemical
959 degradation rates. Moreover, they have a significant influence on the validity of the instantaneous-
960 equilibration assumption (Wilson et al., 2021; Stolzenburg et al., 2018).

961 Adsorption and desorption processes of semi-volatile species are important in indoor
962 environments, as large surface area-to-volume ratios indoors favor heterogeneous interactions. The
963 deposition of semi-volatile organic compounds on impermeable indoor surfaces can lead to the
964 formation of thin organic films (Weschler and Nazaroff, 2017). The desorption lifetime is a critical
965 parameter for the initial film formation via multi-layer adsorption and the subsequent film growth
966 (Lakey et al., 2021). These surface films act as reservoirs of semivolatile compounds and also
967 serve as reaction media, affecting indoor air composition (Wang et al., 2020; Lakey et al., 2023).



968 **Glass Transition.** Molecular corridors yield also significant insight into particle phase state
969 and viscosity. The glass transition temperature (T_g) characterizes the non-equilibrium phase
970 change from a glassy solid state to a more pliable semi-solid state upon an increase of temperature
971 or humidity (Koop et al., 2011). *Shiraiwa et al.* (2017a) has predicted T_g of SOA oxidation
972 products, showing that T_g depends primarily on the molar mass and secondarily on the $O:C$ ratio.
973 Organic compounds with greater molar mass and lower volatility have higher T_g , indicating that
974 these compounds adopt an amorphous (semi-) solid phase with higher viscosity. For weakly
975 functionalized compounds, the trend in viscosity sensitivity to functional group addition is reported
976 to be carboxylic acid (COOH) \approx hydroxyl (OH) $>$ nitrate (ONO₂) $>$ carbonyl (CO) \approx ester (COO)
977 $>$ methylene (CH₂) (Rothfuss and Petters, 2017). It has been demonstrated that on average the
978 addition of one OH group increases the viscosity by a factor of approximately 22 to 45 (Grayson
979 et al., 2017). These studies imply that hydrogen bonding may play an important role in determining
980 viscosity, which is consistent with its role in influencing glass transition temperatures (Nakanishi
981 and Nozaki, 2011; van der Sman, 2013).

982 Application of our parameterization of E_{des}^0 , we can now construct a relationship between E_{des}^0
983 and T_g of the SOA oxidation products shown in Fig. 14. T_g was derived applying the
984 parameterization presented in (Shiraiwa et al., 2017a) using molecular weight and $O:C$ as input
985 variables. E_{des}^0 was derived applying Eqs. (14) and (20). Figure 15 shows that gas species with
986 lower E_{des}^0 have lower T_g and vice versa. Figure 15A demonstrates that for gas species with same
987 E_{des}^0 , an increase in $O:C$ results in a significant increase of T_g pointing to enhance molecular
988 interaction. Hence, alkanes represent species with lowest T_g at given E_{des}^0 . Figure 15B further
989 corroborates this fact. T_g has a strong dependency on molar mass. However, for the same molar
990 mass, T_g can vary by 100 K (which coincides with only small changes in E_{des}^0), which can now be



991 attributed to the impact of $O:C$. In other words, increased molecular interactions can significantly
992 increase T_g , when other parameters remain the same. Similar trends hold for E_{des}^0 , thereby allowing
993 to recognize a relationship between the amorphous phase state of a system and its E_{des}^0 . Figure S7
994 provides the same analysis of the relationship between E_{des}^0 and T_g of the SOA oxidation products
995 using parameterization Eq. (16) for comparison. We see that without knowing the molecular
996 structure, a tighter correlation between E_{des}^0 and T_g is observed due to the linearization of the gas
997 species' polarizability. Similarly to Figs. 14 and S6, the predicted E_{des}^0 values in Fig. S7 are within
998 $\pm 10\%$ of the values shown in Fig. 15 and within the expected general uncertainty of E_{des}^0 .
999

1000 **Summary and Conclusions**

1001 We have compiled computationally and experimentally derived desorption energy data to
1002 provide estimates of E_{des}^0 for a variety of gas species and solid, liquid, and ice substrates, thereby
1003 covering a range of relevant aerosol particle systems. The desorption energies have been placed in
1004 context with intermolecular forces. We were able to express E_{des}^0 as a function of molecular weight
1005 and $O:C$ ratio only, facilitating the application of the proposed parameterization. The important
1006 role of gas species' polarizability and dipole moment governing E_{des}^0 have been recognized. We
1007 demonstrated the importance of correct E_{des}^0 values for interpretation of multiphase chemical
1008 reactions and gas-particle partitioning, especially when extrapolating laboratory findings to
1009 atmospherically relevant temperature ranges. For example, assessment of chemical aging of
1010 aerosol particles during transport relies on E_{des}^0 values for various atmospheric oxidants.

1011 The compiled literature data allowed us to correlate E_{des}^0 with the enthalpy of vaporization and
1012 solvation, thereby evaluating the role of desorption in these interfacial processes. We identified a



1013 positive correlation between E_{des}^0 and ΔH_{vap} , where E_{des}^0 values are often larger than ΔH_{vap} . For
1014 liquid substrates, we observe a correlation with molecule oxidation state as well, indicating the
1015 importance of intermolecular interactions when looking at interfacial processes.

1016 A positive correlation has been observed between E_{des}^0 and ΔH_{solv} in liquid substrates. This
1017 trend could be related to the gas species' dipole moment and the interfacial interactions among the
1018 adsorbed gas species and molecules in the liquid phase.

1019 We demonstrated the relevance of E_{des}^0 in gas-particle partitioning and its relationship to the
1020 concept of molecular corridors. E_{des}^0 values for many SOA components were derived allowing for
1021 in detail simulation of SOA formation and growth processes. Accurate representation of particle
1022 growth and SOA formation processes requires E_{des}^0 for typically oxygenated VOCs. The relevance
1023 of E_{des}^0 for application in indoor air chemistry has been highlighted. Lastly, we outlined the
1024 correlation of glass transition points with E_{des}^0 which adds another layer of complexity when
1025 modeling multiphase chemical reactions (through the potential of viscous phase states). Our
1026 findings identify the following areas of further research needs:

- 1027 - More adsorption and desorption data for environmentally-relevant interfaces, including
1028 multicomponent aerosol particle surfaces, are needed. Experimental and computational
1029 approaches can yield necessary E_{des}^0 values.
- 1030 - Reporting and application of adsorption and/or desorption data should consider applied
1031 standard states and adsorption models to better constrain E_{des}^0 (Donaldson et al., 2012a;
1032 Savara, 2013; Campbell et al., 2016; Knopf and Ammann, 2021).
- 1033 - Experimental and theoretical multiphase chemical kinetics studies should aim to represent
1034 the typical atmospheric temperature range. This can add to further complications with



1035 regard to the underlying thermodynamics and kinetics in addition to possibly phase state
1036 changes of the substrate (Li and Knopf, 2021; Li et al., 2020; Slade et al., 2017; Knopf et
1037 al., 2005; Davies and Wilson, 2015; Chan et al., 2014; Hearn and Smith, 2007).

1038 - Advancing our understanding of the interfacial processes that govern mass
1039 accommodation, solvation, and vaporization is needed. Adsorption and desorption can play
1040 a role in these processes. However, the degree of how much impact E_{des}^0 has on gas species'
1041 solvation or vaporization depends on its relationship with ΔH_{vap} and ΔH_{solv} . Considering
1042 that aerosol particles are chemically complex and exhibit multiple phases and phase states,
1043 these advances will improve representation of gas-particle partitioning.

1044



1045 **Appendix**

1046 This appendix lists the applied data sets to develop the E_{des}^0 parameterization and to produce
 1047 correlation plots. The parameters given in Tables are also available electronically (Knopf et al.,
 1048 2023).

1049

1050 **Table A1.** Compiled adsorbate-substrate data for water vapor and heavy water vapor adsorbed on
 1051 various mineral and clay substrates, inorganics, organics, and carbonaceous substrates. Gas
 1052 species, gas species' molar mass, substrate, experimental or theoretical method, desorption energy
 1053 (E_{des}^0), and desorption lifetimes (τ_{des}) evaluated at 293 K using $A_{des} = 10^{13} \text{ s}^{-1}$, enthalpy of
 1054 vaporization (ΔH_{vap}), gas species' polarizability (α), gas species' dipole moment (μ), substrate's
 1055 relative permittivity (ϵ_r), and gas species' oxygen to carbon ratio ($O:C$) are given.

Gas Species	Molar Mass / g mol ⁻¹	Substrate	Method	E_{des}^0 / kJ mol ⁻¹	$\tau_{des}^{293 K}$ / s	ΔH_{vap} (T) / kJ mol ⁻¹	α / 10 ⁻²⁴ cm ³	μ / D	ϵ_r	O:C
H ₂ O	18.02	clay: orthic luvisol	VM	9.7 (Sokolowska et al., 1993)	5.4×10 ⁻¹²	44 (Chickos and Acree, 2003)	1.45 (Lide, 2008)	1.85 (Lide, 2008)	2 (Daniels, 2004)	0
H ₂ O	18.02	clay: mollic gleysol	VM	11.2 (Sokolowska et al., 1993)	1.0×10 ⁻¹¹	44 (Chickos and Acree, 2003)	1.45 (Lide, 2008)	1.85 (Lide, 2008)	2 (Daniels, 2004)	0
H ₂ O	18.02	clay: eutric cambisol	VM	13.2 (Sokolowska et al., 1993)	2.3×10 ⁻¹¹	44 (Chickos and Acree, 2003)	1.45 (Lide, 2008)	1.85 (Lide, 2008)	2 (Daniels, 2004)	0
H ₂ O	18.02	clay: stagn. phaeozem	VM	12.8 (Sokolowska et al., 1993)	1.9×10 ⁻¹¹	44 (Chickos and Acree, 2003)	1.45 (Lide, 2008)	1.85 (Lide, 2008)	2 (Daniels, 2004)	0
H ₂ O	18.02	clay: eutric cambisol	VM	12.6 (Sokolowska et al., 1993)	1.7×10 ⁻¹¹	44 (Chickos and Acree, 2003)	1.45 (Lide, 2008)	1.85 (Lide, 2008)	2 (Daniels, 2004)	0
H ₂ O	18.02	kaolinite, si, spc/e	GCMC	21.6 (Croteau et al., 2009)	7.1×10 ⁻¹⁰	44 (Chickos and Acree, 2003)	1.45 (Lide, 2008)	1.85 (Lide, 2008)	5.10 (Leluk et al., 2010)	0
H ₂ O	18.02	kaolinite, al, spc/e	GCMC	46.4 (Croteau et al., 2009)	1.9×10 ⁻⁵	44 (Chickos and Acree, 2003)	1.45 (Lide, 2008)	1.85 (Lide, 2008)	5.10 (Leluk et al., 2010)	0
H ₂ O	18.02	kaolinite, unprotonated edge, spc/e	GCMC	73.5 (Croteau et al., 2009)	1.3	44 (Chickos and Acree, 2003)	1.45 (Lide, 2008)	1.85 (Lide, 2008)	5.10 (Leluk et al., 2010)	0
H ₂ O	18.02	kaolinite, protonated edge, spc/e	GCMC	94.1 (Croteau et al., 2009)	6.0×10 ³	44 (Chickos and Acree, 2003)	1.45 (Lide, 2008)	1.85 (Lide, 2008)	5.10 (Leluk et al., 2010)	0
H ₂ O	18.02	kaolinite (Al)	DRIFTS	56.0 (Budi et al., 2018)	9.6×10 ⁻⁴	44 (Chickos and Acree, 2003)	1.45 (Lide, 2008)	1.85 (Lide, 2008)	5.10 (Leluk et al., 2010)	0
H ₂ O	18.02	kaolinite (Si)	DRIFTS	21.2 (Budi et al., 2018)	6.0×10 ⁻¹⁰	44 (Chickos and Acree, 2003)	1.45 (Lide, 2008)	1.85 (Lide, 2008)	5.10 (Leluk et al., 2010)	0



H ₂ O	18.02	Arizona test dust (0-3 μm)	DRIFTS	53.6	3.6×10 ⁻⁴	44 (Chickos and Acree, 2003)	1.45 (Lide, 2008)	1.85 (Lide, 2008)	5.00 (Sharif, 1995)	0
H ₂ O	18.02	Arizona test dust particles (5-10 μm)	DRIFTS	50.5 (Ibrahim et al., 2018)	1.0×10 ⁻⁴	44 (Chickos and Acree, 2003)	1.45 (Lide, 2008)	1.85 (Lide, 2008)	5.00 (Sharif, 1995)	0
H ₂ O	18.02	Arizona test dust particles (10-20 μm)	DRIFTS	49.5 (Ibrahim et al., 2018)	6.7×10 ⁻⁵	44 (Chickos and Acree, 2003)	1.45 (Lide, 2008)	1.85 (Lide, 2008)	5.00 (Sharif, 1995)	0
H ₂ O	18.02	Arizona test dust particles (20-40 μm)	DRIFTS	48.9 (Ibrahim et al., 2018)	5.2×10 ⁻⁵	44 (Chickos and Acree, 2003)	1.45 (Lide, 2008)	1.85 (Lide, 2008)	5.00 (Sharif, 1995)	0
H ₂ O	18.02	Arizona test dust particles (40-80 μm)	DRIFTS	48.3 (Ibrahim et al., 2018)	4.1×10 ⁻⁵	44 (Chickos and Acree, 2003)	1.45 (Lide, 2008)	1.85 (Lide, 2008)	5.00 (Sharif, 1995)	0
H ₂ O	18.02	NaCl (100)	DFT	40.6 (Meyer et al., 2001)	1.7×10 ⁻⁶	44 (Chickos and Acree, 2003)	1.45 (Lide, 2008)	1.85 (Lide, 2008)	5.9 (Lide, 2008)	0
H ₂ O	18.02	KCl (100)	DFT	32.3 (Meyer et al., 2001)	5.7×10 ⁻⁸	44 (Chickos and Acree, 2003)	1.45 (Lide, 2008)	1.85 (Lide, 2008)	4.86 (Lide, 2008)	0
H ₂ O	18.02	NaCl(001)	FTIR	48.0 (Foster and Ewing, 2000)	3.6×10 ⁻⁵	44 (Chickos and Acree, 2003)	1.45 (Lide, 2008)	1.85 (Lide, 2008)	5.9 (Lide, 2008)	0
H ₂ O	18.02	Al(111)	DFT	56 (Hai et al., 2023)	9.6×10 ⁻⁴	44 (Chickos and Acree, 2003)	1.45 (Lide, 2008)	1.85 (Lide, 2008)		0
H ₂ O	18.02	α-Al ₂ O ₃ (0001, hydroxylated)	TPD	134 (Nelson et al., 1998)	7.7×10 ¹⁰	44 (Chickos and Acree, 2003)	1.45 (Lide, 2008)	1.85 (Lide, 2008)	9.34 (Lide, 2008)	0
H ₂ O	18.02	α-Al ₂ O ₃	FTIR	52.0 (Goodman et al., 2001)	1.9×10 ⁻⁴	44 (Chickos and Acree, 2003)	1.45 (Lide, 2008)	1.85 (Lide, 2008)	9.34 (Lide, 2008)	0
H ₂ O	18.02	SiO ₂	FTIR	50.3(Goodman et al., 2001)	9.3×10 ⁻⁵	44 (Chickos and Acree, 2003)	1.45 (Lide, 2008)	1.85 (Lide, 2008)	4.42 (Lide, 2008)	0
H ₂ O	18.02	TiO ₂	FTIR	54.6(Goodman et al., 2001)	5.4×10 ⁻⁴	44 (Chickos and Acree, 2003)	1.45 (Lide, 2008)	1.85 (Lide, 2008)	86 (Lide, 2008)	0
H ₂ O	18.02	γ-Fe ₂ O ₃	FTIR	53.7(Goodman et al., 2001)	3.7×10 ⁻⁴	44 (Chickos and Acree, 2003)	1.45 (Lide, 2008)	1.85 (Lide, 2008)	4.5 (Lide, 2008)	0
H ₂ O	18.02	CaO	FTIR	49.2(Goodman et al., 2001)	5.9×10 ⁻⁵	44 (Chickos and Acree, 2003)	1.45 (Lide, 2008)	1.85 (Lide, 2008)	11.8 (Lide, 2008)	0
H ₂ O	18.02	MgO	FTIR	50.2(Goodman et al., 2001)	8.9×10 ⁻⁵	44 (Chickos and Acree, 2003)	1.45 (Lide, 2008)	1.85 (Lide, 2008)	9.65 (Lide, 2008)	0
H ₂ O	18.02	NaCl powder	DRIFTS	51.7 (Woodill et al., 2013)	1.6×10 ⁻⁴	44 (Chickos and Acree, 2003)	1.45 (Lide, 2008)	1.85 (Lide, 2008)	5.9 (Lide, 2008)	0
H ₂ O	18.02	catechol coated NaCl	DRIFTS	49.0 (Woodill et al., 2013)	5.4×10 ⁻⁵	44 (Chickos and Acree, 2003)	1.45 (Lide, 2008)	1.85 (Lide, 2008)	~3.52(Kronberger and Weiss, 1944)	0
H ₂ O	18.02	catechol coated NaCl + O ₃	DRIFTS	50.1 (Woodill et al., 2013)	8.4×10 ⁻⁵	44 (Chickos and Acree, 2003)	1.45 (Lide, 2008)	1.85 (Lide, 2008)	~3.52(Kronberger and	0



									Weiss, 1944)	
H ₂ O	18.02	Al ₂ O ₃ powder	DRIFTS	55.1 (Woodill et al., 2013)	6.6×10 ⁻⁴	44 (Chickos and Acree, 2003)	1.45 (Lide, 2008)	1.85 (Lide, 2008)	9.34 (Lide, 2008)	0
H ₂ O	18.02	catechol coated Al ₂ O ₃	DRIFTS	49.8 (Woodill et al., 2013)	7.5×10 ⁻⁵	44 (Chickos and Acree, 2003)	1.45 (Lide, 2008)	1.85 (Lide, 2008)	~3.52(Kronberger and Weiss, 1944)	0
H ₂ O	18.02	Catechol coated Al ₂ O ₃ + O ₃	DRIFTS	49.8 (Woodill et al., 2013)	7.5×10 ⁻⁵	44 (Chickos and Acree, 2003)	1.45 (Lide, 2008)	1.85 (Lide, 2008)	~3.52(Kronberger and Weiss, 1944)	0
H ₂ O	18.02	CaCO ₃	DFT	80.0 (Budi et al., 2018)	18	44 (Chickos and Acree, 2003)	1.45 (Lide, 2008)	1.85 (Lide, 2008)	8.67 (Lide, 2008)	0
H ₂ O	18.02	CaCO ₃	TPD	79.1 (Dickbreder et al., 2023)	13	44 (Chickos and Acree, 2003)	1.45 (Lide, 2008)	1.85 (Lide, 2008)	8.67 (Lide, 2008)	0
H ₂ O	18.02	CaCO ₃	TPD	106.1 (Dickbreder et al., 2023)	8.2×10 ⁵	44 (Chickos and Acree, 2003)	1.45 (Lide, 2008)	1.85 (Lide, 2008)	8.67 (Lide, 2008)	0
H ₂ O	18.02	SiO ₂	DFT	53.1 (Budi et al., 2018)	2.9×10 ⁻⁴	44 (Chickos and Acree, 2003)	1.45 (Lide, 2008)	1.85 (Lide, 2008)	4.42 (Lide, 2008)	0
H ₂ O	18.02	Au(111)	DFT	10.1 (Meng et al., 2004)	6.3×10 ⁻¹²	44 (Chickos and Acree, 2003)	1.45 (Lide, 2008)	1.85 (Lide, 2008)	6.9 (Shklyarevskii and Pakhomov, 1973)	0
H ₂ O	18.02	Pt(111)	DFT	28.1 (Meng et al., 2004)	1.0×10 ⁻⁸	44 (Chickos and Acree, 2003)	1.45 (Lide, 2008)	1.85 (Lide, 2008)		0
H ₂ O	18.02	Pd(111)	DFT	29.3 (Meng et al., 2004)	1.7×10 ⁻⁸	44 (Chickos and Acree, 2003)	1.45 (Lide, 2008)	1.85 (Lide, 2008)		0
H ₂ O	18.02	Ru(0001)	DFT	39.5 (Meng et al., 2004)	1.1×10 ⁻⁶	44 (Chickos and Acree, 2003)	1.45 (Lide, 2008)	1.85 (Lide, 2008)		0
H ₂ O	18.02	Rh(111)	DFT	39.4 (Meng et al., 2004)	1.1×10 ⁻⁶	44 (Chickos and Acree, 2003)	1.45 (Lide, 2008)	1.85 (Lide, 2008)		0
H ₂ O	18.02	steel	KU	60.4 (Koch et al., 1997)	5.9×10 ⁻³	44 (Chickos and Acree, 2003)	1.45 (Lide, 2008)	1.85 (Lide, 2008)		0
H ₂ O	18.02	pyrex Glass	KU	56.1 (Koch et al., 1997)	1.0×10 ⁻³	44 (Chickos and Acree, 2003)	1.45 (Lide, 2008)	1.85 (Lide, 2008)	5.0 (Lide, 2008)	0
H ₂ O	18.02	SAM-acid	TPD	45.2 (Dubois et al., 1990)	1.1×10 ⁻⁵	44 (Chickos and Acree, 2003)	1.45 (Lide, 2008)	1.85 (Lide, 2008)	4.1 (Millany and Jonscher, 1980)	0
H ₂ O	18.02	SAM-methyl	TPD	35.1 (Dubois et al., 1990)	1.8×10 ⁻⁷	44 (Chickos and Acree, 2003)	1.45 (Lide, 2008)	1.85 (Lide, 2008)	2.1 (Akkerman et al., 2007; Rampi et al., 1998)	0



H ₂ O	18.02	SAM-alcohol	TPD	39.3 (Dubois et al., 1990)	1.0×10 ⁻⁶	44 (Chickos and Acree, 2003)	1.45 (Lide, 2008)	1.85 (Lide, 2008)		0
H ₂ O	18.02	SAM-amide	TPD	38.5 (Dubois et al., 1990)	7.3×10 ⁻⁷	44 (Chickos and Acree, 2003)	1.45 (Lide, 2008)	1.85 (Lide, 2008)	2 (Romane r et al., 2008)	0
H ₂ O	18.02	SAM-ester	TPD	37.2 (Dubois et al., 1990)	4.3×10 ⁻⁷	44 (Chickos and Acree, 2003)	1.45 (Lide, 2008)	1.85 (Lide, 2008)		0
H ₂ O	18.02	HOPG	TDS	37.2 (Ulbricht et al., 2006)	4.3×10 ⁻⁷	44 (Chickos and Acree, 2003)	1.45 (Lide, 2008)	1.85 (Lide, 2008)	13 (Dovbesh ko et al., 2015)	0
H ₂ O	18.02	graphene	CCSD(T)	13.0 (Voloshina et al., 2011)	1.6×10 ⁻⁵	44 (Chickos and Acree, 2003)	1.45 (Lide, 2008)	1.85 (Lide, 2008)	13 (Dovbesh ko et al., 2015)	0
H ₂ O	18.02	graphene	DFT	12.5 (Liang et al., 2021)	1.7×10 ⁻¹¹	44 (Chickos and Acree, 2003)	1.45 (Lide, 2008)	1.85 (Lide, 2008)	13 (Dovbesh ko et al., 2015)	0
H ₂ O	18.02	graphene, Stone-Wales	DFT	13.5 (Liang et al., 2021)	2.6×10 ⁻¹¹	44 (Chickos and Acree, 2003)	1.45 (Lide, 2008)	1.85 (Lide, 2008)	13 (Dovbesh ko et al., 2015)	0
H ₂ O	18.02	graphene, single vacancy defect	DFT	51.1 (Liang et al., 2021)	1.3×10 ⁻⁴	44 (Chickos and Acree, 2003)	1.45 (Lide, 2008)	1.85 (Lide, 2008)	13 (Dovbesh ko et al., 2015)	0
H ₂ O	18.02	graphene, double vacancy defect	DFT	15.4 (Liang et al., 2021)	5.6×10 ⁻¹¹	44 (Chickos and Acree, 2003)	1.45 (Lide, 2008)	1.85 (Lide, 2008)	13 (Dovbesh ko et al., 2015)	0
H ₂ O	18.02	grey Soot	KU	29.3 (Alcala-Jornod et al., 2002)	1.7×10 ⁻⁸	44 (Chickos and Acree, 2003)	1.45 (Lide, 2008)	1.85 (Lide, 2008)	13 (Dovbesh ko et al., 2015)	0
H ₂ O	18.02	black Soot	KU	37.7 (Alcala-Jornod et al., 2002)	5.3×10 ⁻⁷	44 (Chickos and Acree, 2003)	1.45 (Lide, 2008)	1.85 (Lide, 2008)	13 (Dovbesh ko et al., 2015)	0
H ₂ O	18.02	soot-OH	DFT	18.0 (Collignon et al., 2005)	1.6×10 ⁻¹⁰	44 (Chickos and Acree, 2003)	1.45 (Lide, 2008)	1.85 (Lide, 2008)	~13 (Dovbesh ko et al., 2015)	0
H ₂ O	18.02	soot-COOH	DFT	38.4 (Collignon et al., 2005)	7.0×10 ⁻⁷	44 (Chickos and Acree, 2003)	1.45 (Lide, 2008)	1.85 (Lide, 2008)	~13 (Dovbesh ko et al., 2015)	0
H ₂ O	18.02	benzo[a]pyrene/soot	KU	50.0 (Pöschl et al., 2001)	8.2×10 ⁻⁵	44 (Chickos and Acree, 2003)	1.45 (Lide, 2008)	1.87 (Townes and Schawlow, 1975)	3.52 (Kro nberger and Weiss, 1944)	0
D ₂ O	20.03	SAM-methyl	TPD	34.0 (Grimm et al., 2008)	1.2×10 ⁻⁷	45.14 (Crabtree and Siman-Tov, 1993)	1.26 (Lide, 2008)	1.87 (Townes and Schawlow, 1975)	2.1 (Akkerman et al., 2007;	0



								ow, 1975)	Rampi et al., 1998)	
D ₂ O	20.03	SAM-COOH	TPD	50.0 (Grimm et al., 2008)	8.2×10 ⁻⁵	45.14 (Crabtree and Siman- Tov, 1993)	1.26 (Lide, 2008)	1.87 (Townes and Schawl ow, 1975)	4.1 (Millany and Jonscher , 1980)	0
D ₂ O	20.03	uncoated glass	TPD	50.0 (Moussa et al., 2009)	8.2×10 ⁻⁵	45.14 (Crabtree and Siman- Tov, 1993)	1.26 (Lide, 2008)	1.87 (Townes and Schawl ow, 1975)	4.42 (Lide, 2008)	0
D ₂ O	20.03	C18-SAM	TPD	36.0 (Moussa et al., 2009)	2.6×10 ⁻⁷	45.14 (Crabtree and Siman- Tov, 1993)	1.26 (Lide, 2008)	1.87 (Townes and Schawl ow, 1975)	2.1 (Akkerma n et al., 2007; Rampi et al., 1998)	0
D ₂ O	20.03	C8-SAM	TPD	40.0 (Moussa et al., 2009)	1.4×10 ⁻⁶	45.14 (Crabtree and Siman- Tov, 1993)	1.26 (Lide, 2008)	1.87 (Townes and Schawl ow, 1975)	2.03 (Crossley , 1973)	0
D ₂ O	20.03	KMnO ₄ , O ₃ oxidized SAM	TPD	44.0 (Moussa et al., 2009)	7.0×10 ⁻⁶	45.14 (Crabtree and Siman- Tov, 1993)	1.26 (Lide, 2008)	1.87 (Townes and Schawl ow, 1975)	~4.1 (Millany and Jonscher , 1980)	0
D ₂ O	20.03	methanol on HOPG	MB	45.3 (Thomson et al., 2011)	1.2×10 ⁻⁵	45.14 (Crabtree and Siman- Tov, 1993)	1.26 (Lide, 2008)	1.87 (Townes and Schawl ow, 1975)		0
D ₂ O	20.03	solid butanol	MB	27.0 (Johansson et al., 2019)	6.5×10 ⁻⁹	45.14 (Crabtree and Siman- Tov, 1993)	1.26 (Lide, 2008)	1.87 (Townes and Schawl ow, 1975)	17.84* (Lide, 2008)	0
D ₂ O	20.03	solid acetic acid	DFT	19.0 (Allouche and Bahr, 2006)	2.4×10 ⁻¹⁰	45.14 (Crabtree and Siman- Tov, 1993)	1.26 (Lide, 2008)	1.87 (Townes and Schawl ow, 1975)	6.2* (Lide, 2008)	0
D ₂ O	20.03	solid nopinone	MB	26.0 (Johansson et al., 2020)	4.3×10 ⁻⁹	45.14 (Crabtree and Siman- Tov, 1993)	1.26 (Lide, 2008)	1.87 (Townes and Schawl ow, 1975)		0
D ₂ O	20.03	nitric acid monolayer	MB	49.2 (Thomson et al., 2015)	5.9×10 ⁻⁵	45.14 (Crabtree and Siman- Tov, 1993)	1.26 (Lide, 2008)	1.87 (Townes and Schawl ow, 1975)		0



1056 *Applied the value for liquid phase of substrate species.

1057

1058 **Table A2.** Compiled adsorbate-substrate interaction energies for reactive gases on solid substrates.
 1059 Gas species, gas species' molar mass, substrate, experimental or theoretical method, desorption
 1060 energy (E_{des}^0), and desorption lifetimes (τ_{des}) evaluated at 293 K using $A_{des} = 10^{13} \text{ s}^{-1}$, enthalpy
 1061 of vaporization (ΔH_{vap}), gas species' polarizability (α), gas species' dipole moment (μ),
 1062 substrate's relative permittivity (ϵ_r), and gas species' oxygen to carbon ration ($O:C$) are given.

Gas Species	Molar Mass / g mol ⁻¹	Substrate	Method	E_{des}^0 / kJ mol ⁻¹	$\tau_{des}^{293 K}$ / s	ΔH_{vap} (T) / kJ mol ⁻¹	α / 10 ⁻²⁴ cm ³	μ / D	ϵ_r	O:C
OH	17.01	Al ₂ O ₃	MC	47.5 (Remorov and Bardwell, 2005)	2.9×10 ⁻⁵		7.11 (Zen et al., 2014)	1.65 (Lide, 2008)	9.34 (Lide, 2008)	0
OH	17.01	NaCl	MC	42.7 (Remorov and Bardwell, 2005)	4.1×10 ⁻⁶		7.11 (Zen et al., 2014)	1.65 (Lide, 2008)	5.90 (Lide, 2008)	0
OH	17.01	NH ₄ NO ₃	MC	42.7 (Remorov and Bardwell, 2005)	4.1×10 ⁻⁶		7.11 (Zen et al., 2014)	1.65 (Lide, 2008)	10.70 (Lide, 2008)	0
OH	17.01	NH ₄ HSO ₄	MC	41 (Remorov and Bardwell, 2005)	2.0×10 ⁻⁶		7.11 (Zen et al., 2014)	1.65 (Lide, 2008)	165 (Lide, 2008)	0
OH	17.01	(NH ₄) ₂ SO ₄	MC	43.1 (Remorov and Bardwell, 2005)	4.8×10 ⁻⁶		7.11 (Zen et al., 2014)	1.65 (Lide, 2008)	10 (Lide, 2008)	0
OH	17.01	Ni(100)	ECT	292.9 ^s (Yang and Whitten, 1997)	1.6×10 ³⁹		7.11 (Zen et al., 2014)	1.65 (Lide, 2008)		0
OH	17.01	Ni(111)	ECT	309.6 ^s (Yang and Whitten, 1997)	1.6×10 ⁴²		7.11 (Zen et al., 2014)	1.65 (Lide, 2008)		0
OH	17.01	Fe(110)	ECT	284.5 ^s (Yang and Whitten, 1997)	5.3×10 ³⁷		7.11 (Zen et al., 2014)	1.65 (Lide, 2008)		0
OH	17.01	Ag(110)	DAM	415.9 ^s (Hu and Nakatsuji, 1999)	1.4×10 ⁶¹		7.11 (Zen et al., 2014)	1.65 (Lide, 2008)		0
OH	17.01	Triacontane (solid)	KU	12.7 (Li and	1.8×10 ⁻¹¹		7.11 (Zen et al., 2014)	1.65 (Lide, 2008)	1.91* (Lide, 2008)	0



				Knopf, 2021)						
NO ₃	62.00	oleic acid (monolayer)	K2-SURF	27.8 (Sebastiani et al., 2018)	9.0×10 ⁻⁹		5.15 (Alkorta et al., 2022)		2.34 (Lide, 2008)	0
NO ₃	62.00	palmitoleic acid (monolayer)	K2-SURF	29.5 (Sebastiani et al., 2018)	1.8×10 ⁻⁸		5.15 (Alkorta et al., 2022)		2.34 (Lide, 2008)	0
NO ₃	62.00	methyl oleate (monolayer)	K2-SURF	27.8 (Sebastiani et al., 2018)	9.0×10 ⁻⁹		5.15 (Alkorta et al., 2022)		3.21 (Lide, 2008)	0
NO ₃	62.00	stearic acid (monolayer)	K2-SURF	29.8 (Sebastiani et al., 2018)	2.1×10 ⁻⁸		5.15 (Alkorta et al., 2022)		2.31 (Lide, 2008)	0
O ₃	48.00	BaP/soot	KU	85 (Pöschl et al., 2001)	1.4×10 ²	12.2 (Stull, 1947)	3.21 (Lide, 2008)	0.53 (Mack and Muentner, 1977)	3.52 (Kronberger and Weiss, 1944)	0
O ₃	48.00	graphene, physisorption	DFT	24.1 (Lee et al., 2009)	2.0×10 ⁻⁹	12.2 (Stull, 1947)	3.21 (Lide, 2008)	0.53 (Mack and Muentner, 1977)	13 (Dovbeshko et al., 2015)	0
O ₃	48.00	graphene, chemisorption	DFT	31.8 (Lee et al., 2009)	4.7×10 ⁻⁸	12.2 (Stull, 1947)	3.21 (Lide, 2008)	0.53 (Mack and Muentner, 1977)	13 (Dovbeshko et al., 2015)	0
O, ROI	16.00	BaP/soot	K2-SURF	40 (Shiraiwa et al., 2011b)	1.4×10 ⁻⁶		0.79 (van Duijnen and Swart, 1998; Cambi et al., 1991)		3.52 (Kronberger and Weiss, 1944)	0
O ₂	32.00	Ir(100)	DFT	187 [§] (Cao et al., 2022)	2.2×10 ²⁰					0

1063

1064 [§]Not applied in analysis.

1065 * Applied value for the liquid phase of substrate species.

1066

1067 **Table A3.** Compiled adsorbate-substrate interaction energies for reactive and non-reactive gases
 1068 on soot of light duty vehicle (LDV) and heavy-duty vehicle (HDV), pyrex glass, steel, salt, mineral,
 1069 clay, and highly oriented pyrolyzed graphite (HOPG). Gas species, gas species' molar mass,
 1070 substrate, experimental or theoretical method, desorption energy (E_{des}^0), and desorption lifetimes
 1071 (τ_{des}) evaluated at 293 K using $A_{des} = 10^{13} \text{ s}^{-1}$, enthalpy of vaporization (ΔH_{vap}), gas species'



1072 polarizability (α), gas species' dipole moment (μ), substrate's relative permittivity (ϵ_r), and gas
 1073 species' oxygen to carbon ration ($O:C$) are given.

Gas Species	Molar Mass / g mol ⁻¹	Substrate	Method	E_{des}^0 / kJ mol ⁻¹	$\tau_{des}^{293 K}$ / s	$\Delta H_{vap}(T)$ / kJ mol ⁻¹	α / 10 ⁻²⁴ cm ³	μ / D	ϵ_r	O:C
NO ₂	46.01	soot LDV	KU	54.7 (Messerer et al., 2006)	5.6×10 ⁻⁴	18.89	3.02 (Lide, 2008)	0.316 (Lide, 2008)	~13.00 (Dovbeshko et al., 2015)	0
NO ₂	46.01	soot HDV	KU	37.6 (Messerer et al., 2007)	5.0×10 ⁻⁷	18.89	3.02 (Lide, 2008)	0.316 (Lide, 2008)	~13.00 (Dovbeshko et al., 2015)	0
NO ₂	46.01	NH ₄ Cl	KU	34 (Takenaka and Rossi, 2005)	1.2×10 ⁻⁷	18.89	3.02 (Lide, 2008)	0.316 (Lide, 2008)	6.90 (Lide, 2008)	0
NO ₂	46.01	HOPG	TDS	37 (Ulbricht et al., 2006)	3.9×10 ⁻⁷	18.89	3.02 (Lide, 2008)	0.316 (Lide, 2008)	13.00 (Dovbeshko et al., 2015)	0
NO ₂	46.01	HOPG	TDS	33 (Ulbricht et al., 2006)	7.6×10 ⁻⁸	18.89	3.02 (Lide, 2008)	0.316 (Lide, 2008)	13.00 (Dovbeshko et al., 2015)	0
NO ₂	46.01	Model coal surface	DFT	12.04 (Wang et al., 2021)	1.4×10 ⁻¹¹	18.89	3.02 (Lide, 2008)	0.316 (Lide, 2008)	13.00 (Dovbeshko et al., 2015)	0
HCl	36.46	pyrex glass	KU	56.7 (Koch et al., 1997)	1.3×10 ⁻³	16.15 (Lide, 2008)	2.7 (Lide, 2008)	1.11 (Lide, 2008)	5.00 (Lide, 2008)	0
HCl	36.46	steel	KU	57.4 (Koch et al., 1997)	1.7×10 ⁻³	16.15 (Lide, 2008)	2.7 (Lide, 2008)	1.11 (Lide, 2008)		0
HCl	36.46	α -Al ₂ O ₃ (0001)	TPD	105 (Nelson et al., 2001)	5.2×10 ⁵	16.15 (Lide, 2008)	2.63 (Lide, 2008)	1.11 (Lide, 2008)	9.34 (Lide, 2008)	0
CO ₂	44.01	graphene	TPD	26.1 (Smith and Kay, 2019)	4.5×10 ⁻⁹	16.4 (Chickos and Acree, 2003)	2.91 (Lide, 2008)	0.0001 (Kolomiitsova et al., 2000)	13.00 (Dovbeshko et al., 2015)	2
CO ₂	44.01	HOPG	TDS	24 (Ulbricht et al., 2006)	1.9×10 ⁻⁹	16.4 (Chickos and Acree, 2003)	2.91 (Lide, 2008)	0.0001 (Kolomiitsova et al., 2000)	13.00 (Dovbeshko et al., 2015)	2
CO ₂	44.01	HOPG	TDS	23 (Ulbricht et al., 2006)	1.3×10 ⁻⁹	16.4 (Chickos and Acree, 2003)	2.91 (Lide, 2008)	0.0001 (Kolomiitsova et al., 2000)	13.00 (Dovbeshko et al., 2015)	2
CO ₂	44.01	Calcite	DFT	29.9 (Budi et al., 2018)	2.1×10 ⁻⁸	16.4 (Chickos and Acree, 2003)	2.91 (Lide, 2008)	0.0001 (Kolomiitsova et al., 2000)	8.67 (Lide, 2008)	2
CO ₂	44.01	Quartz	DFT	6.8 (Budi et al., 2018)	1.6×10 ⁻¹²	16.4 (Chickos and Acree, 2003)	2.91 (Lide, 2008)	0.0001 (Kolomiitsova et al., 2000)	4.42 (Lide, 2008)	2



CO ₂	44.01	kaolinite (Al)	DFT	28.9 (Budi et al., 2018)	1.4×10 ⁻⁸	16.4 (Chickos and Acree, 2003)	2.91 (Lide, 2008)	0.0001 (Kolomiitsova et al., 2000)	5.00 (Robinson et al., 2002)	2
CO ₂	44.01	kaolinite (si)	DFT	9.6 (Budi et al., 2018)	5.1×10 ⁻¹²	16.4 (Chickos and Acree, 2003)	2.91 (Lide, 2008)	0.0001 (Kolomiitsova et al., 2000)	5.00 (Robinson et al., 2002)	2
CO	28.01	HOPG	TDS	13 (Ulbricht et al., 2006)	2.1×10 ⁻¹¹	6.0 (Chickos and Acree, 2003)	1.95 (Lide, 2008)	0.122 (Lide, 2008)	13.00 (Dovbeshko et al., 2015)	1
CO	28.01	Au(111)	MB	11.7 (Borodin et al., 2020)	1.2×10 ⁻¹¹	6.0 (Chickos and Acree, 2003)	1.95 (Lide, 2008)	0.122 (Lide, 2008)		1
N ₂	28.01	HOPG	TDS	13 (Ulbricht et al., 2006)	2.1×10 ⁻¹¹	5.57 (Lide, 2008)	1.74 (Lide, 2008)	0.001 (Gustafsson and Andersson, 2006)	13.00 (Dovbeshko et al., 2015)	0
SF ₆	146.06	HOPG	TDS	31 (Ulbricht et al., 2006)	3.4×10 ⁻⁸	8.99 (Lide, 2008)	6.54 (Lide, 2008)	0.08 (Bruska and Piechota, 2008)	13.00 (Dovbeshko et al., 2015)	0
SF ₆	146.06	HOPG	TDS	25 (Ulbricht et al., 2006)	2.9×10 ⁻⁹	8.99 (Lide, 2008)	6.54 (Lide, 2008)	0.08 (Bruska and Piechota, 2008)	13.00 (Dovbeshko et al., 2015)	0
O ₂	32.00	HOPG	TDS	12 (Ulbricht et al., 2006)	1.4×10 ⁻¹¹	6.82 (Lide, 2008)	1.57 (Lide, 2008)	0.002 (on metal) (Gustafsson and Andersson, 2006)	13.00 (Dovbeshko et al., 2015)	0
O ₂	32.00	HOPG	TDS	9 (Ulbricht et al., 2006)	4.0×10 ⁻¹²	6.82 (Lide, 2008)	1.57 (Lide, 2008)	0.002 (on metal) (Gustafsson and Andersson, 2006)	13.00 (Dovbeshko et al., 2015)	0
Xenon	131.29	HOPG	TD	24 (Ulbricht et al., 2006)	1.9×10 ⁻⁹	12.57 (Lide, 2008)	4.04 (Cambiet al., 1991)	0	13.00 (Dovbeshko et al., 2015)	0
Xenon	131.29	HOPG	TD	18 (Ulbricht et al., 2006)	1.6×10 ⁻¹⁰	12.57 (Lide, 2008)	4.04 (Cambiet al., 1991)	0	13.00 (Dovbeshko et al., 2015)	0

1074

1075 **Table A4.** Compiled adsorbate-substrate interaction energies for organic gases on self-assembled
 1076 monolayers, salt, fly ash, and urban aerosol. Gas species, gas species' molar mass, substrate,
 1077 experimental or theoretical method, desorption energy (E_{des}^0), and desorption lifetimes (τ_{des})
 1078 evaluated at 293 K using $A_{des} = 10^{13} \text{ s}^{-1}$, enthalpy of vaporization (ΔH_{vap}), gas species'



1079 polarizability (α), gas species' dipole moment (μ), substrate's relative permittivity (ϵ_r), and gas
 1080 species' oxygen to carbon ration ($O:C$) are given.

Gas Species	Molar Mass / g mol ⁻¹	Substrate	Method	E_{des}^0 / kJ mol ⁻¹	$\tau_{des}^{293 K}$ / s	ΔH_{vap} (T) / kJ mol ⁻¹	α / 10 ⁻²⁴ cm ³	μ / D	ϵ_r	O:C
methanol	32.04	thin nopinone	MB	17.4 (Kong et al., 2021)	1.3×10 ⁻¹⁰	37.8 (Chickos and Acree, 2003)	3.28 (Lide, 2008)	1.7 (Lide, 2008)		1
methanol	32.04	multilayer nopinone	MB	17.4 (Kong et al., 2021)	1.3×10 ⁻¹⁰	37.8 (Chickos and Acree, 2003)	3.28 (Lide, 2008)	1.7 (Lide, 2008)		1
methanol	32.04	SAM-methyl	TPD	47.7 (Dubois et al., 1990)	3.2×10 ⁻⁵	37.8 (Chickos and Acree, 2003)	3.28 (Lide, 2008)	1.7 (Lide, 2008)	4.1 (Millyny and Jonscher, 1980)	1
methanol	32.04	SAM-acid	TPD	35.1 (Dubois et al., 1990)	1.8×10 ⁻⁷	37.8 (Chickos and Acree, 2003)	3.28 (Lide, 2008)	1.7 (Lide, 2008)	2.1 (Akkerman et al., 2007)	1
methanol	32.04	SAM-amide	TPD	41.0 (Dubois et al., 1990)	2.0×10 ⁻⁶	37.8 (Chickos and Acree, 2003)	3.28 (Lide, 2008)	1.7 (Lide, 2008)		1
n-hexane	86.18	SAM-methyl	TPD	38.5 (Dubois et al., 1990)	7.3×10 ⁻⁷	31.5 (Chickos and Acree, 2003)	11.9 (Lide, 2008)	0 (Yaws, 2014)	4.1 (Millyny and Jonscher, 1980)	0
n-hexane	86.18	SAM-acid	TPD	33.9 (Dubois et al., 1990)	1.1×10 ⁻⁷	31.5 (Chickos and Acree, 2003)	11.9 (Lide, 2008)	0 (Yaws, 2014)	2.1 (Akkerman et al., 2007)	0
anthracene	178.23	NaCl	TD	18 (Chu et al., 2010)	1.6×10 ⁻¹⁰	79.6 (Chickos and Acree, 2003)	25.665 (Lide, 2008)	0 (Yaws, 2014)	5.9 (Lide, 2008)	0
pyrene	202.26	NaCl	TD	19.6 (Chu et al., 2010)	3.1×10 ⁻¹⁰	78.6 (Chickos and Acree, 2003)	28.22 (Lide, 2008)	0 (Yaws, 2014)	5.9 (Lide, 2008)	0
benzo(a)pyrene	252.32	NaCl	TD	22.8 (Chu et al., 2010)	1.2×10 ⁻⁹	91 (Chickos and Acree, 2003)	35.8 (McEachran et al., 2018)	0 (Yaws, 2014)	5.9 (Lide, 2008)	0
perylene		NaCl	TD	123.5 (Steiner and Burtscher, 1994)	1.0×10 ⁹	78.6 (Chickos and Acree, 2003)	35.8 (McEachran et al., 2018)	0 (Yaws, 2014)	5.9 (Lide, 2008)	0
phenanthrene	178.23	fly ash	GC	24.3 (Lee and Chen, 1995)	2.2×10 ⁻⁹	78.7 (Chickos and Acree, 2003)	30.75 (Lide, 2008)	0 (Yaws, 2014)	~5 (Sharif, 1995)	0



pyrene	202.26	fly ash	GC	26.6 (Lee and Chen, 1995)	5.5×10^{-9}	78.6 (Chickos and Acree, 2003)	28.22 (Lide, 2008)	0 (Yaws, 2014)	~5 (Sharif, 1995)	0
benzo(a)pyrene	252.33	fly ash	TD	31.2 (Chuet al., 2010)	3.7×10^{-8}	91 (Chickos and Acree, 2003)	35.8 (McEachran et al., 2018)	0 (Yaws, 2014)	~5 (Sharif, 1995)	0
phenanthrene/ anthracene		urban aerosol	TD	18.9 (Yamasaki et al., 1982; Pankow, 1991)	2.3×10^{-10}			0 (Yaws, 2014)		0
pyrene	202.26	urban aerosol	TD	20.4 (Yamasaki et al., 1982; Pankow, 1991)	4.3×10^{-10}	78.6 (Chickos and Acree, 2003)	28.22 (Lide, 2008)	0 (Yaws, 2014)		0
benzo(a)pyrene/ benzo(e)pyrene		urban aerosol	TD	22.3 (Yamasaki et al., 1982; Pankow, 1991)	9.5×10^{-10}			0 (Yaws, 2014)		0
perylene	252.32	carbon	TD	136.5 (Steiner and Burtscher, 1994)	2.2×10^{11}	123.1 (Chickos and Acree, 2003)	35.8 (McEachran et al., 2018)	0 (Yaws, 2014)	13 (Dovbeshko et al., 2015)	0
perylene	252.32	diesel soot	TD	139 (Steiner and Burtscher, 1994)	6.0×10^{11}	123.1 (Chickos and Acree, 2003)	35.8 (McEachran et al., 2018)	0 (Yaws, 2014)	13 (Dovbeshko et al., 2015)	0
perylene	252.32	oil burner soot	TD	140 (Steiner and Burtscher, 1994)	9.1×10^{11}	123.1 (Chickos and Acree, 2003)	35.8 (McEachran et al., 2018)	0 (Yaws, 2014)	13 (Dovbeshko et al., 2015)	0

1081

1082 **Table A5.** Compiled adsorbate-substrate interaction energies of volatile organic compounds
 1083 (VOCs) on graphite (C(0001)), highly oriented pyrolytic graphite (HOPG), granular activated
 1084 carbon (GAC), and soot from combustion of kerosene. Gas species, gas species' molar mass,
 1085 substrate, experimental or theoretical method, desorption energy (E_{des}^0), and desorption lifetimes
 1086 (τ_{des}) evaluated at 293 K using $A_{des} = 10^{13} \text{ s}^{-1}$, enthalpy of vaporization (ΔH_{vap}), gas species'
 1087 polarizability (α), gas species' dipole moment (μ), substrate's relative permittivity (ϵ_r), and gas
 1088 species' oxygen to carbon ration ($O:C$) are given.

Gas Species	Molar Mass / g mol^{-1}	Substrate	Method	$E_{des}^0 / \text{kJ mol}^{-1}$	$\tau_{des}^{293 \text{ K}} / \text{s}$	$\Delta H_{vap} (T) / \text{kJ mol}^{-1}$	$\alpha / 10^{-24} \text{ cm}^3$	μ / D	ϵ_r	O:C
methane	16.04	graphite	TPD	14.1 (Tait et al., 2006)	3.3×10^{-11}	8.5 (Chickos and Acree, 2003)	2.59 (Lide, 2008)	0 (Yaws, 2014)	13.0 (Dovbeshko et al., 2015)	0



ethane	30.07	graphite	TPD	24.6 (Tait et al., 2006)	2.4×10^{-9}	15.3 (Chickos and Acree, 2003)	4.45 (Lide, 2008)	0 (Yaws, 2014)	13.0 (Dovbeshko et al., 2015)	0
propane	44.10	graphite	TPD	32.1 (Tait et al., 2006)	5.3×10^{-8}	18.8 (Chickos and Acree, 2003)	6.33 (Lide, 2008)	0 (Yaws, 2014)	13.0 (Dovbeshko et al., 2015)	0
butane	58.12	graphite	TPD	40.8 (Tait et al., 2006)	1.9×10^{-6}	22.4 (Chickos and Acree, 2003)	8.2 (Lide, 2008)	0 (Yaws, 2014)	13.0 (Dovbeshko et al., 2015)	0
pentane	72.15	graphite	TPD	65 (Paserba and Gellman, 2001)	3.9×10^{-2}	25 (Chickos and Acree, 2003)	9.99 (Lide, 2008)	0 (Yaws, 2014)	13.0 (Dovbeshko et al., 2015)	0
hexane	86.18	graphite	TPD	63 (Tait et al., 2006)	1.7×10^{-2}	31.5 (Chickos and Acree, 2003)	11.9 (Lide, 2008)	0 (Yaws, 2014)	13.0 (Dovbeshko et al., 2015)	0
hexane	86.18	graphite	TPD	73.6 (Paserba and Gellman, 2001)	1.3	31.5 (Chickos and Acree, 2003)	11.9 (Lide, 2008)	0 (Yaws, 2014)	13.0 (Dovbeshko et al., 2015)	0
heptane	100.21	graphite	TPD	81.5 (Paserba and Gellman, 2001)	3.4×10^1	36.6 (Chickos and Acree, 2003)	13.61 (Lide, 2008)	0 (Yaws, 2014)	13.0 (Dovbeshko et al., 2015)	0
octane	114.23	graphite	TPD	72.6 (Tait et al., 2006)	8.8×10^{-1}	41.6 (Chickos and Acree, 2003)	15.9 (Lide, 2008)	0 (Yaws, 2014)	13.0 (Dovbeshko et al., 2015)	0
octane	114.23	graphite	TPD	88.2 (Paserba and Gellman, 2001)	5.3×10^2	41.6 (Chickos and Acree, 2003)	15.9 (Lide, 2008)	0 (Yaws, 2014)	13.0 (Dovbeshko et al., 2015)	0
decane	142.29	graphite	TPD	91.4 (Tait et al., 2006)	2.0×10^3	51.4 (Chickos and Acree, 2003)	19.1 (Lide, 2008)	0 (Yaws, 2014)	13.0 (Dovbeshko et al., 2015)	0
decane	142.29	graphite	TPD	101 (Paserba and Gellman, 2001)	1.0×10^5	51.4 (Chickos and Acree, 2003)	19.1 (Lide, 2008)	0 (Yaws, 2014)	13.0 (Dovbeshko et al., 2015)	0
dodecane	170.33	graphite	TPD	114.8 (Paserba and Gellman, 2001)	2.9×10^7	62.1 (Chickos and Acree, 2003)	22.75 (Lide, 2008)	0 (Yaws, 2014)	13.0 (Dovbeshko et al., 2015)	0
tetradecane	198.39	graphite	TPD	124.7 (Paserba and Gellman, 2001)	1.7×10^9	72.1 (Chickos and Acree, 2003)	26.22 (Laib and Mittleman, 2010)	0 (Yaws, 2014)	13.0 (Dovbeshko et al., 2015)	0



hexadecane	226.41	graphite	TPD	134.3 (Paserba and Gellman, 2001)	8.7×10^{10}	81.4 (Chickos and Acree, 2003)	29.84 (Laib and Mittleman, 2010)	0 (Yaws, 2014)	13.0 (Dovbeshko et al., 2015)	0
octadecane	254.50	graphite	TPD	146.7 (Paserba and Gellman, 2001)	1.4×10^{13}	91.8 (Chickos and Acree, 2003)	33.46 (Laib and Mittleman, 2010)	0 (Yaws, 2014)	13.0 (Dovbeshko et al., 2015)	0
icosane	282.55	graphite	TPD	156.2 (Paserba and Gellman, 2001)	7.0×10^{14}	100 (Chickos and Acree, 2003)	37.08 (Laib and Mittleman, 2010)	0 (Yaws, 2014)	13.0 (Dovbeshko et al., 2015)	0
docosane	310.61	graphite	TPD	166.2 (Paserba and Gellman, 2001)	4.3×10^{16}	115.6 (Chickos and Acree, 2003)	40.7 (Laib and Mittleman, 2010)	0 (Yaws, 2014)	13.0 (Dovbeshko et al., 2015)	0
tetracosane	338.65	graphite	TPD	174.2 (Paserba and Gellman, 2001)	1.1×10^{18}	126.8 (Chickos and Acree, 2003)	44.32 (Laib and Mittleman, 2010)	0 (Yaws, 2014)	13.0 (Dovbeshko et al., 2015)	0
hexacosane	366.71	graphite	TPD	182.3 (Paserba and Gellman, 2001)	3.2×10^{19}	106.1 (Chickos and Acree, 2003)	47.94 (Laib and Mittleman, 2010)	0 (Yaws, 2014)	13.0 (Dovbeshko et al., 2015)	0
octacosane	396.79	graphite	TPD	190.7 (Paserba and Gellman, 2001)	9.9×10^{20}	150.8 (Chickos and Acree, 2003)	51.56 (Laib and Mittleman, 2010)	0 (Yaws, 2014)	13.0 (Dovbeshko et al., 2015)	0
dotriacontane	452.88	graphite	TPD	205.5 (Paserba and Gellman, 2001)	4.3×10^{23}	130.5 (Chickos and Acree, 2003)	58.8 (Laib and Mittleman, 2010)	0 (Yaws, 2014)	13.0 (Dovbeshko et al., 2015)	0
hexatriacontane	506.97	graphite	TPD	219.6 (Paserba and Gellman, 2001)	1.4×10^{26}	157 (Chickos and Acree, 2003)	66.04 (Laib and Mittleman, 2010)	0 (Yaws, 2014)	13.0 (Dovbeshko et al., 2015)	0
tetracontane	563.08	graphite	TPD	232.9 (Paserba and Gellman, 2001)	3.3×10^{28}	132.2 (Chickos and Acree, 2003)	73.28 (Laib and Mittleman, 2010)	0 (Yaws, 2014)	13.0 (Dovbeshko et al., 2015)	0
tetratetracontane	619.19	graphite	TPD	246.2 (Paserba and Gellman, 2001)	7.8×10^{30}	140.1 (Chickos and Acree, 2003)	80.52 (Laib and Mittleman, 2010)	0 (Yaws, 2014)	13.0 (Dovbeshko et al., 2015)	0
octatetracontane	677.31	graphite	TPD	256.7 (Paserba and Gellman, 2001)	5.8×10^{32}	145.9 (Chickos and Acree, 2003)	87.76 (Laib and Mittleman, 2010)	0 (Yaws, 2014)	13.0 (Dovbeshko et al., 2015)	0



hexapentacontane	787.50	graphite	TPD	280.5 (Paserba and Gellman, 2001)	1.0×10^{37}	157.8 (Chickos and Acree, 2003)	102.24 (Laib and Mittleman, 2010)	0 (Yaws, 2014)	13.0 (Dovbeshko et al., 2015)	0
hexacontane	843.61	graphite	TPD	289 (Paserba and Gellman, 2001)	3.3×10^{38}	163 (Chickos and Acree, 2003)	109.48 (Laib and Mittleman, 2010)	0 (Yaws, 2014)	13.0 (Dovbeshko et al., 2015)	0
methanol (monomer)	32.04	graphite	MB	17.4 (Kong et al., 2021)	1.3×10^{-10}	37.8 (Chickos and Acree, 2003)	3.28 (Laib and Mittleman, 2010)	1.7 (Lide, 2008)	13.0 (Dovbeshko et al., 2015)	1
methanol (clusters)	32.04	graphite	MB	34.7 (Kong et al., 2019)	1.5×10^{-7}	37.8 (Chickos and Acree, 2003)	3.28 (Laib and Mittleman, 2010)	1.7 (Lide, 2008)	13.0 (Dovbeshko et al., 2015)	1
methanol (monomer)	32.04	graphene	DFT	20.6 (Schroder, 2013)	4.7×10^{-10}	37.8 (Chickos and Acree, 2003)	3.28 (Laib and Mittleman, 2010)	1.7 (Lide, 2008)	13.0 (Dovbeshko et al., 2015)	1
methanol (3 cluster)	32.04	graphene	DFT	30.4 (Schroder, 2013)	2.6×10^{-8}	37.8 (Chickos and Acree, 2003)	3.28 (Laib and Mittleman, 2010)	1.7 (Lide, 2008)	13.0 (Dovbeshko et al., 2015)	1
methanol (5 cluster)	32.04	graphene	DFT	34.9 (Schroder, 2013)	1.7×10^{-7}	37.8 (Chickos and Acree, 2003)	3.28 (Laib and Mittleman, 2010)	1.7 (Lide, 2008)	13.0 (Dovbeshko et al., 2015)	1
methane	16.04	HOPG	TDS	17 (Ulbricht et al., 2006)	1.1×10^{-10}	8.5 (Chickos and Acree, 2003)	2.59 (Laib and Mittleman, 2010)	0 (Yaws, 2014)	13.0 (Dovbeshko et al., 2015)	0
methanol	32.04	HOPG	TDS	48 (Ulbricht et al., 2006)	3.6×10^{-5}	37.8 (Chickos and Acree, 2003)	3.28 (Laib and Mittleman, 2010)	1.7 (Lide, 2008)	13.0 (Dovbeshko et al., 2015)	1
ethanol	46.07	HOPG	TDS	50 (Ulbricht et al., 2006)	8.2×10^{-5}	42.4 (Chickos and Acree, 2003)	5.26 (Laib and Mittleman, 2010)	1.69 (Lide, 2008)	13.0 (Dovbeshko et al., 2015)	0.5
1,1-dichloroethane	98.96	HOPG	TDS	51 (Ulbricht et al., 2006)	1.2×10^{-4}	33.5 (Chickos and Acree, 2003)	8.64 (Laib and Mittleman, 2010)	2.06 (Lide, 2008)	13.0 (Dovbeshko et al., 2015)	0
trichloromethane	119.38	HOPG	TDS	54 (Ulbricht et al., 2006)	4.2×10^{-4}	31.1 (Chickos and Acree, 2003)	8.87 (Laib and Mittleman, 2010)	1.04 (Lide, 2008)	13.0 (Dovbeshko et al., 2015)	0
benzene	78.11	HOPG	TDS	48 (Ulbricht et al., 2006)	3.6×10^{-5}	42.3 (Chickos and Acree, 2003)	10.53 (Laib and Mittleman, 2010)	0 (Yaws, 2014)	13.0 (Dovbeshko et al., 2015)	0
n,n-dimethylformamide	73.09	HOPG	TDS	53 (Ulbricht et al., 2006)	2.8×10^{-4}	46.9 (Chickos and Acree, 2003)	7.93 (Bosque and Sales, 2002)	3.82 (Lide, 2008)	13.0 (Dovbeshko et al., 2015)	0
ethylbenzene	106.17	HOPG	TDS	79 (Ulbricht et al., 2006)	1.2×10^1	42.3 (Chickos)	14.2 (Laib and)	0.59 (Lide, 2008)	13.0 (Dovbeshko)	0



						and Acree, 2003)	Mittleman, 2010)		o et al., 2015)	
toluene	92.14	HOPG	TDS	68 (Ulbricht et al., 2006)	1.3×10^{-1}	38.9 (Chickos and Acree, 2003)	12.12 (Laib and Mittleman, 2010)	0.375 (Lide, 2008)	13.0 (Dovbeshko et al., 2015)	0
sigma-dichlorobenzene	147.01	HOPG	TDS	69 (Ulbricht et al., 2006)	2.0×10^{-1}	50.9 (Chickos and Acree, 2003)	14.3 (McEachran et al., 2018)	2.5 (Lide, 2008)	13.0 (Dovbeshko et al., 2015)	0
naphthalene	128.17	HOPG	TDS	77 (Ulbricht et al., 2006)	5.3	53.4 (Chickos and Acree, 2003)	17 (Laib and Mittleman, 2010)	0 (Yaws, 2014)	13.0 (Dovbeshko et al., 2015)	0
coronene	300.35	HOPG	TDS	127 (Ulbricht et al., 2006)	4.4×10^9	148 (Chickos and Acree, 2003)	42.5 (Laib and Mittleman, 2010)	0 (Yaws, 2014)	13.0 (Dovbeshko et al., 2015)	0
fullerene	720.66	HOPG	TDS	163 (Ulbricht et al., 2006)	1.1×10^{16}	42.4 (Chickos and Acree, 2003)	76.5	0 (Yaws, 2014)	13.0 (Dovbeshko et al., 2015)	0
ovalene	398.45	HOPG	TDS	230 (Ulbricht et al., 2006)	1.0×10^{28}	31.6 (Chickos and Acree, 2003)	45.8	0 (Yaws, 2014)	13.0 (Dovbeshko et al., 2015)	0
ethanol	46.07	GAC	TG-DSC	56.8 (Giraudet et al., 2006)	1.3×10^{-3}	31.3 (Chickos and Acree, 2003)	5.26 (Lide, 2008)	1.69 (Lide, 2008)	13.0 (Dovbeshko et al., 2015)	0.5
acrylnitrile	53.06	GAC	TG-DSC	49 (Giraudet et al., 2006)	5.4×10^{-5}	28.8 (Chickos and Acree, 2003)	8.05 (Lide, 2008)	3.87 (Lide, 2008)	13.0 (Dovbeshko et al., 2015)	0
acetone	58.08	GAC	TG-DSC	51.1 (Giraudet et al., 2006)	1.3×10^{-4}	47.45 (Chickos and Acree, 2003)	6.37 (Lide, 2008)	2.88 (Lide, 2008)	13.0 (Dovbeshko et al., 2015)	0.33
dichloromethane	84.93	GAC	TG-DSC	45.6 (Giraudet et al., 2006)	1.3×10^{-5}	31.6 (Chickos and Acree, 2003)	7.21 (Lide, 2008)	1.6 (Lide, 2008)	13.0 (Dovbeshko et al., 2015)	0
propanol	60.09	GAC	TG-DSC	52.6 (Giraudet et al., 2006)	2.4×10^{-4}	33.1 (Chickos and Acree, 2003)	6.74 (Lide, 2008)	2.52 (Lide, 2008)	13.0 (Dovbeshko et al., 2015)	0.33
ethyl formate	74.08	GAC	TG-DSC	52 (Giraudet et al., 2006)	1.9×10^{-4}	42.3 (Chickos and Acree, 2003)	6.88 (Lide, 2008)	1.9 (Lide, 2008)	13.0 (Dovbeshko et al., 2015)	0.67
cyclohexane	84.16	GAC	TG-DSC	55.7 (Giraudet et al., 2006)	8.5×10^{-4}	34.5 (Chickos and Acree, 2003)	10.87 (Lide, 2008)	0.61 (Yaws, 2014)	13.0 (Dovbeshko et al., 2015)	0
benzene	78.11	GAC	TG-DSC	56.7 (Giraudet et al., 2006)	1.3×10^{-3}	34.7 (Chickos and Acree, 2003)	10.53 (Lide, 2008)	0 (Yaws, 2014)	13.0 (Dovbeshko et al., 2015)	0
fluorobenzene	96.10	GAC	TG-DSC	57.4 (Giraudet et al., 2006)	1.7×10^{-3}	36.9 (Chickos)	10.3 (Lide, 2008)	1.6 (Lide, 2008)	13.0 (Dovbeshko et al., 2015)	0



						and Acree, 2003)			o et al., 2015)	
methylethylketone	72.11	GAC	TG-DSC	58 (Giraudet et al., 2006)	2.2×10^{-3}	30.6 (Chickos and Acree, 2003)	8.19 (NIST, 2018)	2.78 (Lide, 2008)	13.0 (Dovbeshko et al., 2015)	0.25
3-methylbutane-2-one	86.13	GAC	TG-DSC	60.7 (Giraudet et al., 2006)	6.6×10^{-3}	31.5 (Chickos and Acree, 2003)	10.02 (Bosque and Sales, 2002)	2.77 (Lide, 2008)	13.0 (Dovbeshko et al., 2015)	0.2
hex-1-ene	84.16	GAC	TG-DSC	62.9 (Giraudet et al., 2006)	1.6×10^{-2}	32.1 (Chickos and Acree, 2003)	11.65 (Lide, 2008)	0.4	13.0 (Dovbeshko et al., 2015)	0
hexane	86.18	GAC	TG-DSC	63.4 (Giraudet et al., 2006)	2.0×10^{-2}	34.9 (Chickos and Acree, 2003)	11.9 (Lide, 2008)	0 (Yaws, 2014)	13.0 (Dovbeshko et al., 2015)	0
isopropylether	102.18	GAC	TG-DSC	65.9 (Giraudet et al., 2006)	5.6×10^{-2}	42.4 (Chickos and Acree, 2003)	12.65 (Bosque and Sales, 2002)	1.13 (Lide, 2008)	13.0 (Dovbeshko et al., 2015)	0.17
triethylamine	101.19	GAC	TG-DSC	74.1 (Giraudet et al., 2006)	1.6	31.6 (Chickos and Acree, 2003)	7.97 (Lide, 2008)	0.66 (Lide, 2008)	13.0 (Dovbeshko et al., 2015)	0
phenanthrene	178.23	kerosene soot	KU	85.6 (Guilloteau et al., 2010)	1.8×10^2	78.7 (Chickos and Acree, 2003)	30.75 (Lide, 2008)	0 (Yaws, 2014)	13.0 (Dovbeshko et al., 2015)	0
anthracene	178.23	kerosene soot	KU	88.1 (Guilloteau et al., 2010)	5.1×10^2	79.6 (Chickos and Acree, 2003)	25.67 (Lide, 2008)	0 (Yaws, 2014)	13.0 (Dovbeshko et al., 2015)	0
fluoranthene	202.26	kerosene soot	KU	93.9 (Guilloteau et al., 2008)	5.5×10^3	79.3 (Chickos and Acree, 2003)	23.23	0.23 (Yaws, 2014)	13.0 (Dovbeshko et al., 2015)	0
pyrene	202.26	kerosene soot	KU	95.2 (Guilloteau et al., 2008)	9.4×10^3	78.6 (Chickos and Acree, 2003)	28.22 (Lide, 2008)	0 (Yaws, 2014)	13.0 (Dovbeshko et al., 2015)	0
benzo(ghi)fluoranthene	226.28	kerosene soot	KU	112.1 (Guilloteau et al., 2010)	9.6×10^6	88.5 (Chickos and Acree, 2003)	32.9 (McEachran et al., 2018)	0 (Yaws, 2014)	13.0 (Dovbeshko et al., 2015)	0
acepyrene	226.27	kerosene soot	KU	107.1 (Guilloteau et al., 2010)	1.2×10^6		31.6 (McEachran et al., 2018)	0 (Yaws, 2014)	13.0 (Dovbeshko et al., 2015)	0
benzo(a)anthracene	228.29	kerosene soot	KU	113.9 (Guilloteau et al., 2010)	2.0×10^7	91 (Chickos and Acree, 2003)	32.86 (Lide, 2008)	0 (Yaws, 2014)	13.0 (Dovbeshko et al., 2015)	0
chrysene	228.29	kerosene soot	KU	114.9 (Guilloteau et al., 2010)	3.0×10^7	89.6 (Chickos and Acree, 2003)	33.06 (Lide, 2008)	0 (Yaws, 2014)	13.0 (Dovbeshko et al., 2015)	0
benzo(e)pyrene	252.32	kerosene soot	KU	119.9 (Guilloteau et al., 2010)	2.4×10^8	92 (Chickos and Acree, 2003)	35.8 (McEachran et al., 2018)	0 (Yaws, 2014)	13.0 (Dovbeshko et al., 2015)	0



							n et al., 2018)		o et al., 2015)	
benzo(b)fluoranthene	252.31	kerosene soot	KU	118.7 (Guilloteau et al., 2010)	1.4×10^8	89.7 (Chickos and Acree, 2003)	35.8 (McEachran et al., 2018)	0 (Yaws, 2014)	13.0 (Dovbeshko et al., 2015)	0
benzo(k)fluoranthene	252.32	kerosene soot	KU	120.8 (Guilloteau et al., 2010)	3.4×10^8	88.5 (Chickos and Acree, 2003)	35.8 (McEachran et al., 2018)	0 (Yaws, 2014)	13.0 (Dovbeshko et al., 2015)	0
benzo(a)pyrene	252.32	kerosene soot	KU	121.8 (Guilloteau et al., 2010)	5.2×10^8	91 (Chickos and Acree, 2003)	35.8 (McEachran et al., 2018)	0 (Yaws, 2014)	13.0 (Dovbeshko et al., 2015)	0

1089

1090 **Table A6.** Compiled adsorbate-substrate interaction energies of volatile organic compounds
 1091 (VOCs) on MgO(100), Pt(111), Ni(111), and Pd(111). Gas species, gas species' molar mass,
 1092 substrate, experimental or theoretical method, desorption energy (E_{des}^0), and desorption lifetimes
 1093 (τ_{des}) evaluated at 293 K using $A_{des} = 10^{13} \text{ s}^{-1}$, enthalpy of vaporization (ΔH_{vap}), gas species'
 1094 polarizability (α), gas species' dipole moment (μ), substrate's relative permittivity (ϵ_r), and gas
 1095 species' oxygen to carbon ration ($O:C$) are given.

Gas Species	Molar Mass / g mol ⁻¹	Substrate	Method	E_{des}^0 / kJ mol ⁻¹	$\tau_{des}^{293 K}$ / s	ΔH_{vap} (T) / kJ mol ⁻¹	α / 10 ⁻²⁴ cm ³	μ / D	ϵ_r	O:C
methane	16.04	MgO(100)	TPD	12.1 (Tait et al., 2006)	1.4×10^{-11}	8.5 (Chickos and Acree, 2003)	2.59 (Lide, 2008)	0 (Yaws, 2014)	9.65 (Lide, 2008)	0
ethane	30.07	MgO(100)	TPD	22.2 (Tait et al., 2006)	9.1×10^{-10}	15.3 (Chickos and Acree, 2003)	4.45 (Lide, 2008)	0 (Yaws, 2014)	9.65 (Lide, 2008)	0
propane	44.10	MgO(100)	TPD	29 (Tait et al., 2006)	1.5×10^{-8}	18.8 (Chickos and Acree, 2003)	6.33 (Lide, 2008)	0 (Yaws, 2014)	9.65 (Lide, 2008)	0
butane	58.12	MgO(100)	TPD	34.9 (Tait et al., 2006)	1.7×10^{-7}	22.4 (Chickos and Acree, 2003)	8.2 (Lide, 2008)	0 (Yaws, 2014)	9.65 (Lide, 2008)	0
hexane	86.18	MgO(100)	TPD	46.4 (Tait et al., 2006)	1.9×10^{-5}	31.5 (Chickos and Acree, 2003)	11.9 (Lide, 2008)	0 (Yaws, 2014)	9.65 (Lide, 2008)	0
octane	114.23	MgO(100)	TPD	62.9 (Tait et al., 2006)	1.6×10^{-2}	41.6 (Chickos and Acree, 2003)	15.9 (Lide, 2008)	0 (Yaws, 2014)	9.65 (Lide, 2008)	0
decane	142.29	MgO(100)	TPD	77.9 (Tait et al., 2006)	7.7	51.4 (Chickos and Acree, 2003)	19.1 (Lide, 2008)	0 (Yaws, 2014)	9.65 (Lide, 2008)	0
methane	16.04	Pt(111)	TPD	15.2 (Tait et al., 2006)	5.1×10^{-11}	8.5 (Chickos and Acree, 2003)	2.59 (Lide, 2008)	0 (Yaws, 2014)		0



methane	16.04	Pt(111)	TPD	16.1 (Weaver et al., 2003)	7.4×10^{-11}	8.5 (Chickos and Acree, 2003)	2.59 (Lide, 2008)	0 (Yaws, 2014)		0
ethane	30.07	Pt(111)	TPD	28.9 (Tait et al., 2006)	1.4×10^{-8}	15.3 (Chickos and Acree, 2003)	4.45 (Lide, 2008)	0 (Yaws, 2014)		0
ethane	30.07	Pt(111)	TPD	36.8 (Weaver et al., 2003)	3.6×10^{-7}	15.3 (Chickos and Acree, 2003)	4.45 (Lide, 2008)	0 (Yaws, 2014)		0
propane	44.10	Pt(111)	TPD	41.5 (Tait et al., 2006)	2.5×10^{-6}	18.8 (Chickos and Acree, 2003)	6.33 (Lide, 2008)	0 (Yaws, 2014)		0
propane	44.10	Pt(111)	TPD	41.2 (Weaver et al., 2003)	2.2×10^{-6}	18.8 (Chickos and Acree, 2003)	6.33 (Lide, 2008)	0 (Yaws, 2014)		0
butane	58.12	Pt(111)	TPD	50.9 (Tait et al., 2006)	1.2×10^{-4}	22.4 (Chickos and Acree, 2003)	8.2 (Lide, 2008)	0 (Yaws, 2014)		0
butane	58.12	Pt(111)	TPD	60.2 (Weaver et al., 2003)	5.4×10^{-3}	22.4 (Chickos and Acree, 2003)	8.2 (Lide, 2008)	0 (Yaws, 2014)		0
butane	58.12	Pt(111)	TPD	34.3 (Salmeron and Somorjai, 1981)	1.3×10^{-7}	22.4 (Chickos and Acree, 2003)	8.2 (Lide, 2008)	0 (Yaws, 2014)		0
pentane	72.15	Pt(111)	TPD	42.7 (Salmeron and Somorjai, 1981)	4.1×10^{-6}	25 (Chickos and Acree, 2003)	9.99 (Lide, 2008)	0 (Yaws, 2014)		0
hexane	86.18	Pt(111)	TPD	79.8 (Tait et al., 2006)	1.7×10^1	31.5 (Chickos and Acree, 2003)	11.9 (Lide, 2008)	0 (Yaws, 2014)		0
hexane	86.18	Pt(111)	TPD	61.9 (Bishop et al., 2000)	1.1×10^{-2}	31.5 (Chickos and Acree, 2003)	11.9 (Lide, 2008)	0 (Yaws, 2014)		0
heptane	100.21	Pt(111)	TPD	66.4 (Bishop et al., 2000)	6.9×10^{-2}	36.6 (Chickos and Acree, 2003)	13.61 (Lide, 2008)	0 (Yaws, 2014)		0
octane	114.23	Pt(111)	TPD	72 (Bishop et al., 2000)	6.8×10^{-1}	41.6 (Chickos and Acree, 2003)	15.9 (Lide, 2008)	0 (Yaws, 2014)		0
nonane	128.20	Pt(111)	TPD	74.2 (Bishop et al., 2000)	1.7	46.55 (Chickos and Acree, 2003)	17.36 (Lide, 2008)	0 (Yaws, 2014)		0
decane	142.29	Pt(111)	TPD	76.1 (Bishop et al., 2000)	3.7	51.4 (Chickos)	19.1 (Lide, 2008)	0 (Yaws, 2014)		0



						and Acree, 2003)				
propane	44.10	Ni(111)	DFT	57.9 (Mendes et al., 2019)	1.4×10^8	18.8 (Chickos and Acree, 2003)	6.33 (Lide, 2008)	0 (Yaws, 2014)		0
1-propanol	60.09	Ni(111)	DFT	92.6 (Mendes et al., 2019)	3.3×10^3	47.45 (Chickos and Acree, 2003)	6.74 (Lide, 2008)	1.58 (Lide, 2008)		0.33
2-propanol	60.09	Ni(111)	DFT	89.7 (Mendes et al., 2019)	9.9×10^2	47.45 (Chickos and Acree, 2003)	6.74 (Lide, 2008)	1.58 (Lide, 2008)		0.33
1,2-propanediol	76.09	Ni(111)	DFT	111.0 (Mendes et al., 2019)	6.0×10^6	60.0 (Chickos and Acree, 2003)	7.55 (Bosque and Sales, 2002)	2.25 (Lide, 2008)		0.66
1,3-propanediol	76.09	Ni(111)	DFT	111.0 (Mendes et al., 2019)	6.0×10^6	72.4 (Chickos and Acree, 2003)	7.55 (Bosque and Sales, 2002)	2.55 (Lide, 2008)		0.66
glycerol	92.09	Ni(111)	DFT	118.7 (Mendes et al., 2019)	1.4×10^8	91.7 (Chickos and Acree, 2003)	8.14 (Bosque and Sales, 2002)	2.56 (Lide, 2008)		1
propane	44.10	Pd(111)	DFT	57.9 (Mendes et al., 2019)	2.1×10^{-3}	18.8 (Chickos and Acree, 2003)	6.33 (Lide, 2008)	0 (Yaws, 2014)		0
1-propanol	60.09	Pd(111)	DFT	84.9 (Mendes et al., 2019)	1.4×10^2	47.45 (Chickos and Acree, 2003)	6.74 (Lide, 2008)	1.58 (Lide, 2008)		0.33
2-propanol	60.09	Pd(111)	DFT	85.9 (Mendes et al., 2019)	2.0×10^2	47.45 (Chickos and Acree, 2003)	6.74 (Lide, 2008)	1.58 (Lide, 2008)		0.33
1,2-propanediol	76.09	Pd(111)	DFT	101.3 (Mendes et al., 2019)	1.1×10^5	60.0 (Chickos and Acree, 2003)	7.55 (Bosque and Sales, 2002)	2.25 (Lide, 2008)		0.66
1,3-propanediol	76.09	Pd(111)	DFT	102.3 (Mendes et al., 2019)	1.7×10^5	72.4 (Chickos and Acree, 2003)	7.55 (Bosque and Sales, 2002)	2.55 (Lide, 2008)		0.66
glycerol	92.09	Pd(111)	DFT	116.7 (Mendes et al., 2019)	6.5×10^7	91.7 (Chickos and Acree, 2003)	8.14 (Bosque and Sales, 2002)	2.56 (Lide, 2008)		1
propane	44.10	Pt(111)	DFT	65.6 (Mendes et al., 2019)	5.0×10^{-2}	18.8 (Chickos and Acree, 2003)	6.33 (Lide, 2008)	0 (Yaws, 2014)		0
1-propanol	60.09	Pt(111)	DFT	100.3 (Mendes et al., 2019)	7.7×10^4	47.45 (Chickos and Acree, 2003)	6.74 (Lide, 2008)	1.58 (Lide, 2008)		0.33
2-propanol	60.09	Pt(111)	DFT	99.4 (Mendes et al., 2019)	5.2×10^4	47.45 (Chickos and Acree, 2003)	6.74 (Lide, 2008)	1.58 (Lide, 2008)		0.33



						and Acree, 2003)				
1,2-propanediol	76.09	Pt(111)	DFT	114.8 (Mendes et al., 2019)	2.9×10^7	60.0 (Chickos and Acree, 2003)	7.55 (Bosque and Sales, 2002)	2.25 (Lide, 2008)		0.66
1,3-propanediol	76.09	Pt(111)	DFT	119.6 (Mendes et al., 2019)	2.1×10^8	72.4 (Chickos and Acree, 2003)	7.55 (Bosque and Sales, 2002)	2.55 (Lide, 2008)		0.66
glycerol	92.09	Pt(111)	DFT	133.1 (Mendes et al., 2019)	5.5×10^{10}	91.7 (Chickos and Acree, 2003)	8.14 (Bosque and Sales, 2002)	2.56 (Lide, 2008)		1

1096

1097

1098 **Table A7.** Compiled adsorbate-substrate interaction energies of volatile organic compounds
 1099 (VOCs) on mineral surrogates and minerals and clays. Gas species, gas species' molar mass,
 1100 substrate, experimental or theoretical method, desorption energy (E_{des}^0), and desorption lifetimes
 1101 (τ_{des}) evaluated at 293 K using $A_{des} = 10^{13} \text{ s}^{-1}$, enthalpy of vaporization (ΔH_{vap}), gas species'
 1102 polarizability (α), gas species' dipole moment (μ), substrate's relative permittivity (ϵ_r), and gas
 1103 species' oxygen to carbon ration (O:C) are given.

Gas Species	Molar Mass / g mol ⁻¹	Substrate	Method	E_{des}^0 / kJ mol ⁻¹	$\tau_{des}^{293 K}$ / s	ΔH_{vap} (T) / kJ mol ⁻¹	α / 10 ⁻²⁴ cm ³	μ / D	ϵ_r	O:C
n-decane	142.29	α -Al ₂ O ₃	IGC	28.5 (Goss and Eisenreich, 1996)	1.2×10^{-8}	51.4 (Chickos and Acree, 2003)	19.1 (Lide, 2008)	0 (Yaws, 2014)	9.34 (Lide, 2008)	0
o-xylene	106.17	α -Al ₂ O ₃	IGC	26.6 (Goss and Eisenreich, 1996)	5.5×10^{-9}	42.9 (Chickos and Acree, 2003)	14.25 (Bosque and Sales, 2002)	0.64 (Lide, 2008)	9.34 (Lide, 2008)	0
propylbenzene	120.19	α -Al ₂ O ₃	IGC	30.3 (Goss and Eisenreich, 1996)	2.5×10^{-8}	46.2 (Chickos and Acree, 2003)	16 (McEachran et al., 2018)	0.369 (Yaws, 2014)	9.34 (Lide, 2008)	0
1,2-dichlorobenzene	147.01	α -Al ₂ O ₃	IGC	28.0 (Goss and Eisenreich, 1996)	9.7×10^{-9}	49.9 (Chickos and Acree, 2003)	14.3 (Bosque and Sales, 2002)	2.5 (Lide, 2008)	9.34 (Lide, 2008)	0
1,4-dichlorobenzene	147.01	α -Al ₂ O ₃	IGC	26.6 (Goss and Eisenreich, 1996)	5.5×10^{-9}	54.8 (Chickos and Acree, 2003)	14.3 (McEachran et al., 2018)	1.72 (Lide, 2008)	9.34 (Lide, 2008)	0
1,2,3,4-tetrachlorobenzene	215.89	α -Al ₂ O ₃	IGC	42.7 (Goss and Eisenreich, 1996)	4.0×10^{-6}	60.1 (Chickos and Acree, 2003)	18.2 (McEachran et al., 2018)	2.42 (Lide, 2008)	9.34 (Lide, 2008)	0
naphthalene	128.17	α -Al ₂ O ₃	IGC	38.0 (Goss and Eisenreich, 1996)	5.9×10^{-7}	53.4 (Chickos and Acree, 2003)	17 (Lide, 2008)	0 (Yaws, 2014)	9.34 (Lide, 2008)	0
anisole	108.14	α -Al ₂ O ₃	IGC	37.7 (Goss and	5.2×10^{-7}	45.3 (Chickos	13.1 (Lide, 2008)	1.38 (Lide, 2008)	9.34 (Lide, 2008)	0.14



				Eisenreich, 1996)		and Acree, 2003)				
pyridine	79.10	α -Al ₂ O ₃	IGC	47.0 (Goss and Eisenreich, 1996)	2.4×10^{-5}	40.2 (Chickos and Acree, 2003)	9.34 (Lide, 2008)	2.215 (Lide, 2008)	9.34 (Lide, 2008)	0
ethanol	46.07	α -Al ₂ O ₃	IGC	48.4 (Goss and Eisenreich, 1996)	4.2×10^{-5}	42.4 (Chickos and Acree, 2003)	5.41 (Lide, 2008)	1.69 (Lide, 2008)	9.34 (Lide, 2008)	0.5
ethyl acetate	88.11	α -Al ₂ O ₃	IGC	40.2 (Goss and Eisenreich, 1996)	1.5×10^{-6}	35 (Chickos and Acree, 2003)	8.62 (Lide, 2008)	1.78 (Lide, 2008)	9.34 (Lide, 2008)	0.5
acetone	58.08	α -Al ₂ O ₃	IGC	38.0 (Goss and Eisenreich, 1996)	5.9×10^{-7}	31.3 (Chickos and Acree, 2003)	6.37 (Lide, 2008)	2.88 (Lide, 2008)	9.34 (Lide, 2008)	0.33
n-nonane	128.26	CaCO ₃	IGC	30.4 (Goss and Eisenreich, 1996)	2.7×10^{-8}	46.55 (Chickos and Acree, 2003)	17.36 (Lide, 2008)	0 (Yaws, 2014)	8.67 (Lide, 2008)	0
p-xylene	106.17	CaCO ₃	IGC	35.5 (Goss and Eisenreich, 1996)	2.2×10^{-7}	42.3 (Chickos and Acree, 2003)	14.35 (Bosque and Sales, 2002)	0 (Yaws, 2014)	8.67 (Lide, 2008)	0
ethylbenzene	106.17	CaCO ₃	IGC	34.1 (Goss and Eisenreich, 1996)	1.2×10^{-7}	42.3 (Chickos and Acree, 2003)	14.2 (Lide, 2008)	0.59 (Lide, 2008)	8.67 (Lide, 2008)	0
chlorobenzene	112.56	CaCO ₃	IGC	28.1 (Goss and Eisenreich, 1996)	1.0×10^{-8}	40.3 (Chickos and Acree, 2003)	13.2 (Lide, 2008)	1.69 (Lide, 2008)	8.67 (Lide, 2008)	0
1,2-dichlorobenzene	147.01	CaCO ₃	IGC	36.8 (Goss and Eisenreich, 1996)	3.7×10^{-7}	49.9 (Chickos and Acree, 2003)	14.3 (Bosque and Sales, 2002)	2.5 (Lide, 2008)	8.67 (Lide, 2008)	0
anisole	108.14	CaCO ₃	IGC	38.8 (Goss and Eisenreich, 1996)	8.4×10^{-7}	45.3 (Chickos and Acree, 2003)	13.1 (Lide, 2008)	1.38 (Lide, 2008)	8.67 (Lide, 2008)	0.14
diethyl ether	74.12	CaCO ₃	IGC	39.3 (Goss and Eisenreich, 1996)	1.0×10^{-6}	27.1 (Chickos and Acree, 2003)	9.47 (Lide, 2008)	1.098 (Lide, 2008)	8.67 (Lide, 2008)	0.25
methanol	32.04	CaCO ₃	DFT	77.2 (Budi et al., 2018)	5.8	37.8 (Chickos and Acree, 2003)	3.28 (Lide, 2008)	1.7 (Lide, 2008)	8.67 (Lide, 2008)	1
ethanol	46.07	CaCO ₃	DFT	80.1 (Budi et al., 2018)	19	42.4 (Chickos and Acree, 2003)	5.41 (Lide, 2008)	1.69 (Lide, 2008)	8.67 (Lide, 2008)	0.5
ethanol	46.07	CaCO ₃	TPD	83.9 (Dickbreder et al., 2023)	91	42.4 (Chickos and Acree, 2003)	5.41 (Lide, 2008)	1.69 (Lide, 2008)	8.67 (Lide, 2008)	0.5
ethanol	46.07	CaCO ₃	TPD	100.3 (Dickbreder et al., 2023)	7.6×10^4	42.4 (Chickos)	5.41 (Lide, 2008)	1.69 (Lide, 2008)	8.67 (Lide, 2008)	0.5



						and Acree, 2003)				
formic acid	46.03	CaCO ₃	DFT	94.6 (Budi et al., 2018)	7.3×10 ³	36 (Chickos and Acree, 2003)	3.4 (Lide, 2008)	1.425 (Lide, 2008)	8.67 (Lide, 2008)	2
acetic acid	60.05	CaCO ₃	DFT	95.5 (Budi et al., 2018)	1.1×10 ⁴	41.6 (Chickos and Acree, 2003)	5.1 (Lide, 2008)	1.7 (Lide, 2008)	8.67 (Lide, 2008)	1
methane	16.04	CaCO ₃	DFT	12.5 (Budi et al., 2018)	1.7×10 ⁻¹¹	8.5 (Chickos and Acree, 2003)	2.59 (Lide, 2008)	0 (Yaws, 2014)	8.67 (Lide, 2008)	0
ethane	30.07	CaCO ₃	DFT	17.4 (Budi et al., 2018)	1.3×10 ⁻¹⁰	15.3 (Chickos and Acree, 2003)	4.45 (Lide, 2008)	0 (Yaws, 2014)	8.67 (Lide, 2008)	0
benzene	78.11	CaCO ₃	DFT	30.9 (Budi et al., 2018)	3.2×10 ⁻⁸	42.3 (Chickos and Acree, 2003)	10 (Lide, 2008)	0 (Yaws, 2014)	8.67 (Lide, 2008)	0
n-octane	114.23	α-Fe ₂ O ₃	IGC	25.0 (Goss and Eisenreich, 1996)	2.9×10 ⁻⁹	41.6 (Chickos and Acree, 2003)	15.9 (Lide, 2008)	0 (Yaws, 2014)	12.00 (Lide, 2008)	0
n-nonane	128.26	α-Fe ₂ O ₃	IGC	31.3 (Goss and Eisenreich, 1996)	3.9×10 ⁻⁸	46.55 (Chickos and Acree, 2003)	17.36 (Lide, 2008)	0 (Yaws, 2014)	12.00 (Lide, 2008)	0
toluene	92.14	α-Fe ₂ O ₃	IGC	27.5 (Goss and Eisenreich, 1996)	8.1×10 ⁻⁹	38.9 (Chickos and Acree, 2003)	11.8 (Lide, 2008)	0.375 (Lide, 2008)	12.00 (Lide, 2008)	0
p-xylene	106.17	α-Fe ₂ O ₃	IGC	32.7 (Goss and Eisenreich, 1996)	6.9×10 ⁻⁸	42.3 (Chickos and Acree, 2003)	14.35 (Bosque and Sales, 2002)	0 (Yaws, 2014)	12.00 (Lide, 2008)	0
o-xylene	106.17	α-Fe ₂ O ₃	IGC	33.6 (Goss and Eisenreich, 1996)	1.0×10 ⁻⁷	42.9 (Chickos and Acree, 2003)	14.25 (Bosque and Sales, 2002)	0.64 (Lide, 2008)	12.00 (Lide, 2008)	0
ethylbenzene	106.17	α-Fe ₂ O ₃	IGC	32.4 (Goss and Eisenreich, 1996)	6.1×10 ⁻⁸	42.3 (Chickos and Acree, 2003)	14.2 (Lide, 2008)	0.59 (Lide, 2008)	12.00 (Lide, 2008)	0
chlorobenzene	112.56	α-Fe ₂ O ₃	IGC	26.4 (Goss and Eisenreich, 1996)	5.2×10 ⁻⁹	40.3 (Chickos and Acree, 2003)	13.2 (Lide, 2008)	1.69 (Lide, 2008)	12.00 (Lide, 2008)	0
1,2-dichlorobenzene	147.01	α-Fe ₂ O ₃	IGC	35.5 (Goss and Eisenreich, 1996)	2.2×10 ⁻⁷	49.9 (Chickos and Acree, 2003)	14.3 (Bosque and Sales, 2002)	2.5 (Lide, 2008)	12.00 (Lide, 2008)	0
1,4-dichlorobenzene	147.01	α-Fe ₂ O ₃	IGC	32.5 (Goss and Eisenreich, 1996)	6.3×10 ⁻⁸	54.8 (Chickos and Acree, 2003)	14.3 (McEachran et al., 2018)	1.72 (Lide, 2008)	12.00 (Lide, 2008)	0
anisole	108.14	α-Fe ₂ O ₃	IGC	41.0 (Goss and	2.1×10 ⁻⁶	45.3 (Chickos	13.1 (Lide, 2008)	1.38 (Lide, 2008)	12.00 (Lide, 2008)	0.143



				Eisenreich, 1996)		and Acree, 2003)				
acetone	58.08	α -Fe ₂ O ₃	IGC	39.3 (Goss and Eisenreich, 1996)	1.0×10 ⁻⁶	31.3 (Chickos and Acree, 2003)	6.37 (Lide, 2008)	2.88 (Lide, 2008)	12.00 (Lide, 2008)	0.33
diethyl ether	74.12	α -Fe ₂ O ₃	IGC	38.2 (Goss and Eisenreich, 1996)	6.6×10 ⁻⁷	27.1 (Chickos and Acree, 2003)	9.47 (Lide, 2008)	1.098 (Lide, 2008)	12.00 (Lide, 2008)	0.25
n-octane	114.23	quartz/kaolinite	IGC	27.9 (Goss and Eisenreich, 1996)	9.5×10 ⁻⁹	41.6 (Chickos and Acree, 2003)	15.9 (Lide, 2008)	0 (Yaws, 2014)	~4.0 (Leluk et al., 2010)	0
n-nonane	128.26	quartz/kaolinite	IGC	31.6 (Goss and Eisenreich, 1996)	4.3×10 ⁻⁸	46.55 (Chickos and Acree, 2003)	17.36 (Lide, 2008)	0 (Yaws, 2014)	~4.0 (Leluk et al., 2010)	0
n-decane	142.29	quartz/kaolinite	IGC	35.6 (Goss and Eisenreich, 1996)	2.2×10 ⁻⁷	51.4 (Chickos and Acree, 2003)	19.1 (Lide, 2008)	0 (Yaws, 2014)	~4.0 (Leluk et al., 2010)	0
toluene	92.14	quartz/kaolinite	IGC	31.3 (Goss and Eisenreich, 1996)	3.8×10 ⁻⁸	38.9 (Chickos and Acree, 2003)	11.8 (Lide, 2008)	0.375 (Lide, 2008)	~4.0 (Leluk et al., 2010)	0
p-xylene	106.17	quartz/kaolinite	IGC	35.6 (Goss and Eisenreich, 1996)	2.2×10 ⁻⁷	42.3 (Chickos and Acree, 2003)	14.35 (Bosque and Sales, 2002)	0 (Yaws, 2014)	~4.0 (Leluk et al., 2010)	0
o-xylene	106.17	quartz/kaolinite	IGC	36.5 (Goss and Eisenreich, 1996)	3.2×10 ⁻⁷	42.9 (Chickos and Acree, 2003)	14.25 (Bosque and Sales, 2002)	0.64 (Lide, 2008)	~4.0 (Leluk et al., 2010)	0
ethylbenzene	106.17	quartz/kaolinite	IGC	35.4 (Goss and Eisenreich, 1996)	2.1×10 ⁻⁷	42.3 (Chickos and Acree, 2003)	14.2 (Lide, 2008)	0.59 (Lide, 2008)	~4.0 (Leluk et al., 2010)	0
propylbenzene	120.19	quartz/kaolinite	IGC	40.2 (Goss and Eisenreich, 1996)	1.5×10 ⁻⁶	46.2 (Chickos and Acree, 2003)	16 (McEachra n et al., 2018)	0.369 (Yaws, 2014)	~4.0 (Leluk et al., 2010)	0
chlorobenzene	112.56	quartz/kaolinite	IGC	32.1 (Goss and Eisenreich, 1996)	5.3×10 ⁻⁸	40.3 (Chickos and Acree, 2003)	13.2 (Lide, 2008)	1.69 (Lide, 2008)	~4.0 (Leluk et al., 2010)	0
1,2-dichlorobenzene	147.01	quartz/kaolinite	IGC	36.6 (Goss and Eisenreich, 1996)	3.4×10 ⁻⁷	49.9 (Chickos and Acree, 2003)	14.3 (Bosque and Sales, 2002)	2.5 (Lide, 2008)	~4.0 (Leluk et al., 2010)	0
1,4-dichlorobenzene	147.01	quartz/kaolinite	IGC	37.2 (Goss and Eisenreich, 1996)	4.3×10 ⁻⁷	54.8 (Chickos and Acree, 2003)	14.3 (McEachra n et al., 2018)	1.72 (Lide, 2008)	~4.0 (Leluk et al., 2010)	0
1,2,3,4-tetrachlorobenzene	215.89	quartz/kaolinite	IGC	45.3 (Goss and Eisenreich, 1996)	1.2×10 ⁻⁵	60.1 (Chickos and Acree, 2003)	18.2 (McEachra n et al., 2018)	2.42 (Lide, 2008)	~4.0 (Leluk et al., 2010)	0
naphthalene	128.17	quartz/kaolinite	IGC	46.9 (Goss and	2.3×10 ⁻⁵	53.4 (Chickos	17 (Lide, 2008)	0 (Yaws, 2014)	~4.0 (Leluk	0



				Eisenreich, 1996)		and Acree, 2003)			et al., 2010)	
anisole	108.14	quartz/kaolinite	IGC	44.2 (Goss and Eisenreich, 1996)	7.7×10^{-6}	45.3 (Chickos and Acree, 2003)	13.1 (Lide, 2008)	1.38 (Lide, 2008)	~4.0 (Leluk et al., 2010)	0.143
pyridine	79.10	quartz/kaolinite	IGC	48.6 (Goss and Eisenreich, 1996)	4.7×10^{-5}	40.2 (Chickos and Acree, 2003)	9.34 (Lide, 2008)	2.215 (Lide, 2008)	~4.0 (Leluk et al., 2010)	0
ethanol	46.07	quartz/kaolinite	IGC	46.6 (Goss and Eisenreich, 1996)	2.1×10^{-5}	42.4 (Chickos and Acree, 2003)	5.41 (Lide, 2008)	1.38 (Lide, 2008)	~4.0 (Leluk et al., 2010)	0.5
ethyl acetate	88.11	quartz/kaolinite	IGC	45.0 (Goss and Eisenreich, 1996)	1.1×10^{-5}	35 (Chickos and Acree, 2003)	8.62 (Lide, 2008)	2.215	~4.0 (Leluk et al., 2010)	0.5
acetone	58.08	quartz/kaolinite	IGC	43.6 (Goss and Eisenreich, 1996)	6.0×10^{-6}	31.3 (Chickos and Acree, 2003)	6.37 (Lide, 2008)	2.88 (Lide, 2008)	~4.0 (Leluk et al., 2010)	0.33
diethyl ether	74.12	quartz/kaolinite	IGC	40.0 (Goss and Eisenreich, 1996)	1.4×10^{-6}	27.1 (Chickos and Acree, 2003)	9.47 (Lide, 2008)	1.098 (Lide, 2008)	~4.0 (Leluk et al., 2010)	0.25
methanol	32.04	quartz	DFT	60.8 (Budi et al., 2018)	6.9×10^{-3}	37.8 (Chickos and Acree, 2003)	3.28 (Lide, 2008)	1.7 (Lide, 2008)	3.75 (Lide, 2008)	1
ethanol	46.07	quartz	DFT	64.6 (Budi et al., 2018)	3.3×10^{-2}	42.4 (Chickos and Acree, 2003)	5.41 (Lide, 2008)	1.69 (Lide, 2008)	3.75 (Lide, 2008)	0.5
formic acid	46.03	quartz	DFT	57.9 (Budi et al., 2018)	2.1×10^{-3}	36 (Chickos and Acree, 2003)	3.4 (Lide, 2008)	1.425 (Lide, 2008)	3.75 (Lide, 2008)	2
acetic acid	60.05	quartz	DFT	60.8 (Budi et al., 2018)	6.9×10^{-3}	41.6 (Chickos and Acree, 2003)	5.1 (Lide, 2008)	1.7 (Lide, 2008)	3.75 (Lide, 2008)	1
methane	16.04	quartz	DFT	6.8 (Budi et al., 2018)	1.6×10^{-12}	8.5 (Chickos and Acree, 2003)	2.59 (Lide, 2008)	0 (Yaws, 2014)	3.75 (Lide, 2008)	0
ethane	30.07	quartz	DFT	12.5 (Budi et al., 2018)	1.7×10^{-11}	15.3 (Chickos and Acree, 2003)	4.45 (Lide, 2008)	0 (Yaws, 2014)	3.75 (Lide, 2008)	0
benzene	78.11	quartz	DFT	33.8 (Budi et al., 2018)	1.1×10^{-7}	42.3 (Chickos and Acree, 2003)	10 (Lide, 2008)	0 (Yaws, 2014)	3.75 (Lide, 2008)	0
methanol	32.04	kaolinite (Al)	DFT	61.8 (Budi et al., 2018)	1.0×10^{-2}	37.8 (Chickos and Acree, 2003)	3.28 (Lide, 2008)	1.7 (Lide, 2008)	5.10 (Leluk et al., 2010)	1
ethanol	46.07	kaolinite (Al)	DFT	64.6 (Budi et al., 2018)	3.3×10^{-2}	42.4 (Chickos and Acree, 2003)	5.41 (Lide, 2008)	1.69 (Lide, 2008)	5.10 (Leluk et al., 2010)	0.5



formic acid	46.03	kaolinite (Al)	DFT	79.1 (Budi et al., 2018)	1.3×10^1	36 (Chickos and Acree, 2003)	3.4 (Lide, 2008)	1.425 (Lide, 2008)	5.10 (Leluk et al., 2010)	2
acetic acid	60.05	kaolinite (Al)	DFT	82.0 (Budi et al., 2018)	4.2×10^1	41.6 (Chickos and Acree, 2003)	5.1 (Lide, 2008)	1.7 (Lide, 2008)	5.10 (Leluk et al., 2010)	1
methane	16.04	kaolinite (Al)	DFT	16.4 (Budi et al., 2018)	8.4×10^{-11}	8.5 (Chickos and Acree, 2003)	2.59 (Lide, 2008)	0 (Yaws, 2014)	5.10 (Leluk et al., 2010)	0
ethane	30.07	kaolinite (Al)	DFT	22.2 (Budi et al., 2018)	9.1×10^{-10}	15.3 (Chickos and Acree, 2003)	4.45 (Lide, 2008)	0 (Yaws, 2014)	5.10 (Leluk et al., 2010)	0
benzene	78.11	kaolinite (Al)	DFT	37.6 (Budi et al., 2018)	5.0×10^{-7}	42.3 (Chickos and Acree, 2003)	10 (Lide, 2008)	0 (Yaws, 2014)	5.10 (Leluk et al., 2010)	0
methanol	32.04	kaolinite (Si)	DFT	21.2 (Budi et al., 2018)	6.0×10^{-10}	37.8 (Chickos and Acree, 2003)	3.28 (Lide, 2008)	1.7 (Lide, 2008)	5.10 (Leluk et al., 2010)	1
ethanol	46.07	kaolinite (Si)	DFT	23.2 (Budi et al., 2018)	1.4×10^{-9}	42.4 (Chickos and Acree, 2003)	5.41 (Lide, 2008)	1.69 (Lide, 2008)	5.10 (Leluk et al., 2010)	0.5
formic acid	46.03	kaolinite (Si)	DFT	21.2 (Budi et al., 2018)	6.0×10^{-10}	36 (Chickos and Acree, 2003)	3.4 (Lide, 2008)	1.425 (Lide, 2008)	5.10 (Leluk et al., 2010)	2
acetic acid	60.05	kaolinite (Si)	DFT	21.2 (Budi et al., 2018)	6.0×10^{-10}	41.6 (Chickos and Acree, 2003)	5.1 (Lide, 2008)	1.7 (Lide, 2008)	5.10 (Leluk et al., 2010)	1
methane	16.04	kaolinite (Si)	DFT	7.7 (Budi et al., 2018)	2.4×10^{-12}	8.5 (Chickos and Acree, 2003)	2.59 (Lide, 2008)	0 (Yaws, 2014)	5.10 (Leluk et al., 2010)	0
ethane	30.07	kaolinite (Si)	DFT	11.6 (Budi et al., 2018)	1.2×10^{-11}	15.3 (Chickos and Acree, 2003)	4.45 (Lide, 2008)	0 (Yaws, 2014)	5.10 (Leluk et al., 2010)	0
benzene	78.11	kaolinite (Si)	DFT	18.3 (Budi et al., 2018)	1.8×10^{-10}	42.3 (Chickos and Acree, 2003)	10 (Lide, 2008)	0 (Yaws, 2014)	5.10 (Leluk et al., 2010)	0
limonene up	136.24	SiO ₂	DFT	46.3 (Fang et al., 2019)	1.8×10^{-5}	49.6 (Chickos and Acree, 2003)	17.94 (Helburn et al., 2008)	0.7 (Svirbely et al., 1935)	4.42 (Lide, 2008)	0
limonene down	136.24	SiO ₂	DFT	41.6 (Fang et al., 2019)	2.6×10^{-6}	49.6 (Chickos and Acree, 2003)	17.94 (Helburn et al., 2008)	0.7 (Svirbely et al., 1935)	4.42 (Lide, 2008)	0
benzene	78.11	SiO ₂	DFT	27.5 (Fang et al., 2019)	8.0×10^{-9}	33.83 (Chickos and Acree, 2003)	10.44 (Bosque and Sales, 2002)	0 (Yaws, 2014)	4.42 (Lide, 2008)	0



cyclohexene	82.143	SiO ₂	DFT	29.2 (Fang et al., 2019)	1.6×10 ⁻⁸	33.5 (Chickos and Acree, 2003)	10.79 (Bosque and Sales, 2002)	0 (Yaws, 2014)	4.42 (Lide, 2008)	0
cyclohexane	84.16	SiO ₂	DFT	24.3 (Fang et al., 2019)	2.1×10 ⁻⁹	33 (Chickos and Acree, 2003)	11.04 (Bosque and Sales, 2002)	0 (Yaws, 2014)	4.42 (Lide, 2008)	0
limonene	136.24	Hydroxylated TiO ₂	MD	71 (Fan et al., 2022)	0.5	49.6 (Chickos and Acree, 2003)	17.94 (Helburn et al., 2008)	1.57 (Yaws, 2014)	86 (Lide, 2008)	0
carvone	150.22	Hydroxylated TiO ₂	MD	148.8 (Fan et al., 2022)	3.4×10 ¹³	58.2 (Hoskovec et al., 2005)	18.25 (Yankova et al., 2019)	3.56 (Yankova et al., 2019)	86 (Lide, 2008)	0.1
toluene	92.14	Nefta dust	DRIFTS	88.8 (Romanias et al., 2016)	6.9×10 ²	38.9 (Chickos and Acree, 2003)	12.12 (Lide, 2008)	0.375 (Lide, 2008)	~4.5 (Lide, 2008; Leluk et al., 2010)	0
toluene	92.14	Touggourt dust	DRIFTS	88.9 (Romanias et al., 2016)	7.0×10 ²	38.9 (Chickos and Acree, 2003)	12.12 (Lide, 2008)	0.375 (Lide, 2008)	~4.5 (Lide, 2008; Leluk et al., 2010)	0
toluene	92.14	N'Goussa dust	DRIFTS	88.5 (Romanias et al., 2016)	6.0×10 ²	38.9 (Chickos and Acree, 2003)	12.12 (Lide, 2008)	0.375 (Lide, 2008)	~4.5 (Lide, 2008; Leluk et al., 2010)	0
toluene	92.14	Bordj dust	DRIFTS	88.6 (Romanias et al., 2016)	6.1×10 ²	38.9 (Chickos and Acree, 2003)	12.12 (Lide, 2008)	0.375 (Lide, 2008)	~4.5 (Lide, 2008; Leluk et al., 2010)	0
toluene	92.14	Laayoune dust	DRIFTS	87.9 (Romanias et al., 2016)	4.6×10 ²	38.9 (Chickos and Acree, 2003)	12.12 (Lide, 2008)	0.375 (Lide, 2008)	~4.5 (Lide, 2008; Leluk et al., 2010)	0
toluene	92.14	Tarfaya dust	DRIFTS	87.7 (Romanias et al., 2016)	4.3×10 ²	38.9 (Chickos and Acree, 2003)	12.12 (Lide, 2008)	0.375 (Lide, 2008)	~4.5 (Lide, 2008; Leluk et al., 2010)	0
limonene	136.24	Nefta dust	DRIFTS	91.4 (Romanias et al., 2016)	2.0×10 ³	49.6 (Chickos and Acree, 2003)	17.94 (Helburn et al., 2008)	1.57 (Yaws, 2014)	~4.5 (Lide, 2008; Leluk et al., 2010)	0
limonene	136.24	Touggourt dust	DRIFTS	88.5 (Romanias et al., 2016)	6.0×10 ²	49.6 (Chickos)	17.94 (Helburn)	1.57 (Yaws, 2014)	~4.5 (Lide, 2008;)	0



						and Acree, 2003)	et al., 2008)		Leluk et al., 2010)	
limonene	136.24	N'Goussa dust	DRIFTS	91.6 (Romanias et al., 2016)	2.1×10^3	49.6 (Chickos and Acree, 2003)	17.94 (Helburn et al., 2008)	1.57 (Yaws, 2014)	~4.5 (Lide, 2008; Leluk et al., 2010)	0
limonene	136.24	Bordj dust	DRIFTS	91.8 (Romanias et al., 2016)	2.3×10^3	49.6 (Chickos and Acree, 2003)	17.94 (Helburn et al., 2008)	1.57 (Yaws, 2014)	~4.5 (Lide, 2008; Leluk et al., 2010)	0
limonene	136.24	Laayoune dust	DRIFTS	88.7 (Romanias et al., 2016)	6.4×10^2	49.6 (Chickos and Acree, 2003)	17.94 (Helburn et al., 2008)	1.57 (Yaws, 2014)	~4.5 (Lide, 2008; Leluk et al., 2010)	0
limonene	136.24	Tarfaya dust	DRIFTS	88.1 (Romanias et al., 2016)	5.0×10^2	49.6 (Chickos and Acree, 2003)	17.94 (Helburn et al., 2008)	1.57 (Yaws, 2014)	~4.5 (Lide, 2008; Leluk et al., 2010)	0

1104

1105

1106 **Table A8.** Compiled adsorbate-substrate interaction energies of inorganic and organic gas
 1107 species on ice. Gas species, gas species' molar mass, substrate, experimental or theoretical method,
 1108 desorption energy (E_{des}^0), and desorption lifetimes (τ_{des}) evaluated at 293 K using $A_{des} = 10^{13} \text{ s}^{-1}$,
 1109 enthalpy of vaporization (ΔH_{vap}), gas species' polarizability (α), gas species' dipole moment (μ),
 1110 substrate's relative permittivity (ϵ_r), and gas species' oxygen to carbon ration ($O:C$) are given.

Gas Species	Molar Mass / g mol ⁻¹	Substrate	Method	E_{des}^0 / kJ mol ⁻¹	$\tau_{des}^{293 K}$ / s	ΔH_{vap} (T) / kJ mol ⁻¹	α / 10 ⁻²⁴ cm ³	μ / D	ϵ_r	O:C
H ₂ O	18.02	ice	MB	48.3 (Brown et al., 1996)	4.1×10^{-5}	44 (Chickos and Acree, 2003)	1.45 (Lide, 2008)	1.85 (Lide, 2008)	97.5 (Lide, 2008; Auty and Cole, 1952)	0
H ₂ O	18.02	ice (170-230 K)	VM	43.1 (Delval and Rossi, 2005; Delval et al., 2003)	4.8×10^{-6}	44 (Chickos and Acree, 2003)	1.45 (Lide, 2008)	1.85 (Lide, 2008)	119.5 (Lide, 2008; Auty and Cole, 1952)	0
H ₂ O	18.02	ice	MD	50.0 (Schlesinger et al., 2020)	8.2×10^{-5}	44 (Chickos and Acree, 2003)	1.45 (Lide, 2008)	1.85 (Lide, 2008)	97.5 (Lide, 2008; Auty and Cole, 1952)	0
D ₂ O	20.03	ice	MB	42 (Kong et al., 2014a)	3.1×10^{-6}	45.14 (Crabtree	1.26 (Lide, 2008)	1.87 (Townes	97.5 (Lide,	0



						and Siman-Tov, 1993)		and Schawlow, 1975)	2008; Auty and Cole, 1952)	
CO ₂	44.01	amorphous ice	TPD	22.5 (Kim et al., 2008)	1.0×10 ⁻⁹	16.4 (Chickos and Acree, 2003)	2.91 (Lide, 2008)	0.0001 (Kolomiitsova et al., 2000)	97.5 (Lide, 2008; Auty and Cole, 1952)	0.5
n-hexane	86.18	ice	IGC	23.0 (Langenberg and Schurath, 2018)	1.3×10 ⁻⁹	31.5 (Chickos and Acree, 2003)	11.9 (Lide, 2008)	0	97.5 (Lide, 2008; Auty and Cole, 1952)	0
formaldehyde	30.03	ice	GCMC	30.0 (Hantal et al., 2007)	2.2×10 ⁻⁸	24.3 (Chickos and Acree, 2003)	2.63 (Lide, 2008)	2.33 (Lide, 2008)	97.5 (Lide, 2008; Auty and Cole, 1952)	1
acetaldehyde	44.05	ice	KU	29.1 (Crowley et al., 2010)	1.5×10 ⁻⁸	27.6 (Chickos and Acree, 2003)	4.6 (Lide, 2008)	2.75 (Lide, 2008)	97.5 (Lide, 2008; Auty and Cole, 1952)	0.5
methanol	32.04	ice	KU	51.0 (Winkler et al., 2002)	1.2×10 ⁻⁴	37.8 (Chickos and Acree, 2003)	3.28 (Lide, 2008)	1.7 (Lide, 2008)	97.5 (Lide, 2008; Auty and Cole, 1952)	0
acetone	58.08	ice	KU	48.6 (Crowley et al., 2010)	4.6×10 ⁻⁵	31.3 (Chickos and Acree, 2003)	6.37 (Lide, 2008)	2.88 (Lide, 2008)	97.5 (Lide, 2008; Auty and Cole, 1952)	0.33
formic acid	46.03	ice	KU	48.1 (Crowley et al., 2010)	3.8×10 ⁻⁵	36 (Chickos and Acree, 2003)	3.4 (Lide, 2008)	1.43 (Lide, 2008)	97.5 (Lide, 2008; Auty and Cole, 1952)	2
acetic acid	60.05	ice	KU	70.7 (Crowley et al., 2010)	0.4	41.6 (Chickos and Acree, 2003)	5.1 (Lide, 2008)	1.7 (Lide, 2008)	97.5 (Lide, 2008; Auty and Cole, 1952)	1
acetic acid	60.05	ice	KU	73.2 (Sokolov and Abbatt, 2002)	1.1	41.6 (Chickos and Acree, 2003)	5.1 (Lide, 2008)	1.7 (Lide, 2008)	97.5 (Lide, 2008; Auty and Cole, 1952)	1
1-pentanol	88.15	ice	KU	71.5 (Sokolov and Abbatt, 2002)	0.6	57.8 (Chickos and Acree, 2003)	10.61 (Bosque and Sales, 2002)	1.7 (liq.)(Lide, 2008)	97.5 (Lide, 2008; Auty and	0.2



									Cole, 1952)	
1-butanol	74.12	ice	KU	67.8 (Sokolov and Abbatt, 2002)	0.1	52.5 (Chickos and Acree, 2003)	8.88 (Lide, 2008)	1.66 (Lide, 2008)	97.5 (Lide, 2008; Auty and Cole, 1952)	0.25
ethanol	46.07	ice	KU	62.4 (Crowley et al., 2010)	1.3×10^{-2}	42.4 (Chickos and Acree, 2003)	5.41 (Lide, 2008)	1.69 (Lide, 2008)	97.5 (Lide, 2008; Auty and Cole, 1952)	0.5
ethanol	46.07	ice	KU	61.9 (Sokolov and Abbatt, 2002)	1.1×10^{-2}	42.4 (Chickos and Acree, 2003)	5.41 (Lide, 2008)	1.69 (Lide, 2008)	97.5 (Lide, 2008; Auty and Cole, 1952)	0.5
1-propanol	60.09	ice	GCMC	70.0 (Joliat et al.)	0.3	47.45 (Chickos and Acree, 2003)	6.74 (Lide, 2008)	1.58 (Lide, 2008)	97.5 (Lide, 2008; Auty and Cole, 1952)	0.33
2-propanol	60.09	ice	GCMC	71.5 (Joliat et al.)	0.6	47.45 (Chickos and Acree, 2003)	6.74 (Lide, 2008)	1.58 (Lide, 2008)	97.5 (Lide, 2008; Auty and Cole, 1952)	0.33
hexanal	100.16	ice	KU	64.9 (Sokolov and Abbatt, 2002)	3.7×10^{-2}	42.3 (Chickos and Acree, 2003)	11.9 (McEachran et al., 2018)	2.6 (Wiberg and Rablen, 1993; Bak et al., 2000)	97.5 (Lide, 2008; Auty and Cole, 1952)	0
peroxyacetylnitrate	121.05	ice	IGC	30.0 (Bartels-Rausch et al., 2002)	2.2×10^{-8}	34.6 (Stephenson and Malanowski, 1987)	8.27 (McEachran et al., 2018)		97.5 (Lide, 2008; Auty and Cole, 1952)	2.5
acetylene	26.04	ice	VS	15.5 (Silva and Devlin, 1994)	5.8×10^{-11}	16.7	3.40 (Gussoni et al., 1998)	0	97.5 (Lide, 2008; Auty and Cole, 1952)	0
ethylene	28.05	ice	VS	15.9 (Silva and Devlin, 1994)	6.8×10^{-11}	13.8	4.09 (Gussoni et al., 1998)	0	97.5 (Lide, 2008; Auty and Cole, 1952)	
benzene	78.11	ice	VS	18.0 (Silva and Devlin, 1994)	1.6×10^{-10}	33.5	9.96 (Gussoni et al., 1998)	0	97.5 (Lide, 2008; Auty and	



									Cole, 1952)	
HCl	36.46	ice (100-170 K)	TPD	28.0 (Isakson and Sitz, 1999)	9.8×10^{-9}	16.15 (Lide, 2008)	2.63 (Lide, 2008)	1.11 (Lide, 2008)	119.5 (Lide, 2008; Auty and Cole, 1952)	0
HOCl	52.46	ice (185-225K)	KU	39.6 (Crowley et al., 2010)	1.1×10^{-6}	36.66 (Joback and Reid, 1987)	3.31 (Hait and Head-Gordon, 2018)	1.3 (Lide, 2008)	119.5 (Lide, 2008; Auty and Cole, 1952)	0
H ₂ O ₂	34.01	ice	KU	31.6 (Pouvesle et al., 2010; Crowley et al., 2010)	4.3×10^{-8}	51.6 (Lide, 2008)	2.3 (Giguere, 1983)	1.57 (Lide, 2008)	97.5 (Lide, 2008; Auty and Cole, 1952)	0
NO	30.01	ice (93-150 K)	MB	15.4 (Lejonthun et al., 2014)	5.7×10^{-11}	13.83 (Lide, 2008)	1.7 (Lide, 2008)	0.16 (Lide, 2008)	119.5 (Lide, 2008; Auty and Cole, 1952)	0
NO ₂	46.01	ice (150-171 K)	MB	25.1 (Lejonthun et al., 2014)	3.0×10^{-9}	18.89	3.02 (Lide, 2008)	0.32 (Lide, 2008)	119.5 (Lide, 2008; Auty and Cole, 1952)	0
NO ₂	46.01	ice	IGC	22.0 (Bartels-Rausch et al., 2002)	8.4×10^{-10}	18.89	3.02 (Lide, 2008)	0.32 (Lide, 2008)	97.5 (Lide, 2008; Auty and Cole, 1952)	0
HONO	47.01	ice	KU	43.0 (Crowley et al., 2010)	4.6×10^{-6}		2.81 (Jensen et al., 2002)	1.42 (Lide, 2008)	97.5 (Lide, 2008; Auty and Cole, 1952)	0
N ₂ O ₅	108.01	ice (135-168 K)	MB	34.7 (Lejonthun et al., 2014)	1.6×10^{-7}	57.4 (Stull, 1947)	7.7 (Wincel et al., 1995)	0.5 (Grabow et al., 1996)	119.5 (Lide, 2008; Auty and Cole, 1952)	0
N ₂ O ₅	108.01	ice covered HNO ₃ (135-168 K)	MB	23.2 (Lejonthun et al., 2014)	1.3×10^{-9}	57.4 (Stull, 1947)	7.7 (Wincel et al., 1995)	0.5 (Grabow et al., 1996)	119.5 (Lide, 2008; Auty and Cole, 1952)	0
HNO ₃	63.01	ice	KU	38.1 (Crowley et al., 2010)	6.2×10^{-7}	39.1 (Lide, 2008)	3.55 (Jensen et al., 2002)	2.17 (Lide, 2008)	97.5 (Lide, 2008; Auty and Cole, 1952)	0



HO ₂ NO ₂	79.01	ice	KU	59.0 (Ulrich et al., 2012)	3.3×10 ⁻³			2.44 (Wei et al., 2011)	97.5 (Lide, 2008; Auty and Cole, 1952)	0
OH	17.01	ice (205-230 K)	MC	31.2 (Remorov and Bardwell, 2005)	3.6×10 ⁻⁸		7.11 (Zen et al., 2014)	1.65 (Lide, 2008)	119.5 (Lide, 2008; Auty and Cole, 1952)	0
O ₃	48.00	amorphous ice	TPD	20.0 (Borget et al., 2001)	3.7×10 ⁻¹⁰	12.2 (Stull, 1947)	3.21 (Lide, 2008)	0.53 (Lide, 2008)	97.5 (Lide, 2008; Auty and Cole, 1952)	0
SO ₂	64.07	ice	KU	17.2 (Crowley et al., 2010)	1.2×10 ⁻¹⁰	24.9 (Chickos and Acree, 2003)	4 (Lide, 2008)	1.63 (Lide, 2008)	97.5 (Lide, 2008; Auty and Cole, 1952)	0

1111

1112

1113 **Table A9.** Compiled adsorbate-substrate data for water vapor and inorganic gases adsorbed on
 1114 water and aqueous substrates. Gas species, gas species' molar mass, substrate, experimental or
 1115 theoretical method, desorption energy (E_{des}^0), and desorption lifetimes (τ_{des}) evaluated at 293 K
 1116 using $A_{des} = 10^{13} \text{ s}^{-1}$, enthalpy of vaporization (ΔH_{vap}) and solvation (ΔH_{solv}), gas species'
 1117 polarizability (α), gas species' dipole moment (μ), substrate's relative permittivity (ϵ_r), and gas
 1118 species' oxygen to carbon ration (O:C) are given.

Gas Species	Molar Mass / g mol ⁻¹	Substrate	Method	E_{des}^0 / kJ mol ⁻¹	$\tau_{des}^{293 K}$ / s	ΔH_{vap} (T) / kJ mol ⁻¹	α / 10 ⁻²⁴ cm ³	μ / D	ϵ_r	ΔH_{solv} (T) / kJ mol ⁻¹	O:C
H ₂ O	18.02	H ₂ O	MD	9.2 (Vieceli et al., 2004)	4.4×10 ⁻¹²	44 (Chickos and Acree, 2003)	1.45 (Lide, 2008)	1.85 (Lide, 2008)	80.2 (Lide, 2008)		0
H ₂ O	18.02	H ₂ O, 1.92 nm radius	MD	10.6 (Julin et al., 2013)	7.8×10 ⁻¹²	44 (Chickos and Acree, 2003)	1.45 (Lide, 2008)	1.85 (Lide, 2008)	80.2 (Lide, 2008)		0
H ₂ O	18.02	H ₂ O, 4.14 nm radius	MD	10.9 (Julin et al., 2013)	8.8×10 ⁻¹²	44 (Chickos and Acree, 2003)	1.45 (Lide, 2008)	1.85 (Lide, 2008)	80.2 (Lide, 2008)		0
H ₂ O	18.02	H ₂ O, planar	MD	11.4 (Julin et al., 2013)	1.1×10 ⁻¹¹	44 (Chickos and Acree, 2003)	1.45 (Lide, 2008)	1.85 (Lide, 2008)	80.2 (Lide, 2008)		0



H ₂ O	18.02	H ₂ O, planar	MD	9.05 (Julin et al., 2013)	4.1×10^{12}	44 (Chickos and Acree, 2003)	1.45 (Lide, 2008)	1.85 (Lide, 2008)	80.2 (Lide, 2008)		0
H ₂ O	18.02	H ₂ O, planar	MD	10.4 (Julin et al., 2013)	7.1×10^{12}	44 (Chickos and Acree, 2003)	1.45 (Lide, 2008)	1.85 (Lide, 2008)	80.2 (Lide, 2008)		0
H ₂ O	18.02	H ₂ O, planar	MD	10.3 (Julin et al., 2013)	6.9×10^{12}	44 (Chickos and Acree, 2003)	1.45 (Lide, 2008)	1.85 (Lide, 2008)	80.2 (Lide, 2008)		0
SO ₂	64.07	H ₂ O	KU	44.2 (Ammann et al., 2013; Jayne et al., 1990)	7.6×10^6	24.9 (Chickos and Acree, 2003)	4 (Lide, 2008)	1.633 (Lide, 2008)	80.2 (Lide, 2008)	24.11 (Sander et al., 2011)	0
NH ₃	17.03	H ₂ O	ST	41 (Donaldson, 1999)	2.0×10^6	22.7 (Chickos and Acree, 2003)	2.35 (Lide, 2008)	1.472 (Lide, 2008)	80.2 (Lide, 2008)	34.92 (Sander et al., 2011)	0
O ₃	48.00	H ₂ O	MD	14.7 (Vieceli et al., 2005)	4.2×10^{11}	12.2 (Stull, 1947)	3.21 (Lide, 2008)	0.533 (Lide, 2008)	80.2 (Lide, 2008)	23.28 (Sander et al., 2011)	0
H ₂ O ₂	34.01	H ₂ O	KU	26 (Worsnop et al., 1989)	4.3×10^9	51.16	2.3 (Giguere, 1983)	1.573 (Lide, 2008)	80.2 (Lide, 2008)	63.19 (Sander et al., 2011)	0
HCl	36.46	H ₂ SO ₄	KU	14.1 (Ammann et al., 2013; Behr et al., 2009; Robinson et al., 1998)	3.3×10^{11}	16.15	2.63 (Lide, 2008)	1.11 (Lide, 2008)	95 (Hall and Cole, 1981)	19.12 (Marsh and McElroy, 1985)	0
O ₃	48.00	shikimic acid (aqueous)	KU	20 (Berkemeier et al., 2016; Steimer et al., 2015)	3.7×10^{10}	12.2 (Stull, 1947)	3.21 (Lide, 2008)	0.533 (Lide, 2008)		23.28 (Sander et al., 2011)	0
N ₂ O ₅	108.01	H ₂ O	MD	15.4 (Cruzeiro et al., 2022)	5.6×10^{11}	57.4 (Stull, 1947)	7.7 (Wincel et al., 1995)	0.5 (Grabow et al., 1996)	80.2 (Lide, 2008)		0

1119

1120

1121 **Table A10.** Compiled absorbate-substrate data for volatile aromatic gases adsorbed on water. Gas
 1122 species, gas species' molar mass, substrate, experimental or theoretical method, desorption energy
 1123 (E_{des}^0), and desorption lifetimes (τ_{des}) evaluated at 293 K using $A_{des} = 10^{13} \text{ s}^{-1}$, enthalpy of
 1124 vaporization (ΔH_{vap}) and solvation (ΔH_{solv}), gas species' polarizability (α), gas species' dipole
 1125 moment (μ), substrate's relative permittivity (ϵ_r), and gas species' oxygen to carbon ration ($O:C$)
 1126 are given.



Gas Species	Molar Mass / g mol ⁻¹	Substrate	Method	E_{des}^0 / kJ mol ⁻¹	$\tau_{des}^{293 K}$ / s	$\Delta H_{vap}(T)$ / kJ mol ⁻¹	α / 10 ⁻²⁴ cm ³	μ / D	ϵ_r	$\Delta H_{solv}(T)$ / kJ mol ⁻¹	O:C
toluene	92.14	H ₂ O	ST	31 (Blank and Ottewill, 1964)	3.4×10^{-8}	38.9 (Chickos and Acree, 2003)	11.8 (Lide, 2008)	0.375 (Lide, 2008)	80.2 (Lide, 2008)	35.75 (Staudinger and Roberts, 2001; Sander, 2015)	0
toluene	92.14	H ₂ O	IGC	37.2 (Hartkopf and Karger, 1973)	4.3×10^{-7}	38.9 (Chickos and Acree, 2003)	11.8 (Lide, 2008)	0.375 (Lide, 2008)	80.2 (Lide, 2008)	35.75 (Staudinger and Roberts, 2001; Sander, 2015)	0
toluene	92.14	H ₂ O	ST	43.4 (Hauxwell and Ottewill, 1968)	5.5×10^{-6}	38.9 (Chickos and Acree, 2003)	11.8 (Lide, 2008)	0.375 (Lide, 2008)	80.2 (Lide, 2008)	35.75 (Staudinger and Roberts, 2001; Sander, 2015)	0
toluene	92.14	H ₂ O	IGC	28.8 (Goss, 2009)	1.4×10^{-8}	38.9 (Chickos and Acree, 2003)	11.8 (Lide, 2008)	0.375 (Lide, 2008)	80.2 (Lide, 2008)	35.75 (Staudinger and Roberts, 2001; Sander, 2015)	0
toluene	92.14	H ₂ O	ST	47.1 (Bruant and Conklin, 2002)	2.5×10^{-5}	38 (Chickos and Acree, 2003)	11.8 (Lide, 2008)	0.375 (Lide, 2008)	80.2 (Lide, 2008)	35.75 (Staudinger and Roberts, 2001; Sander, 2015)	0
benzene	78.11	H ₂ O	ST	41 (Bruant and Conklin, 2002)	2.0×10^{-6}	42.3 (Chickos and Acree, 2003)	10.53 (Lide, 2008)	0 (Yaws, 2014)	80.2 (Lide, 2008)	34.92 (Staudinger and Roberts, 2001; Sander, 2015)	0
benzene	78.11	H ₂ O	ST	25.8 (Blank and Ottewill, 1964)	4.0×10^{-9}	42.3 (Chickos and Acree, 2003)	10.53 (Lide, 2008)	0 (Yaws, 2014)	80.2 (Lide, 2008)	34.92 (Staudinger and Roberts, 2001; Sander, 2015)	0
benzene	78.11	H ₂ O	IGC	31.4 (Hartkopf and Karger, 1973)	4.0×10^{-8}	42.3 (Chickos and Acree, 2003)	10.53 (Lide, 2008)	0 (Yaws, 2014)	80.2 (Lide, 2008)	34.92 (Staudinger and Roberts, 2001; Sander, 2015)	0



benzene	78.11	H ₂ O	IGC	41 (Raja et al., 2002)	2.0×10^{-6}	42.3 (Chickos and Acree, 2003)	10.53 (Lide, 2008)	0 (Yaws, 2014)	80.2 (Lide, 2008)	34.92 (Staudinger and Roberts, 2001; Sander, 2015)	0
1,2-dimethylbenzene	106.17	H ₂ O	ST	45.9 (Bruant and Conklin, 2002)	1.5×10^{-5}	43.4 (Chickos and Acree, 2003)	14.5 (Lide, 2008)	0.63 (Yaws, 2014)	80.2 (Lide, 2008)	34.92 (Staudinger and Roberts, 2001; Sander, 2015)	0
1,3-dimethylbenzene	106.17	H ₂ O	ST	51.6 (Bruant and Conklin, 2002)	1.6×10^{-4}	42.7 (Chickos and Acree, 2003)	14.2 (Lide, 2008)	0.3 (Yaws, 2014)	80.2 (Lide, 2008)	34.92 (Staudinger and Roberts, 2001; Sander, 2015)	0
1,4-dimethylbenzene	106.17	H ₂ O	ST	46.5 (Bruant and Conklin, 2002)	1.9×10^{-5}	42.3 (Chickos and Acree, 2003)	14.27 (Lide, 2008)	0 (Yaws, 2014)	80.2 (Lide, 2008)	34.92 (Staudinger and Roberts, 2001; Sander, 2015)	0
1,3,5-trimethylbenzene	120.20	H ₂ O	ST	56.2 (Bruant and Conklin, 2002)	1.0×10^{-3}	47.6 (Chickos and Acree, 2003)	15.82 (Lide, 2008)	0.6 (Yaws, 2014)	80.2 (Lide, 2008)	34.92 (Sander, 2015)	0
ethylbenzene	106.17	H ₂ O	IGC	41.4 (Hartkopf and Karger, 1973)	2.4×10^{-6}	42.3 (Chickos and Acree, 2003)	14.2 (Lide, 2008)	0.59 (Lide, 2008)	80.2 (Lide, 2008)	42.40 (Staudinger and Roberts, 2001; Sander, 2015)	0
fluorobenzene	96.10	H ₂ O	IGC	32.6 (Hartkopf and Karger, 1973)	6.5×10^{-8}	34.5 (Chickos and Acree, 2003)	10.3 (Lide, 2008)	1.6 (Lide, 2008)	80.2 (Lide, 2008)	34.92 (Staudinger and Roberts, 2001; Sander, 2015)	0
chlorobenzene	112.56	H ₂ O	IGC	36.4 (Arp et al., 2006)	3.1×10^{-7}	46.2 (Chickos and Acree, 2003)	13.2 (Lide, 2008)	1.69 (Yaws, 2014)	80.2 (Lide, 2008)	31.59 (Staudinger and Roberts, 2001; Sander, 2015)	0
chlorobenzene	112.56	H ₂ O	IGC	35.1 (Hartkopf and Karger, 1973)	1.8×10^{-7}	46.2 (Chickos and Acree, 2003)	13.2 (Lide, 2008)	1.69 (Yaws, 2014)	80.2 (Lide, 2008)	31.59 (Staudinger and Roberts, 2001; Sander, 2015)	0



naphthalene	128.17	H ₂ O	IGC	67 (Raja et al., 2002)	8.8×10 ⁻²	53.4 (Chickos and Acree, 2003)	16.99 (Lide, 2008)	0 (Yaws, 2014)	80.2 (Lide, 2008)	44.07 (Fogg and Sangster, 2003; Sander, 2015)	0
naphthalene	128.17	H ₂ O	IGC	50.4 (Arp et al., 2006)	9.7×10 ⁻⁵	53.4 (Chickos and Acree, 2003)	16.99 (Lide, 2008)	0 (Yaws, 2014)	80.2 (Lide, 2008)	44.07 (Fogg and Sangster, 2003; Sander, 2015)	0
phenanthrene	178.23	H ₂ O	IGC	104 (Raja et al., 2002)	3.5×10 ⁵	78.7 (Chickos and Acree, 2003)	30.75 (Lide, 2008)	0 (Yaws, 2014)	80.2 (Lide, 2008)	34.92 (Fogg and Sangster, 2003; Sander, 2015)	0
1,2,3,4-tetrachlorobenzene	215.88	H ₂ O	IGC	54.5 (Arp et al., 2006)	5.2×10 ⁻⁴	60.1 (Chickos and Acree, 2003)	18.2 (McEachran et al., 2018)	2.42 (Lide, 2008)	80.2 (Lide, 2008)	39.91 (Sander, 2015; Tenhulshcher et al., 1992)	0
1,2,3,5-tetrachlorobenzene	215.88	H ₂ O	IGC	50.7 (Arp et al., 2006)	1.1×10 ⁻⁴	60.7 (Chickos and Acree, 2003)	18.2 (McEachran et al., 2018)	1.46 (Lide, 2008)	80.2 (Lide, 2008)		0
1,2,4,5-tetrachlorobenzene	215.88	H ₂ O	IGC	64.7 (Arp et al., 2006)	3.4×10 ⁻²	60.7 (Chickos and Acree, 2003)	18.2 (McEachran et al., 2018)	0.06 (Baron and Arevalo, 1988)	80.2 (Lide, 2008)		0
1,2,4-trichlorobenzene	181.44	H ₂ O	IGC	57.2 (Arp et al., 2006)	1.6×10 ⁻³	55.5 (Chickos and Acree, 2003)	16.32 (Bosque and Sales, 2002)	1.26 (in benzene) (Yaws, 2014)	80.2 (Lide, 2008)	37.62 (Sander, 2015)	0
1,2-dinitrobenzene	168.11	H ₂ O	IGC	69.2 (Goss, 2009)	2.2×10 ⁻¹	60 (Chickos and Acree, 2003)	15.6 (McEachran et al., 2018)	6.3 (in benzene) (Yaws, 2014)	80.2 (Lide, 2008)		0.67
1,3-dinitrobenzene	168.11	H ₂ O	IGC	59.2 (Goss, 2009)	3.6×10 ⁻³	96.7 (Chickos and Acree, 2003)	15.6 (McEachran et al., 2018)	3.84 (in benzene) (Yaws, 2014)	80.2 (Lide, 2008)		0.67
2,4-dinitrotoluene	168.11	H ₂ O	IGC	78.1 (Goss, 2009)	8.4	76.9 (Chickos and Acree, 2003)	17.5 (McEachran et al., 2018)	4.32 (in benzene) (Yaws, 2014)	80.2 (Lide, 2008)	24.11 (Sander, 2015; Goldstein, 1982)	0.67
1-methylnaphthalene	142.20	H ₂ O	IGC	48.4 (Arp et al., 2006)	4.2×10 ⁻⁵	62.4 (Chickos and Acree, 2003)	19.35 (Lide, 2008)	0.51 (in benzene) (Yaws, 2014)	80.2 (Lide, 2008)	50.72 (Fogg and Sangster, 2003; Sander, 2015)	0



2,3-dichlorophenol	163.0	H ₂ O	IGC	75.6 (Arp et al., 2006)	3.0	60.8 (Chickos and Acree, 2003)	15 (McEachran et al., 2018)		80.2 (Lide, 2008)		0.17
2,6-dichlorophenol	163.0	H ₂ O	IGC	65.4 (Arp et al., 2006)	4.6×10 ⁻²	57.9 (Chickos and Acree, 2003)	15 (McEachran et al., 2018)	5.03 (in benzene) (Oszust and Ratajczak, 1981)	80.2 (Lide, 2008)		0.17
2-chlorophenol	128.56	H ₂ O	IGC	57.9 (Arp et al., 2006)	2.1×10 ⁻³	47 (Chickos and Acree, 2003)	13.1 (McEachran et al., 2018)	1.33 (in benzene) (Yaws, 2014)	80.2 (Lide, 2008)	47.39 (Tabai et al., 1997; Sander, 2015)	0.17
2,4,5-trichlorophenol	197.44	H ₂ O	IGC	85.4 (Arp et al., 2006)	1.7×10 ²	54.5 (Chickos and Acree, 2003)	17 (McEachran et al., 2018)	2.4 (Baron and Arevalo, 1988)	80.2 (Lide, 2008)		0.17
2-nitroanisole	153.14	H ₂ O	IGC	65.4 (Arp et al., 2006)	4.6×10 ⁻²	58.6 (Chickos and Acree, 2003)	15.7 (Lide, 2008)	5 (liq.) (Lide, 2008)	80.2 (Lide, 2008)		0.43
2-nitrotoluene	137.14	H ₂ O	IGC	50.1 (Arp et al., 2006)	8.5×10 ⁻⁵	59.1 (Chickos and Acree, 2003)	14.9 (McEachran et al., 2018)	3.75 (in benzene) (Yaws, 2014)	80.2 (Lide, 2008)	24.11 (Sander, 2015; Baron and Arevalo, 1988)	0.29
2-phenylethyl acetate	164.20	H ₂ O	IGC	77.4 (Goss, 2009)	6.3	64.5 (Chickos and Acree, 2003)	18.6 (McEachran et al., 2018)	1.85 (in benzene) (Rajyam and Murty, 1966; Mopsik, 1967)	80.2 (Lide, 2008)		0.2
3(m)-nitroanisole	153.14	H ₂ O	IGC	55.6 (Arp et al., 2006)	8.2×10 ⁻⁴	49.8 (Chickos and Acree, 2003)	15.7 (Lide, 2008)	4.51 (Groves and Sudden, 1937)	80.2 (Lide, 2008)		0.43
4(p)-nitroanisole	153.14	H ₂ O	IGC	69.7 (Arp et al., 2006)	2.7×10 ⁻¹	54.2 (Chickos and Acree, 2003)	15.7 (Lide, 2008)	5.22 (Groves and Sudden, 1937)	80.2 (Lide, 2008)		0.43
acenaphthene	154.21	H ₂ O	IGC	60.8 (Arp et al., 2006)	6.9×10 ⁻³	66.2 (Chickos and Acree, 2003)	20.61 (Lide, 2008)	~0.85 (Lide, 2008)	80.2 (Lide, 2008)	54.04 (Fogg and Sangster, 2003; Sander, 2015)	0
acetophenone	120.15	H ₂ O	IGC	52.2 (Arp et al., 2006)	2.0×10 ⁻⁴	55.4 (Chickos and Acree, 2003)	15 (Lide, 2008)	3.02 (Lide, 2008)	80.2 (Lide, 2008)	64.02 (Staudinger and Roberts, 2001;	0



										Sander, 2015)	
α -HCH	290.81	H ₂ O	IGC	85.5 (Goss, 2009)	1.7×10^2		22.5 (McEachran et al., 2018)	2.2	80.2 (Lide, 2008)	54.04 (Sander, 2015)	0
anthracene	178.23	H ₂ O	IGC	64 (Arp et al., 2006)	2.6×10^{-2}	79.6 (Chickos and Acree, 2003)	25.67 (Lide, 2008)	0 (Yaws, 2014)	80.2 (Lide, 2008)	47.39 (Fogg and Sangster, 2003; Sander, 2015)	0
azobenzene	182.23	H ₂ O	IGC	74.4 (Arp et al., 2006)	1.8	72.8 (Chickos and Acree, 2003)	23.3 (McEachran et al., 2018)	0 (Merino and Ribagorda, 2012)	80.2 (Lide, 2008)		0
benzaldehyde	106.12	H ₂ O	IGC	53.9 (Goss, 2009)	4.1×10^{-4}	49.1 (Chickos and Acree, 2003)	12.7 (Bosque and Sales, 2002)	3 (liq.) (Lide, 2008)	80.2 (Lide, 2008)	45.73 (Fogg and Sangster, 2003; Sander, 2015)	0.14
benzyl acetate	150.18	H ₂ O	IGC	70.5 (Goss, 2009)	3.7×10^{-1}	55.5 (Chickos and Acree, 2003)	16.7 (McEachran et al., 2018)	1.22 (liq.) (Lide, 2008)	80.2 (Lide, 2008)		0.22
biphenyl	154.21	H ₂ O	IGC	59.5 (Arp et al., 2006)	4.0×10^{-3}	64.5 (Chickos and Acree, 2003)	20.2 (McEachran et al., 2018)	0 (Yaws, 2014)	80.2 (Lide, 2008)	38.80 (Sander, 2015)	0
bromobenzene	157.01	H ₂ O	IGC	31.2 (Arp et al., 2006)	3.6×10^{-8}	44.5 (Chickos and Acree, 2003)	13.62 (Lide, 2008)	1.7 (Lide, 2008)	80.2 (Lide, 2008)	34.92 (Fogg and Sangster, 2003; Sander, 2015)	0
dibenzofurane	168.20	H ₂ O	IGC	61.5 (Arp et al., 2006)	9.2×10^{-3}	66.2 (Chickos and Acree, 2003)	21.5	0.88 (in benzene) (Yaws, 2014)	80.2 (Lide, 2008)		0.08
ethylbenzene	106.17	H ₂ O	IGC	35.9 (Goss, 2009)	2.5×10^{-7}	42.3 (Chickos and Acree, 2003)	14.2 (Lide, 2008)	0.6 (Yaws, 2014)	80.2 (Lide, 2008)	41.16 (Sander, 2015)	0
<i>m</i> -cresol	108.14	H ₂ O	IGC	64.8 (Arp et al., 2006)	3.6×10^{-2}	62.5 (Chickos and Acree, 2003)	13.1 (McEachran et al., 2018)	1.48 (liq.) (Lide, 2008)	80.2 (Lide, 2008)	62.36 (Sander, 2015)	0.14
methylbenzoate	136.15	H ₂ O	IGC	54.8 (Goss, 2009)	5.9×10^{-4}	55.6 (Chickos and Acree, 2003)	15.06 (Bosque and Sales, 2002)	1.94 (liq.) (Lide, 2008)	80.2 (Lide, 2008)		0.25



<i>p</i> -cresol	108.14	H ₂ O	IGC	66.6 (Arp et al., 2006)	7.5×10 ⁻²	62 (Chickos and Acree, 2003)	13.2 (Bosque and Sales, 2002)	1.48 (liq.) (Lide, 2008)	80.2 (Lide, 2008)	62.63 (Sander, 2015)	0.14
phenanthrene	178.23	H ₂ O	IGC	66.5 (Arp et al., 2006)	7.2×10 ⁻²	78.7 (Chickos and Acree, 2003)	30.75 (Lide, 2008)	0 (Yaws, 2014)	80.2 (Lide, 2008)	34.92 (Fogg and Sangster, 2003; Sander, 2015)	0
phenol	94.11	H ₂ O	IGC	63 (Arp et al., 2006)	1.7×10 ⁻²	58.8 (Chickos and Acree, 2003)	10.52 (Lide, 2008)	1.224 (Lide, 2008)	80.2 (Lide, 2008)	49.61 (Sander, 2015)	0.17
propylbenzene	120.20	H ₂ O	IGC	47.2 (Goss, 2009)	2.6×10 ⁻⁵	46.2 (Chickos and Acree, 2003)	16 (McEachran et al., 2018)	0.37 (in benzene) (Yaws, 2014)	80.2 (Lide, 2008)	34.75 (Sander, 2015)	0
<i>p</i> -xylene	106.17	H ₂ O	IGC	35.5 (Goss, 2009)	2.1×10 ⁻⁷	42.3 (Chickos and Acree, 2003)	14.35 (Bosque and Sales, 2002)	0 (Yaws, 2014)	80.2 (Lide, 2008)	34.92 (Fogg and Sangster, 2003; Sander, 2015)	0
tetrahydrofuran	72.11	H ₂ O	IGC	42.6 (Arp et al., 2006)	3.9×10 ⁻⁶	32 (Chickos and Acree, 2003)	7.97 (Bosque and Sales, 2002)	1.75 (Lide, 2008)	80.2 (Lide, 2008)	35.75 (Sander, 2015)	0.25

1127

1128

1129 **Table A11.** Compiled adsorbate-substrate data for volatile amine and alcohol compounds
 1130 adsorbed on water. Gas species, gas species' molar mass, substrate, experimental or theoretical
 1131 method, desorption energy (E_{des}^0), and desorption lifetimes (τ_{des}) evaluated at 293 K using A_{des}
 1132 = 10^{13} s^{-1} , enthalpy of vaporization (ΔH_{vap}) and solvation (ΔH_{solv}), gas species' polarizability (α),
 1133 gas species' dipole moment (μ), substrate's relative permittivity (ϵ_r), and gas species' oxygen to
 1134 carbon ration ($O:C$) are given.

Gas Species	Molar Mass / g mol ⁻¹	Substrate	Method	E_{des}^0 / kJ mol ⁻¹	$\tau_{des}^{293 K}$ / s	ΔH_{vap} (T) / kJ mol ⁻¹	α / 10 ⁻²⁴ cm ³	μ / D	ϵ_r	ΔH_{solv} (T) / kJ mol ⁻¹	O:C
methylamine	31.06	H ₂ O	ST	28 (Mmerek i et al., 2000)	9.8×10 ⁻⁹	26.1 (Chickos and Acree, 2003)	4.24 (Lide, 2008)	1.31 (Lide, 2008)	80.2 (Lide, 2008)	33.67 (Sander, 2015)	0
dimethylamine	45.09	H ₂ O	ST	37 (Mmerek i et al., 2000)	3.9×10 ⁻⁷	27 (Chickos and Acree, 2003)	6.37 (Hickey and Rowley, 2014)	1.01 (Lide, 2008)	80.2 (Lide, 2008)	43.23 (Sander, 2015)	0
trimethylamine	59.11	H ₂ O	ST	34 (Mmerek i et al., 2000)	1.2×10 ⁻⁷	24.1 (Chickos and Acree, 2003)	8.15 (Hickey and Rowley, 2014)	0.612 (Lide, 2008)	80.2 (Lide, 2008)	49.6 (Leng et al., 2015)	0



methanol	32.04	H ₂ O	ST	39.2 (Donaldson and Anderson, 1999)	9.7×10 ⁻⁷	37.8 (Chickos and Acree, 2003)	3.28 (Lide, 2008)	1.7 (Lide, 2008)	80.2 (Lide, 2008)	46.56 (Sander, 2015; Sander et al., 2011)	0
1-propanol	60.09	H ₂ O	ST	68.2 (Donaldson and Anderson, 1999)	1.4×10 ⁻¹	47.45 (Chickos and Acree, 2003)	6.74 (Lide, 2008)	1.58 (Lide, 2008)	80.2 (Lide, 2008)	57.37 (Sander, 2015; Sander et al., 2011)	0.33
2-propanol	60.09	H ₂ O	ST	68.9 (Donaldson and Anderson, 1999)	1.9×10 ⁻¹	45.34 (Chickos and Acree, 2003)	7.29 (Lide, 2008)	1.58 (Lide, 2008)	80.2 (Lide, 2008)	62.36 (Sander, 2015; Sander et al., 2011)	0.33
1-propanol	60.09	H ₂ O	ST	58.8 (Demou and Donaldson, 2002)	3.0×10 ⁻³	47.45 (Chickos and Acree, 2003)	6.74 (Lide, 2008)	1.58 (Lide, 2008)	80.2 (Lide, 2008)	57.37 (Sander, 2015; Sander et al., 2011)	0.33
1-propanol	60.09	H ₂ O	ST	56.7 (Goss, 2009)	1.3×10 ⁻³	47.45 (Chickos and Acree, 2003)	6.74 (Lide, 2008)	1.58 (Lide, 2008)	80.2 (Lide, 2008)	57.37 (Sander, 2015; Sander et al., 2011)	0.33
1-butanol	74.12	H ₂ O	ST	62.8 (Donaldson and Anderson, 1999)	1.6×10 ⁻²	52.34 (Chickos and Acree, 2003)	8.88 (Lide, 2008)	1.66 (Lide, 2008)	80.2 (Lide, 2008)	62.36 (Sander, 2015; Sander et al., 2011)	0.25
2-butanol	74.12	H ₂ O	ST	63.5 (Donaldson and Anderson, 1999)	2.1×10 ⁻²	49.74 (Chickos and Acree, 2003)	8.77 (Bosque and Sales, 2002)	1.66 (Yaws, 2014)	80.2 (Lide, 2008)	60.70 (Sander, 2015; Sander et al., 2011)	0.25
1-butanol	74.12	H ₂ O	IGC	56.1 (Goss, 2009)	1.0×10 ⁻³	52.34 (Chickos and Acree, 2003)	8.88 (Lide, 2008)	1.66 (Lide, 2008)	80.2 (Lide, 2008)	62.36 (Sander, 2015; Sander et al., 2011)	0.25
ethanediol	62.07	H ₂ O	IGC	84.8 (Goss, 2009)	1.3×10 ²	65.6 (Chickos and Acree, 2003)	5.72 (Bosque and Sales, 2002)	2.36 (Lide, 2008)	80.2 (Lide, 2008)	73.17 (Compernelle and Muller, 2014; Sander, 2015)	1
ethanol	46.07	H ₂ O	IGC	51.1 (Goss, 2009)	1.3×10 ⁻⁴	42.4 (Chickos and Acree, 2003)	5.41 (Lide, 2008)	1.69 (Lide, 2008)	80.2 (Lide, 2008)	53.21 (Sander, 2015; Sander et al., 2011)	0.5
cyclohexanol	100.16	H ₂ O	IGC	79.5 (Goss, 2009)	1.5×10 ¹	62 (Chickos and Acree, 2003)	11.56 (Lide, 2008)	1.86 (in CCl ₄) (Yaws, 2014)	80.2 (Lide, 2008)	66.51 (Sander, 2015)	0.17
cyclopentanol	86.13	H ₂ O	IGC	62.7 (Goss, 2009)	1.5×10 ⁻²	57.5 (Chickos and Acree, 2003)	9.72 (Lide, 2008)		80.2 (Lide, 2008)	63.19 (Sander, 2015)	0.2



3-methylbutan-1-ol	88.15	H ₂ O	IGC	61.6 (Goss, 2009)	9.6×10 ⁻³	54.3 (Chickos and Acree, 2003)	10.61 (Lide, 2008)	1.88 (2- Methylbuta n-1-ol) (Lide, 2008)	80.2 (Lide, 2008)	63.19 (Kuhne et al., 2005)	0.2
1,2-propanediol	76.10	H ₂ O	IGC	64.5 (Goss, 2009)	3.2×10 ⁻²	58.6 (Chickos and Acree, 2003)	7.55 (Bosque and Sales, 2002)	2.25 (liq.) (Lide, 2008)	80.2 (Lide, 2008)	78.99 (Comperno lle and Muller, 2014; Sander, 2015)	0.67
1,3-propanediol	76.10	H ₂ O	IGC	75 (Goss, 2009)	2.3	72.4 (Chickos and Acree, 2003)	7.54 (McEachran et al., 2018)	2.55 (liq.) (Lide, 2008)	80.2 (Lide, 2008)	78.99 (Comperno lle and Muller, 2014; Sander, 2015)	0.67
1,4-butanediol	90.12	H ₂ O	IGC	105.1 (Goss, 2009)	5.4×10 ⁵	79.3 (Chickos and Acree, 2003)	9.35 (Bosque and Sales, 2002)	2.48 (liq.) (Lide, 2008)	80.2 (Lide, 2008)	91.46 (Comperno lle and Muller, 2014; Sander, 2015)	0.5
1-decanol	158.29	H ₂ O	IGC	94.8 (Goss, 2009)	7.9×10 ³	81.5 (Chickos and Acree, 2003)	19.83 (Bosque and Sales, 2002)	1.70 (Crossley, 1971)	80.2 (Lide, 2008)	49.47 (Sander, 2015)	0.1
1-heptanol	116.20	H ₂ O	IGC	75.7 (Goss, 2009)	3.1	66.5 (Chickos and Acree, 2003)	14.3 (Bosque and Sales, 2002)	1.74 (in benzene) (Yaws, 2014)	80.2 (Lide, 2008)	56.12 (Sander, 2015)	0.14
1-hexanol	102.18	H ₂ O	IGC	66.2 (Goss, 2009)	6.3×10 ⁻²	61.6 (Chickos and Acree, 2003)	12.46 (Bosque and Sales, 2002)	1.55 (Speight, 2017)	80.2 (Lide, 2008)	51.96 (Sander, 2015)	0.17
1-nonanol	144.26	H ₂ O	IGC	86.3 (Goss, 2009)	2.4×10 ²	76.9 (Chickos and Acree, 2003)	18 (McEachran et al., 2018)	1.61 (in benzene) (Yaws, 2014)	80.2 (Lide, 2008)	51.96 (Sander, 2015)	0.11
1-octanol	130.23	H ₂ O	IGC	75.7 (Goss, 2009)	3.1	71 (Chickos and Acree, 2003)	16.14 (Bosque and Sales, 2002)	1.76 (liq.) (Lide, 2008)	80.2 (Lide, 2008)	53.63 (Sander, 2015)	0.13
1-pentanol	88.15	H ₂ O	IGC	68.9 (Goss, 2009)	1.9×10 ⁻¹	57.8 (Chickos and Acree, 2003)	10.61 (Bosque and Sales, 2002)	1.7 (liq.) (Lide, 2008)	80.2 (Lide, 2008)	55.91 (Sander, 2015)	0.2
1-undecanol	172.31	H ₂ O	IGC	88 (Goss, 2009)	4.9×10 ²	83.5 (Chickos and Acree, 2003)	21.6 (McEachran et al., 2018)	1.67 (Yaws, 2014)	80.2 (Lide, 2008)		0.09
2-methylpropan-1-ol	74.12	H ₂ O	IGC	50.7 (Goss, 2009)	1.1×10 ⁻⁴	54.1 (Chickos and Acree, 2003)	8.92 (Lide, 2008)	1.64 (Lide, 2008)	80.2 (Lide, 2008)	59.86 (Kuhne et al., 2005)	0.25

1135

1136



1137 **Table A12.** Compiled adsorbate-substrate data for alkene and ketone compounds adsorbed on
 1138 water. Gas species, gas species' molar mass, substrate, experimental or theoretical method,
 1139 desorption energy (E_{des}^0), and desorption lifetimes (τ_{des}) evaluated at 293 K using $A_{des} = 10^{13} \text{ s}^{-1}$,
 1140 enthalpy of vaporization (ΔH_{vap}) and solvation (ΔH_{solv}), gas species' polarizability (α), gas
 1141 species' dipole moment (μ), substrate's relative permittivity (ϵ_r), and gas species' oxygen to
 1142 carbon ratio ($O:C$) are given.

Gas Species	Molar Mass / g mol ⁻¹	Substrate	Method	E_{des}^0 / kJ mol ⁻¹	$\tau_{des}^{293 K}$ / s	ΔH_{vap} (T) / kJ mol ⁻¹	α / 10 ⁻²⁴ cm ³	μ / D	ϵ_r	ΔH_{solv} (T) / kJ mol ⁻¹	O:C
1-decene	140.27	H ₂ O	IGC	47.5 (Goss, 2009)	2.9×10 ⁻⁵	50.4 (Chickos and Acree, 2003)	19.1 (McEachran et al., 2018)	0.42 (in benzene) (Yaws, 2014)	80.2 (Lide, 2008)		0
1-dodecene	168.32	H ₂ O	IGC	49 (Goss, 2009)	5.4×10 ⁻⁵	60.8 (Chickos and Acree, 2003)	22.7 (McEachran et al., 2018)	0.52 (in benzene) (Yaws, 2014)	80.2 (Lide, 2008)		0
1-tridecene	182.35	H ₂ O	IGC	52.7 (Goss, 2009)	2.5×10 ⁻⁴	65.3 (Chickos and Acree, 2003)	24.6 (McEachran et al., 2018)	0 (Yaws, 2014)	80.2 (Lide, 2008)		0
cis-2-octene	112.22	H ₂ O	IGC	36 (Hartkopf and Karger, 1973)	2.6×10 ⁻⁷	40.2 (Chickos and Acree, 2003)	15.5 (McEachran et al., 2018)	0.31 (Yaws, 2014)	80.2 (Lide, 2008)		0
trans-2-octene	112.22	H ₂ O	IGC	36 (Hartkopf and Karger, 1973)	2.6×10 ⁻⁷	40.2 (Chickos and Acree, 2003)	15.5 (McEachran et al., 2018)	0 (Yaws, 2014)	80.2 (Lide, 2008)		0
1-nonene	126.24	H ₂ O	IGC	44.3 (Goss, 2009)	7.9×10 ⁻⁶	44.7 (Chickos and Acree, 2003)	17.2 (McEachran et al., 2018)	0.36 (Yaws, 2014)	80.2 (Lide, 2008)		0
1-undecene	154.30	H ₂ O	IGC	54.1 (Goss, 2009)	4.4×10 ⁻⁴	54.3 (Chickos and Acree, 2003)	20.9 (McEachran et al., 2018)	0.53 (in benzene) (Yaws, 2014)	80.2 (Lide, 2008)		0
acetone	58.08	H ₂ O	ST	50.3 (Donaldson and Anderson, 1999)	9.3×10 ⁻⁵	31.3 (Chickos and Acree, 2003)	6.37 (Lide, 2008)	2.88 (Lide, 2008)	80.2 (Lide, 2008)	44.27 (Sander, 2015)	0.33
propanone	58.08	H ₂ O	IGC	42.9 (Arp et al., 2006)	4.4×10 ⁻⁶	31.3 (Chickos and Acree, 2003)	6.37 (Lide, 2008)	2.88 (=acetone) (Yaws, 2014)	80.2 (Lide, 2008)	44.27 (Sander, 2015)	0.33
pentanal	86.13	H ₂ O	IGC	46.7 (Goss, 2009)	2.1×10 ⁻⁵	38.3 (Chickos and Acree, 2003)	10.1 (McEachran et al., 2018)	2.57 (in benzene) (Yaws, 2014)	80.2 (Lide, 2008)	51.55 (Sander, 2015)	0.2
2,3-butanedione	86.09	H ₂ O	IGC	46.9 (Goss, 2009)	2.3×10 ⁻⁵	38.5 (Chickos and Acree, 2003)	8.2 (Lide, 2008)	1.03 (Henderson and Meyer, 1976)	80.2 (Lide, 2008)	51.55 (Sander, 2015)	0.5



2,5-hexanedione	114.14	H ₂ O	IGC	64.1 (Goss, 2009)	2.7×10 ⁻²	50.1 (Chickos and Acree, 2003)	11.9 (McEachran et al., 2018)	2.5 (in dioxane) (Wittwer et al., 1988)	80.2 (Lide, 2008)		0.33
2-butanone	72.11	H ₂ O	IGC	49.3 (Arp et al., 2006)	6.1×10 ⁻⁵	34.8 (Chickos and Acree, 2003)	8.25 (Bosque and Sales, 2002)	2.78 (Lide, 2008)	80.2 (Lide, 2008)	99.77	0.25
2-heptanone	114.19	H ₂ O	IGC	59.7 (Arp et al., 2006)	4.4×10 ⁻³	47.4 (Chickos and Acree, 2003)	13.7 (McEachran et al., 2018)	2.59 (liq.) (Lide, 2008)	80.2 (Lide, 2008)	46.56 (Sander, 2015)	0.14
2-hexanone	100.16	H ₂ O	IGC	47 (Arp et al., 2006)	2.4×10 ⁻⁵	43.1 (Chickos and Acree, 2003)	11.95 (Bosque and Sales, 2002)	2.66 (liq.) (Lide, 2008)	80.2 (Lide, 2008)	52.05 (Sander, 2015)	0.17
2-octanone	128.22	H ₂ O	IGC	63.2 (Arp et al., 2006)	1.8×10 ⁻²	52.6 (Chickos and Acree, 2003)	15.5 (McEachran et al., 2018)	2.7 (liq.) (Lide, 2008)	80.2 (Lide, 2008)	60.69 (Kuhne et al., 2005; Sander, 2015)	0.13
2-pentanone	86.13	H ₂ O	IGC	43.2 (Arp et al., 2006)	5.0×10 ⁻⁶	38.3 (Chickos and Acree, 2003)	9.93 (Lide, 2008)	2.7 (liq.) (Lide, 2008)	80.2 (Lide, 2008)	41.85 (Sander, 2015)	0.2
cyclopentanone	84.19	H ₂ O	IGC	54.1 (Arp et al., 2006)	4.4×10 ⁻⁴	42.7 (Chickos and Acree, 2003)	9.19 (McEachran et al., 2018)	3.3 (liq.) (Lide, 2008)	80.2 (Lide, 2008)	48.22 (Kuhne et al., 2005; Sander, 2015)	0.2

1143

1144

1145 **Table A13.** Compiled absorbate-substrate data for volatile acid and ether compounds adsorbed on
 1146 water. Gas species, gas species' molar mass, substrate, experimental or theoretical method,
 1147 desorption energy (E_{des}^0), and desorption lifetimes (τ_{des}) evaluated at 293 K using $A_{des} = 10^{13} \text{ s}^{-1}$,
 1148 enthalpy of vaporization (ΔH_{vap}) and solvation (ΔH_{solv}), gas species' polarizability (α), gas
 1149 species' dipole moment (μ), substrate's relative permittivity (ϵ_r), and gas species' oxygen to
 1150 carbon ration (O:C) are given.

Gas Species	Molar Mass / g mol ⁻¹	Substrate	Method	E_{des}^0 / kJ mol ⁻¹	$\tau_{des}^{293 \text{ K}}$ / s	ΔH_{vap} (T) / kJ mol ⁻¹	α / 10 ⁻²⁴ cm ³	μ / D	ϵ_r	ΔH_{solv} (T) / kJ mol ⁻¹	O:C
acetic acid	60.05	H ₂ O	ST	58.8 (Donaldson and Anderson, 1999)	3.0×10 ⁻³	41.6 (Chickos and Acree, 2003)	5.1 (Lide, 2008)	1.7 (Lide, 2008)	80.2 (Lide, 2008)	51.96 (Sander, 2015)	1
propionic acid	74.08	H ₂ O	ST	61.4 (Donaldson and Anderson, 1999)	8.8×10 ⁻³	31.1 (Chickos and Acree, 2003)	6.9 (Lide, 2008)	1.75 (Lide, 2008)	80.2 (Lide, 2008)	56.54 (Abraham, 1984; Sander, 2015)	0.67
butanoic acid	88.11	H ₂ O	ST	58.6 (Donaldson and Anderson, 1999)	2.8×10 ⁻³	40.5 (Chickos and Acree, 2003)	8.58 (Lide, 2008)	1.65 (liq.) (Lide, 2008)	80.2 (Lide, 2008)	59.86 (Abraham, 1984; Sander, 2015)	0.5



hexanoic acid	116.16	H ₂ O	ST	57.6 (Demou and Donaldson, 2002)	1.9×10 ⁻³	69.2 (Chickos and Acree, 2003)	12.5	1.13 (liq.) (Lide, 2008)	80.2 (Lide, 2008)	50.72 (Staudinger and Roberts, 2001; Sander, 2015)	0.33
methyl formate	60.05	H ₂ O	IGC	32.6 (Hartkopf and Karger, 1973)	6.5×10 ⁻⁸	31.6 (Chickos and Acree, 2003)	5.05 (Lide, 2008)	1.77 (Lide, 2008)	80.2 (Lide, 2008)	33.26 (Sander, 2015; Sander et al., 2011)	1
ethyl formate	74.08	H ₂ O	IGC	28.9 (Hartkopf and Karger, 1973)	1.4×10 ⁻⁸	31.6 (Chickos and Acree, 2003)	6.88 (Lide, 2008)	1.93 (Lide, 2008)	80.2 (Lide, 2008)	38.25 (Sander, 2015; Sander et al., 2011)	0.67
butyl acetate	116.16	H ₂ O	IGC	60.4 (Goss, 2009)	5.9×10 ⁻³	41.3 (Chickos and Acree, 2003)	12.57 (Bosque and Sales, 2002)	1.87 (liq.) (Lide, 2008)	80.2 (Lide, 2008)	46.01 (Sander, 2015)	0.33
Diethyl phthalate	222.24	H ₂ O	IGC	94.6 (Goss, 2009)	7.3×10 ³	81.8 (Chickos and Acree, 2003)	23.4 (McEachran et al., 2018)	2.73 (in benzene) (Yaws, 2014)	80.2 (Lide, 2008)	100.7 (Kuhne et al., 2005)	0.33
dimethyl oxalate	118.09	H ₂ O	IGC	48.2 (Goss, 2009)	3.9×10 ⁻⁵	48.8 (Chickos and Acree, 2003)	9.57 (McEachran et al., 2018)	2 (in m-xylene) (Aihara and Davies, 1956)	80.2 (Lide, 2008)		1
dimethyl phthalate	194.19	H ₂ O	IGC	84 (Goss, 2009)	9.4×10 ¹	77.2 (Chickos and Acree, 2003)	19.7 (McEachran et al., 2018)	2.78 (in benzene) (Yaws, 2014)	80.2 (Lide, 2008)		0.4
dimethyl succinate	146.14	H ₂ O	IGC	63.3 (Goss, 2009)	1.9×10 ⁻²	49.3 (Chickos and Acree, 2003)	13.2 (McEachran et al., 2018)	2.16 (in benzene) (Yaws, 2014)	80.2 (Lide, 2008)	64.85 (Sander, 2015)	0.5
pentyl acetate	130.19	H ₂ O	IGC	58.3 (Goss, 2009)	2.5×10 ⁻³	48.6 (Chickos and Acree, 2003)	14.9 (Lide, 2008)	1.75 (Lide, 2008)	80.2 (Lide, 2008)	54.04 (Kieckbusch and King, 1979; Sander, 2015)	0.29
ethyl acetate	88.11	H ₂ O	IGC	47 (Goss, 2009)	2.4×10 ⁻⁵	35.1 (Chickos and Acree, 2003)	8.62 (Lide, 2008)	1.78 (Lide, 2008)	80.2 (Lide, 2008)	49.05 (Sander, 2015; Sander et al., 2011)	0.5
di-n-butyl ether	130.23	H ₂ O	IGC	57.4 (Arp et al., 2006)	1.7×10 ⁻³	45 (Chickos and Acree, 2003)	16.31 (Bosque and Sales, 2002)	~1.17 (Lide, 2008)	80.2 (Lide, 2008)	54.87 (Kuhne et al., 2005; Sander, 2015)	0.125
di-n-pentyl ether	158.28	H ₂ O	IGC	59.6 (Arp et al., 2006)	4.2×10 ⁻³	46.2 (Chickos and Acree, 2003)	19.9 (McEachran et al., 2018)	~1.2 (liq.) (Lide, 2008)	80.2 (Lide, 2008)		0.1
ethyl-t-butyl ether	102.18	H ₂ O	IGC	47.9 (Arp et al., 2006)	3.5×10 ⁻⁵	33.5 (Chickos and Acree, 2003)	12.5 (McEachran et al., 2018)	1.22 (in benzene)	80.2 (Lide, 2008)	39.2 (Kuhne et al., 2005)	0.17



				al., 2006)		and Acree, 2003)		(Yaws, 2014)			
methyl tert-butyl ether	88.15	H ₂ O	IGC	38.7 (Arp et al., 2006)	7.9×10 ⁻⁷	30.4 (Chickos and Acree, 2003)	10.7 (McEachran et al., 2018)	1.36 (in benzene) (Yaws, 2014)	80.2 (Lide, 2008)	45.97 (Sander, 2015)	0.2
n-propyl ether	102.18	H ₂ O	IGC	53.6 (Hartkopf and Karger, 1973)	3.6×10 ⁻⁴	35.7 (Chickos and Acree, 2003)	12.5 (McEachran et al., 2018)	1.21 (Yaws, 2014)	80.2 (Lide, 2008)	61.80 (Sander, 2015)	0.17

1151

1152

1153 **Table A14.** Compiled adsorbate-substrate data for volatile alkane compounds adsorbed on water.

1154 Gas species, gas species' molar mass, substrate, experimental or theoretical method, desorption energy (E_{des}^0), and desorption lifetimes (τ_{des}) evaluated at 293 K using $A_{des} = 10^{13} \text{ s}^{-1}$, enthalpy of vaporization (ΔH_{vap}) and solvation (ΔH_{solv}), gas species' polarizability (α), gas species' dipole moment (μ), substrate's relative permittivity (ϵ_r), and gas species' oxygen to carbon ratio (O:C) are given.

Gas Species	Molar Mass / g mol ⁻¹	Substrate	Method	E_{des}^0 / kJ mol ⁻¹	$\tau_{des}^{293 K}$ / s	ΔH_{vap} (T) / kJ mol ⁻¹	α / 10 ⁻²⁴ cm ³	μ / D	ϵ_r	ΔH_{solv} (T) / kJ mol ⁻¹	O:C
decane	142.29	H ₂ O	IGC	46.5 (Goss, 2009)	1.9×10 ⁻⁵	51.4 (Chickos and Acree, 2003)	19.1 (Lide, 2008)	0 (Yaws, 2014)	80.2 (Lide, 2008)		0
dodecane	170.34	H ₂ O	IGC	58.1 (Goss, 2009)	2.3×10 ⁻³	62.1 (Chickos and Acree, 2003)	22.75 (Laib and Mittleman, 2010)	0 (Yaws, 2014)	80.2 (Lide, 2008)		0
nonane	128.26	H ₂ O	IGC	34.6 (Goss, 2009)	1.5×10 ⁻⁷	46.55 (Chickos and Acree, 2003)	17.36 (Laib and Mittleman, 2010)	0 (Yaws, 2014)	80.2 (Lide, 2008)	34.50 (Sander et al., 2011)	0
tetradecane	198.39	H ₂ O	IGC	67.6 (Goss, 2009)	1.1×10 ⁻¹	71.73 (Chickos and Acree, 2003)	26.22 (Laib and Mittleman, 2010)	0 (Yaws, 2014)	80.2 (Lide, 2008)		0
tridecane	184.37	H ₂ O	IGC	58.2 (Goss, 2009)	2.4×10 ⁻³	66.68 (Chickos and Acree, 2003)	24.41 (Laib and Mittleman, 2010)	0 (Yaws, 2014)	80.2 (Lide, 2008)		0
trimethyl phosphite	124.08	H ₂ O	IGC	77.4 (Arp et al., 2006)	6.3	42.5 (Chickos and Acree, 2003)	28.6 (Aroney et al., 1964)		80.2 (Lide, 2008)		1
undecane	156.31	H ₂ O	IGC	52.8 (Goss, 2009)	2.6×10 ⁻⁴	56.58 (Chickos and Acree, 2003)	21.03 (Lide, 2008)	0 (Yaws, 2014)	80.2 (Lide, 2008)		0
n-pentane	72.15	H ₂ O	IGC	23.8 (Hartkopf and Karger, 1973)	1.7×10 ⁻⁹	25 (Chickos and Acree, 2003)	9.99 (Lide, 2008)	0 (Yaws, 2014)	80.2 (Lide, 2008)	25.77 (Sander et al., 2011)	0



n-hexane	86.18	H ₂ O	IGC	27.6 (Hartkopf and Karger, 1973)	8.3×10 ⁻⁹	31.5 (Chickos and Acree, 2003)	11.9 (Lide, 2008)	0 (Yaws, 2014)	80.2 (Lide, 2008)	46.89 (Sander et al., 2011)	0
n-heptane	100.21	H ₂ O	IGC	31.4 (Hartkopf and Karger, 1973)	4.0×10 ⁻⁸	36.6 (Chickos and Acree, 2003)	13.61 (Lide, 2008)	0 (Yaws, 2014)	80.2 (Lide, 2008)	34.64 (Sander et al., 2011)	0
n-octane	114.23	H ₂ O	IGC	35.6 (Hartkopf and Karger, 1973)	2.2×10 ⁻⁷	41.6 (Chickos and Acree, 2003)	15.9 (Lide, 2008)	0 (Yaws, 2014)	80.2 (Lide, 2008)	45.31 (Sander et al., 2011)	0
n-nonane	128.26	H ₂ O	IGC	39.7 (Hartkopf and Karger, 1973)	1.2×10 ⁻⁶	46.55 (Chickos and Acree, 2003)	17.36 (Lide, 2008)	0 (Yaws, 2014)	80.2 (Lide, 2008)	34.50 (Sander et al., 2011)	0
n-decane	142.29	H ₂ O	IGC	44.8 (Hartkopf and Karger, 1973)	9.7×10 ⁻⁶	51.4 (Chickos and Acree, 2003)	19.1 (Lide, 2008)	0 (Yaws, 2014)	80.2 (Lide, 2008)		0
2-methylheptane	114.23	H ₂ O	IGC	34.7 (Hartkopf and Karger, 1973)	1.5×10 ⁻⁷	46.55 (Chickos and Acree, 2003)	15.5 (McEachran et al., 2018)	0 (Yaws, 2014)	80.2 (Lide, 2008)		0
2,4-dimethylhexane	114.23	H ₂ O	IGC	33.5 (Hartkopf and Karger, 1973)	9.4×10 ⁻⁸	71.73 (Chickos and Acree, 2003)	15.5 (McEachran et al., 2018)	0 (Yaws, 2014)	80.2 (Lide, 2008)	38.5 (2,5-dimethylhexane) (Kuhne et al., 2005)	0
2,2,4-trimethylpentane	114.23	H ₂ O	IGC	32.2 (Hartkopf and Karger, 1973)	5.5×10 ⁻⁸	66.68 (Chickos and Acree, 2003)	15.44 (Lide, 2008)	0 (Yaws, 2014)	80.2 (Lide, 2008)	36.17 (Sander et al., 2011)	0
cycloheptane	98.19	H ₂ O	IGC	31.4 (Hartkopf and Karger, 1973)	4.0×10 ⁻⁸	42.5 (Chickos and Acree, 2003)	12.84 (Bosque and Sales, 2002)	0 (Yaws, 2014)	80.2 (Lide, 2008)		0
cyclooctane	112.22	H ₂ O	IGC	35.6 (Hartkopf and Karger, 1973)	2.2×10 ⁻⁷	56.58 (Chickos and Acree, 2003)	14.62 (Bosque and Sales, 2002)	0 (Yaws, 2014)	80.2 (Lide, 2008)	39.63 (Sander et al., 2011)	0
trichloroethane	133.40	H ₂ O	ST	26.3 (Bruant and Conklin, 2001)	4.9×10 ⁻⁹	32.5 (Chickos and Acree, 2003)	10.7 (Lide, 2008)	1.78 (Yaws, 2014)	80.2 (Lide, 2008)	32.15 (Sander et al., 2011)	0
dichloromethane	84.93	H ₂ O	IGC	23.4 (Hartkopf and Karger, 1973)	1.5×10 ⁻⁹	30.6 (Chickos and Acree, 2003)	6.49 (McEachran et al., 2018)	1.60 (Yaws, 2014)	80.2 (Lide, 2008)	33.26 (Sander et al., 2011)	0



				r_r , 1973)							
chloroform	119.37	H ₂ O	IGC	26.8 (Hartkopf and Karger, 1973)	6.0×10^{-9}	31.1 (Chickos and Acree, 2003)	8.87 (Lide, 2008)	1.01 (Yaws, 2014)	80.2 (Lide, 2008)	37.00 (Sander et al., 2011)	0
carbon tetrachloride	153.81	H ₂ O	IGC	23.4 (Hartkopf and Karger, 1973)	1.5×10^{-9}	32.4 (Chickos and Acree, 2003)	10.85 (Lide, 2008)	0 (Yaws, 2014)	80.2 (Lide, 2008)	35.13 (Sander et al., 2011)	0
1,2-dichloroethane	98.95	H ₂ O	IGC	32.6 (Hartkopf and Karger, 1973)	6.5×10^{-8}	35.2 (Chickos and Acree, 2003)	8 (Lide, 2008)	1.83 (Lide, 2008)	80.2 (Lide, 2008)	35.47 (Sander et al., 2011)	0

1159

1160

1161 **Table A15.** Compiled absorbate-substrate data for volatile acid and alcohol compounds adsorbed
 1162 on aqueous solutions. Gas species, gas species' molar mass, substrate, experimental or theoretical
 1163 method, desorption energy (E_{des}^0), and desorption lifetimes (τ_{des}) evaluated at 293 K using A_{des}
 1164 = 10^{13} s^{-1} , enthalpy of vaporization (ΔH_{vap}) and solvation (ΔH_{solv}), gas species' polarizability (α),
 1165 gas species' dipole moment (μ), substrate's relative permittivity (ϵ_r), and gas species' oxygen to
 1166 carbon ration (O:C) are given.

Gas Species	Molar Mass / g mol ⁻¹	Substrate	Method	E_{des}^0 / kJ mol ⁻¹	$\tau_{des}^{293 K}$ / s	ΔH_{vap} (T) / kJ mol ⁻¹	α / 10 ⁻²⁴ cm ³	μ / D	ϵ_r	ΔH_{solv} (T) / kJ mol ⁻¹	O:C
hexanoic acid	116.16	4 M NaCl (aq)	ST	54.2 (Demou and Donaldson, 2002)	4.6×10^{-4}	69.2 (Chickos and Acree, 2003)	12.5 (McEachran et al., 2018)	1.13 (liq.) (Lide, 2008)	40 (Maribomogensen et al., 2013)	50.72 (Staudinger and Roberts, 2001; Sander, 2015)	0.33
hexanoic acid	116.16	4 M (NH ₄) ₂ SO ₄ (aq)	ST	55.4 (Demou and Donaldson, 2002)	7.5×10^{-4}	69.2 (Chickos and Acree, 2003)	12.5 (McEachran et al., 2018)	1.13 (liq.) (Lide, 2008)	42 (Lileev and Lyashchenko, 2009)	50.72 (Staudinger and Roberts, 2001; Sander, 2015)	0.33
1-propanol	60.09	4 M NaCl (aq)	ST	58.7 (Demou and Donaldson, 2002)	2.9×10^{-3}	47.45 (Chickos and Acree, 2003)	6.74 (Lide, 2008)	1.58 (Lide, 2008)	40 (Maribomogensen et al., 2013)	57.37 (Sander, 2015; Sander et al., 2011)	0.33



1-propanol	60.09	4 M (NH ₄) ₂ SO ₄ (aq)	ST	58.9 (Demou and Donalds on, 2002)	3.2×10 ⁻³	47.45 (Chickos and Acree, 2003)	6.74 (Lide, 2008)	1.58 (Lide, 2008)	42 (Lileev and Lyashch enko, 2009)	57.37 (Sander, 2015; Sander et al., 2011)	0.33
------------	-------	--	----	--	----------------------	--	----------------------	----------------------	---	---	------

1167

1168 **Data availability.** Data needed to draw the conclusions in the present study are given in the paper
1169 and in the Supplement. In addition, the datasets required to reproduce the results and corresponding
1170 figures are available on Zenodo (Knopf et al., 2023).

1171

1172 **Supplement.** The supplement related to this article is available online at: XYZ

1173

1174 **Author contributions.** DAK and MS envisioned the project. DAK supervised project, performed
1175 correlation analyses, and wrote first draft of manuscript. MS performed kinetic flux modeling.
1176 MA, TB, and UP critically discussed analyses and results and were involved in representation of
1177 data. All authors discussed interpretation of the data and contributed to the writing of the paper.

1178

1179 **Competing interests.** At least one of the (co-)authors is a member of the editorial board of
1180 Atmospheric Chemistry and Physics.

1181

1182

1183 **Disclaimer.** Publisher's note: Copernicus Publications remains neutral with regard to
1184 jurisdictional claims in published maps and institutional affiliations.



1185

1186 **Acknowledgments.** D.K. acknowledges support by the U.S. National Science Foundation (grant
1187 no. AGS-1446286) and the Max-Planck Society to support a sabbatical stay in 2014 that initiated
1188 this project. M.S. acknowledges support by the U.S. National Science Foundation (grant no. AGS-
1189 1654104) and the U.S. Department of Energy (grant no DE-SC0022139). M. A. acknowledges
1190 support by the Swiss National Science Foundation (grant no. 188662).

1191

1192 **Financial support.** This research has been supported by the U.S. National Science Foundation
1193 (grant nos. AGS-1446286 and AGS-1654104), the U.S. Department of Energy (DE-SC0022139),
1194 and the Swiss National Science Foundation (grant no. 188662).

1195

1196

1197

1198

1199

1200

1201

1202

1203

1204

1205

1206

1207

1208

1209

1210



1211 **Table 1.** Intermolecular forces for selected functional groups and gases (Jeffrey, 1997; Jeffrey
1212 and Saenger, 1991; Vinogradov and Linnell, 1971; IUPAC, 1997).

Functional Group	London dispersion force	Keesom force	Hydrogen Bonding
Alkane	Increases with chain length	none	None with itself.
Ether	Increases with chain length	Slightly polar, 1 O	None with itself. H-bond acceptor (max. 2) of other molecules
Ester	Increases with chain length	More polar than ether, 1 O	None with itself. H-bond acceptor (max. 2) of other molecules
Amine	Increases with chain length	Polar, 1 N	0-2 H-bonds with itself. <i>Primary:</i> H-bond donor (max. 2) and acceptor (max. 1). <i>Secondary:</i> H-bond donor (max. 1) and acceptor (max. 1). <i>Tertiary:</i> H-bond acceptor (max. 1).
Imine	Increases with chain length	Polar, 1 N	1-2 H-bonds with itself. <i>Primary:</i> H-bond donor (max. 1) and acceptor (max. 1). <i>Secondary:</i> H-bond acceptor (max. 1). <i>Tertiary:</i> H-bond acceptor (max. 1).
Aldehyde / Ketone	Increases with chain length	Polar C=O manifest strong dipole	None with itself. H-bond acceptor (max. 2) of other molecules
Alcohol	Increases with chain length	Polar, 1 O	2 H-bonds with itself. H-bond donor (max. 1) and acceptor (max. 2).
Acid	Increases with chain length	Polar, 2 O	2 H-bonds with itself forming dimer increasing molecule size. H-bond donor (max. 1) and acceptor (max. 4).
Amide	Increases with chain length	Polar, strong dipole 1 N & 1 O	2 H-bonds with itself. H-bond donor (max. 2) and acceptor (max. 3).
Other Species	Vapor pressure	Polar	
N ₂ O ₅	100 hPa @ 3.9 °C	Yes	None with itself. H-bond acceptor (max. 12).
HONO		Yes	2 H-bonds with itself. H-bond donor (max. 1) and acceptor (max. 5).
NH ₃	100 hPa @ -71.3 °C	Yes	2 H-bonds with itself.



			H-bond donor (max. 3) and acceptor (max. 1).
HNO ₃	100 hPa @ 28.4 °C	Yes	2 H-bonds with itself. H-bond donor (max. 1) and acceptor (max. 7).
H ₂ SO ₄	100 hPa @ 248 °C	Yes	4 H-bonds with itself. H-bond donor (max. 2) and acceptor (max. 8).
H ₂ O	100 hPa @ 45.8 °C	Yes	4 H-bonds with itself. H-bond donor (max. 2) and acceptor (max. 2).

1213

1214

1215

1216

1217

1218

1219

1220

1221

1222

1223

1224

1225

1226

1227

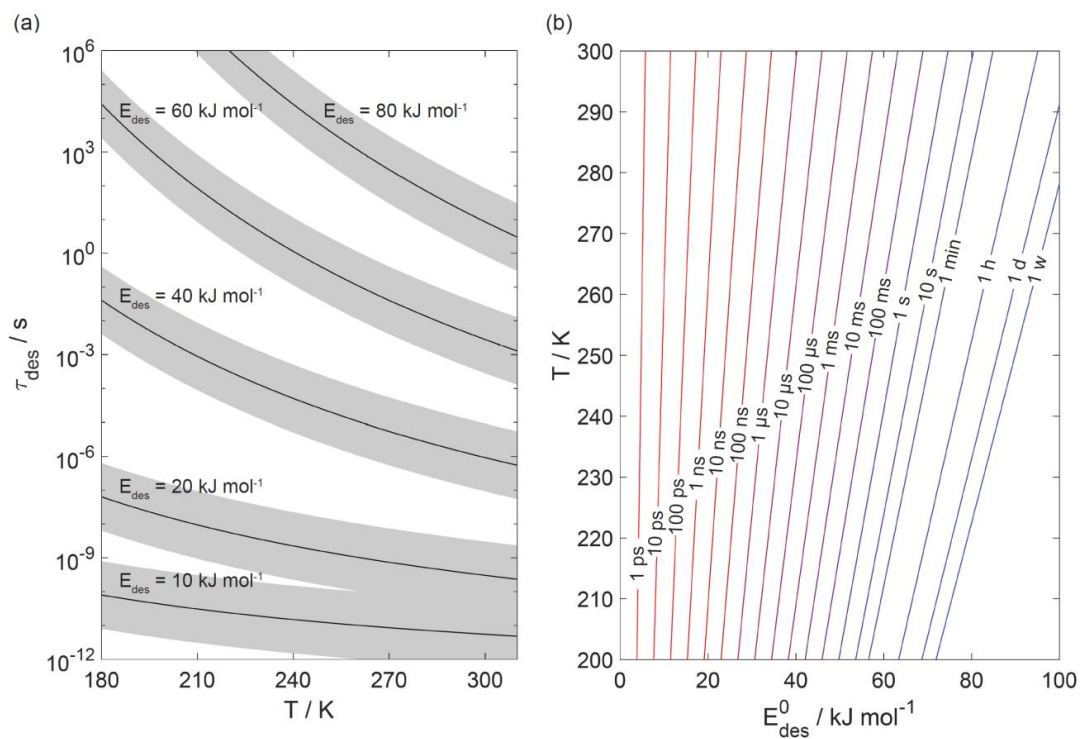
1228

1229

1230

1231

1232



1233

1234 **Figure 1.** The dependence of the desorption lifetime (τ_{des}) on temperature (T) and desorption
 1235 energy (E_{des}^0). (a) τ_{des} as a function of T for various E_{des}^0 values. The shaded area covers the range
 1236 of the pre-exponential factor (A_{des}) varied by ± 1 order of magnitude. (b) Iso- τ_{des} lines for various
 1237 combination of T and E_{des}^0 . All presented data calculated applying Eq. (1) and using $A_{\text{des}} = 1 \times 10^{13}$
 1238 s^{-1} .

1239

1240

1241

1242

1243

1244

1245

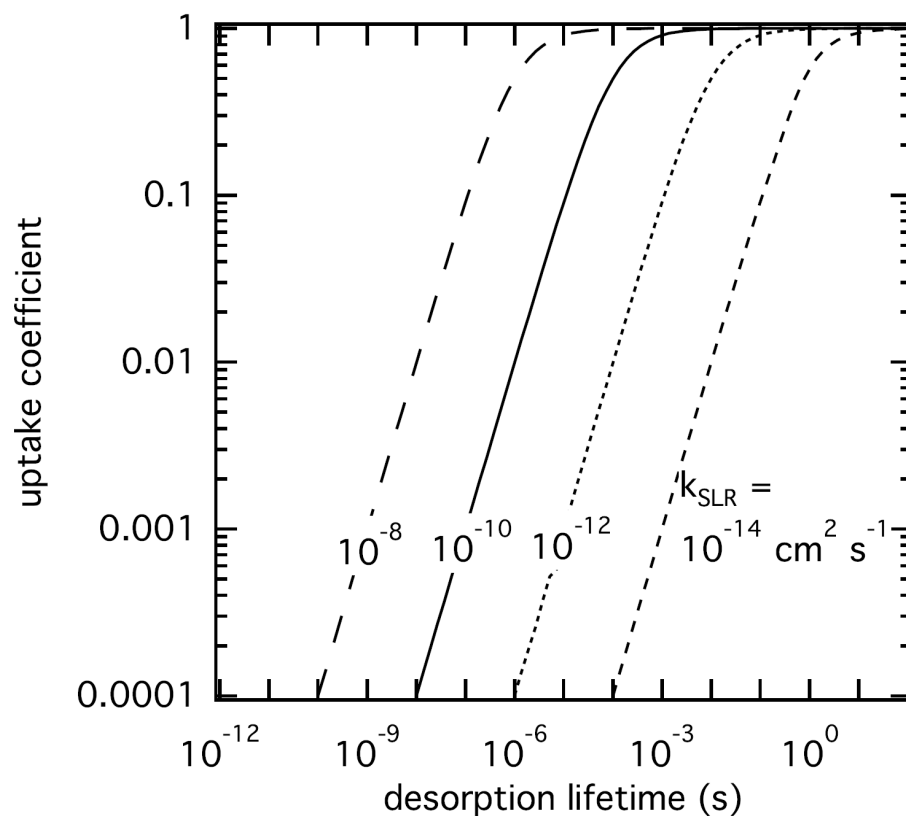
1246

1247

1248



1249



1250

1251 **Figure 2.** The response in reactive uptake coefficient of a reactive gas species X with a condensed-
1252 phase species Y when varying the desorption lifetime and second-order rate coefficients derived
1253 by the numerical diffusion model K2-SURF. The gas phase concentration of X and the surface
1254 concentration of Y remained fixed during the calculations. The surface accommodation coefficient
1255 is assumed to be equal to one.

1256

1257

1258

1259

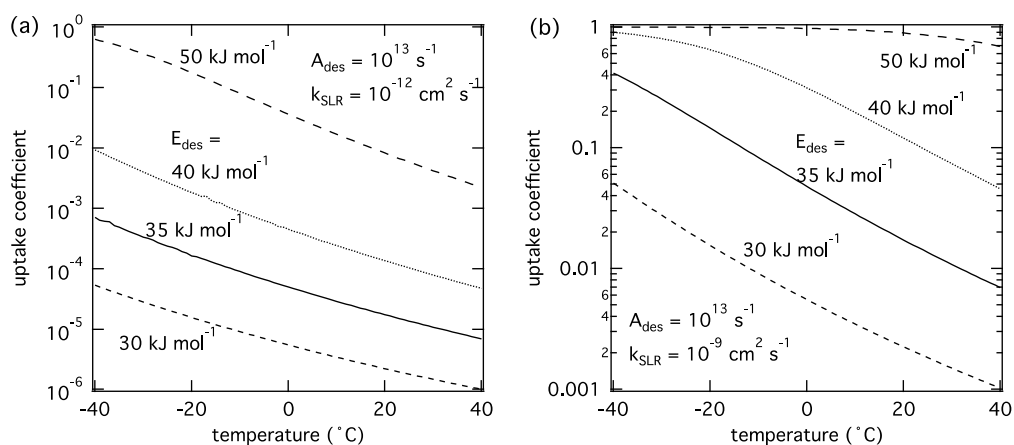
1260

1261

1262



1263



1264

1265 **Figure 3.** The response of the reactive uptake coefficient as temperature and adsorption energy are
 1266 varied for two different second-order rate coefficients derived by K2-SURF. The gas phase
 1267 concentration of X remained fixed during the calculations. The pre-exponential factor A_{des} is fixed
 1268 for both cases. The surface accommodation coefficient is assumed to be one.

1269

1270

1271

1272

1273

1274

1275

1276

1277

1278

1279

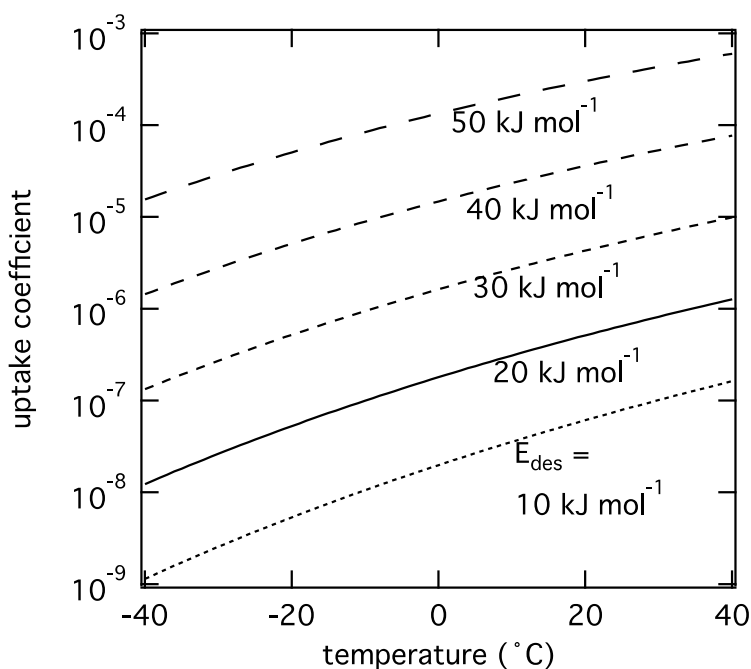
1280

1281

1282



1283



1284

1285 **Figure 4.** The response of the reactive uptake coefficient of O₃ by PAH coated on soot including
1286 formation of reactive oxygen intermediates (ROIs) following Shiraiwa et al. (2011) as temperature
1287 and adsorption energy are varied using the numerical diffusion model K2-SURF. ROI formation
1288 and oxidation reaction rates are adjusted using an Arrhenius-based temperature scaling. The pre-
1289 exponential factor A_{des} is fixed at 10^{13} s^{-1} .

1290

1291

1292

1293

1294

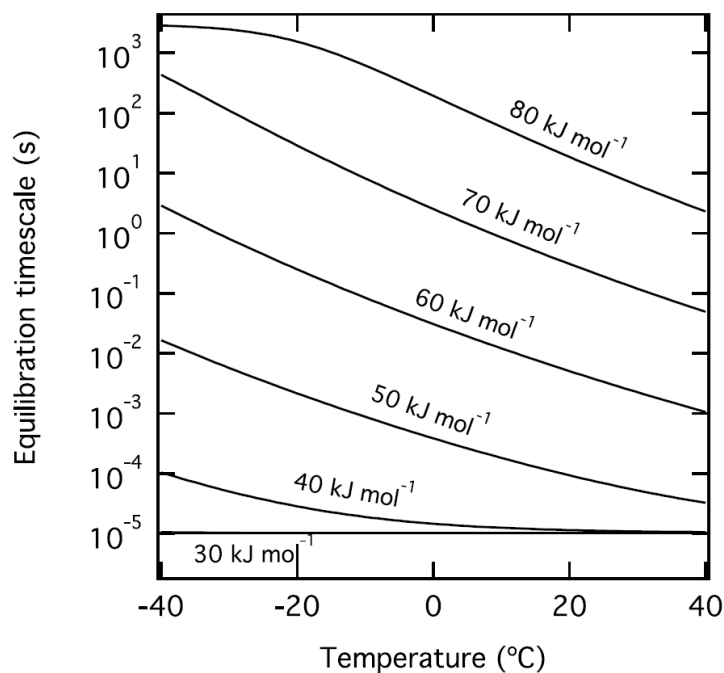
1295

1296

1297

1298

1299



1300

1301 **Figure 5.** Equilibration timescale of non-reactive uptake of gas molecules into particles with the
1302 diameter of 100 nm with different desorption energies by a liquid substrate. Gas-phase mixing
1303 ratio is fixed to be 1 ppb.

1304

1305

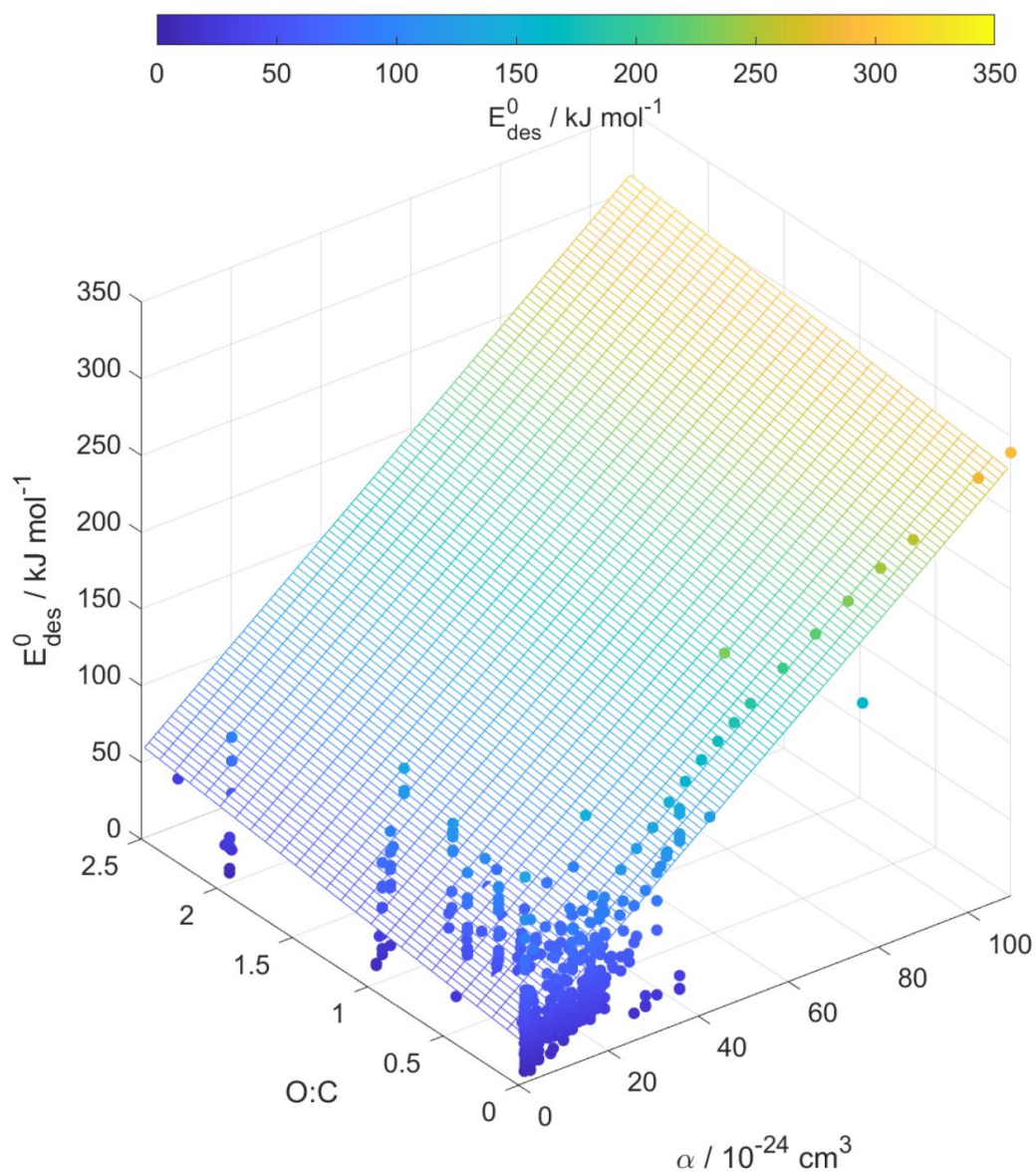
1306

1307

1308

1309

1310



1311

1312

1313 **Figure 6.** Multilinear regression analysis of E_{des}^0 , oxygen to carbon ratio of gas species expressed
1314 as $O:C$, and gas species polarizability (α) using data from Tables A1-A15. Gridded surface shows
1315 regression model and color shading indicates changes in E_{des}^0 .

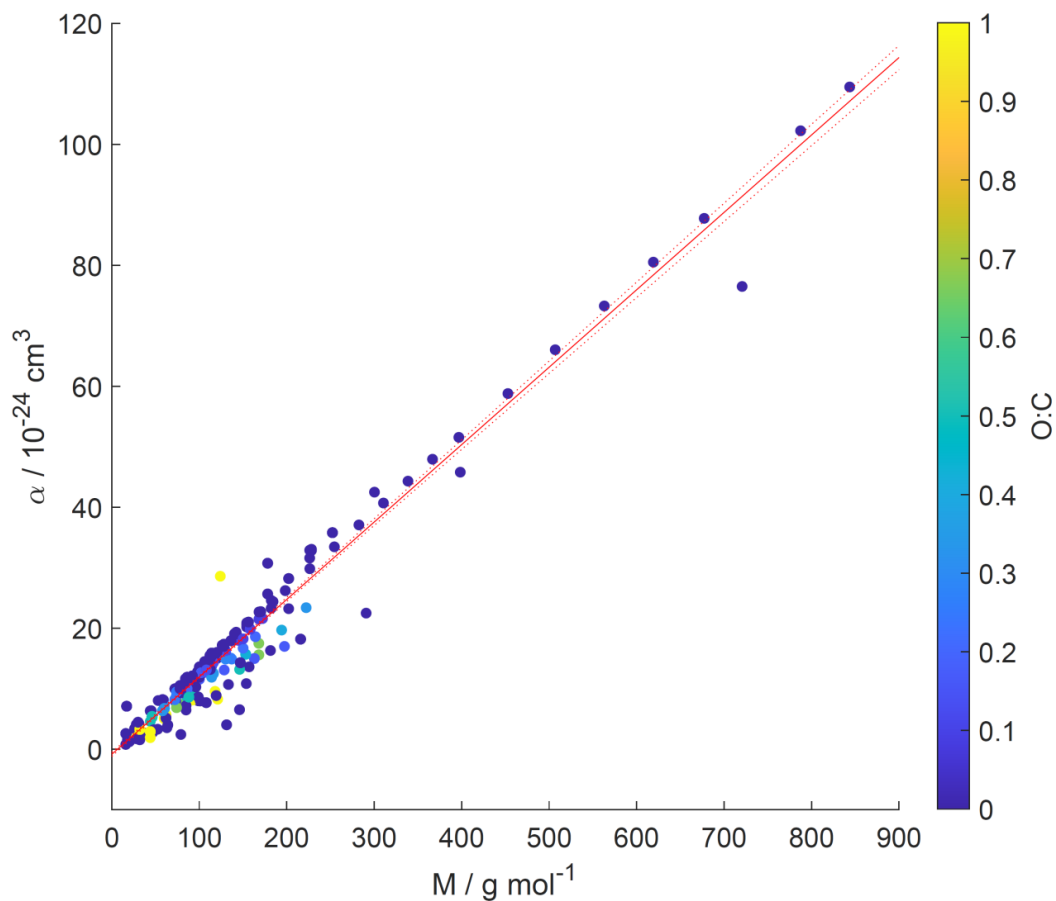
1316

1317



1318

1319



1320

1321 **Figure 7.** Gas species polarizability (α) as a function of molar mass (M) and its dependence on
1322 oxygen to carbon ratio expressed as $O:C$. $O:C$ is given as color shading. Red solid and dotted lines
1323 represent a linear fit to the data and its 95% prediction bands, respectively. Note that three gas
1324 species with $O:C > 1$ (CO_2 , formic acid, and peroxyacetyl nitrate) are included in this plot as
1325 having $O:C = 1$ to allow for better visualization of entire data set.

1326

1327

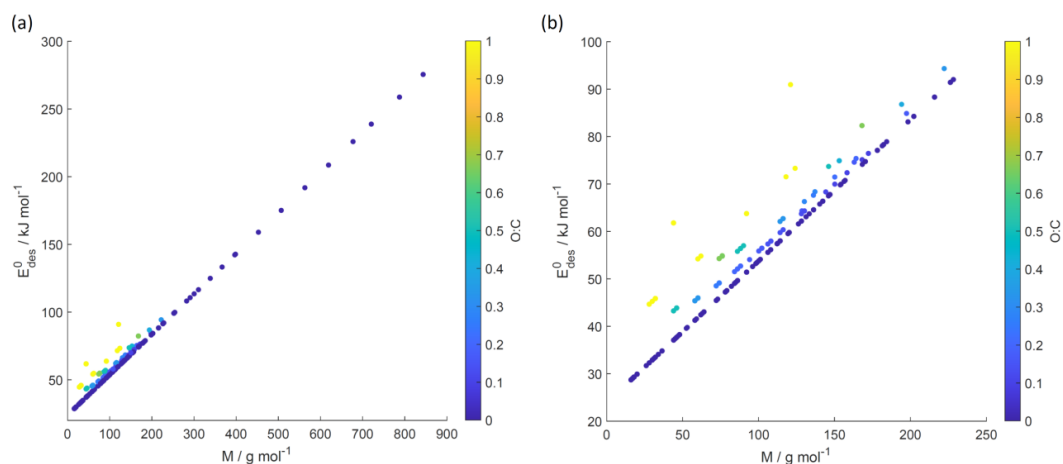
1328

1329

1330



1331



1332

1333 **Figure 8.** E_{des}^0 values derived from the new parameterization (Eq. (16)) applying the training
1334 dataset of gas species with molar mass (M) and $O:C$, the latter coded as symbol color described
1335 by the color bar. (b) is an enlarged view of (a). Note that three gas species with $O:C > 1$ (CO_2 ,
1336 formic acid, and peroxyacetyl nitrate) are included in these plots as having $O:C = 1$ to allow for
1337 better visualization of entire data set.

1338

1339

1340

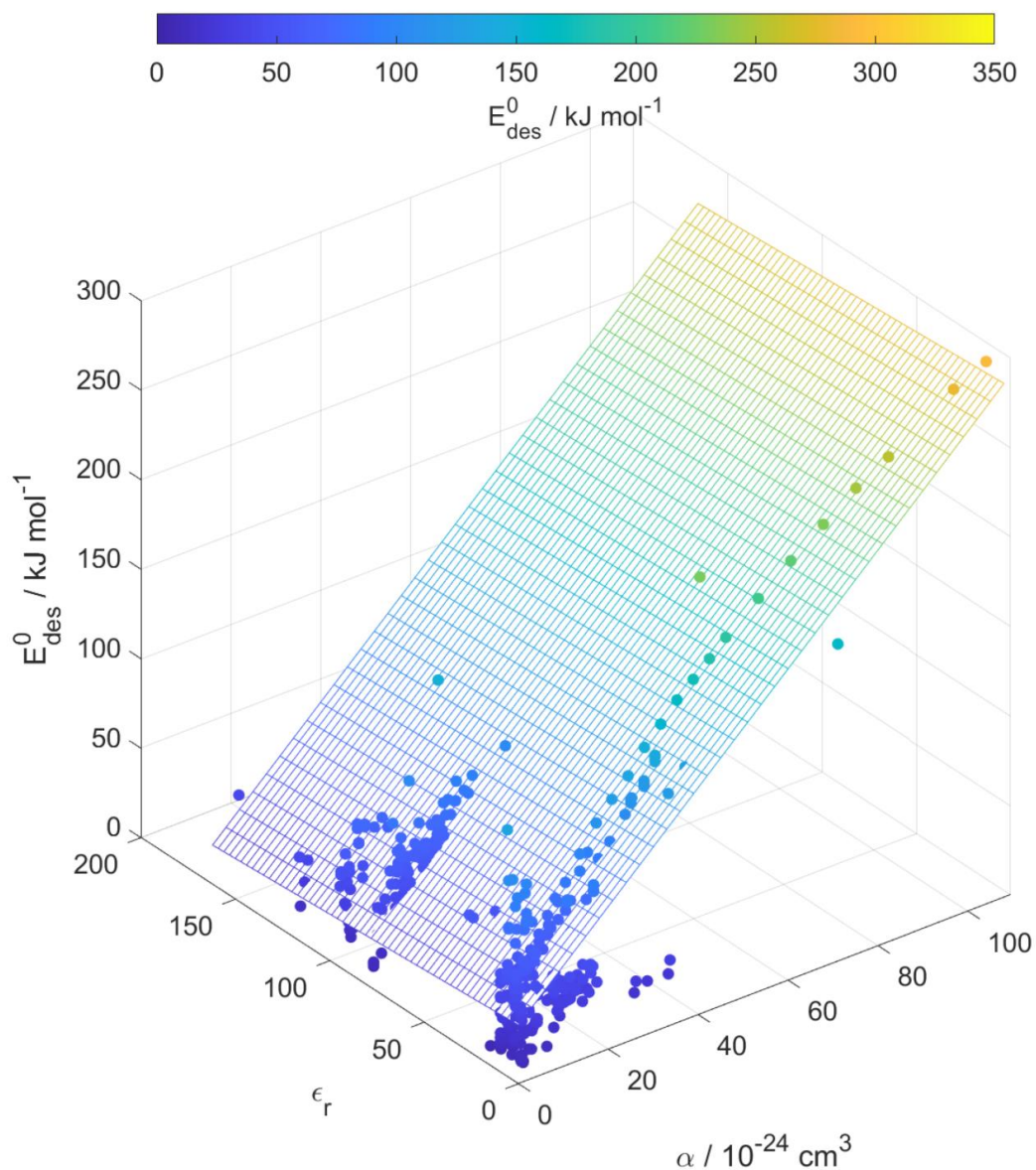
1341

1342

1343

1344

1345



1346

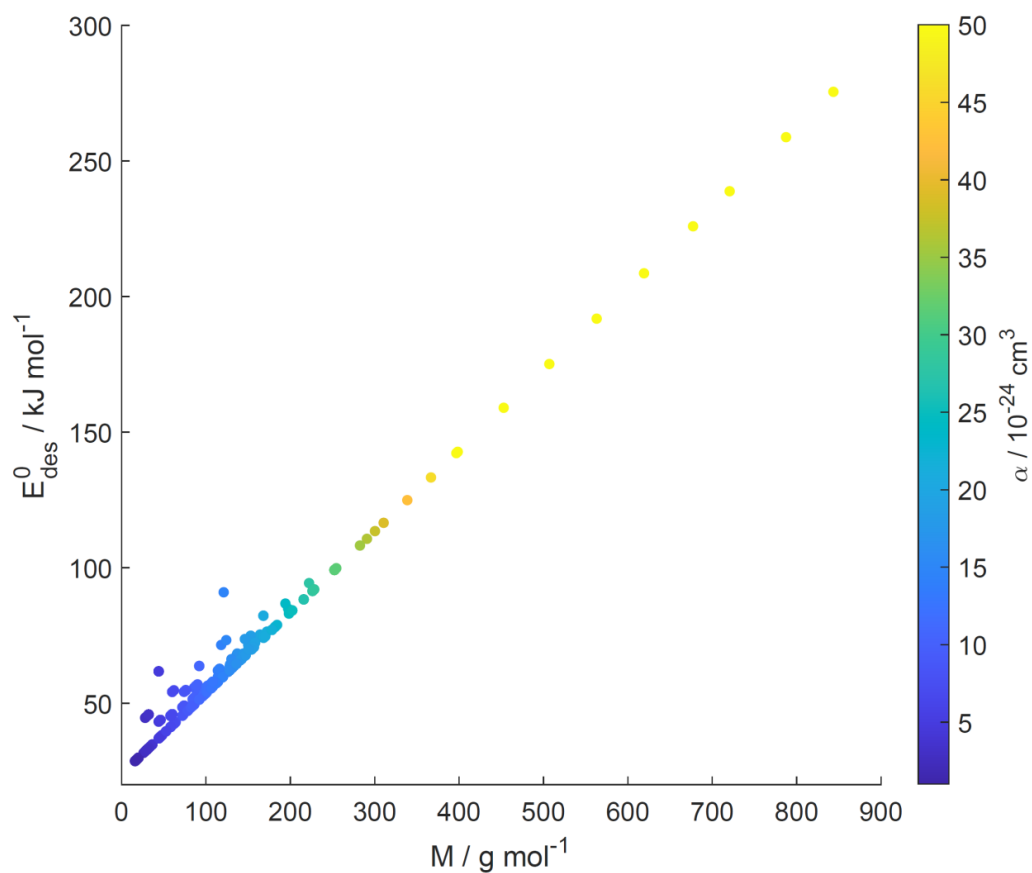
1347 **Figure 9.** Multilinear regression analysis of E_{des}^0 , substrate relative permittivity (ϵ_r), and gas
1348 species polarizability (α) using data from Tables A1-A15. Gridded surface shows regression
1349 model and color shading indicates changes in E_{des}^0 .

1350

1351



1352



1353

1354 **Figure 10.** Parameterized E_{des}^0 values as a function of gas species molar mass (M) and
1355 polarizability (α) given as color bar following Eq. (16).

1356

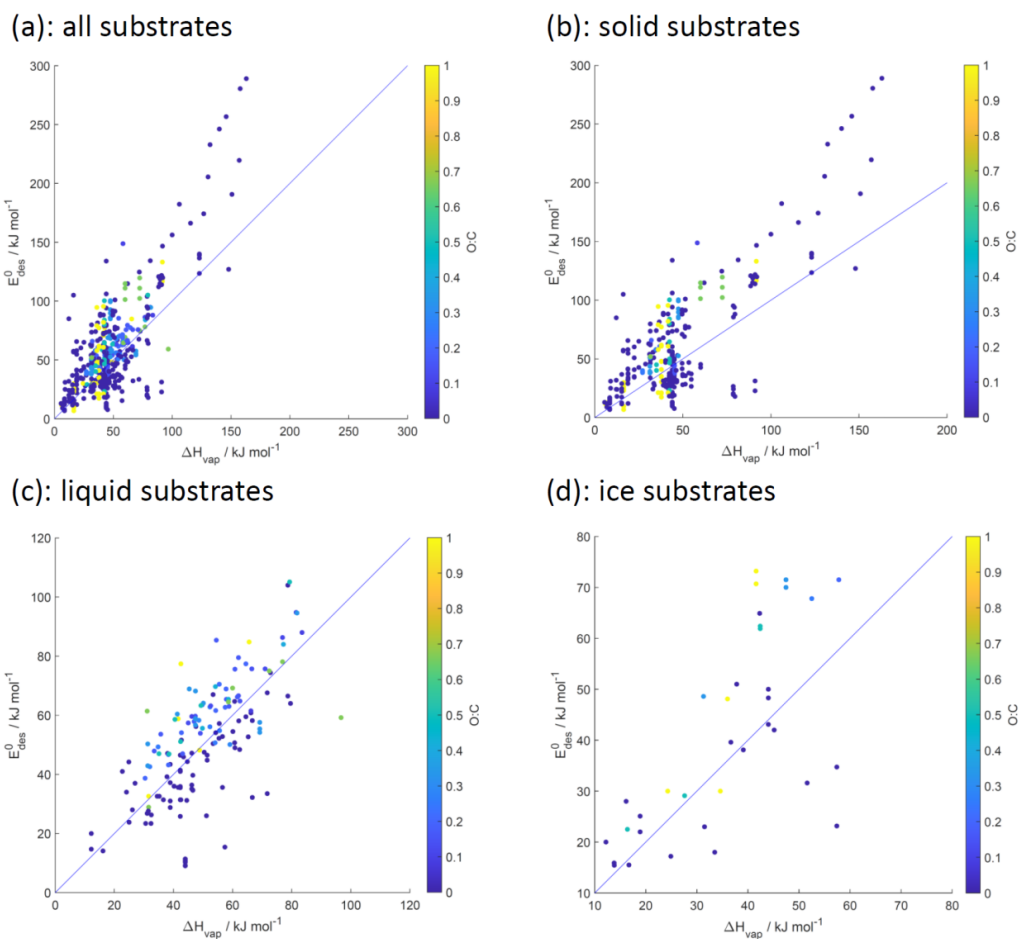
1357

1358

1359

1360

1361



1362

1363 **Figure 11.** Desorption energy (E_{des}^0) as a function of enthalpy of vaporization (ΔH_{vap}) and its
1364 dependence on O:C for all (a), solid (b), liquid (c), and ice (d) substrates. Blue lines indicate 1:1
1365 lines.

1366

1367

1368

1369

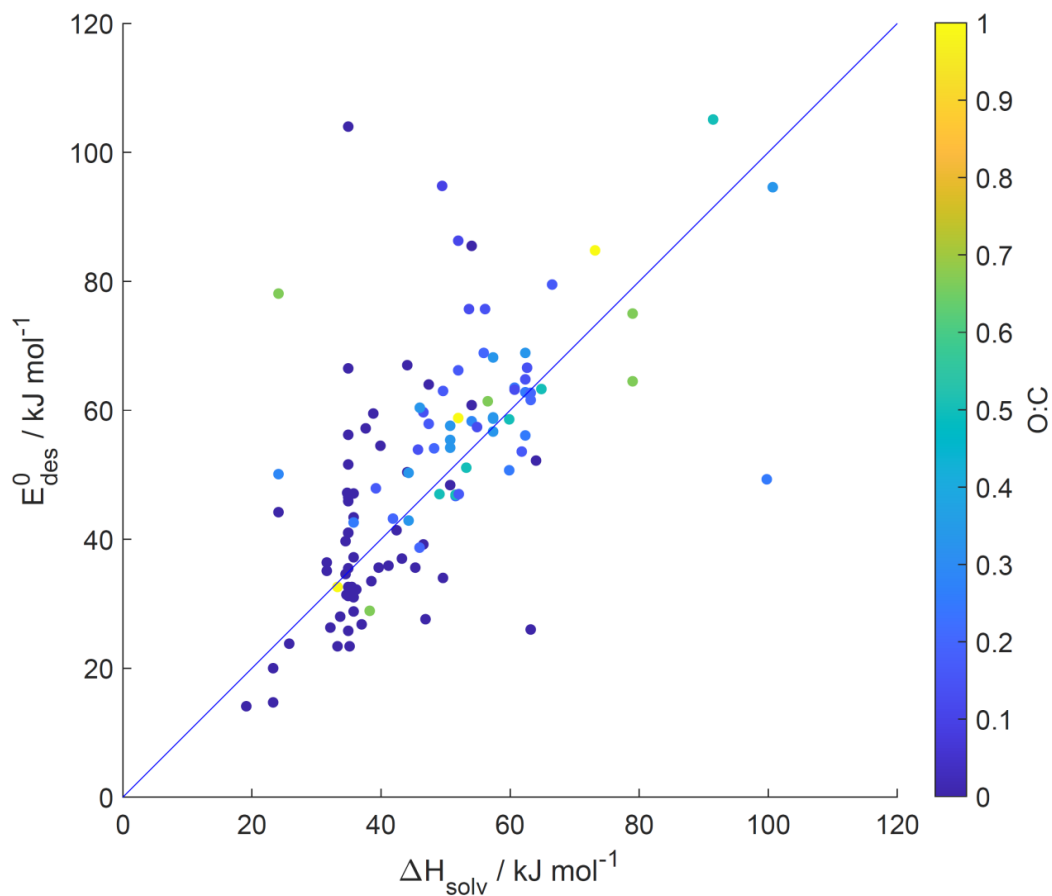
1370

1371

1372



1373



1374

1375 **Figure 12.** Desorption energy (E_{des}^0) as a function of enthalpy of solvation (ΔH_{solv}) and its
1376 dependence on $O:C$ for liquid substrates. Blue line indicates 1:1 line.

1377

1378

1379

1380

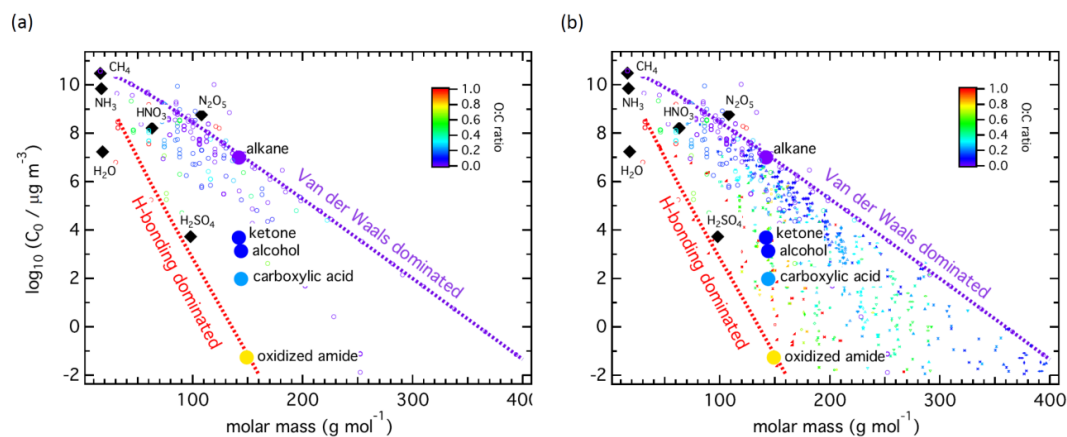
1381

1382

1383



1384



1385

1386 **Figure 13.** Molecular corridors of saturation mass concentration (C_0) vs. molar mass (M). The
1387 small markers represent individual gas species color-coded by $O:C$ ratio. (a) displays data from
1388 Tables S1-S15. (b) includes SOA oxidation products data discussed in (Shiraiwa et al., 2014). The
1389 dotted lines represent linear alkanes C_nH_{2n+2} (purple with $O:C = 0$) and sugar alcohols $C_nH_{2n+2}O_n$
1390 (red with $O:C = 1$). Inorganic species (diamonds) and organic species with similar molar mass but
1391 with different functional groups (circles) are plotted.

1392

1393

1394

1395

1396

1397

1398

1399

1400

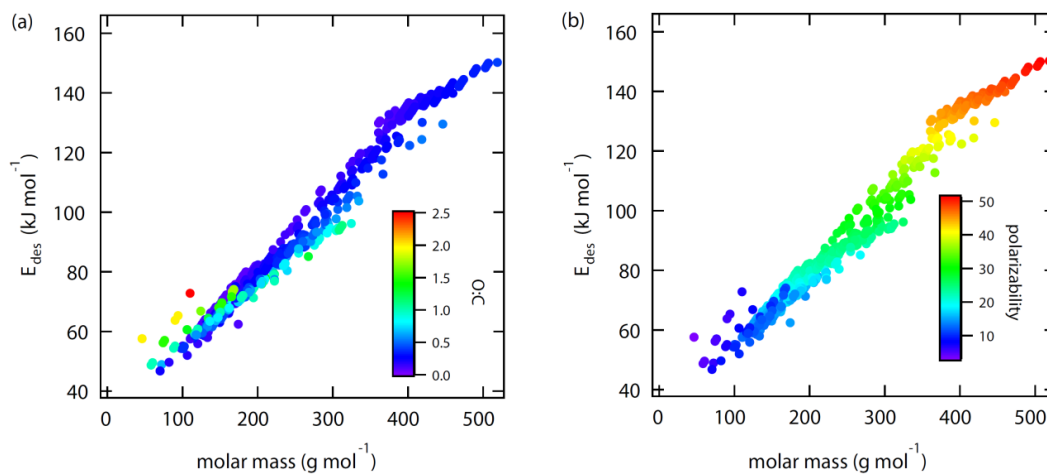
1401

1402

1403

1404

1405



1406

1407 **Figure 14.** Calculated desorption energies (E_{des}^0) of SOA precursor gases from (Shiraiwa et al.,
1408 2014) as a function molar mass and its dependence on $O:C$ (a) and polarizability (b). This analysis
1409 applies parameterizations given in Eqs. (14) and (20).

1410

1411

1412

1413

1414

1415

1416

1417

1418

1419

1420

1421

1422

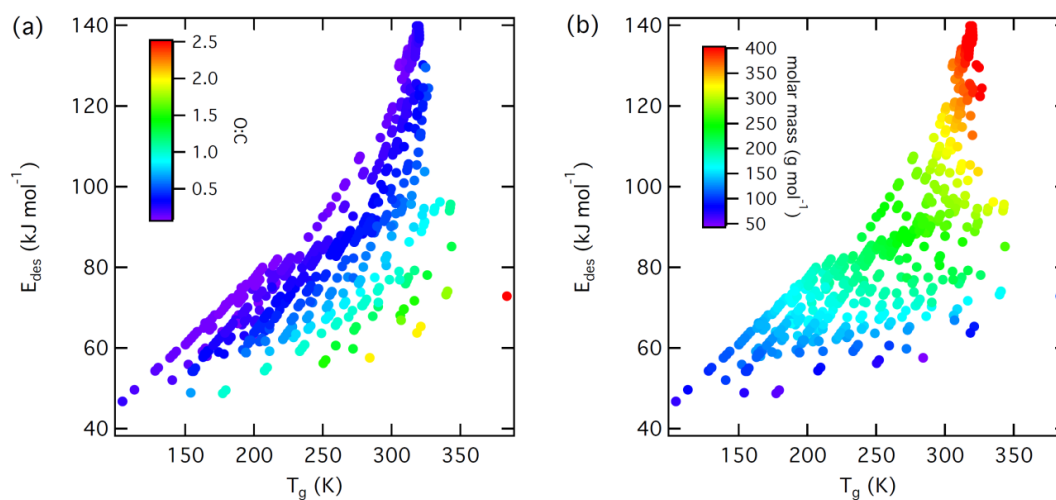
1423

1424

1425



1426



1427

1428 **Figure 15.** Relationship between calculated desorption energies (E_{des}^0) of SOA precursor gases
1429 from (Shiraiwa et al., 2014) and species' glass transition temperature (T_g) and its dependence on
1430 O: C (a) and molar mass (b). This analysis applies parameterizations given in Eqs. (14) and (20).

1431

1432

1433

1434

1435

1436

1437

1438

1439

1440

1441

1442

1443

1444



1445 References

- 1446 Abbatt, J. P. D. and Ravishankara, A. R.: Opinion: Atmospheric multiphase chemistry – past,
1447 present, and future, *Atmos. Chem. Phys.*, 23, 9765–9785, 10.5194/acp-23-9765-2023, 2023.
- 1448 Abbatt, J. P. D., Lee, A. K. Y., and Thornton, J. A.: Quantifying trace gas uptake to tropospheric
1449 aerosol: recent advances and remaining challenges, *Chem. Soc. Rev.*, 41, 6555–6581,
1450 10.1039/C2cs35052a, 2012.
- 1451 Abraham, M. H.: Measurement of Enthalpies of Solution of Electrolytes, in: *Thermochemistry
1452 and Its Applications to Chemical and Biochemical Systems. NATO ASI Series (Series C:
1453 Mathematical and Physical Sciences)*, edited by: Ribeiro da Silva, M. A. V., 119, Springer,
1454 Dordrecht, 10.1007/978-94-009-6312-2_20, 1984.
- 1455 Ahmed, M., Blum, M., Crumlin, E. J., Geissler, P. L., Head-Gordon, T., Limmer, D. T.,
1456 Mandadapu, K. K., Saykally, R. J., and Wilson, K. R.: Molecular Properties and Chemical
1457 Transformations Near Interfaces, *J. Phys. Chem. B*, 125, 9037–9051, 10.1021/acs.jpcc.1c03756,
1458 2021.
- 1459 Aihara, A. and Davies, M.: Dielectric relaxation times of some nonrigid polar molecules, *J. Coll.
1460 Sci. Imp. U. Tok.*, 11, 671–687, 10.1016/0095-8522(56)90182-9, 1956.
- 1461 Akkerman, H. B., Naber, R. C. G., Jongbloed, B., van Hal, P. A., Blom, P. W. M., de Leeuw, D.
1462 M., and de Boer, B.: Electron tunneling through alkanedithiol self-assembled monolayers in
1463 large-area molecular junctions, *Proc. Natl. Acad. Sci. U. S. A.*, 104, 11161–11166,
1464 10.1073/pnas.0701472104, 2007.
- 1465 Alcalá-Jornod, C., van den Bergh, H., and Rossi, M. J.: Reactivity of NO₂ and H₂O on soot
1466 generated in the laboratory: a diffusion tube study at ambient temperature, *Phys. Chem. Chem.
1467 Phys.*, 2, 5584–5593, 2000.
- 1468 Alcalá-Jornod, C., van den Bergh, H., and Rossi, M. J.: Can soot particles emitted by airplane
1469 exhaust contribute to the formation of aviation contrails and cirrus clouds?, *Geophys. Res. Lett.*,
1470 29, 4, 10.1029/2001gl014115, 2002.
- 1471 Alkorta, I., Plane, J. M. C., Elguero, J., Davalos, J. Z., Acuna, A. U., and Saiz-Lopez, A.:
1472 Theoretical study of the NO₃ radical reaction with CH₂ClBr, CH₂ICl, CH₂BrI, CHCl₂Br, and
1473 CHClBr₂, *Phys. Chem. Chem. Phys.*, 24, 14365–14374, 10.1039/d2cp00021k, 2022.
- 1474 Allouche, A. and Bahr, S.: Acetic acid-water interaction in solid interfaces, *Journal of Physical
1475 Chemistry B*, 110, 8640–8648, 10.1021/jp0559736, 2006.
- 1476 Ammann, M. and Pöschl, U.: Kinetic model framework for aerosol and cloud surface chemistry
1477 and gas-particle interactions - Part 2: Exemplary practical applications and numerical
1478 simulations, *Atmos. Chem. Phys.*, 7, 6025–6045, 2007.
- 1479 Ammann, M., Pöschl, U., and Rudich, Y.: Effects of reversible adsorption and Langmuir-
1480 Hinshelwood surface reactions on gas uptake by atmospheric particles, *Phys. Chem. Chem.
1481 Phys.*, 5, 351–356, 2003.
- 1482 Ammann, M., Cox, R. A., Crowley, J. N., Jenkin, M. E., Mellouki, A., Rossi, M. J., Troe, J., and
1483 Wallington, T. J.: Evaluated kinetic and photochemical data for atmospheric chemistry: Volume
1484 VI - heterogeneous reactions with liquid substrates, *Atmos. Chem. Phys.*, 13, 8045–8228,
1485 10.5194/acp-13-8045-2013, 2013.
- 1486 Arangio, A. M., Slade, J. H., Berkemeier, T., Pöschl, U., Knopf, D. A., and Shiraiwa, M.:
1487 Multiphase Chemical Kinetics of OH Radical Uptake by Molecular Organic Markers of Biomass
1488 Burning Aerosols: Humidity and Temperature Dependence, Surface Reaction, and Bulk
1489 Diffusion, *J. Phys. Chem. A*, 119, 4533–4544, 10.1021/jp510489z, 2015.



- 1490 Aroney, M. J., Saxby, J. D., Lefevre, R. J. W., and Chia, L. H. L.: Molecular polarisability.
1491 Dipole moments molar Kerr constants + conformations of 11 phosphate + phosphite triesters as
1492 solutes in benzene, *J. Chem. Soc.*, 2948-2954, 10.1039/jr9640002948, 1964.
- 1493 Arp, H. P. H., Goss, K. U., and Schwarzenbach, R. P.: Evaluation of a predictive model for
1494 air/surface adsorption equilibrium constants and enthalpies, *Environ. Toxicol. Chem.*, 25, 45-51,
1495 10.1897/05-291r.1, 2006.
- 1496 Arrhenius, S. A.: Über die Dissociationswärme und den Einfluß der Temperatur auf den
1497 Dissociationsgrad der Elektrolyte, *Z. Phys. Chem.*, 4, 96-116, 1889a.
- 1498 Arrhenius, S. A.: Über die Reaktionsgeschwindigkeit bei der Inversion von Rohrzucker durch
1499 Säuren, *Z. Phys. Chem.*, 4, 226-248, 1889b.
- 1500 Artiglia, L., Edebeli, J., Orlando, F., Chen, S. Z., Lee, M. T., Arroyo, P. C., Gilgen, A., Bartels-
1501 Rausch, T., Kleibert, A., Vazdar, M., Carignano, M. A., Francisco, J. S., Shepson, P. B., Gladich,
1502 I., and Ammann, M.: A surface-stabilized ozonide triggers bromide oxidation at the aqueous
1503 solution-vapour interface, *Nat. Commun.*, 8, 8, 10.1038/s41467-017-00823-x, 2017.
- 1504 Asakawa, H., Sazaki, G., Nagashima, K., Nakatsubo, S., and Furukawa, Y.: Two types of quasi-
1505 liquid layers on ice crystals are formed kinetically, *Proc. Natl. Acad. Sci. U. S. A.*, 113, 1749-
1506 1753, 10.1073/pnas.1521607113, 2016.
- 1507 Auty, R. P. and Cole, R. H.: Dielectric properties of ice and solid D₂O, *J. Chem. Phys.*, 20,
1508 1309-1314, 10.1063/1.1700726, 1952.
- 1509 Bak, K. L., Gauss, J., Helgaker, T., Jorgensen, P., and Olsen, J.: The accuracy of molecular
1510 dipole moments in standard electronic structure calculations, *Chemical Physics Letters*, 319,
1511 563-568, 10.1016/s0009-2614(00)00198-6, 2000.
- 1512 Baron, M. and Arevalo, E. S.: Dipole-moment values from single-solution measurements, *J.*
1513 *Chem. Educ.*, 65, 644-645, 10.1021/ed065p644, 1988.
- 1514 Bartels-Rausch, T.: Ten things we need to know about ice and snow, *Nature*, 494, 27-29,
1515 10.1038/494027a, 2013.
- 1516 Bartels-Rausch, T., Huthwelker, T., Gaggeler, H. W., and Ammann, M.: Atmospheric pressure
1517 coated-wall flow-tube study of acetone adsorption on ice, *J. Phys. Chem. A*, 109, 4531-4539,
1518 10.1021/jp0451871, 2005.
- 1519 Bartels-Rausch, T., Eichler, B., Zimmermann, P., Gaggeler, H. W., and Ammann, M.: The
1520 adsorption enthalpy of nitrogen oxides on crystalline ice, *Atmos. Chem. Phys.*, 2, 235-247,
1521 10.5194/acp-2-235-2002, 2002.
- 1522 Bartels-Rausch, T., Orlando, F., Kong, X. R., Artiglia, L., and Ammann, M.: Experimental
1523 Evidence for the Formation of Solvation Shells by Soluble Species at a Nonuniform Air-Ice
1524 Interface, *ACS Earth Space Chem.*, 1, 572-579, 10.1021/acsearthspacechem.7b00077, 2017.
- 1525 Bartels-Rausch, T., Jacobi, H. W., Kahan, T. F., Thomas, J. L., Thomson, E. S., Abbatt, J. P. D.,
1526 Ammann, M., Blackford, J. R., Bluhm, H., Boxe, C., Domine, F., Frey, M. M., Gladich, I.,
1527 Guzman, M. I., Heger, D., Huthwelker, T., Klan, P., Kuhs, W. F., Kuo, M. H., Maus, S., Moussa,
1528 S. G., McNeill, V. F., Newberg, J. T., Pettersson, J. B. C., Roeselova, M., and Sodeau, J. R.: A
1529 review of air-ice chemical and physical interactions (AICI): liquids, quasi-liquids, and solids in
1530 snow, *Atmos. Chem. Phys.*, 14, 1587-1633, 10.5194/acp-14-1587-2014, 2014.
- 1531 Behr, P., Scharfenort, U., Ataya, K., and Zellner, R.: Dynamics and mass accommodation of HCl
1532 molecules on sulfuric acid-water surfaces, *Phys. Chem. Chem. Phys.*, 11, 8048-8055,
1533 10.1039/b904629a, 2009.



- 1534 Behr, P., Morris, J. R., Antman, M. D., Ringeisen, B. R., Splan, J. R., and Nathanson, G. M.:
1535 Reaction and desorption of HCl and HBr following collisions with supercooled sulfuric acid,
1536 *Geophys. Res. Lett.*, 28, 1961-1964, 10.1029/2000gl012716, 2001.
- 1537 Beller, M., Renken, A., and van Santen, R. A.: *Catalysis: From Principles to Applications*, John
1538 Wiley & Sons, Inc., Hoboken, New Jersey, USA2012.
- 1539 Berkemeier, T., Takeuchi, M., Eris, G., and Ng, N. L.: Kinetic modeling of formation and
1540 evaporation of secondary organic aerosol from NO₃ oxidation of pure and mixed monoterpenes,
1541 *Atmos. Chem. Phys.*, 20, 15513-15535, 10.5194/acp-20-15513-2020, 2020.
- 1542 Berkemeier, T., Huisman, A. J., Ammann, M., Shiraiwa, M., Koop, T., and Pöschl, U.: Kinetic
1543 regimes and limiting cases of gas uptake and heterogeneous reactions in atmospheric aerosols
1544 and clouds: a general classification scheme, *Atmos. Chem. Phys.*, 13, 6663-6686, 10.5194/acp-
1545 13-6663-2013, 2013.
- 1546 Berkemeier, T., Mishra, A., Mattei, C., Huisman, A. J., Krieger, U. K., and Poschl, U.:
1547 Ozonolysis of Oleic Acid Aerosol Revisited: Multiphase Chemical Kinetics and Reaction
1548 Mechanisms, *ACS Earth Space Chem.*, 5, 3313-3323, 10.1021/acsearthspacechem.1c00232,
1549 2021.
- 1550 Berkemeier, T., Steimer, S. S., Krieger, U. K., Peter, T., Pöschl, U., Ammann, M., and Shiraiwa,
1551 M.: Ozone uptake on glassy, semi-solid and liquid organic matter and the role of reactive oxygen
1552 intermediates in atmospheric aerosol chemistry, *Phys. Chem. Chem. Phys.*, 18, 12662-12674,
1553 10.1039/c6cp00634e, 2016.
- 1554 Bertram, A. K., Martin, S. T., Hanna, S. J., Smith, M. L., Bodsworth, A., Chen, Q., Kuwata, M.,
1555 Liu, A., You, Y., and Zorn, S. R.: Predicting the relative humidities of liquid-liquid phase
1556 separation, efflorescence, and deliquescence of mixed particles of ammonium sulfate, organic
1557 material, and water using the organic-to-sulfate mass ratio of the particle and the oxygen-to-
1558 carbon elemental ratio of the organic component, *Atmos. Chem. Phys.*, 11, 10995-11006,
1559 10.5194/acp-11-10995-2011, 2011.
- 1560 Bishop, A. R., Girolami, G. S., and Nuzzo, R. G.: Structural models and thermal desorption
1561 energetics for multilayer assemblies of the n-alkanes on Pt(111), *J. Phys. Chem. B*, 104, 754-
1562 763, 10.1021/jp9926488, 2000.
- 1563 Blank, M. and Ottewill, R. H.: Adsorption of aromatic vapors on water surfaces, *J. Phys. Chem.*,
1564 68, 2206-2211, 10.1021/j100790a030, 1964.
- 1565 Bolis, V.: Fundamentals in Adsorption at the Solid-Gas Interface. Concepts and
1566 Thermodynamics, in: *Calorimetry and Thermal Methods in Catalysis*, edited by: Auroux, A.,
1567 154, Springer-Verlag Berlin Heidelberg, Berlin, 3-50, 10.1007/978-3-642-11954-5, 2013.
- 1568 Bond, T. C., Doherty, S. J., Fahey, D. W., Forster, P. M., Berntsen, T., DeAngelo, B. J., Flanner,
1569 M. G., Ghan, S., Karcher, B., Koch, D., Kinne, S., Kondo, Y., Quinn, P. K., Sarofim, M. C.,
1570 Schultz, M. G., Schulz, M., Venkataraman, C., Zhang, H., Zhang, S., Bellouin, N., Guttikunda,
1571 S. K., Hopke, P. K., Jacobson, M. Z., Kaiser, J. W., Klimont, Z., Lohmann, U., Schwarz, J. P.,
1572 Shindell, D., Storelvmo, T., Warren, S. G., and Zender, C. S.: Bounding the role of black carbon
1573 in the climate system: A scientific assessment, *J. Geophys. Res.*, 118, 5380-5552,
1574 10.1002/jgrd.50171, 2013.
- 1575 Borget, F., Chiavassa, T., Allouche, A., and Aycard, J. P.: Experimental and quantum study of
1576 adsorption of ozone (O₃) on amorphous water ice film, *J. Phys. Chem. B*, 105, 449-454,
1577 10.1021/jp001785y, 2001.
- 1578 Borodin, D., Rahinov, I., Shirhatti, P. R., Huang, M., Kandratsenka, A., Auerbach, D. J., Zhong,
1579 T. L., Guo, H., Schwarzer, D., Kitsopoulos, T. N., and Wodtke, A. M.: Following the



- 1580 microscopic pathway to adsorption through chemisorption and physisorption wells, *Science*, 369,
1581 1461-1465, 10.1126/science.abc9581, 2020.
- 1582 Borrmann, S., Solomon, S., Dye, J. E., and Luo, B. P.: The potential of cirrus clouds for
1583 heterogeneous chlorine activation, *Geophys. Res. Lett.*, 23, 2133-2136, 1996.
- 1584 Bosque, R. and Sales, J.: Polarizabilities of solvents from the chemical composition, *J. Chem.*
1585 *Inf. Comput. Sci.*, 42, 1154-1163, 10.1021/ci025528x, 2002.
- 1586 Brastad, S. M., Albert, D. R., Huang, M. W., and Nathanson, G. M.: Collisions of DCI with a
1587 Solution Covered with Hydrophobic and Hydrophilic Ions: Tetrahexylammonium Bromide in
1588 Glycerol, *J. Phys. Chem. A*, 113, 7422-7430, 10.1021/jp900232v, 2009.
- 1589 Brini, E., Fennell, C. J., Fernandez-Serra, M., Hribar-Lee, B., Luksic, M., and Dill, K. A.: How
1590 Water's Properties Are Encoded in Its Molecular Structure and Energies, *Chem. Rev.*, 117,
1591 12385-12414, 10.1021/acs.chemrev.7b00259, 2017.
- 1592 Broderick, A., Rocha, M. A., Khalifa, Y., Shiflett, M. B., and Newberg, J. T.: Mass Transfer
1593 Thermodynamics through a Gas-Liquid Interface, *J. Phys. Chem. B*, 123, 2576-2584,
1594 10.1021/acs.jpcc.9b00958, 2019.
- 1595 Brown, D. E., George, S. M., Huang, C., Wong, E. K. L., Rider, K. B., Smith, R. S., and Kay, B.
1596 D.: H₂O condensation coefficient and refractive index for vapor-deposited ice from molecular
1597 beam and optical interference measurements, *J. Phys. Chem.*, 100, 4988-4995,
1598 10.1021/jp952547j, 1996.
- 1599 Bruant, R. G. and Conklin, M. H.: Adsorption of trichloroethene at the vapor/water interface,
1600 *Environ. Sci. Technol.*, 35, 362-364, 10.1021/es000994t, 2001.
- 1601 Bruant, R. G. and Conklin, M. H.: Adsorption of benzene and methyl-substituted benzenes at the
1602 vapor/water interface. 2. Single-component VHOC adsorption, *J. Phys. Chem. B*, 106, 2224-
1603 2231, 10.1021/jp0029156, 2002.
- 1604 Bruska, M. K. and Piechota, J.: Density functional study of sulphur hexafluoride (SF₆) and its
1605 hydrogen derivatives, *Mol. Simul.*, 34, 1041-1050, 10.1080/08927020802258708, 2008.
- 1606 Budi, A., Stipp, S. L. S., and Andersson, M. P.: Calculation of Entropy of Adsorption for Small
1607 Molecules on Mineral Surfaces, *J. Phys. Chem. C*, 122, 8236-8243, 10.1021/acs.jpcc.7b11860,
1608 2018.
- 1609 Caloz, F., Fenter, F. F., Tabor, K. D., and Rossi, M. J.: Paper I: Design and construction of a
1610 Knudsen-cell reactor for the study of heterogeneous reactions over the temperature range 130-
1611 750 K: Performances and limitations, *Rev. Sci. Instrum.*, 68, 3172-3179, 1997.
- 1612 Cambi, R., Cappelletti, D., Liuti, G., and Pirani, F.: Generalized correlations in terms of
1613 polarizability for vanderwaals interaction potential parameter calculations, *J. Chem. Phys.*, 95,
1614 1852-1861, 10.1063/1.461035, 1991.
- 1615 Campbell, C. T., Sprowl, L. H., and Arnadottir, L.: Equilibrium Constants and Rate Constants
1616 for Adsorbates: Two-Dimensional (2D) Ideal Gas, 2D Ideal Lattice Gas, and Ideal Hindered
1617 Translator Models, *J. Phys. Chem. C*, 120, 10283-10297, 10.1021/acs.jpcc.6b00975, 2016.
- 1618 Cao, X., Liu, C. L., Zhang, T. F., Xu, Q., Zhang, D. L., Liu, X. T., Jiao, H. J., Wen, X. D., Yang,
1619 Y., Li, Y. W., Niemantsverdriet, J. W., and Zhu, J. F.: Revisiting Oxygen Adsorption on Ir(100),
1620 *J. Phys. Chem. C*, 126, 10035-10044, 10.1021/acs.jpcc.2c01237, 2022.
- 1621 Cappa, C. D., Onasch, T. B., Massoli, P., Worsnop, D. R., Bates, T. S., Cross, E. S., Davidovits,
1622 P., Hakala, J., Hayden, K. L., Jobson, B. T., Kolesar, K. R., Lack, D. A., Lerner, B. M., Li, S.
1623 M., Mellon, D., Nuaaman, I., Olfert, J. S., Petaja, T., Quinn, P. K., Song, C., Subramanian, R.,
1624 Williams, E. J., and Zaveri, R. A.: Radiative Absorption Enhancements Due to the Mixing State
1625 of Atmospheric Black Carbon, *Science*, 337, 1078-1081, 10.1126/science.1223447, 2012.



- 1626 Chan, M. N., Zhang, H., Goldstein, A. H., and Wilson, K. R.: Role of Water and Phase in the
1627 Heterogeneous Oxidation of Solid and Aqueous Succinic Acid Aerosol by Hydroxyl Radicals, *J.*
1628 *Phys. Chem. C*, 118, 28978-28992, 10.1021/jp5012022, 2014.
- 1629 Chandler, D.: Interfaces and the driving force of hydrophobic assembly, *Nature*, 437, 640-647,
1630 10.1038/nature04162, 2005.
- 1631 Charnawskas, J. C., Alpert, P. A., Lambe, A. T., Berkemeier, T., O'Brien, R. E., Massoli, P.,
1632 Onasch, T. B., Shiraiwa, M., Moffet, R. C., Gilles, M. K., Davidovits, P., Worsnop, D. R., and
1633 Knopf, D. A.: Condensed-phase biogenic-anthropogenic interactions with implications for cold
1634 cloud formation, *Faraday Discuss.*, 200, 164-195, 10.1039/C7FD00010C, 2017.
- 1635 Chickos, J. S. and Acree, W. E.: Enthalpies of vaporization of organic and organometallic
1636 compounds, 1880-2002, *J. Phys. Chem. Ref. Data*, 32, 519-878, 10.1063/1.1529214, 2003.
- 1637 China, S., Mazzoleni, C., Gorkowski, K., Aiken, A. C., and Dubey, M. K.: Morphology and
1638 mixing state of individual freshly emitted wildfire carbonaceous particles, *Nat. Commun.*, 4,
1639 2122, 10.1038/ncomms3122, 2013.
- 1640 Cho, H., Shepson, P. B., Barrie, L. A., Cowin, J. P., and Zaveri, R.: NMR investigation of the
1641 quasi-brine layer in ice/brine mixtures, *J. Phys. Chem. B*, 106, 11226-11232,
1642 10.1021/jp020449+, 2002.
- 1643 Chorkendorff, I. and Niemantsverdriet, J. W.: *Concepts of Modern Catalysis and Kinetics*, 2nd,
1644 Wiley-VCH Verlag GmbH & Co. KGaA, Weinheim, 477 pp.2007.
- 1645 Chu, S. N., Sands, S., Tomasik, M. R., Lee, P. S., and McNeill, V. F.: Ozone Oxidation of
1646 Surface-Adsorbed Polycyclic Aromatic Hydrocarbons: Role of PAH-Surface Interaction, *J. Am.*
1647 *Chem. Soc.*, 132, 15968-15975, 10.1021/ja1014772, 2010.
- 1648 Collignon, B., Hoang, P. N. M., Picaud, S., and Rayez, J. C.: Ab initio study of the water
1649 adsorption on hydroxylated graphite surfaces, *Chemical Physics Letters*, 406, 430-435,
1650 10.1016/j.cplett.2005.03.026, 2005.
- 1651 Compernelle, S. and Muller, J. F.: Henry's law constants of polyols, *Atmos. Chem. Phys.*, 14,
1652 12815-12837, 10.5194/acp-14-12815-2014, 2014.
- 1653 Compernelle, S., Ceulemans, K., and Muller, J. F.: EVAPORATION: a new vapour pressure
1654 estimation method for organic molecules including non-additivity and intramolecular
1655 interactions, *Atmos. Chem. Phys.*, 11, 9431-9450, 10.5194/acp-11-9431-2011, 2011.
- 1656 Crabtree, A. and Siman-Tov, M.: Thermophysical properties of saturated light and heavy water
1657 for advanced neutron source applications, Oak Ridge National Laboratory ORNL/TM-12322,
1658 1993.
- 1659 Crossley, J.: Dielectric relaxation of 1-butanol and 1-decanol in several solvents, *J. Phys. Chem.*,
1660 75, 1790-&, 10.1021/j100681a005, 1971.
- 1661 Crossley, J.: Dielectric-relaxation of 1-alkenes, *J. Chem. Phys.*, 58, 5315-5318,
1662 10.1063/1.1679145, 1973.
- 1663 Croteau, T., Bertram, A. K., and Patey, G. N.: Simulation of Water Adsorption on Kaolinite
1664 under Atmospheric Conditions, *J. Phys. Chem. A*, 113, 7826-7833, 10.1021/jp902453f, 2009.
- 1665 Crowley, J. N., Ammann, M., Cox, R. A., Hynes, R. G., Jenkin, M. E., Mellouki, A., Rossi, M.
1666 J., Troc, J., and Wallington, T. J.: Evaluated kinetic and photochemical data for atmospheric
1667 chemistry: Volume V - heterogeneous reactions on solid substrates (vol 10, pg 9059, 2010),
1668 *Atmos. Chem. Phys.*, 13, 7359-7359, 10.5194/acp-13-7359-2013, 2013.
- 1669 Crowley, J. N., Ammann, M., Cox, R. A., Hynes, R. G., Jenkin, M. E., Mellouki, A., Rossi, M.
1670 J., Troc, J., and Wallington, T. J.: Evaluated kinetic and photochemical data for atmospheric



- 1671 chemistry: Volume V - heterogeneous reactions on solid substrates, *Atmos. Chem. Phys.*, 10,
1672 9059-9223, 10.5194/acp-10-9059-2010, 2010.
- 1673 Cruzeiro, V. W. D., Galib, M., Limmer, D. T., and Gotz, A. W.: Uptake of N₂O₅ by aqueous
1674 aerosol unveiled using chemically accurate many-body potentials, *Nat. Commun.*, 13, 7,
1675 10.1038/s41467-022-28697-8, 2022.
- 1676 Cussler, E. L.: *Diffusion - Mass Transfer in Fluid Systems*, 2009.
- 1677 Cwiertny, D. M., Young, M. A., and Grassian, V. H.: Chemistry and photochemistry of mineral
1678 dust aerosol, *Annu. Rev. Phys. Chem.*, 59, 27-51,
1679 10.1146/annurev.physchem.59.032607.093630, 2008.
- 1680 Daniels, D. J., Daniels, D. J. (Ed.): *Ground Penetrating Radar*, 2nd, The Institution of Engineering
1681 and Technology, London, United Kingdom, 726 pp.2004.
- 1682 Davidovits, P., Kolb, C. E., Williams, L. R., Jayne, J. T., and Worsnop, D. R.: Mass
1683 accommodation and chemical reactions at gas-liquid interfaces, *Chem. Rev.*, 106, 1323-1354,
1684 10.1021/cr040366k, 2006.
- 1685 Davidovits, P., Kolb, C. E., Williams, L. R., Jayne, J. T., and Worsnop, D. R.: Update 1 of: Mass
1686 Accommodation and Chemical Reactions at Gas-Liquid Interfaces, *Chem. Rev.*, 111, PR76-
1687 PR109, 10.1021/cr100360b, 2011.
- 1688 Davies, J. F. and Wilson, K. R.: Nanoscale interfacial gradients formed by the reactive uptake of
1689 OH radicals onto viscous aerosol surfaces, *Chem. Sci.*, 6, 7020-7027, 10.1039/c5sc02326b,
1690 2015.
- 1691 Delval, C. and Rossi, M. J.: Influence of monolayer amounts of HNO₃ on the evaporation rate of
1692 H₂O over ice in the range 179 to 208 K: A quartz crystal microbalance study, *J. Phys. Chem. A*,
1693 109, 7151-7165, 10.1021/jp0505072, 2005.
- 1694 Delval, C., Fluckiger, B., and Rossi, M. J.: The rate of water vapor evaporation from ice
1695 substrates in the presence of HCl and HBr: implications for the lifetime of atmospheric ice
1696 particles, *Atmos. Chem. Phys.*, 3, 1131-1145, 10.5194/acp-3-1131-2003, 2003.
- 1697 Demou, E. and Donaldson, D. J.: Adsorption of atmospheric gases at the air-water interface. 4:
1698 The influence of salts, *J. Phys. Chem. A*, 106, 982-987, 10.1021/jp0128628, 2002.
- 1699 Desjonqueres, M.-C. and Spanjaard, D.: *Concepts in Surface Physics*, Springer-Verlag Berlin
1700 Heidelberg, 10.1007/978-3-642-61400-2, 1996.
- 1701 Devlin, J. P., Joyce, C., and Buch, V.: Infrared spectra and structures of large water clusters, *J.*
1702 *Phys. Chem. A*, 104, 1974-1977, 2000.
- 1703 Dickbreder, T., Lautner, D., Kohler, A., Klausfering, L., Bechstein, R., and Kuhnle, A.: How
1704 water desorbs from calcite, *Phys. Chem. Chem. Phys.*, 25, 12694, 10.1039/d3cp01159c, 2023.
- 1705 Donahue, N. M., Epstein, S. A., Pandis, S. N., and Robinson, A. L.: A two-dimensional volatility
1706 basis set: 1. organic-aerosol mixing thermodynamics, *Atmos. Chem. Phys.*, 11, 3303-3318,
1707 10.5194/acp-11-3303-2011, 2011.
- 1708 Donahue, N. M., Kroll, J. H., Pandis, S. N., and Robinson, A. L.: A two-dimensional volatility
1709 basis set - Part 2: Diagnostics of organic-aerosol evolution, *Atmos. Chem. Phys.*, 12, 615-634,
1710 10.5194/acp-12-615-2012, 2012.
- 1711 Donaldson, D. J.: Adsorption of atmospheric gases at the air-water interface. I. NH₃, *J. Phys.*
1712 *Chem. A*, 103, 62-70, 1999.
- 1713 Donaldson, D. J. and Anderson, D.: Adsorption of atmospheric gases at the air-water interface. 2.
1714 C-1-C-4 alcohols, acids, and acetone, *J. Phys. Chem. A*, 103, 871-876, 1999.
- 1715 Donaldson, D. J., Guest, J. A., and Goh, M. C.: Evidence For Adsorbed So₂ At the Aqueous Air
1716 Interface, *J. Phys. Chem.*, 99, 9313-9315, 1995.



- 1717 Donaldson, D. J., Ammann, M., Bartels-Rausch, T., and Pöschl, U.: Standard States and
1718 Thermochemical Kinetics in Heterogeneous Atmospheric Chemistry, *J. Phys. Chem. A*, 116,
1719 6312-6316, 10.1021/jp212015g, 2012a.
- 1720 Donaldson, D. J., Ammann, M., Bartels-Rausch, T., and Pöschl, U.: Standard States and
1721 Thermochemical Kinetics in Heterogeneous Atmospheric Chemistry, *J. Phys. Chem. A*, 116,
1722 6312-6316, 10.1021/jp212015g, 2012b.
- 1723 Dovbeshko, G. I., Romanyuk, V. R., Pidgirnyi, D. V., Cherepanov, V. V., Andreev, E. O., Levin,
1724 V. M., Kuzhir, P. P., Kaplas, T., and Svirko, Y. P.: Optical Properties of Pyrolytic Carbon Films
1725 Versus Graphite and Graphene, *Nanoscale Res. Lett.*, 10, 234, 10.1186/s11671-015-0946-8,
1726 2015.
- 1727 Dubois, L. H., Zegarski, B. R., and Nuzzo, R. G.: Fundamental-studies of microscopic wetting
1728 on organic-surfaces .2. interaction of secondary adsorbates with chemically textured organic
1729 monolayers, *J. Am. Chem. Soc.*, 112, 570-579, 10.1021/ja00158a013, 1990.
- 1730 Edebeli, J., Ammann, M., and Bartels-Rausch, T.: Microphysics of the aqueous bulk counters the
1731 water activity driven rate acceleration of bromide oxidation by ozone from 289-245 K, *Environ.*
1732 *Sci.-Process Impacts*, 21, 63-73, 10.1039/c8em00417j, 2019.
- 1733 Edwards, K. C., Klodt, A. L., Galeazzo, T., Schervish, M., Wei, J. L., Fang, T., Donahue, N. M.,
1734 Aumont, B., Nizkorodov, S. A., and Shiraiwa, M.: Effects of Nitrogen Oxides on the Production
1735 of Reactive Oxygen Species and Environmentally Persistent Free Radicals from alpha-Pinene
1736 and Naphthalene Secondary Organic Aerosols, *J. Phys. Chem. A*, 126, 7361-7372,
1737 10.1021/acs.jpca.2c05532, 2022.
- 1738 Ekholm, V., Coleman, C., Prytz, N. B., Walz, M. M., Werner, J., Ohrwall, G., Rubensson, J. E.,
1739 and Bjornholm, O.: Strong enrichment of atmospherically relevant organic ions at the aqueous
1740 interface: the role of ion pairing and cooperative effects, *Phys. Chem. Chem. Phys.*, 20, 27185-
1741 27191, 10.1039/c8cp04525a, 2018.
- 1742 Epstein, S. A., Riipinen, I., and Donahue, N. M.: A Semiempirical Correlation between Enthalpy
1743 of Vaporization and Saturation Concentration for Organic Aerosol, *Environ. Sci. Technol.*, 44,
1744 743-748, 10.1021/es902497z, 2010.
- 1745 Fan, H. Y., Lakey, P. S. J., Frank, E. S., Tobias, D. J., Shiraiwa, M., and Grassian, V. H.:
1746 Comparison of the Adsorption-Desorption Kinetics of Limonene and Carvone on TiO₂ and SiO₂
1747 Surfaces under Different Relative Humidity Conditions, *J. Phys. Chem. C*, 126, 21253-21262,
1748 10.1021/acs.jpcc.2c06853, 2022.
- 1749 Fang, Y., Riahi, S., McDonald, A. T., Shrestha, M., Tobias, D. J., and Grassian, V. H.: What Is
1750 the Driving Force behind the Adsorption of Hydrophobic Molecules on Hydrophilic Surfaces?, *J.*
1751 *Phys. Chem. Lett.*, 10, 468-473, 10.1021/acs.jpcclett.8b03484, 2019.
- 1752 Faust, J. A. and Nathanson, G. M.: Microjets and coated wheels: versatile tools for exploring
1753 collisions and reactions at gas-liquid interfaces, *Chem. Soc. Rev.*, 45, 3609-3620,
1754 10.1039/c6cs00079g, 2016.
- 1755 Faust, J. A., Dempsey, L. P., and Nathanson, G. M.: Surfactant-Promoted Reactions of Cl₂ and
1756 Br₂ with Br⁻ in Glycerol, *J. Phys. Chem. B*, 117, 12602-12612, 10.1021/jp4079037, 2013.
- 1757 Faust, J. A., Sobyra, T. B., and Nathanson, G. M.: Gas-Microjet Reactive Scattering: Collisions
1758 of HCl and DCl with Cool Salty Water, *J. Phys. Chem. Lett.*, 7, 730-735,
1759 10.1021/acs.jpcclett.5b02848, 2016.
- 1760 Fichthorn, K. A. and Miron, R. A.: Thermal desorption of large molecules from solid surfaces,
1761 *Phys. Rev. Lett.*, 89, 4, 10.1103/PhysRevLett.89.196103, 2002.



- 1762 Finlayson-Pitts, B. J. and Pitts, J. N.: Chemistry of the Upper and Lower Atmosphere: Theory,
1763 Experiments and Applications, Academic Press, San Diego, Calif. ; London, xxii, 969 pp.2000.
1764 Fogg, P. G. T. and Sangster, J. M.: Chemicals in the Atmosphere: Solubility, Sources and
1765 Reactivity, John Wiley & Sons Inc., Hoboken, New Jersey2003.
1766 Foster, M. C. and Ewing, G. E.: Adsorption of water on the NaCl(001) surface. II. An infrared
1767 study at ambient temperatures, *J. Chem. Phys.*, 112, 6817-6826, 10.1063/1.481256, 2000.
1768 Frenkel, J.: Theory of the adsorption and related occurrences, *Z. Phys.*, 26, 117-138,
1769 10.1007/bf01327320, 1924.
1770 Fuchs, N. A.: Mechanics of Aerosols, Pergamon, New York1964.
1771 Fuchs, N. A. and Sutugin, A. G.: High-dispersed aerosols, in: Topics in current aerosol research,
1772 edited by: Hidy, G. M., and Brock, J. R., Pergamon, New York, 1971.
1773 Gao, X. F. and Nathanson, G. M.: Exploring Gas-Liquid Reactions with Microjets: Lessons We
1774 Are Learning, *Accounts Chem. Res.*, 55, 3294-3302, 10.1021/acs.accounts.2c00602, 2022.
1775 George, C., Ammann, M., D'Anna, B., Donaldson, D. J., and Nizkorodov, S. A.: Heterogeneous
1776 Photochemistry in the Atmosphere, *Chem. Rev.*, 115, 4218-4258, 10.1021/cr500648z, 2015.
1777 George, I. J. and Abbatt, J. P. D.: Heterogeneous oxidation of atmospheric aerosol particles by
1778 gas-phase radicals, *Nat. Chem.*, 2, 713-722, 10.1038/Nchem.806, 2010.
1779 Giguere, P. A.: Molecular association and structure of hydrogen-peroxide, *J. Chem. Educ.*, 60,
1780 399-401, 10.1021/ed060p399, 1983.
1781 Giraudet, S., Pre, P., Tezel, H., and Le Cloirec, P.: Estimation of adsorption energies using
1782 physical characteristics of activated carbons and VOCs' molecular properties, *Carbon*, 44, 1873-
1783 1883, 10.1016/j.carbon.2006.02.018, 2006.
1784 Goldstein, D. J.: Air and steam stripping of toxic pollutants, Industrial Environmental Research
1785 Laboratory, Cincinnati, OH, USAEPA-68-03-002, 1982.
1786 Goodman, A. L., Bernard, E. T., and Grassian, V. H.: Spectroscopic study of nitric acid and
1787 water adsorption on oxide particles: Enhanced nitric acid uptake kinetics in the presence of
1788 adsorbed water, *J. Phys. Chem. A*, 105, 6443-6457, 2001.
1789 Goss, K. U.: Adsorption of organic vapors on ice and quartz sand at temperatures below 0 C,
1790 *Environ. Sci. Technol.*, 27, 2826-2830, 10.1021/es00049a024, 1993.
1791 Goss, K. U.: Predicting the enrichment of organic-compounds in fog caused by adsorption on the
1792 water-surface, *Atmos. Environ.*, 28, 3513-3517, 10.1016/1352-2310(94)90008-6, 1994a.
1793 Goss, K. U.: Adsorption of organic vapors on polar mineral surfaces and on a bulk water-surface
1794 - development of an empirical predictive model, *Environ. Sci. Technol.*, 28, 640-645,
1795 10.1021/es00053a017, 1994b.
1796 Goss, K. U.: Predicting Adsorption of Organic Chemicals at the Air-Water Interface, *J. Phys.*
1797 *Chem. A*, 113, 12256-12259, 10.1021/jp907347p, 2009.
1798 Goss, K. U. and Eisenreich, S. J.: Adsorption of organic-compounds from water to mineral
1799 surfaces - a theoretical approach, *Abstr. Pap. Am. Chem. Soc.*, 209, 157-ENVR, 1995a.
1800 Goss, K. U. and Eisenreich, S. J.: Effects of temperature and relative-humidity on the adsorption
1801 of organic vapors on hematite, corundum and lime, *Abstr. Pap. Am. Chem. Soc.*, 209, 84-ENVR,
1802 1995b.
1803 Goss, K. U. and Eisenreich, S. J.: Adsorption of VOCs from the gas phase to different minerals
1804 and a mineral mixture, *Environ. Sci. Technol.*, 30, 2135-2142, 10.1021/es950508f, 1996.
1805 Grabow, J. U., Andrews, A. M., Fraser, G. T., Irikura, K. K., Suenram, R. D., Lovas, F. J.,
1806 Lafferty, W. J., and Domenech, J. L.: Microwave spectrum, large-amplitude motions, and ab
1807 initio calculations for N₂O₅, *J. Chem. Phys.*, 105, 7249-7262, 10.1063/1.472586, 1996.



- 1808 Grayson, J. W., Evoy, E., Song, M., Chu, Y. X., Maclean, A., Nguyen, A., Upshur, M. A.,
1809 Ebrahimi, M., Chan, C. K., Geiger, F. M., Thomson, R. J., and Bertram, A. K.: The effect of
1810 hydroxyl functional groups and molar mass on the viscosity of non-crystalline organic and
1811 organic-water particles, *Atmos. Chem. Phys.*, 17, 8509-8524, 10.5194/acp-17-8509-2017, 2017.
1812 Grimm, R. L., Barrentine, N. M., Knox, C. J. H., and Hemminger, J. C.: D2O water interaction
1813 with mixed alkane thiol monolayers of tuned hydrophobic and hydrophilic character, *J. Phys.*
1814 *Chem. C*, 112, 890-894, 10.1021/jp710257q, 2008.
1815 Groves, L. G. and Sudden, S.: The dipole moments of vapours - Part V Aromatic compounds,
1816 *Journal of the Chemical Society*, 1782-1784, 10.1039/jr9370001782, 1937.
1817 Guilloteau, A., Bedjanian, Y., Nguyen, M. L., and Tomas, A.: Desorption of Polycyclic
1818 Aromatic Hydrocarbons from a Soot Surface: Three- to Five-Ring PAHs, *J. Phys. Chem. A*, 114,
1819 942-948, 10.1021/jp908862c, 2010.
1820 Guilloteau, A., Nguyen, M. L., Bedjanian, Y., and Le Bras, G.: Desorption of Polycyclic
1821 Aromatic Hydrocarbons from Soot Surface: Pyrene and Fluoranthene, *J. Phys. Chem. A*, 112,
1822 10552-10559, 10.1021/jp803043s, 2008.
1823 Gussoni, M., Rui, M., and Zerbi, G.: Electronic and relaxation contribution to linear molecular
1824 polarizability. An analysis of the experimental values, *J. Mol. Struct.*, 447, 163-215,
1825 10.1016/s0022-2860(97)00292-5, 1998.
1826 Gustafsson, K. and Andersson, S.: Dipole active vibrations and dipole moments of N-2 and O-2
1827 physisorbed on a metal surface, *J. Chem. Phys.*, 125, 5, 10.1063/1.2218842, 2006.
1828 Hai, P., Wu, C., Ding, X., and Li, Y.: Coverage-dependent adsorption and dissociation of H2O
1829 on Al surfaces, *Phys. Chem. Chem. Phys.*, 25, 13041, 10.1039/d2cp04386f, 2023.
1830 Hait, D. and Head-Gordon, M.: How accurate are static polarizability predictions from density
1831 functional theory? An assessment over 132 species at equilibrium geometry, *Phys. Chem. Chem.*
1832 *Phys.*, 20, 19800-19810, 10.1039/c8cp03569e, 2018.
1833 Hakem, I. F., Boussaid, A., Benchouk-Taleb, H., and Bockstaller, M. R.: Temperature, pressure,
1834 and isotope effects on the structure and properties of liquid water: A lattice approach, *J. Chem.*
1835 *Phys.*, 127, 10, 10.1063/1.2804418, 2007.
1836 Hall, D. G. and Cole, R. H.: Dielectric polarization of sulfuric-acid-solutions, *J. Phys. Chem.*, 85,
1837 1065-1069, 10.1021/j150608a029, 1981.
1838 Hallquist, M., Wenger, J. C., Baltensperger, U., Rudich, Y., Simpson, D., Claeys, M., Dommen,
1839 J., Donahue, N. M., George, C., Goldstein, A. H., Hamilton, J. F., Herrmann, H., Hoffmann, T.,
1840 Iinuma, Y., Jang, M., Jenkin, M. E., Jimenez, J. L., Kiendler-Scharr, A., Maenhaut, W.,
1841 McFiggans, G., Mentel, T. F., Monod, A., Prevot, A. S. H., Seinfeld, J. H., Surratt, J. D.,
1842 Szmigielski, R., and Wildt, J.: The formation, properties and impact of secondary organic
1843 aerosol: current and emerging issues, *Atmos. Chem. Phys.*, 9, 5155-5236, 2009.
1844 Hanefeld, U. and Lefferts, L.: *Catalysis*, John Wiley & Sons, Inc., Hoboken, New Jersey, USA,
1845 384 pp.2018.
1846 Hanson, D. R.: Surface-specific reactions on liquids, *J. Phys. Chem. B*, 101, 4998-5001, 1997.
1847 Hanson, D. R. and Lovejoy, E. R.: The Reaction of ClONO2 With Submicrometer Sulfuric-Acid
1848 Aerosol, *Science*, 267, 1326-1328, 1995.
1849 Hanson, D. R. and Ravishankara, A. R.: The Loss of CF2O On Ice, Nat, and Sulfuric-Acid-
1850 Solutions, *Geophys. Res. Lett.*, 18, 1699-1701, 1991.
1851 Hanson, D. R., Ravishankara, A. R., and Lovejoy, E. R.: Reaction of BrONO2 with H2O on
1852 submicron sulfuric acid aerosol and the implications for the lower stratosphere, *J. Geophys. Res.*,
1853 101, 9063-9069, 1996.



- 1854 Hanson, D. R., Ravishankara, A. R., and Solomon, S.: Heterogeneous Reactions in Sulfuric-Acid
1855 Aerosols - a Framework For Model-Calculations, *J. Geophys. Res.*, 99, 3615-3629, 1994.
1856 Hantal, G., Jedlovszky, P., Hoang, P. N. M., and Picaud, S.: Calculation of the adsorption
1857 isotherm of formaldehyde on ice by grand canonical Monte Carlo simulation, *J. Phys. Chem. C*,
1858 111, 14170-14178, 10.1021/jp0742564, 2007.
1859 Hao, H. X., Leven, I., and Head-Gordon, T.: Can electric fields drive chemistry for an aqueous
1860 microdroplet?, *Nat. Commun.*, 13, 8, 10.1038/s41467-021-27941-x, 2022.
1861 Hartkopf, A. and Karger, B. L.: Study of interfacial properties of water by gas-chromatography,
1862 *Accounts Chem. Res.*, 6, 209-216, 10.1021/ar50066a006, 1973.
1863 Hauxwell, F. and Ottewill, R. H.: Adsorption of toluene vapor on water surfaces, *J. Colloid*
1864 *Interface Sci.*, 28, 514-&, 10.1016/0021-9797(68)90084-2, 1968.
1865 Hearn, J. D. and Smith, G. A.: Ozonolysis of mixed oleic acid/n-docosane particles: The roles of
1866 phase, morphology, and metastable states, *J. Phys. Chem. A*, 111, 11059-11065,
1867 10.1021/jp0755701, 2007.
1868 Helburn, R., Albritton, J., Howe, G., Michael, L., and Franke, D.: Henry's law constants for
1869 fragrance and organic solvent compounds in aqueous industrial surfactants, *J. Chem. Eng. Data*,
1870 53, 1071-1079, 10.1021/je700418a, 2008.
1871 Hems, R. F., Schnitzler, E. G., Liu-Kang, C., Cappa, C. D., and Abbatt, J. P. D.: Aging of
1872 Atmospheric Brown Carbon Aerosol, *ACS Earth Space Chem.*, 5, 722-748,
1873 10.1021/acsearthspacechem.0c00346, 2021.
1874 Henderson, G. L. and Meyer, G. H.: Intramolecular torsional potential and dielectric properties
1875 of 2,3-butanedione, *J. Phys. Chem.*, 80, 2422-2425, 10.1021/j100562a020, 1976.
1876 Hickey, A. L. and Rowley, C. N.: Benchmarking Quantum Chemical Methods for the
1877 Calculation of Molecular Dipole Moments and Polarizabilities, *J. Phys. Chem. A*, 118, 3678-
1878 3687, 10.1021/jp502475e, 2014.
1879 Hildebrand, J. and Scott, R.: The solubility of nonelectrolytes, 3rd ed., Dover Publications, New
1880 York 1964.
1881 Hill, T. L.: An Introduction to Statistical Thermodynamics, Dover Publications, Inc., New York,
1882 501 pp. 1986.
1883 Hoffmann, M. R. and Edwards, J. O.: Kinetics of oxidation of sulfite by hydrogen-peroxide in
1884 acidic solution, *J. Phys. Chem.*, 79, 2096-2098, 10.1021/j100587a005, 1975.
1885 Hoffmann, M. R., Martin, S. T., Choi, W. Y., and Bahnemann, D. W.: Environmental
1886 Applications of Semiconductor Photocatalysis, *Chem. Rev.*, 95, 69-96, 10.1021/cr00033a004,
1887 1995.
1888 Hoose, C. and Möhler, O.: Heterogeneous ice nucleation on atmospheric aerosols: a review of
1889 results from laboratory experiments, *Atmos. Chem. Phys.*, 12, 9817-9854, 10.5194/acp-12-9817-
1890 2012, 2012.
1891 Hoskovec, M., Grygarova, D., Cvacka, J., Streinz, L., Zima, J., Verevkin, S. P., and Koutek, B.:
1892 Determining the vapour pressures of plant volatiles from gas chromatographic retention data, *J.*
1893 *Chromatogr. A*, 1083, 161-172, 10.1016/j.chroma.2005.06.006, 2005.
1894 Houle, F. A., Wiegel, A. A., and Wilson, K. R.: Predicting Aerosol Reactivity Across Scales:
1895 from the Laboratory to the Atmosphere, *Environ. Sci. Technol.*, 52, 13774-13781,
1896 10.1021/acs.est.8b04688, 2018.
1897 Hu, Z. M. and Nakatsuji, H.: Adsorption and disproportionation reaction of OH on Ag surfaces:
1898 dipped adcluster model study, *Surf. Sci.*, 425, 296-312, 10.1016/s0039-6028(99)00215-0, 1999.



- 1899 Huang, Y. Z., Mahrt, F., Xu, S., Shiraiwa, M., Zuend, A., and Bertram, A. K.: Coexistence of
1900 three liquid phases in individual atmospheric aerosol particles, *Proc. Natl. Acad. Sci. U. S. A.*,
1901 118, 9, 10.1073/pnas.2102512118, 2021.
- 1902 Hvidt, A.: Interactions of water with non-polar solutes, *Annual Review of Biophysics and*
1903 *Bioengineering*, 12, 1-20, 10.1146/annurev.bb.12.060183.000245, 1983.
- 1904 Ibrahim, S., Romanias, M. N., Alleman, L. Y., Zeineddine, M. N., Angeli, G. K., Trikalitis, P.
1905 N., and Thevenet, F.: Water Interaction with Mineral Dust Aerosol: Particle Size and
1906 Hygroscopic Properties of Dust, *ACS Earth Space Chem.*, 2, 376–386,
1907 10.1021/acsearthspacechem.7b00152, 2018.
- 1908 Ingram, S., Rovelli, G., Song, Y. C., Topping, D., Dutcher, C. S., Liu, S. H., Nandy, L.,
1909 Shiraiwa, M., and Reid, J. P.: Accurate Prediction of Organic Aerosol Evaporation Using Kinetic
1910 Multilayer Modeling and the Stokes-Einstein Equation, *J. Phys. Chem. A*, 125, 3444-3456,
1911 10.1021/acs.jpca.1c00986, 2021.
- 1912 Isaacman-VanWertz, G., Massoli, P., O'Brien, R., Lim, C., Franklin, J. P., Moss, J. A., Hunter, J.
1913 F., Nowak, J. B., Canagaratna, M. R., Misztal, P. K., Arata, C., Roscioli, J. R., Herndon, S. T.,
1914 Onasch, T. B., Lambe, A. T., Jayne, J. T., Su, L., Knopf, D. A., Goldstein, A. H., Worsnop, D.
1915 R., and Kroll, J. H.: Chemical evolution of atmospheric organic carbon over multiple generations
1916 of oxidation, *Nat. Chem.*, 10.1038/s41557-018-0002-2, 2018.
- 1917 Isakson, M. J. and Sitz, G. O.: Adsorption and desorption of HCl on ice, *J. Phys. Chem. A*, 103,
1918 2044-2049, 10.1021/jp984106g, 1999.
- 1919 IUPAC, McNaught, A. D., and Wilkinson, A. (Eds.): *Compendium of Chemical Terminology*,
1920 (the "Gold Book"), 2nd, Blackwell Scientific Publications, Oxford, 10.1351/goldbook, 1997.
- 1921 Jayne, J. T., Davidovits, P., Worsnop, D. R., Zahniser, M. S., and Kolb, C. E.: Uptake of $\text{SO}_2(\text{G})$
1922 By Aqueous Surfaces As a Function of Ph - the Effect of Chemical-Reaction At the Interface, *J.*
1923 *Phys. Chem.*, 94, 6041-6048, 1990.
- 1924 Jeffrey, G. A.: *An Introduction to Hydrogen Bonding*, Oxford University Press, Oxford, 303
1925 pp. 1997.
- 1926 Jeffrey, G. A. and Saenger, W.: *Hydrogen Bonding in Biological Structures*, Springer-Verlag,
1927 Berlin, 569 pp., 10.1007/978-3-642-85135-3, 1991.
- 1928 Jensen, L., Astrand, P. O., Osted, A., Kongsted, J., and Mikkelsen, K. V.: Polarizability of
1929 molecular clusters as calculated by a dipole interaction model, *J. Chem. Phys.*, 116, 4001-4010,
1930 10.1063/1.1433747, 2002.
- 1931 Jeong, D., McNamara, S. M., Barget, A. J., Raso, A. R. W., Upchurch, L. M., Thanekar, S.,
1932 Quinn, P. K., Simpson, W. R., Fuentes, J. D., Shepson, P. B., and Pratt, K. A.: Multiphase
1933 Reactive Bromine Chemistry during Late Spring in the Arctic: Measurements of Gases, Particles,
1934 and Snow, *ACS Earth Space Chem.*, 6, 2877-2887, 10.1021/acsearthspacechem.2c00189, 2022.
- 1935 Jimenez, J. L., Canagaratna, M. R., Donahue, N. M., Prevot, A. S. H., Zhang, Q., Kroll, J. H.,
1936 DeCarlo, P. F., Allan, J. D., Coe, H., Ng, N. L., Aiken, A. C., Docherty, K. S., Ulbrich, I. M.,
1937 Grieshop, A. P., Robinson, A. L., Duplissy, J., Smith, J. D., Wilson, K. R., Lanz, V. A., Hueglin,
1938 C., Sun, Y. L., Tian, J., Laaksonen, A., Raatikainen, T., Rautiainen, J., Vaattovaara, P., Ehn, M.,
1939 Kulmala, M., Tomlinson, J. M., Collins, D. R., Cubison, M. J., Dunlea, E. J., Huffman, J. A.,
1940 Onasch, T. B., Alfarra, M. R., Williams, P. I., Bower, K., Kondo, Y., Schneider, J., Drewnick, F.,
1941 Borrmann, S., Weimer, S., Demerjian, K., Salcedo, D., Cottrell, L., Griffin, R., Takami, A.,
1942 Miyoshi, T., Hatakeyama, S., Shimono, A., Sun, J. Y., Zhang, Y. M., Dzepina, K., Kimmel, J.
1943 R., Sueper, D., Jayne, J. T., Herndon, S. C., Trimborn, A. M., Williams, L. R., Wood, E. C.,



- 1944 Middlebrook, A. M., Kolb, C. E., Baltensperger, U., and Worsnop, D. R.: Evolution of Organic
1945 Aerosols in the Atmosphere, *Science*, 326, 1525-1529, 10.1126/science.1180353, 2009.
- 1946 Joback, K. G. and Reid, R. C.: Estimation of pure-component properties from group-
1947 contributions, *Chem. Eng. Commun.*, 57, 233-243, 10.1080/00986448708960487, 1987.
- 1948 Johansson, S. M., Lovric, J., Kong, X. R., Thomson, E. S., Hallquist, M., and Pettersson, J. B.
1949 C.: Experimental and Computational Study of Molecular Water Interactions with Condensed
1950 Nopinone Surfaces Under Atmospherically Relevant Conditions, *J. Phys. Chem. A*, 124, 3652-
1951 3661, 10.1021/acs.jpca.9b10970, 2020.
- 1952 Johansson, S. M., Lovric, J., Kong, X. R., Thomson, E. S., Papagiannakopoulos, P., Briquez, S.,
1953 Toubin, C., and Pettersson, J. B. C.: Understanding water interactions with organic surfaces:
1954 environmental molecular beam and molecular dynamics studies of the water-butanol system,
1955 *Phys. Chem. Chem. Phys.*, 21, 1141-1151, 10.1039/c8cp04151b, 2019.
- 1956 Joliat, J., Lenoir, T., and Picaud, S.: Comparative Study of the Adsorption of 1-and 2-Propanol
1957 on Ice by Means of Grand Canonical Monte Carlo Simulations, *ACS Earth Space Chem.*, 13,
1958 10.1021/acsearthspacechem.2c00390, 2023.
- 1959 Julin, J., Shiraiwa, M., Miles, R. E. H., Reid, J. P., Pöschl, U., and Riipinen, I.: Mass
1960 Accommodation of Water: Bridging the Gap Between Molecular Dynamics Simulations and
1961 Kinetic Condensation Models, *J. Phys. Chem. A*, 117, 410-420, 10.1021/jp310594e, 2013.
- 1962 Jungwirth, P., Finlayson-Pitts, B. J., and Tobias, D. J.: Introduction: Structure and chemistry at
1963 aqueous interfaces, *Chem. Rev.*, 106, 1137-1139, 2006.
- 1964 Kahan, T. F., Kwamena, N. O. A., and Donaldson, D. J.: Heterogeneous ozonation kinetics of
1965 polycyclic aromatic hydrocarbons on organic films, *Atmos. Environ.*, 40, 3448-3459,
1966 10.1016/j.atmosenv.2006.02.004, 2006.
- 1967 Kaiser, J. C., Riemer, N., and Knopf, D. A.: Detailed heterogeneous oxidation of soot surfaces in
1968 a particle-resolved aerosol model, *Atmos. Chem. Phys.*, 11, 4505-4520, 2011.
- 1969 Kanakidou, M., Seinfeld, J. H., Pandis, S. N., Barnes, I., Dentener, F. J., Facchini, M. C., Van
1970 Dingenen, R., Ervens, B., Nenes, A., Nielsen, C. J., Swietlicki, E., Putaud, J. P., Balkanski, Y.,
1971 Fuzzi, S., Horth, J., Moortgat, G. K., Winterhalter, R., Myhre, C. E. L., Tsigaridis, K., Vignati,
1972 E., Stephanou, E. G., and Wilson, J.: Organic aerosol and global climate modelling: a review,
1973 *Atmos. Chem. Phys.*, 5, 1053-1123, 2005.
- 1974 Kanji, Z. A., Ladino, L. A., Wex, H., Boose, Y., Burkert-Kohn, M., Cziczo, D. J., and Krämer,
1975 M.: Overview of Ice Nucleating Particles, in: *Ice Formation and Evolution in Clouds and
1976 Precipitation: Measurement and Modeling Challenges*, Meteorological Monographs, American
1977 Meteorological Society, 1.1-1.33, DOI: 10.1175/AMSMONOGRAPHS-D-16-0006.1, 2017.
- 1978 Kerbrat, M., Huthwelker, T., Gaggeler, H. W., and Ammann, M.: Interaction of Nitrous Acid
1979 with Polycrystalline Ice: Adsorption on the Surface and Diffusion into the Bulk, *J. Phys. Chem.
1980 C*, 114, 2208-2219, 10.1021/jp909535c, 2010.
- 1981 Keyser, L. F., Moore, S. B., and Leu, M. T.: Surface-Reaction and Pore Diffusion in Flow-Tube
1982 Reactors, *J. Phys. Chem.*, 95, 5496-5502, 1991.
- 1983 Kieckbusch, T. G. and King, C. J.: Partition-coefficients for acetates in food systems, *J. Agric.
1984 Food Chem.*, 27, 504-507, 10.1021/jf60223a033, 1979.
- 1985 Kim, Y. K., Park, S. C., Kim, J. H., Lee, C. W., and Kang, H.: Interaction of Carbon Dioxide and
1986 Hydroxide Ion at the Surface of Ice Films, *J. Phys. Chem. C*, 112, 18104-18109,
1987 10.1021/jp806643e, 2008.
- 1988 Kisliuk, P.: The sticking probabilities of gases chemisorbed on the surfaces of solids, *J. Phys.
1989 Chem. Solids*, 3, 95-101, 10.1016/0022-3697(57)90054-9, 1957.



- 1990 Kisliuk, P.: The sticking probabilities of gases chemisorbed on the surfaces of solids. 2., *J. Phys.*
1991 *Chem. Solids*, 5, 78-84, 1958.
- 1992 Klassen, J. K., Fiehrer, K. M., and Nathanson, G. M.: Collisions of organic molecules with
1993 concentrated sulfuric acid: Scattering, trapping, and desorption, *J. Phys. Chem. B*, 101, 9098-
1994 9106, 10.1021/jp972329l, 1997.
- 1995 Klassen, J. K., Hu, Z. J., and Williams, L. R.: Diffusion coefficients for HCl and HBr in 30 wt %
1996 to 72 wt % sulfuric acid at temperatures between 220 and 300 K, *J. Geophys. Res.-Atmospheres*,
1997 103, 16197-16202, 10.1029/98jd01252, 1998.
- 1998 Knopf, D. A. and Alpert, P. A.: Atmospheric ice nucleation, *Nat. Rev. Phys.*, 10.1038/s42254-
1999 023-00570-7, 2023.
- 2000 Knopf, D. A. and Ammann, M.: Technical note: Adsorption and desorption equilibria from
2001 statistical thermodynamics and rates from transition state theory, *Atmos. Chem. Phys.*, 21,
2002 15725-15753, 10.5194/acp-21-15725-2021, 2021.
- 2003 Knopf, D. A. and Koop, T.: Heterogeneous nucleation of ice on surrogates of mineral dust, *J.*
2004 *Geophys. Res.*, 111, D12201, 10.1029/2005jd006894, 2006.
- 2005 Knopf, D. A., Alpert, P. A., and Wang, B.: The Role of Organic Aerosol in Atmospheric Ice
2006 Nucleation: A Review, *ACS Earth Space Chem.*, 2, 168–202,
2007 10.1021/acsearthspacechem.7b00120, 2018.
- 2008 Knopf, D. A., Anthony, L. M., and Bertram, A. K.: Reactive uptake of O₃ by multicomponent
2009 and multiphase mixtures containing oleic acid, *J. Phys. Chem. A*, 109, 5579-5589, 2005.
- 2010 Knopf, D. A., Forrester, S. M., and Slade, J. H.: Heterogeneous oxidation kinetics of organic
2011 biomass burning aerosol surrogates by O₃, NO₂, N₂O₅, and NO₃, *Phys. Chem. Chem. Phys.*,
2012 13, 21050-21062, 10.1039/C1cp22478f, 2011.
- 2013 Knopf, D. A., Pöschl, U., and Shiraiwa, M.: Radial Diffusion and Penetration of Gas Molecules
2014 and Aerosol Particles through Laminar Flow Reactors, Denuders, and Sampling Tubes, *Anal.*
2015 *Chem.*, 87, 3746-3754, 10.1021/ac5042395, 2015.
- 2016 Knopf, D. A., Ammann, M., Berkemeier, T., Pöschl, U., and Shiraiwa, M.: Desorption Lifetimes
2017 and Activation Energies influencing Gas-Surface Interactions and Multiphase Chemical
2018 Kinetics: Atmospheric and Environmental Implications [dataset], XYZ, 2023.
- 2019 Knox, C. J. H. and Phillips, L. F.: Capillary-wave model of gas-liquid exchange, *J. Phys. Chem.*
2020 *B*, 102, 8469-8472, 10.1021/jp973183t, 1998.
- 2021 Koch, T. G. and Rossi, M. J.: Direct measurement of surface residence times: Nitryl chloride and
2022 chlorine nitrate on alkali halides at room temperature, *J. Phys. Chem. A*, 102, 9193-9201, 1998a.
- 2023 Koch, T. G. and Rossi, M. J.: Direct measurement of surface residence times: Nitryl chloride and
2024 chlorine nitrate on alkali halides at room temperature, *J. Phys. Chem. A*, 102, 9193-9201,
2025 10.1021/jp982539d, 1998b.
- 2026 Koch, T. G., Fenter, F. F., and Rossi, M. J.: Real-time measurement of residence times of gas
2027 molecules on solid surfaces, *Chemical Physics Letters*, 275, 253-260, 1997.
- 2028 Kolasinski, K. W.: *Surface Science: Foundations of Catalysis and Nanoscience*, 3rd, John Wiley
2029 & Sons, Ltd., West Sussex, United Kingdom, 556 pp., 10.1002/9781119941798, 2012.
- 2030 Kolb, C. E., Worsnop, D. R., Zahniser, M. S., Davidovits, P., Keyser, L. F., Leu, M.-T., Molina,
2031 M. J., Hanson, D. R., Ravishankara, A. R., Williams, L. R., and Tolbert, M. A.: Laboratory
2032 Studies of Atmospheric Heterogeneous Chemistry, in: *Progress and Problems in Atmospheric*
2033 *Chemistry*, edited by: Barker, J. R., World Scientific, Singapore, 771-875, 1995.
- 2034 Kolb, C. E., Cox, R. A., Abbatt, J. P. D., Ammann, M., Davis, E. J., Donaldson, D. J., Garrett, B.
2035 C., George, C., Griffiths, P. T., Hanson, D. R., Kulmala, M., McFiggans, G., Pöschl, U.,



- 2036 Riipinen, I., Rossi, M. J., Rudich, Y., Wagner, P. E., Winkler, P. M., Worsnop, D. R., and O'
2037 Dowd, C. D.: An overview of current issues in the uptake of atmospheric trace gases by aerosols
2038 and clouds, *Atmos. Chem. Phys.*, 10, 10561-10605, 2010.
- 2039 Kolomiitsova, T. D., Lyaptsev, A. V., and Shchepkin, D. N.: Determination of parameters of the
2040 dipole moment of the CO₂ molecule, *Opt. Spectrosc.*, 88, 648-660, 10.1134/1.626856, 2000.
- 2041 Kong, X. R., Thomson, E. S., Markovic, N., and Pettersson, J. B. C.: Dynamics and Kinetics of
2042 Methanol-Graphite Interactions at Low Surface Coverage, *ChemPhysChem*, 20, 2171-2178,
2043 10.1002/cphc.201900457, 2019.
- 2044 Kong, X. R., Lovri, J., Johansson, S. M., Prisle, N. L., and Pettersson, J. B. C.: Dynamics and
2045 Sorption Kinetics of Methanol Monomers and Clusters on Nopinone Surfaces, *J. Phys. Chem. A*,
2046 125, 6263-6272, 10.1021/acs.jpca.1c02309, 2021.
- 2047 Kong, X. R., Papagiannakopoulos, P., Thomson, E. S., Markovic, N., and Pettersson, J. B. C.:
2048 Water Accommodation and Desorption Kinetics on Ice, *J. Phys. Chem. A*, 118, 3973-3979,
2049 10.1021/jp503504e, 2014a.
- 2050 Kong, X. R., Thomson, E. S., Papagiannakopoulos, P., Johansson, S. M., and Pettersson, J. B.
2051 C.: Water Accommodation on Ice and Organic Surfaces: Insights from Environmental Molecular
2052 Beam Experiments, *J. Phys. Chem. B*, 118, 13378-13386, 10.1021/jp5044046, 2014b.
- 2053 Kong, X. R., Waldner, A., Orlando, F., Artiglia, L., Huthwelker, T., Ammann, M., and Bartels-
2054 Rausch, T.: Coexistence of Physisorbed and Solvated HCl at Warm Ice Surfaces, *J. Phys. Chem.*
2055 *Lett.*, 8, 4757-4762, 10.1021/acs.jpcllett.7b01573, 2017.
- 2056 Koop, T., Bookhold, J., Shiraiwa, M., and Pöschl, U.: Glass transition and phase state of organic
2057 compounds: dependency on molecular properties and implications for secondary organic
2058 aerosols in the atmosphere, *Phys. Chem. Chem. Phys.*, 13, 19238-19255, 10.1039/c1cp22617g,
2059 2011.
- 2060 Kroll, J. H., Donahue, N. M., Jimenez, J. L., Kessler, S. H., Canagaratna, M. R., Wilson, K. R.,
2061 Altieri, K. E., Mazzoleni, L. R., Wozniak, A. S., Bluhm, H., Mysak, E. R., Smith, J. D., Kolb, C.
2062 E., and Worsnop, D. R.: Carbon oxidation state as a metric for describing the chemistry of
2063 atmospheric organic aerosol, *Nat Chem*, 3, 133-139, 10.1038/nchem.948, 2011.
- 2064 Kronberg, B.: The hydrophobic effect, *Curr. Opin. Colloid Interface Sci.*, 22, 14-22,
2065 10.1016/j.cocis.2016.02.001, 2016.
- 2066 Kronberger, H. and Weiss, J.: Formation and structure of some organic molecular compounds.
2067 Part III. The dielectric polarisation of some solid crystalline molecular compounds, *J. Chem.*
2068 *Soc.*, 464-469, 10.1039/jr9440000464, 1944.
- 2069 Kuhne, R., Ebert, R. U., and Schuurmann, G.: Prediction of the temperature dependency of
2070 Henry's law constant from chemical structure, *Environ. Sci. Technol.*, 39, 6705-6711,
2071 10.1021/es050527h, 2005.
- 2072 Kwamena, N. O. A., Thornton, J. A., and Abbatt, J. P. D.: Kinetics of surface-bound benzo a
2073 pyrene and ozone on solid organic and salt aerosols, *J. Phys. Chem. A*, 108, 11626-11634,
2074 10.1021/jp046161x, 2004.
- 2075 Laib, J. P. and Mittleman, D. M.: Temperature-Dependent Terahertz Spectroscopy of Liquid n-
2076 alkanes, *J. Infrared Millim. Terahertz Waves*, 31, 1015-1021, 10.1007/s10762-010-9678-0, 2010.
- 2077 Laidler, K. J.: The mechanisms of some elementary surface reactions, *J. Phys. Colloid Chem.*,
2078 53, 712-732, 10.1021/j150470a010, 1949.
- 2079 Laidler, K. J., Glasstone, S., and Eyring, H.: Application of the Theory of Absolute Reaction
2080 Rates to Heterogeneous Processes II. Chemical Reactions on Surfaces, *J. Chem. Phys.*, 8, 667-
2081 676, 10.1063/1.1750737, 1940.



- 2082 Lakey, P. S. J., Cummings, B. E., Waring, M. S., Morrison, G. C., and Shiraiwa, M.: Effective
2083 mass accommodation for partitioning of organic compounds into surface films with different
2084 viscosities, *Environ. Sci.-Process Impacts*, 15, 10.1039/d3em00213f, 2023.
- 2085 Lakey, P. S. J., Eichler, C. M. A., Wang, C. Y., Little, J. C., and Shiraiwa, M.: Kinetic multi-
2086 layer model of film formation, growth, and chemistry (KM-FILM): Boundary layer processes,
2087 multi-layer adsorption, bulk diffusion, and heterogeneous reactions, *Indoor Air*, 31, 2070-2083,
2088 10.1111/ina.12854, 2021.
- 2089 Lakey, P. S. J., Berkemeier, T., Krapf, M., Dommen, J., Steimer, S. S., Whalley, L. K., Ingham,
2090 T., Baeza-Romero, M. T., Pöschl, U., Shiraiwa, M., Ammann, M., and Heard, D. E.: The effect
2091 of viscosity and diffusion on the HO₂ uptake by sucrose and secondary organic aerosol particles,
2092 *Atmos. Chem. Phys.*, 16, 13035-13047, 10.5194/acp-16-13035-2016, 2016.
- 2093 Langenberg, S. and Schurath, U.: Gas chromatography using ice-coated fused silica columns:
2094 study of adsorption of sulfur dioxide on water ice, *Atmos. Chem. Phys.*, 18, 7527-7537,
2095 10.5194/acp-18-7527-2018, 2018.
- 2096 Langmuir, I.: A theory of adsorption, *Phys. Rev.*, 6, 79-80, 1915.
- 2097 Langmuir, I.: The evaporation, condensation and reflection of molecules and the mechanism of
2098 adsorption, *Phys. Rev.*, 8, 149-176, 10.1103/PhysRev.8.149, 1916.
- 2099 Langmuir, I.: The adsorption of gases on plane surfaces of glass, mica and platinum, *J. Am.*
2100 *Chem. Soc.*, 40, 1361-1403, 10.1021/ja02242a004, 1918.
- 2101 Laskin, A., Laskin, J., and Nizkorodov, S. A.: Chemistry of Atmospheric Brown Carbon, *Chem.*
2102 *Rev.*, 115, 4335-4382, 10.1021/cr5006167, 2015.
- 2103 Lee, G., Lee, B., Kim, J., and Cho, K.: Ozone Adsorption on Graphene: Ab Initio Study and
2104 Experimental Validation, *J. Phys. Chem. C*, 113, 14225-14229, 10.1021/jp904321n, 2009.
- 2105 Lee, M. T., Orlando, F., Artiglia, L., Chen, S. Z., and Ammann, M.: Chemical Composition and
2106 Properties of the Liquid-Vapor Interface of Aqueous C₁ to C₄ Monofunctional Acid and Alcohol
2107 Solutions, *J. Phys. Chem. A*, 120, 9749-9758, 10.1021/acs.jpca.6b09261, 2016.
- 2108 Lee, M. T., Orlando, F., Khabiri, M., Roeselova, M., Brown, M. A., and Ammann, M.: The
2109 opposing effect of butanol and butyric acid on the abundance of bromide and iodide at the
2110 aqueous solution-air interface, *Phys. Chem. Chem. Phys.*, 21, 8418-8427, 10.1039/c8cp07448h,
2111 2019.
- 2112 Lee, W. M. G. and Chen, J. C.: Partitioning coefficients of polycyclic aromatic-hydrocarbons in
2113 stack gas from a municipal incinerator, *Environ. Int.*, 21, 827-831, 10.1016/0160-
2114 4120(95)00092-4, 1995.
- 2115 Lejonhuthun, L., Andersson, P. U., Hallquist, M., Thomson, E. S., and Pettersson, J. B. C.:
2116 Interactions of N₂O₅ and Related Nitrogen Oxides with Ice Surfaces: Desorption Kinetics and
2117 Collision Dynamics, *J. Phys. Chem. B*, 118, 13427-13434, 10.1021/jp5053826, 2014.
- 2118 Leluk, K., Orzechowski, K., Jerie, K., Baranowski, A., Slonka, T., and Glowinski, J.: Dielectric
2119 permittivity of kaolinite heated to high temperatures, *J. Phys. Chem. Solids*, 71, 827-831,
2120 10.1016/j.jpcs.2010.02.008, 2010.
- 2121 Leng, C. B., Kish, J. D., Roberts, J. E., Dwebi, I., Chon, N., and Liu, Y.: Temperature-Dependent
2122 Henry's Law Constants of Atmospheric Amines, *J. Phys. Chem. A*, 119, 8884-8891,
2123 10.1021/acs.jpca.5b05174, 2015.
- 2124 Li, G., Su, H., Kuhn, U., Meusel, H., Ammann, M., Shao, M., Pöschl, U., and Cheng, Y. F.:
2125 Technical note: Influence of surface roughness and local turbulence on coated-wall flow tube
2126 experiments for gas uptake and kinetic studies, *Atmos. Chem. Phys.*, 18, 2669-2686,
2127 10.5194/acp-18-2669-2018, 2018.



- 2128 Li, J. and Knopf, D. A.: Representation of Multiphase OH Oxidation of Amorphous Organic
2129 Aerosol for Tropospheric Conditions, *Environ. Sci. Technol.*, *55*, 7266-7275,
2130 10.1021/acs.est.0c07668, 2021.
- 2131 Li, J. N., Forrester, S. M., and Knopf, D. A.: Heterogeneous oxidation of amorphous organic
2132 aerosol surrogates by O₃, NO₃, and OH at typical tropospheric temperatures, *Atmos. Chem.*
2133 *Phys.*, *20*, 6055-6080, 10.5194/acp-20-6055-2020, 2020.
- 2134 Li, Y. and Shiraiwa, M.: Timescales of secondary organic aerosols to reach equilibrium at
2135 various temperatures and relative humidities, *Atmos. Chem. Phys.*, *19*, 5959-5971, 10.5194/acp-
2136 19-5959-2019, 2019.
- 2137 Li, Y., Pöschl, U., and Shiraiwa, M.: Molecular corridors and parameterizations of volatility in
2138 the chemical evolution of organic aerosols, *Atmos. Chem. Phys.*, *16*, 3327-3344, 10.5194/acp-
2139 16-3327-2016, 2016.
- 2140 Liang, Z., Li, K. J., Wang, Z. M., Bu, Y. S., and Zhang, J. L.: Adsorption and reaction
2141 mechanisms of single and double H₂O molecules on graphene surfaces with defects: a density
2142 functional theory study, *Phys. Chem. Chem. Phys.*, *23*, 19071-19082, 10.1039/d1cp02595c,
2143 2021.
- 2144 Lide, D. R.: *CRC Handbook of Chemistry and Physics*, 82nd, CRC Press., Boca Raton 2008.
- 2145 Lileev, A. and Lyashchenko, A.: Dielectric properties of ammonium salt aqueous solutions, *J.*
2146 *Mol. Liq.*, *150*, 4-8, 10.1016/j.molliq.2009.08.008, 2009.
- 2147 Longfellow, C. A., Imamura, T., Ravishankara, A. R., and Hanson, D. R.: HONO solubility and
2148 heterogeneous reactivity on sulfuric acid surfaces, *J. Phys. Chem. A*, *102*, 3323-3332, 1998.
- 2149 Mack, K. M. and Muentzer, J. S.: Stark and Zeeman properties of ozone from molecular-beam
2150 spectroscopy, *J. Chem. Phys.*, *66*, 5278-5283, 10.1063/1.433909, 1977.
- 2151 Mader, B. T., Goss, K. U., and Eisenreich, S. J.: Sorption of nonionic, hydrophobic organic
2152 chemicals to mineral surfaces, *Environ. Sci. Technol.*, *31*, 1079-1086, 10.1021/es960606g, 1997.
- 2153 Maribo-Mogensen, B., Kontogeorgis, G. M., and Thomsen, K.: Modeling of Dielectric
2154 Properties of Aqueous Salt Solutions with an Equation of State, *J. Phys. Chem. B*, *117*, 10523-
2155 10533, 10.1021/jp403375t, 2013.
- 2156 Marsh, A. R. W. and McElroy, W. J.: The dissociation-constant and Henry law constant of HCl
2157 in aqueous-solution, *Atmos. Environ.*, *19*, 1075-1080, 10.1016/0004-6981(85)90192-1, 1985.
- 2158 Marshall, F. H., Berkemeier, T., Shiraiwa, M., Nandy, L., Ohm, P. B., Dutcher, C. S., and Reid,
2159 J. P.: Influence of particle viscosity on mass transfer and heterogeneous ozonolysis kinetics in
2160 aqueous-sucrose-maleic acid aerosol, *Phys. Chem. Chem. Phys.*, *20*, 15560-15573,
2161 10.1039/c8cp01666f, 2018.
- 2162 Marshall, F. H., Miles, R. E. H., Song, Y. C., Ohm, P. B., Power, R. M., Reid, J. P., and Dutcher,
2163 C. S.: Diffusion and reactivity in ultraviscous aerosol and the correlation with particle viscosity,
2164 *Chem. Sci.*, *7*, 1298-1308, 10.1039/c5sc03223g, 2016.
- 2165 Masel, R. I.: *Principles of Adsorption and Reaction on Solid Surfaces*, Wiley Series in Chemical
2166 Engineering 1996.
- 2167 McEachran, A. D., Mansouri, K., Grulke, C., Schymanski, E. L., Ruttkies, C., and Williams, A.
2168 J.: "MS-Ready" structures for non-targeted high-resolution mass spectrometry screening studies,
2169 *J. Cheminformatics*, *10*, 16, 10.1186/s13321-018-0299-2, 2018.
- 2170 McNamara, S. M., Chen, Q. J., Edebeli, J., Kulju, K. D., Mumpfield, J., Fuentes, J. D., Bertman,
2171 S. B., and Pratt, K. A.: Observation of N₂O₅ Deposition and ClNO₂ Production on the Saline
2172 Snowpack, *ACS Earth Space Chem.*, *5*, 1020-1031, 10.1021/acsearthspacechem.0c00317, 2021.



- 2173 McNeill, V. F., Loerting, T., Geiger, F. M., Trout, B. L., and Molina, M. J.: Hydrogen chloride-
2174 induced surface disordering on ice, *Proc. Natl. Acad. Sci. U. S. A.*, 103, 9422-9427,
2175 10.1073/pnas.0603494103, 2006.
- 2176 McNeill, V. F., Geiger, F. M., Loerting, T., Trout, B. L., Molina, L. T., and Molina, M. J.:
2177 Interaction of hydrogen chloride with ice surfaces: The effects of grain size, surface roughness,
2178 and surface disorder, *J. Phys. Chem. A*, 111, 6274-6284, 10.1021/jp068914g, 2007.
- 2179 McNeill, V. F., Grannas, A. M., Abbatt, J. P. D., Ammann, M., Ariya, P., Bartels-Rausch, T.,
2180 Domine, F., Donaldson, D. J., Guzman, M. I., Heger, D., Kahan, T. F., Klan, P., Masclin, S.,
2181 Toubin, C., and Voisin, D.: Organics in environmental ices: sources, chemistry, and impacts,
2182 *Atmos. Chem. Phys.*, 12, 9653-9678, 10.5194/acp-12-9653-2012, 2012.
- 2183 Mendes, P. C. D., Costa-Amaral, R., Gomes, J. F., and Da Silva, J. L. F.: The influence of
2184 hydroxy groups on the adsorption of three-carbon alcohols on Ni(111), Pd(111) and Pt(111)
2185 surfaces: a density functional theory study within the D3 dispersion correction, *Phys. Chem.*
2186 *Chem. Phys.*, 21, 8434, 10.1039/c9cp00752k, 2019.
- 2187 Meng, S., Wang, E. G., and Gao, S. W.: Water adsorption on metal surfaces: A general picture
2188 from density functional theory studies, *Phys. Rev. B*, 69, 13, 10.1103/PhysRevB.69.195404,
2189 2004.
- 2190 Merino, E. and Ribagorda, M.: Control over molecular motion using the cis-trans
2191 photoisomerization of the azo group, *Beilstein J. Org. Chem.*, 8, 1071-1090, 10.3762/bjoc.8.119,
2192 2012.
- 2193 Messerer, A., Niessner, R., and Pöschl, U.: Comprehensive kinetic characterization of the
2194 oxidation and gasification of model and real diesel soot by nitrogen oxides and oxygen under
2195 engine exhaust conditions: Measurement, Langmuir-Hinshelwood, and Arrhenius parameters,
2196 *Carbon*, 44, 307-324, 10.1016/j.carbon.2005.07.017, 2006.
- 2197 Messerer, A., Schmatloch, V., Pöschl, U., and Niessner, R.: Combined particle emission
2198 reduction and heat recovery from combustion exhaust - A novel approach for small wood-fired
2199 appliances, *Biomass & Bioenergy*, 31, 512-521, 10.1016/j.biombioe.2007.01.022, 2007.
- 2200 Meyer, H., Entel, P., and Hafner, J.: Physisorption of water on salt surfaces, *Surf. Sci.*, 488, 177-
2201 192, 10.1016/s0039-6028(01)01136-0, 2001.
- 2202 Mikhailov, E., Vlasenko, S., Martin, S. T., Koop, T., and Poschl, U.: Amorphous and crystalline
2203 aerosol particles interacting with water vapor: conceptual framework and experimental evidence
2204 for restructuring, phase transitions and kinetic limitations, *Atmos. Chem. Phys.*, 9, 9491-9522,
2205 2009.
- 2206 Millany, H. M. and Jonscher, A. K.: Dielectric-properties of stearic-acid multilayers, *Thin Solid*
2207 *Films*, 68, 257-273, 10.1016/0040-6090(80)90151-0, 1980.
- 2208 Mmereki, B. T., Hicks, J. M., and Donaldson, D. J.: Adsorption of atmospheric gases at the air-
2209 water interface. 3: Methylamines, *J. Phys. Chem. A*, 104, 10789-10793, 10.1021/jp0023258,
2210 2000.
- 2211 Moise, T., Flores, J. M., and Rudich, Y.: Optical properties of secondary organic aerosols and
2212 their changes by chemical processes, *Chem. Rev.*, 115, 4400-4439, 10.1021/cr5005259, 2015.
- 2213 Mopsik, F. I.: Digest of Literature on Dielectrics: National Academy of Sciences, National
2214 Research Council Washington, D. C. , 1967.
- 2215 Morris, J. R., Behr, P., Antman, M. D., Ringeisen, B. R., Splan, J., and Nathanson, G. M.:
2216 Molecular beam scattering from supercooled sulfuric acid: Collisions of HCl, HBr, and HNO₃
2217 with 70 wt % D₂SO₄, *J. Phys. Chem. A*, 104, 6738-6751, 10.1021/jp000105o, 2000.



- 2218 Moussa, S. G., McIntire, T. M., Szori, M., Roeselova, M., Tobias, D. J., Grimm, R. L.,
2219 Hemminger, J. C., and Finlayson-Pitts, B. J.: Experimental and Theoretical Characterization of
2220 Adsorbed Water on Self-Assembled Monolayers: Understanding the Interaction of Water with
2221 Atmospherically Relevant Surfaces, *J. Phys. Chem. A*, 113, 2060-2069, 10.1021/jp808710n,
2222 2009.
- 2223 Mu, Q., Shiraiwa, M., Octaviani, M., Ma, N., Ding, A. J., Su, H., Lammel, G., Poschl, U., and
2224 Cheng, Y. F.: Temperature effect on phase state and reactivity controls atmospheric multiphase
2225 chemistry and transport of PAHs, *Sci. Adv.*, 4, 8, 10.1126/sciadv.aap7314, 2018.
- 2226 Nakanishi, M. and Nozaki, R.: Systematic study of the glass transition in polyhydric alcohols,
2227 *Phys. Rev. E*, 83, 5, 10.1103/PhysRevE.83.051503, 2011.
- 2228 Nakatsuji, H.: Dipped adcluster model for chemisorptions and catalytic reactions on a metal-
2229 surface, *J. Chem. Phys.*, 87, 4995-5001, 10.1063/1.452814, 1987.
- 2230 Nathanson, G. M.: Molecular beam studies of gas-liquid interfaces, *Annu. Rev. Phys. Chem.*, 55,
2231 231-255, 10.1146/annurev.physchem.55.091602.094357, 2004.
- 2232 Nathanson, G. M., Davidovits, P., Worsnop, D. R., and Kolb, C. E.: Dynamics and kinetics at the
2233 gas-liquid interface, *J. Phys. Chem.*, 100, 13007-13020, 1996.
- 2234 Nelson, C. E., Elam, J. W., Tolbert, M. A., and George, S. M.: H₂O and HCl adsorption on
2235 single crystal alpha-Al₂O₃(0001) at stratospheric temperatures, *Appl. Surf. Sci.*, 171, 21-33,
2236 2001.
- 2237 Nelson, C. E., Elam, J. W., Cameron, M. A., Tolbert, M. A., and George, S. M.: Desorption of
2238 H₂O from a hydroxylated single-crystal alpha-Al₂O₃(0001) surface, *Surf. Sci.*, 416, 341-353,
2239 10.1016/s0039-6028(98)00439-7, 1998.
- 2240 NIST: NIST Computational Chemistry Comparison and Benchmark Database,
2241 10.18434/T47C7Z, 2018.
- 2242 Nizkorodov, S. A., Laskin, J., and Laskin, A.: Molecular chemistry of organic aerosols through
2243 the application of high resolution mass spectrometry, *Phys. Chem. Chem. Phys.*, 13, 3612-3629,
2244 10.1039/c0cp02032j, 2011.
- 2245 Ohrwall, G., Prisle, N. L., Ottosson, N., Werner, J., Ekholm, V., Walz, M. M., and Bjorneholm,
2246 O.: Acid-Base Speciation of Carboxylate Ions in the Surface Region of Aqueous Solutions in the
2247 Presence of Ammonium and Aminium Ions, *J. Phys. Chem. B*, 119, 4033-4040,
2248 10.1021/jp509945g, 2015.
- 2249 Oszust, J. and Ratajczak, H.: Dipole-moments and spectral features of some phenol-diethylamine
2250 complexes, *J. Chem. Soc. Farad. T* 1, 77, 1215-1221, 10.1039/f19817701215, 1981.
- 2251 Pankow, J. F.: Common gamma-intercept and single compound regressions of gas particle
2252 partitioning data vs 1/t, *Atmos. Environ. A-Gen.*, 25, 2229-2239, 10.1016/0960-1686(91)90098-
2253 r, 1991.
- 2254 Paserba, K. R. and Gellman, A. J.: Effects of conformational isomerism on the desorption
2255 kinetics of n-alkanes from graphite, *J. Chem. Phys.*, 115, 6737-6751, 10.1063/1.1398574, 2001.
- 2256 Penkett, S. A., Jones, B. M. R., Brice, K. A., and Eggleton, A. E. J.: Importance of atmospheric
2257 ozone and hydrogen-peroxide in oxidizing sulfur-dioxide in cloud and rainwater, *Atmos.*
2258 *Environ.*, 13, 123-137, 10.1016/0004-6981(79)90251-8, 1979.
- 2259 Perraud, V., Bruns, E. A., Ezell, M. J., Johnson, S. N., Yu, Y., Alexander, M. L., Zelenyuk, A.,
2260 Imre, D., Chang, W. L., Dabdub, D., Pankow, J. F., and Finlayson-Pitts, B. J.: Nonequilibrium
2261 atmospheric secondary organic aerosol formation and growth, *P. Natl. Acad. Sci. USA*, 109,
2262 2836-2841, 10.1073/pnas.1119909109, 2012.



- 2263 Petters, M. D., Prenni, A. J., Kreidenweis, S. M., DeMott, P. J., Matsunaga, A., Lim, Y. B., and
2264 Ziemann, P. J.: Chemical aging and the hydrophobic-to-hydrophilic conversion of carbonaceous
2265 aerosol, *Geophys. Res. Lett.*, 33, 10.1029/2006gl027249, 2006.
- 2266 Poe, S. H., Valsaraj, K. T., Thibodeaux, L. J., and Springer, C.: Equilibrium vapor-phase
2267 adsorption of volatile organic-chemicals on dry soils, *J. Hazard. Mater.*, 19, 17-32,
2268 10.1016/0304-3894(88)85071-4, 1988.
- 2269 Pöschl, U. and Shiraiwa, M.: Multiphase Chemistry at the Atmosphere-Biosphere Interface
2270 Influencing Climate and Public Health in the Anthropocene, *Chem. Rev.*, 115, 4440-4475,
2271 10.1021/cr500487s, 2015.
- 2272 Pöschl, U., Rudich, Y., and Ammann, M.: Kinetic model framework for aerosol and cloud
2273 surface chemistry and gas-particle interactions - Part 1: General equations, parameters, and
2274 terminology, *Atmos. Chem. Phys.*, 7, 5989-6023, 2007.
- 2275 Pöschl, U., Letzel, T., Schauer, C., and Niessner, R.: Interaction of ozone and water vapor with
2276 spark discharge soot aerosol particles coated with benzo a pyrene: O₃ and H₂O adsorption,
2277 benzo a pyrene degradation, and atmospheric implications, *J. Phys. Chem. A*, 105, 4029-4041,
2278 2001.
- 2279 Pouvesle, N., Kippenberger, M., Schuster, G., and Crowley, J. N.: The interaction of H₂O₂ with
2280 ice surfaces between 203 and 233 K, *Phys. Chem. Chem. Phys.*, 12, 15544-15550,
2281 10.1039/c0cp01656j, 2010.
- 2282 Raja, S., Yaccone, F. S., Ravikrishna, R., and Valsaraj, K. T.: Thermodynamic parameters for
2283 the adsorption of aromatic hydrocarbon vapors at the gas-water interface, *J. Chem. Eng. Data*,
2284 47, 1213-1219, 10.1021/je025520j, 2002.
- 2285 Rajyam, B. S. and Murty, C. R. K.: Dipole moments of some alkyl phenylacetates, *Indian J. Pure*
2286 *Appl. Phys.*, 4, 327-&, 1966.
- 2287 Rampi, M. A., Schueller, O. J. A., and Whitesides, G. M.: Alkanethiol self-assembled
2288 monolayers as the dielectric of capacitors with nanoscale thickness, *Appl. Phys. Lett.*, 72, 1781-
2289 1783, 10.1063/1.121183, 1998.
- 2290 Raso, A. R. W., Custard, K. D., May, N. W., Tanner, D., Newburn, M. K., Walker, L., Moore, R.
2291 J., Huey, L. G., Alexander, L., Shepson, P. B., and Pratt, K. A.: Active molecular iodine
2292 photochemistry in the Arctic, *Proc. Natl. Acad. Sci. U. S. A.*, 114, 10053-10058,
2293 10.1073/pnas.1702803114, 2017.
- 2294 Ravishankara, A. R.: Heterogeneous and multiphase chemistry in the troposphere, *Science*, 276,
2295 1058-1065, 1997.
- 2296 Redhead, P. A.: Thermal desorption of gases, *Vacuum*, 12, 203-211, 10.1016/0042-
2297 207X(62)90978-8, 1962.
- 2298 Remorov, R. G. and Bardwell, M. W.: Model of uptake of OH radicals on nonreactive solids, *J.*
2299 *Phys. Chem. B*, 109, 20036-20043, 2005.
- 2300 Rettner, C. T., Auerbach, D. J., Tully, J. C., and Kleyn, A. W.: Chemical dynamics at the gas-
2301 surface interface, *J. Phys. Chem.*, 100, 13021-13033, 10.1021/jp9536007, 1996.
- 2302 Ringeisen, B. R., Muentner, A. H., and Nathanson, G. M.: Collisions of DCl with liquid glycerol:
2303 Evidence for rapid, near-interfacial D → H exchange and desorption, *J. Phys. Chem. B*, 106,
2304 4999-5010, 10.1021/jp013959x, 2002a.
- 2305 Ringeisen, B. R., Muentner, A. H., and Nathanson, G. M.: Collisions of HCl, DCl, and HBr with
2306 liquid glycerol: Gas uptake, D → H exchange, and solution thermodynamics, *J. Phys. Chem. B*,
2307 106, 4988-4998, 10.1021/jp013960w, 2002b.



- 2308 Robinson, D. A., Cooper, J. D., and Gardner, C. M. K.: Modelling the relative permittivity of
2309 soils using soil hygroscopic water content, *J. Hydrol.*, 255, 39-49, 10.1016/s0022-
2310 1694(01)00508-x, 2002.
- 2311 Robinson, G. N., Worsnop, D. R., Jayne, J. T., Kolb, C. E., Swartz, E., and Davidovits, P.:
2312 Heterogeneous uptake of HCl by sulfuric acid solutions, *J. Geophys. Res.*, 103, 25371-25381,
2313 1998.
- 2314 Romaner, L., Heimel, G., Ambrosch-Draxl, C., and Zojer, E.: The Dielectric Constant of Self-
2315 Assembled Monolayers, *Adv. Funct. Mater.*, 18, 3999-4006, 10.1002/adfm.200800876, 2008.
- 2316 Romanias, M. N., Ourrad, H., Thevenet, F., and Riffault, V.: Investigating the Heterogeneous
2317 Interaction of VOCs with Natural Atmospheric Particles: Adsorption of Limonene and Toluene
2318 on Saharan Mineral Dusts, *J. Phys. Chem. A*, 120, 1197-1212, 10.1021/acs.jpca.5b10323, 2016.
- 2319 Rothfuss, N. E. and Petters, M. D.: Influence of Functional Groups on the Viscosity of Organic
2320 Aerosol, *Environ. Sci. Technol.*, 51, 271-279, 10.1021/acs.est.6b04478, 2017.
- 2321 Rouquerol, J. and Davy, L.: Automatic gravimetric apparatus for recording adsorption-isotherms
2322 of gases or vapors onto solids, *Thermochim. Acta*, 24, 391-397, 10.1016/0040-6031(78)80027-6,
2323 1978.
- 2324 Rowland, F. S.: Stratospheric ozone depletion, *Annu. Rev. Phys. Chem.*, 42, 731-768,
2325 10.1146/annurev.physchem.42.1.731, 1991.
- 2326 Rudich, Y., Donahue, N. M., and Mentel, T. F.: Aging of organic aerosol: Bridging the gap
2327 between laboratory and field studies, *Annu. Rev. Phys. Chem.*, 58, 321-352,
2328 10.1146/annurev.physchem.58.032806.104432, 2007.
- 2329 Salmeron, M. and Somorjai, G. A.: Adsorption and bonding of butane and pentane on the
2330 Pt(111) crystal-surfaces - effects of oxygen treatments and deuterium pre-adsorption, *J. Phys.*
2331 *Chem.*, 85, 3835-3840, 10.1021/j150625a025, 1981.
- 2332 Sander, R.: Compilation of Henry's law constants (version 4.0) for water as solvent, *Atmos.*
2333 *Chem. Phys.*, 15, 4399-4981, 10.5194/acp-15-4399-2015, 2015.
- 2334 Sander, S. P., Abbatt, J., Barker, J. R., Burkholder, J. B., Friedl, R. R., Golden, D. M., Huie, R.
2335 E., Kolb, C. E., Kurylo, M. J., Moortgat, G. K., Orkin, V. L., and Wine, P. H.: Chemical Kinetics
2336 and Photochemical Data for Use in Atmospheric Studies, Evaluation No. 17, NASA Jet
2337 Propulsion Laboratory, Pasadena 2011.
- 2338 Savara, A.: Standard States for Adsorption on Solid Surfaces: 2D Gases, Surface Liquids, and
2339 Langmuir Adsorbates, *J. Phys. Chem. C*, 117, 15710-15715, 10.1021/jp404398z, 2013.
- 2340 Savara, A., Schmidt, C. M., Geiger, F. M., and Weitz, E.: Adsorption Entropies and Enthalpies
2341 and Their Implications for Adsorbate Dynamics, *J. Phys. Chem. C*, 113, 2806-2815,
2342 10.1021/jp806221j, 2009.
- 2343 Schervish, M. and Shiraiwa, M.: Impact of phase state and non-ideal mixing on equilibration
2344 timescales of secondary organic aerosol partitioning, *Atmos. Chem. Phys.*, 23, 221-233,
2345 10.5194/acp-23-221-2023, 2023.
- 2346 Schlesinger, D., Lowe, S. J., Olenius, T., Kong, X. R., Pettersson, J. B. C., and Riipinen, I.:
2347 Molecular Perspective on Water Vapor Accommodation into Ice and Its Dependence on
2348 Temperature, *J. Phys. Chem. A*, 124, 10879-10889, 10.1021/acs.jpca.0c09357, 2020.
- 2349 Schroder, E.: Methanol Adsorption on Graphene, *J. Nanomater.*, 2013, 6, 10.1155/2013/871706,
2350 2013.
- 2351 Schwartz, S. E.: Mass-transport considerations pertinent to aqueous phase reactions of gases in
2352 liquid-water clouds, in: Chemistry of multiphase atmospheric systems, edited by: Jaeschke, W.,
2353 NATO ASI Series, G6, Springer, New York, 1986.



- 2354 Sebastiani, F., Campbell, R. A., Rastogi, K., and Pfrang, C.: Nighttime oxidation of surfactants at
2355 the air-water interface: effects of chain length, head group and saturation, *Atmos. Chem. Phys.*,
2356 18, 3249-3268, 10.5194/acp-18-3249-2018, 2018.
- 2357 Seinfeld, J. H. and Pandis, S. N.: *Atmospheric Chemistry and Physics. From Air Pollution to*
2358 *Climate Change*, John Wiley, New York, 1326 pp.1998.
- 2359 Sharif, S.: Chemical and mineral-composition of dust and its effect on the dielectric-constant,
2360 *IEEE Trans. Geosci. Remote Sensing*, 33, 353-359, 10.1109/36.377935, 1995.
- 2361 Shen, C. Y., Zhang, W., Choczynski, J., Davies, J. F., and Zhang, H. F.: Phase State and Relative
2362 Humidity Regulate the Heterogeneous Oxidation Kinetics and Pathways of Organic-Inorganic
2363 Mixed Aerosols, *Environ. Sci. Technol.*, 56, 15398-15407, 10.1021/acs.est.2c04670, 2022.
- 2364 Shi, Q., Jayne, J. T., Kolb, C. E., Worsnop, D. R., and Davidovits, P.: Kinetic model for reaction
2365 of ClONO₂ with H₂O and HCl and HOCl with HCl in sulfuric acid solutions, *J. Geophys. Res.*,
2366 106, 24259-24274, 2001.
- 2367 Shinoda, K.: Iceberg formation and solubility, *J. Phys. Chem.*, 81, 1300-1302,
2368 10.1021/j100528a016, 1977.
- 2369 Shinoda, K.: Characteristic property in aqueous-solutions - effect of iceberg formation of water
2370 surrounding solute on the solubility (or cmc) and its peculiar temperature-dependence, *Adv.*
2371 *Colloid Interface Sci.*, 41, 81-100, 10.1016/0001-8686(92)80008-1, 1992.
- 2372 Shiraiwa, M. and Pöschl, U.: Mass accommodation and gas-particle partitioning in secondary
2373 organic aerosols: dependence on diffusivity, volatility, particle-phase reactions, and penetration
2374 depth, *Atmos. Chem. Phys.*, 21, 1565-1580, 10.5194/acp-21-1565-2021, 2021.
- 2375 Shiraiwa, M. and Seinfeld, J. H.: Equilibration timescale of atmospheric secondary organic
2376 aerosol partitioning, *Geophys. Res. Lett.*, 39, L24801, 10.1029/2012gl054008, 2012.
- 2377 Shiraiwa, M., Garland, R. M., and Pöschl, U.: Kinetic double-layer model of aerosol surface
2378 chemistry and gas-particle interactions (K2-SURF): Degradation of polycyclic aromatic
2379 hydrocarbons exposed to O₃, NO₂, H₂O, OH and NO₃, *Atmos. Chem. Phys.*, 9, 9571-9586,
2380 2009.
- 2381 Shiraiwa, M., Pfrang, C., and Pöschl, U.: Kinetic multi-layer model of aerosol surface and bulk
2382 chemistry (KM-SUB): the influence of interfacial transport and bulk diffusion on the oxidation
2383 of oleic acid by ozone, *Atmos. Chem. Phys.*, 10, 3673-3691, 2010.
- 2384 Shiraiwa, M., Ammann, M., Koop, T., and Pöschl, U.: Gas uptake and chemical aging of
2385 semisolid organic aerosol particles, *P. Natl. Acad. Sci. USA*, 108, 11003-11008, 2011a.
- 2386 Shiraiwa, M., Pfrang, C., Koop, T., and Pöschl, U.: Kinetic multi-layer model of gas-particle
2387 interactions in aerosols and clouds (KM-GAP): linking condensation, evaporation and chemical
2388 reactions of organics, oxidants and water, *Atmos. Chem. Phys.*, 12, 2777-2794, 2012.
- 2389 Shiraiwa, M., Zuend, A., Bertram, A. K., and Seinfeld, J. H.: Gas-particle partitioning of
2390 atmospheric aerosols: interplay of physical state, non-ideal mixing and morphology, *Phys.*
2391 *Chem. Chem. Phys.*, 15, 11441-11453, 10.1039/c3cp51595h, 2013a.
- 2392 Shiraiwa, M., Berkemeier, T., Schilling-Fahnestock, K. A., Seinfeld, J. H., and Pöschl, U.:
2393 Molecular corridors and kinetic regimes in the multiphase chemical evolution of secondary
2394 organic aerosol, *Atmos. Chem. Phys.*, 14, 8323-8341, 10.5194/acp-14-8323-2014, 2014.
- 2395 Shiraiwa, M., Sosedova, Y., Rouviere, A., Yang, H., Zhang, Y. Y., Abbatt, J. P. D., Ammann,
2396 M., and Pöschl, U.: The role of long-lived reactive oxygen intermediates in the reaction of ozone
2397 with aerosol particles, *Nature Chemistry*, 3, 291-295, 2011b.



- 2398 Shiraiwa, M., Yee, L. D., Schilling, K. A., Loza, C. L., Craven, J. S., Zuend, A., Ziemann, P. J.,
2399 and Seinfeld, J. H.: Size distribution dynamics reveal particle-phase chemistry in organic aerosol
2400 formation, *Proc. Natl. Acad. Sci. U. S. A.*, 110, 11746-11750, 10.1073/pnas.1307501110, 2013b.
2401 Shiraiwa, M., Li, Y., Tsimpidi, A. P., Karydis, V. A., Berkemeier, T., Pandis, S. N., Lelieveld, J.,
2402 Koop, T., and Pöschl, U.: Global distribution of particle phase state in atmospheric secondary
2403 organic aerosols, *Nat. Commun.*, 8, 10.1038/ncomms15002, 2017a.
2404 Shiraiwa, M., Li, Y., Tsimpidi, A. P., Karydis, V. A., Berkemeier, T., Pandis, S. N., Lelieveld, J.,
2405 Koop, T., and Pöschl, U.: Global distribution of particle phase state in atmospheric secondary
2406 organic aerosols, *Nat. Commun.*, 8, 15002, 10.1038/ncomms15002, 2017b.
2407 Shiraiwa, M., Ueda, K., Pozzer, A., Lammel, G., Kampf, C. J., Fushimi, A., Enami, S., Arangio,
2408 A. M., Frohlich-Nowoisky, J., Fujitani, Y., Furuyama, A., Lakey, P. S. J., Lelieveld, J., Lucas,
2409 K., Morino, Y., Pöschl, U., Takaharna, S., Takami, A., Tong, H. J., Weber, B., Yoshino, A., and
2410 Sato, K.: Aerosol Health Effects from Molecular to Global Scales, *Environ. Sci. Technol.*, 51,
2411 13545-13567, 10.1021/acs.est.7b04417, 2017c.
2412 Shklyarevskii, I. N. and Pakhomov, P. L.: Separation of contributions from free and coupled
2413 electrons into real and imaginary parts of a dielectric-constant of gold, *Opt. Spektrosk.*, 34, 163-
2414 166, 1973.
2415 Shrivastava, M., Lou, S. J., Zelenyuk, A., Easter, R. C., Corley, R. A., Thrall, B. D., Rasch, P. J.,
2416 Fast, J. D., Simonich, S. L. M., Shen, H. Z., and Tao, S.: Global long-range transport and lung
2417 cancer risk from polycyclic aromatic hydrocarbons shielded by coatings of organic aerosol (vol
2418 114, pg 1246, 2017), *Proc. Natl. Acad. Sci. U. S. A.*, 114, E2263-E2263,
2419 10.1073/pnas.1702221114, 2017a.
2420 Shrivastava, M., Cappa, C. D., Fan, J. W., Goldstein, A. H., Guenther, A. B., Jimenez, J. L.,
2421 Kuang, C., Laskin, A., Martin, S. T., Ng, N. L., Petaja, T., Pierce, J. R., Rasch, P. J., Roldin, P.,
2422 Seinfeld, J. H., Shilling, J., Smith, J. N., Thornton, J. A., Volkamer, R., Wang, J., Worsnop, D.
2423 R., Zaveri, R. A., Zelenyuk, A., and Zhang, Q.: Recent advances in understanding secondary
2424 organic aerosol: Implications for global climate forcing, *Rev. Geophys.*, 55, 509-559,
2425 10.1002/2016rg000540, 2017b.
2426 Silva, S. C. and Devlin, J. P.: Interaction of acetylene, ethylene, and benzene with ice surfaces, *J.*
2427 *Phys. Chem.*, 98, 10847-10852, 10.1021/j100093a027, 1994.
2428 Slade, J. H. and Knopf, D. A.: Heterogeneous OH oxidation of biomass burning organic aerosol
2429 surrogate compounds: assessment of volatilisation products and the role of OH concentration on
2430 the reactive uptake kinetics, *Phys. Chem. Chem. Phys.*, 15, 5898-5915, 10.1039/c3cp44695f,
2431 2013.
2432 Slade, J. H. and Knopf, D. A.: Multiphase OH oxidation kinetics of organic aerosol: The role of
2433 particle phase state and relative humidity, *Geophys. Res. Lett.*, 41, 5297-5306,
2434 10.1002/2014gl060582, 2014.
2435 Slade, J. H., Thalman, R., Wang, J., and Knopf, D. A.: Chemical aging of single and
2436 multicomponent biomass burning aerosol surrogate particles by OH: implications for cloud
2437 condensation nucleus activity, *Atmos. Chem. Phys.*, 15, 10183-10201, 10.5194/acp-15-10183-
2438 2015, 2015.
2439 Slade, J. H., Shiraiwa, M., Arangio, A., Su, H., Pöschl, U., Wang, J., and Knopf, D. A.: Cloud
2440 droplet activation through oxidation of organic aerosol influenced by temperature and particle
2441 phase state, *Geophys. Res. Lett.*, 44, 1583-1591, 10.1002/2016gl072424, 2017.
2442 Slater, B. and Michaelides, A.: Surface premelting of water ice, *Nat. Rev. Chem.*, 3, 172-188,
2443 10.1038/s41570-019-0080-8, 2019.



- 2444 Smith, R. S. and Kay, B. D.: Desorption Kinetics of Carbon Dioxide from a Graphene-Covered
2445 Pt(111) Surface, *J. Phys. Chem. A*, 123, 3248–3254 10.1021/acs.jpca.9b00674, 2019.
- 2446 Sokolov, O. and Abbatt, J. P. D.: Adsorption to ice of n-alcohols (ethanol to 1-hexanol), acetic
2447 acid, and hexanal, *J. Phys. Chem. A*, 106, 775-782, 2002.
- 2448 Sokolowska, Z., Jozefaciuk, G., Sokolowski, S., and Ourumovapesheva, A.: Adsorption of
2449 water-vapor by soils - investigations of the influence of organic-matter, iron, and aluminum on
2450 energetic heterogeneity of soil clays, *Clay Clay Min.*, 41, 346-352, 10.1346/ccmn.1993.0410310,
2451 1993.
- 2452 Solomon, S.: Stratospheric ozone depletion: A review of concepts and history, *Rev. Geophys.*,
2453 37, 275-316, 1999.
- 2454 Speight, J. G.: in: *Lange's Handbook of Chemistry*, 17th ed., McGraw-Hill Education, New
2455 York, 2017.
- 2456 Springmann, M., Knopf, D. A., and Riemer, N.: Detailed heterogeneous chemistry in an urban
2457 plume box model: reversible co-adsorption of O₃, NO₂, and H₂O on soot coated with benzo
2458 a pyrene, *Atmos. Chem. Phys.*, 9, 7461-7479, 2009.
- 2459 Sprowl, L. H., Campbell, C. T., and Arnadottir, L.: Hindered Translator and Hindered Rotor
2460 Models for Adsorbates: Partition Functions and Entropies, *J. Phys. Chem. C*, 120, 9719-9731,
2461 10.1021/acs.jpcc.5b11616, 2016.
- 2462 Staudinger, J. and Roberts, P. V.: A critical compilation of Henry's law constant temperature
2463 dependence relations for organic compounds in dilute aqueous solutions, *Chemosphere*, 44, 561-
2464 576, 10.1016/s0045-6535(00)00505-1, 2001.
- 2465 Steimer, S. S., Berkemeier, T., Gilgen, A., Krieger, U. K., Peter, T., Shiraiwa, M., and Ammann,
2466 M.: Shikimic acid ozonolysis kinetics of the transition from liquid aqueous solution to highly
2467 viscous glass, *Phys. Chem. Chem. Phys.*, 17, 31101-31109, 10.1039/c5cp04544d, 2015.
- 2468 Steiner, D. and Burtscher, H. K.: Desorption of perylene from combustion, nacl, and carbon
2469 particles, *Environ. Sci. Technol.*, 28, 1254-1259, 10.1021/es00056a012, 1994.
- 2470 Steiner, T.: The hydrogen bond in the solid state, *Angew. Chem.-Int. Edit.*, 41, 48-76,
2471 10.1002/1521-3773(20020104)41:1<48::Aid-anie48>3.0.Co;2-u, 2002.
- 2472 Stephenson, R. M. and Malanowski, S.: *Handbook of the Thermodynamics of Organic*
2473 *Compounds*, Elsevier Science Publishing Co., Inc., Dordrecht, 10.1007/978-94-009-3173-2,
2474 1987.
- 2475 Stolzenburg, D., Fischer, L., Vogel, A. L., Heinritzi, M., Schervish, M., Simon, M., Wagner, A.
2476 C., Dada, L., Ahonen, L. R., Amorim, A., Baccarini, A., Bauer, P. S., Baumgartner, B., Bergen,
2477 A., Bianchi, F., Breitenlechner, M., Brilke, S., Mazon, S. B., Chen, D. X., Dias, A., Draper, D.
2478 C., Duplissy, J., Haddad, I., Finkenzeller, H., Frege, C., Fuchs, C., Garmash, O., Gordon, H., He,
2479 X., Helm, J., Hofbauer, V., Hoyle, C. R., Kim, C., Kirkby, J., Kontkanen, J., Kuerten, A.,
2480 Lampilahti, J., Lawler, M., Lehtipalo, K., Leiminger, M., Mai, H., Mathot, S., Mentler, B.,
2481 Molteni, U., Nie, W., Nieminen, T., Nowak, J. B., Ojdanic, A., Onnela, A., Passananti, M.,
2482 Petaja, T., Quelever, L. L. J., Rissanen, M. P., Sarnela, N., Schallhart, S., Tauber, C., Tome, A.,
2483 Wagner, R., Wang, M., Weitz, L., Wimmer, D., Xiao, M., Yan, C., Ye, P., Zha, Q.,
2484 Baltensperger, U., Curtius, J., Dommen, J., Flagan, R. C., Kulmala, M., Smith, J. N., Worsnop,
2485 D. R., Hansel, A., Donahue, N. M., and Winkler, P. M.: Rapid growth of organic aerosol
2486 nanoparticles over a wide tropospheric temperature range, *Proc. Natl. Acad. Sci. U. S. A.*, 115,
2487 9122-9127, 10.1073/pnas.1807604115, 2018.
- 2488 Stull, D. R.: Vapor pressure of pure substances - inorganic compounds, *Industrial and*
2489 *Engineering Chemistry*, 4, 540-550, 10.1021/ie50448a023, 1947.



- 2490 Su, H., Cheng, Y. F., and Pöschl, U.: New Multiphase Chemical Processes Influencing
2491 Atmospheric Aerosols, Air Quality, and Climate in the Anthropocene, *Accounts Chem. Res.*, 53,
2492 2034-2043, 10.1021/acs.accounts.0c00246, 2020.
- 2493 Svribely, W. J., Ablard, J. E., and Warner, J. C.: Molar polarizations in extremely dilute
2494 solutions. The dipole moments of d-limonene, d-pinene, methyl benzoate and ethyl benzoate, *J.*
2495 *Am. Chem. Soc.*, 57, 652-655, 10.1021/ja01307a015, 1935.
- 2496 Tabai, S., Rogalski, M., Solimando, R., and Malanowski, S. K.: Activity coefficients of
2497 chlorophenols in water at infinite dilution, *J. Chem. Eng. Data*, 42, 1147-1150,
2498 10.1021/je960336h, 1997.
- 2499 Tait, S. L., Dohnalek, Z., Campbell, C. T., and Kay, B. D.: n-alkanes on Pt(111) and on
2500 C(0001)/Pt(111): Chain length dependence of kinetic desorption parameters, *J. Chem. Phys.*,
2501 125, 15, 10.1063/1.2400235, 2006.
- 2502 Takenaka, N. and Rossi, M. J.: The heterogeneous reaction of NO₂ with NH₄Cl: A molecular
2503 diffusion tube study, *J. Atmos. Chem.*, 50, 171-194, 10.1007/s10874-005-5898-4, 2005.
- 2504 Tang, M. J., Cziczo, D. J., and Grassian, V. H.: Interactions of Water with Mineral Dust Aerosol:
2505 Water Adsorption, Hygroscopicity, Cloud Condensation, and Ice Nucleation, *Chem. Rev.*, 116,
2506 4205-4259, 10.1021/acs.chemrev.5b00529, 2016.
- 2507 Tenhulscher, T. E. M., Vandervelde, L. E., and Bruggeman, W. A.: Temperature-dependence of
2508 Henry law constants for selected chlorobenzenes, polychlorinated-biphenyls and polycyclic
2509 aromatic-hydrocarbons, *Environ. Toxicol. Chem.*, 11, 1595-1603, 10.1897/1552-
2510 8618(1992)11[1595:Tdohlc]2.0.Co;2, 1992.
- 2511 Thomas, J. M. and Williams, B. R.: Theory and applications of vacuum microbalance
2512 techniques, *Quarterly Reviews*, 19, 231+, 10.1039/qr9651900231, 1965.
- 2513 Thomson, E. S., Kong, X., Papagiannakopoulos, P., and Pettersson, J. B. C.: Deposition-mode
2514 ice nucleation reexamined at temperatures below 200 K, *Atmos. Chem. Phys.*, 15, 1621-1632,
2515 10.5194/acp-15-1621-2015, 2015.
- 2516 Thomson, E. S., Kong, X. R., Andersson, P. U., Markovic, N., and Pettersson, J. B. C.: Collision
2517 Dynamics and Solvation of Water Molecules in a Liquid Methanol Film, *J. Phys. Chem. Lett.*, 2,
2518 2174-2178, 10.1021/jz200929y, 2011.
- 2519 Tolbert, M. A., Rossi, M. J., Malhotra, R., and Golden, D. M.: Reaction of chlorine nitrate with
2520 hydrogen-chloride and water at antarctic stratospheric temperatures, *Science*, 238, 1258-1260,
2521 10.1126/science.238.4831.1258, 1987.
- 2522 Townes, C. H. and Schawlow, A. L.: *Microwave Spectroscopy*, Dover Publications, Inc., New
2523 York 1975.
- 2524 Tully, J. C.: The dynamics of adsorption and desorption, *Surf. Sci.*, 299, 667-677, 10.1016/0039-
2525 6028(94)90688-2, 1994.
- 2526 Ulbricht, H., Zacharia, R., Cindir, N., and Hertel, T.: Thermal desorption of gases and solvents
2527 from graphite and carbon nanotube surfaces, *Carbon*, 44, 2931-2942,
2528 10.1016/j.carbon.2006.05.040, 2006.
- 2529 Ulrich, T., Ammann, M., Leutwyler, S., and Bartels-Rausch, T.: The adsorption of peroxyntic
2530 acid on ice between 230 K and 253 K, *Atmos. Chem. Phys.*, 12, 1833-1845, 10.5194/acp-12-
2531 1833-2012, 2012.
- 2532 Usher, C. R., Michel, A. E., and Grassian, V. H.: Reactions on mineral dust, *Chem. Rev.*, 103,
2533 4883-4939, 2003.



- 2534 Valsaraj, K. T.: Binding constants for non-polar hydrophobic organics at the air-water-interface -
2535 comparison of experimental and predicted values, *Chemosphere*, 17, 2049-2053, 10.1016/0045-
2536 6535(88)90015-x, 1988a.
- 2537 Valsaraj, K. T.: On the physicochemical aspects of partitioning of non-polar hydrophobic
2538 organics at the air-water-interface, *Chemosphere*, 17, 875-887, 10.1016/0045-6535(88)90060-4,
2539 1988b.
- 2540 Valsaraj, K. T.: Hydrophobic compounds in the environment - adsorption equilibrium at the air-
2541 water-interface, *Water Res.*, 28, 819-830, 10.1016/0043-1354(94)90088-4, 1994.
- 2542 Valsaraj, K. T.: Trace gas adsorption thermodynamics at the air-water interface: Implications in
2543 atmospheric chemistry, *Pure Appl. Chem.*, 81, 1889-1901, 10.1351/pac-con-08-07-06, 2009.
- 2544 Valsaraj, K. T. and Thibodeaux, L. J.: Equilibrium adsorption of chemical vapors on surface
2545 soils, landfills and landfarms - a review, *J. Hazard. Mater.*, 19, 79-99, 10.1016/0304-
2546 3894(88)85075-1, 1988.
- 2547 Valsaraj, K. T., Thoma, G. J., Reible, D. D., and Thibodeaux, L. J.: On the enrichment of
2548 hydrophobic organic-compounds in fog droplets, *Atmospheric Environment Part a-General*
2549 *Topics*, 27, 203-210, 10.1016/0960-1686(93)90351-x, 1993.
- 2550 van der Sman, R. G. M.: Predictions of Glass Transition Temperature for Hydrogen Bonding
2551 Biomaterials, *J. Phys. Chem. B*, 117, 16303-16313, 10.1021/jp408184u, 2013.
- 2552 van Duijnen, P. T. and Swart, M.: Molecular and atomic polarizabilities: Thole's model revisited,
2553 *J. Phys. Chem. A*, 102, 2399-2407, 10.1021/jp980221f, 1998.
- 2554 Vega, C. P., Pohjola, V. A., Samyn, D., Pettersson, R., Isaksson, E., Bjorkman, M. P., Martma,
2555 T., Marca, A., and Kaiser, J.: First ice core records of NO₃- stable isotopes from
2556 Lomonosovfonna, Svalbard, *J. Geophys. Res.-Atmos.*, 120, 313-330, 10.1002/2013jd020930,
2557 2015.
- 2558 Vieceli, J., Roeselova, M., and Tobias, D. J.: Accommodation coefficients for water vapor at the
2559 air/water interface, *Chemical Physics Letters*, 393, 249-255, 10.1016/j.cplett.2004.06.038, 2004.
- 2560 Vieceli, J., Roeselova, M., Potter, N., Dang, L. X., Garrett, B. C., and Tobias, D. J.: Molecular
2561 dynamics simulations of atmospheric oxidants at the air-water interface: Solvation and
2562 accommodation of OH and O₃, *J. Phys. Chem. B*, 109, 15876-15892, 10.1021/jp051361+, 2005.
- 2563 Vinogradov, S. N. and Linnell, R. H.: *Hydrogen Bonding*, Van Nostrand Reinhold Company,
2564 London, 319 pp.1971.
- 2565 Virtanen, A., Joutsensaari, J., Koop, T., Kannosto, J., Yli-Pirila, P., Leskinen, J., Makela, J. M.,
2566 Holopainen, J. K., Pöschl, U., Kulmala, M., Worsnop, D. R., and Laaksonen, A.: An amorphous
2567 solid state of biogenic secondary organic aerosol particles, *Nature*, 467, 824-827,
2568 10.1038/nature09455, 2010.
- 2569 Vlasenko, A., Huthwelker, T., Gaggeler, H. W., and Ammann, M.: Kinetics of the heterogeneous
2570 reaction of nitric acid with mineral dust particles: an aerosol flowtube study, *Phys. Chem. Chem.*
2571 *Phys.*, 11, 7921-7930, 10.1039/b904290n, 2009.
- 2572 Voigt, C., Schlager, H., Ziereis, H., Karcher, B., Luo, B. P., Schiller, C., Kramer, M., Popp, P. J.,
2573 Irie, H., and Kondo, Y.: Nitric acid in cirrus clouds, *Geophys. Res. Lett.*, 33, L05803,
2574 10.1029/2005gl025159, 2006.
- 2575 Voloshina, E., Usvyat, D., Schutz, M., Dedkov, Y., and Paulus, B.: On the physisorption of
2576 water on graphene: a CCSD(T) study, *Phys. Chem. Chem. Phys.*, 13, 12041-12047,
2577 10.1039/c1cp20609e, 2011.



- 2578 von Domaros, M., Lakey, P. S. J., Shiraiwa, M., and Tobias, D. J.: Multiscale Modeling of
2579 Human Skin Oil-Induced Indoor Air Chemistry: Combining Kinetic Models and Molecular
2580 Dynamics, *J. Phys. Chem. B*, 124, 3836-3843, 10.1021/acs.jpcc.0c02818, 2020.
- 2581 von Hessberg, P., Pouvesle, N., Winkler, A. K., Schuster, G., and Crowley, J. N.: Interaction of
2582 formic and acetic acid with ice surfaces between 187 and 227 K. Investigation of single species-
2583 and competitive adsorption, *Phys. Chem. Chem. Phys.*, 10, 2345-2355, 10.1039/b800831k, 2008.
- 2584 Wang, B. and Knopf, D. A.: Heterogeneous ice nucleation on particles composed of humic-like
2585 substances impacted by O₃, *J. Geophys. Res.*, 116, D03205, 10.1029/2010jd014964, 2011.
- 2586 Wang, B., Lambe, A. T., Massoli, P., Onasch, T. B., Davidovits, P., Worsnop, D. R., and Knopf,
2587 D. A.: The deposition ice nucleation and immersion freezing potential of amorphous secondary
2588 organic aerosol: Pathways for ice and mixed-phase cloud formation, *J. Geophys. Res.*, 117,
2589 D16209, 10.1029/2012jd018063, 2012.
- 2590 Wang, C., Collins, D. B., Arata, C., Goldstein, A. H., Mattila, J. M., Farmer, D. K., Ampollini,
2591 L., DeCarlo, P. F., Novoselac, A., Vance, M. E., Nazaroff, W. W., and Abbatt, J. P. D.: Surface
2592 reservoirs dominate dynamic gas-surface partitioning of many indoor air constituents, *Sci. Adv.*,
2593 6, 11, 10.1126/sciadv.aay8973, 2020.
- 2594 Wang, X. F., Qiao, L., Deng, C. B., Chu, G., Li, X. F., Zhao, Q., and Wang, G. L.: Study on the
2595 characteristics of nitrogen dioxide adsorption and storage of coal residue in coal-fired power
2596 plants in goaf, *Sci Rep*, 11, 11, 10.1038/s41598-021-87855-y, 2021.
- 2597 Weaver, J. F., Carlsson, A. F., and Madix, R. J.: The adsorption and reaction of low molecular
2598 weight alkanes on metallic single crystal surfaces, *Surf. Sci. Rep.*, 50, 107-199, 10.1016/s0167-
2599 5729(03)00031-1, 2003.
- 2600 Wei, W. M., Zheng, R. H., Jing, Y. Y., Liu, Y. T., Hu, J. C., Ye, Y., and Shi, Q.: Theoretical
2601 Study on Raman Spectra of Aqueous Peroxynitric Acid, *Chin. J. Chem. Phys.*, 24, 625-630,
2602 10.1088/1674-0068/24/05/625-630, 2011.
- 2603 Weschler, C. J. and Nazaroff, W. W.: Growth of organic films on indoor surfaces, *Indoor Air*,
2604 27, 1101-1112, 10.1111/ina.12396, 2017.
- 2605 Whitten, J. L.: Theoretical-studies of surface-reactions - Embedded-cluster theory, *Chemical*
2606 *Physics*, 177, 387-397, 10.1016/0301-0104(93)80020-a, 1993.
- 2607 Wiberg, K. B. and Rablen, P. R.: Comparison of atomic charges derived via different procedures,
2608 *J. Comput. Chem.*, 14, 1504-1518, 10.1002/jcc.540141213, 1993.
- 2609 Wiegel, A. A., Liu, M. J., Hinsberg, W. D., Wilson, K. R., and Houle, F. A.: Diffusive
2610 confinement of free radical intermediates in the OH radical oxidation of semisolid aerosols,
2611 *Phys. Chem. Chem. Phys.*, 19, 6814-6830, 10.1039/c7cp00696a, 2017.
- 2612 Willis, M. D. and Wilson, K. R.: Coupled Interfacial and Bulk Kinetics Govern the Timescales
2613 of Multiphase Ozonolysis Reactions, *J. Phys. Chem. A*, 126, 4991-5010,
2614 10.1021/acs.jpca.2c03059, 2022.
- 2615 Wilson, J., Poschl, U., Shiraiwa, M., and Berkemeier, T.: Non-equilibrium interplay between
2616 gas-particle partitioning and multiphase chemical reactions of semi-volatile compounds:
2617 mechanistic insights and practical implications for atmospheric modeling of polycyclic aromatic
2618 hydrocarbons, *Atmos. Chem. Phys.*, 21, 6175-6198, 10.5194/acp-21-6175-2021, 2021.
- 2619 Wilson, K. R., Prophet, A. M., and Willis, M. D.: A Kinetic Model for Predicting Trace Gas
2620 Uptake and Reaction, *J. Phys. Chem. A*, 126, 7291-7308, 10.1021/acs.jpca.2c03559, 2022.
- 2621 Wincel, H., Mereand, E., and Castleman, A. W.: Gas-Phase Reactions of N₂O₅ with NO₂-
2622 (H₂O)(N=0-2), NO₃-(H₂O)(N=1,2), and NON=2,3-HNO₂, *J. Chem. Phys.*, 102, 9228-9234,
2623 10.1063/1.468872, 1995.



- 2624 Winkler, A. K., Holmes, N. S., and Crowley, J. N.: Interaction of methanol, acetone and
2625 formaldehyde with ice surfaces between 198 and 223 K, *Phys. Chem. Chem. Phys.*, 4, 5270-
2626 5275, 10.1039/b206258e, 2002.
- 2627 Wittwer, H., Pino, P., and Suter, U. W.: Dipole-moments and conformational-analysis of
2628 copolymers of ethylene and carbon-monoxide, *Macromolecules*, 21, 1262-1269,
2629 10.1021/ma00183a015, 1988.
- 2630 Woodill, L. A., O'Neill, E. M., and Hinrichs, R. Z.: Impacts of Surface Adsorbed Catechol on
2631 Tropospheric Aerosol Surrogates: Heterogeneous Ozonolysis and Its Effects on Water Uptake, *J.*
2632 *Phys. Chem. A*, 117, 5620-5631, 10.1021/jp400748r, 2013.
- 2633 Worsnop, D. R., Morris, J. W., Shi, Q., Davidovits, P., and Kolb, C. E.: A chemical kinetic
2634 model for reactive transformations of aerosol particles, *Geophys. Res. Lett.*, 29, 2002.
- 2635 Worsnop, D. R., Zahniser, M. S., Kolb, C. E., Gardner, J. A., Watson, L. R., Vandoren, J. M.,
2636 Jayne, J. T., and Davidovits, P.: Temperature-Dependence of Mass Accommodation of So₂ and
2637 H₂O₂ On Aqueous Surfaces, *J. Phys. Chem.*, 93, 1159-1172, 1989.
- 2638 Yamasaki, H., Kuwata, K., and Miyamoto, H.: Effects of ambient-temperature on aspects of
2639 airborne polycyclic aromatic-hydrocarbons, *Environ. Sci. Technol.*, 16, 189-194,
2640 10.1021/es00098a003, 1982.
- 2641 Yang, H. and Whitten, J. L.: Energetics of hydroxyl and influence of coadsorbed oxygen on
2642 metal surfaces, *J. Phys. Chem. B*, 101, 4090-4096, 10.1021/jp9702311, 1997.
- 2643 Yankova, R., Dimov, M., Dobрева, K., and Stoyanova, A.: Electronic structure, reactivity, and
2644 Hirshfeld surface analysis of carvone, *J. Chem. Res*, 43, 319-329, 10.1177/1747519819863957,
2645 2019.
- 2646 Yaws, C. L.: *Thermophysical Properties of Chemicals and Hydrocarbons 2nd*, Elsevier, Oxford,
2647 1000 pp.2014.
- 2648 You, Y. and Bertram, A. K.: Effects of molecular weight and temperature on liquid-liquid phase
2649 separation in particles containing organic species and inorganic salts, *Atmos. Chem. Phys.*, 15,
2650 1351-1365, 10.5194/acp-15-1351-2015, 2015.
- 2651 You, Y., Smith, M. L., Song, M. J., Martin, S. T., and Bertram, A. K.: Liquid-liquid phase
2652 separation in atmospherically relevant particles consisting of organic species and inorganic salts,
2653 *Int. Rev. Phys. Chem.*, 33, 43-77, 10.1080/0144235x.2014.890786, 2014.
- 2654 You, Y., Renbaum-Wolff, L., Carreras-Sospedra, M., Hanna, S. J., Hiranuma, N., Kamal, S.,
2655 Smith, M. L., Zhang, X. L., Weber, R. J., Shilling, J. E., Dabdub, D., Martin, S. T., and Bertram,
2656 A. K.: Images reveal that atmospheric particles can undergo liquid-liquid phase separations, *P.*
2657 *Natl. Acad. Sci. USA*, 109, 13188-13193, 10.1073/pnas.1206414109, 2012.
- 2658 Zen, A., Trout, B. L., and Guidoni, L.: Properties of reactive oxygen species by quantum Monte
2659 Carlo, *J. Chem. Phys.*, 141, 14, 10.1063/1.4885144, 2014.
- 2660 Zheng, G. J., Su, H., Wang, S. W., Andreae, M. O., Poschl, U., and Cheng, Y. F.: Multiphase
2661 buffer theory explains contrasts in atmospheric aerosol acidity, *Science*, 369, 1374-+,
2662 10.1126/science.aba3719, 2020.
- 2663 Zhou, S., Shiraiwa, M., McWhinney, R. D., Pöschl, U., and Abbatt, J. P. D.: Kinetic limitations
2664 in gas-particle reactions arising from slow diffusion in secondary organic aerosol, *Faraday*
2665 *Discuss.*, 165, 391-406, 10.1039/c3fd00030c, 2013.
- 2666 Zimmermann, S., Kippenberger, M., Schuster, G., and Crowley, J. N.: Adsorption isotherms for
2667 hydrogen chloride (HCl) on ice surfaces between 190 and 220 K, *Phys. Chem. Chem. Phys.*, 18,
2668 13799-13810, 10.1039/c6cp01962e, 2016.



2669 Zobrist, B., Marcolli, C., Pedernera, D. A., and Koop, T.: Do atmospheric aerosols form
2670 glasses?, *Atmos. Chem. Phys.*, 8, 5221-5244, 2008.

2671